Synthesis and evaluation of fluorinated sialic acid derivatives as novel 'mechanism-based' neuraminidase inhibitors

Hader, Stefan

Award date:
2011

Awarding institution:
University of Bath

Synthesis and evaluation of fluorinated sialic acid derivatives as novel ‘mechanism-based’ neuraminidase inhibitors

Stefan Hader

A thesis submitted for the degree of Doctor of Philosophy

University of Bath

Department of Pharmacy and Pharmacology

November 2011

This research has been carried out under the supervision of Dr. Andrew G. Watts

Signed……

Date……

Abstract

Synthesis and evaluation of fluorinated sialic acid derivatives as novel ‘mechanism-based’ neuraminidase inhibitors

Doctor of Philosophy

by Stefan Hader

Increasing drug resistance towards the front line influenza neuraminidase inhibitor Oseltamivir (Tamiflu®, Roche) has recently been reported, emphasising the need to perform further studies to gain insight into receptor ligand interactions.

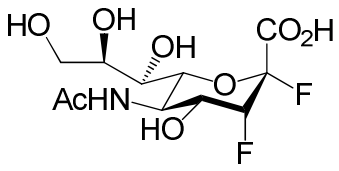

Recently, influenza neuraminidase activity has been tackled using a novel class of mechanism-based inactivator, which incorporates fluorine atoms at positions C-2 and C-3 of sialic acid. These inactivators are anticipated to be less susceptible to drug induced resistance as they target essential catalytic amino acids. However, individual hydrogen-bonding interactions formed between these inactivators and the neuraminidase in both the Michaelis complex and at the transition-state remain unclear.

The aim of this project is to synthesise a series of monodeoxygenated 2,3-difluoro-*N*-acetyl-neuraminic acid derivatives, designed to probe the importance of individual hydrogen-bonding interactions towards transition-state stabilisation.

The syntheses of the four novel monodeoxygenated 2,3-difluorosialic acid inactivators at position C-4,C-7, C-8 and C-9 deploying a Barton-McCombie protocol were accomplished. The time-dependant inactivation of wild type influenza neuraminidase N9 G70C by these monodeoxygenated 2,3-difluorosialic acid inactivators was tested in a fluorescent kinetic assay. Further biochemical evaluation (performed by our collaborators) in IC_{50} measurements against a panel of influenza viruses including wild types (wt.) and Oseltamivir resistant mutants showed potent inhibition of influenza B and H1N1 strains.

We also wished to develop a further understanding of the effects of the monodeoxygenated 2,3-difluorosialic acid inactivators upon inactivation on a physical basis. Hence, we will discuss X-ray crystallographic structures, (obtained by our collaborators) of influenza neuraminidase N9 in complex with the monodeoxygenated 2,3-difluoro-sialic acid inactivators.

Acknowledgements

First of all, I would like to acknowledge my supervisor Dr. Andrew G. Watts for giving me the opportunity to do this PhD. This Capacity PhD Studentship had been funded by the Medical Research Council, which I am grateful for.

I am thankful for the successful collaboration with Dr. Jennifer McKimm-Breschkin at Molecular and Health Technologies, CSIRO, Australia. She provided the neuraminidases, did the biological testing of my compounds and without her expertise it would not have been possible to perform this project. I would also like to acknowledge Dr. Victor Streltsov at Livestock Industries, CSIRO Australia and at the Australian Synchrotron MX-2, who did the X-ray crystal structures.

I would like to thank Dr Anneke Lubben for her inspiring dedication to provide an excellent mass spectrometry service and Dr. Timothy Woodman for running countless NMR spectra and his trust to let me use the 500 on my own.

I cannot imagine what the last 2 and half years would have been without Dr. Patricia Marcé-Villá in the lab. Thank you for the laugh and joy you brought, but also thank you for your time to discuss chemistry and sharing your expertise.

Over the years I was lucky to meet a lot of inspiring chemists in this department with Dr. Francesca Giuntini and Dr. Dan Furkert, only to name a few.

I would also like to thank Benjamin Butterfield, Dr. François D'Hooge, Dr. Christian Glover, Terrence Kantner, Deena LaSheen, and Dr. Ricardo Resende in the group for having dealt with me in the lab.

I am grateful for the company at lunch breaks of Rachel Carlton, Hannah Family, Hanne Kinnunen, Dr. Harshal Kubavat, Cormac Sammon, Ioana Stupariu and Irini Terzakis and I cannot wait to meet up with you all and catch up on the latest.

I also would like to thank my landlords Rob and Fhiona McKie for making me feel welcome and becoming close friends over the last four years.

I am thankful to my mother for being supportive and always there to talk, although moving to the UK meant not to be with her as often as I would have liked to. Danke Mama !

Finally, the last paragraph is for you, Patrick. You gave my life a meaning and I am blessed with you as my partner. I am looking forward to rise to new challenges together with you.

Table of Contents

List of Figures

List of Graphs

List of Schemes

List of Tables

Abbreviations

Abbreviation	Meaning
Å	Angstrom
Ac	Acetyl
AIBN	Azobisisobutyronitrile
Ala	Alanine
Arg	Arginine
Asn	Asparagine
Asp	Aspartic acid
CAZy	Carbohydrate active enzyme database
CMP-Neu5Ac	Cytidine 5'-monophosphate sialic acid
DANA	2-Deoxy-2,3-didehydro-*N*-acetylneuraminic acid
DAST	(Diethylamino)sulphur trifuloride
DBU	Diazabicycloundecene
dec.	decomposition
Deoxo-fluor®	Bis(2-methoxyethyl)aminosulphur trifluoride
DMAP	4-(Dimethylamino)pyridine
DMF	Dimethylformamide
DNA	Deoxyribonucleic acid

Abbreviation	Meaning
DNP	2,4-Dinitrophenyl
e.g.	*Exempli gratia* (as an example)
EC	Enzyme commission
et al.	*Et alii* (and others)
EtOAc	Ethyl acetate
FDA	US Food and Drug Administration
Gc	Glycolyl
GH	Glycoside hydrolase
Glu	Glutamic acid
Gly	Glycine
GTP	Guanosine 5'-triphosphate
h	Hours
His	Histidine
HLG	Protonated leaving group
HMPA	Hexamethylphosphoramide
HPLC/MS	High performance liquid chromatography mass spectrometry
Hz	Hertz
IC_{50}	Half maximal (50%) inhibitory concentration
Im	Imidazole
IMP	Inosine 5'-monophosphate
in vitro	Within glass
in vivo	Within the living
J	Coupling constant
k	Rate constant

Abbreviation	Meaning
kcal	Kilocalorie
k_{cat}	Catalytic rate constant
k_{cat}/K_M	Apparent rate constant
KDN	3-Deoxy-2-keto-*D*-glycero-*D*-galactononulosonic acid
K_i	Dissociation constant for inhibition/inactivation
k_{inact}	Rate constant for inactivation
K_M	Michaelis constant
K_S	Substrate dissociation constant
LG	Leaving group
Lt	Lactyl
Lys	Lysine
M1	Matrix protein
M2	Matrix protein
Man-6-P	Mannose-6-phosphate
ManNAc-6-P	2-*N*-Acetylmannosamine-6-phosphate
Me	Methyl
MeCN	Acetonitrile
MeOH	Methanol
min	Minutes
mL	Milliliter
mM	Millimolar
mmol	Millimole
mol	Mole
m.p	Melting point
MUNANA	2'-(4-Methylumbelliferyl) α-*D*-*N*-acetylneuraminic acid

Abbreviation	Meaning
n.d.	not determined
Neu	5-*N*-Amino-3,5-dideoxy-2-keto-*D*-glycero-*D*-galactononulosonic acid
Neu5Ac	5-*N*-Acetamido-3,5-dideoxy-2-keto-*D*-glycero-*D*-galactononulosonic acid
Neu5Gc	5-*N*-Gycolylamido-3,5-dideoxy-2-keto-*D*-glycero-*D*-galacto-nonulosonic acid
NP	Nucleoprotein
NS1	Non-structural protein 1
NS2	Non-structural protein 2
O/N	Over night
PA	Polymerase polypeptide A
PB1	Polymerase polypeptide B1
PB2	Polymerase polypeptide B2
PDB	Protein data bank
Ph	Phenyl
PEP	Phosphoenolpyruvate
pK_a	Acid dissociation constant
ppm	Parts per million
PMHS	Poly(methylhydrosiloxane)
*p*TSA	*p*-Toluenesulphonic acid
r.t.	Room temperature
RNPs	RNA + nucleoprotein
RMSD	Root-mean-square deviation
sec	Second
Selectfluor®	1-Chloromethyl-4-fluoro-1,4-diazoniabicyclo[2.2.2]octane bis(tetrafluoroborate)
TASF	Tris(dimethylamino)sulphonium difluorotrimethylsiliconate
TBAF	Tetrabutylammonium fluoride

Abbreviation	Meaning
TBDMS	*tert*-Butyldimethylsilyl
TFA	Trifluoroacetic acid
TLC	Thin layer chromatography
TMEDA	Tetramethylethylenediamine
TMS	Tetramethylsilyl
TNP	2,4,6-Trinitrophenyl
tRNA	Transfer ribonucleic acid
Tyr	Tyrosine
Val	Valine
wt.	wild type
δ	Chemical shift
$\Delta G^{\ddagger}$	Gibbs free energy of bond making and breaking
$\Delta G^{\ddagger}_{T}$	Gibbs free energy for k_{cat}/K_M
ΔG_S	Gibbs free energy of binding
$\Delta\Delta G - I_S$	Difference in Gibbs free energy of binding for the transition-state inhibitor and substrate

Their specific effect on the glycosides might thus be explained by assuming that the intimate contact between the molecules necessary for the release of the chemical reaction is possible only with similar geometrical configurations. To give an illustration I will say that enzyme and glycoside must fit together like lock and key in order to be able to exercise a chemical action on each other.
This concept has undoubtedly gained in probability and value for stereochemical research, after the phenomenon itself was transferred from the biological to the purely chemical field. It is an extension of the theory of asymmetry without being a direct consequence of it: for the conviction that the geometrical structure of the molecule even for optical isomers exercises such a great influence on the chemical affinities, in my opinion could only be gained by new actual observations.

— Emil Fischer

'Einfluss der Configuration auf die Wirkung der Enzyme', *Berichte der deutschen Chemischen Gesellschaft*, 1894, **27**, 2985-93. Trans. B. Holmstedt and G. Liljestrand (eds.) *Readings in Pharmacology* (1963), 251

Chapter 1 - Introduction

1.1 Preface

Infection caused by the influenza virus is a persistent problem in the human population and the recent H1N1 pandemic influenza outbreak in 2009 demonstrated the on-going global need for specific influenza anti-virals. The current production time of vaccines is too slow to have an impact on the first wave of an influenza pandemic and recently reported increases in resistance towards the existing front-line neuraminidase inhibitor Oseltamivir emphasises the urgent need for novel anti-influenza therapeutics.[3-5]

Neuraminidase is a feasible target for antiviral therapy but, in order to be able to develop novel anti-influenza therapeutics, more detailed kinetic and X-ray crystallographic studies are needed to gain insight into receptor-ligand interactions.

The first study performed to embrace the systematic removal of side chains involved in hydrogen-bonding interactions with the substrate through site-specific mutagenesis and measurement of the affinity of the ligand for each mutant generated was accomplished by Fersht *et al*. on tyrosyl tRNA synthetase.[6] The study quantified tyrosyl tRNA synthetase mutants generated in terms of Michaelis-Menten parameters compared to the wild type enzyme.

In a complementary approach by Street *et al.*, substrate/protein interactions have also been investigated through specific modifications of the substrate rather than the protein, creating carefully selected analogues that differ in their electronic properties and hydrogen-bonding capability but retain the ability to be accepted and/or processed by the enzyme.[7,8]

Detailed studies of modified substrates performed by Street *et al.* on glycogen phosphorylase demonstrated the usefulness of fluorinated and deoxygenated substrates to gain insight into both the electronic structure of the enzymatic ground-state Michaelis complex and transition-state of the reaction.[7,8] The experiments of Street *et al.* initiated the development of 2-deoxy-2-fluoro glycosides, which were amongst the first derivatives of representing a specific class of mechanism-based inactivators for glycoside hydrolase activity.[9,10]

Targeting influenza neuraminidase, the auspicious class of novel mechanism-based neuraminidase inactivators reported by Watts *et al.*[11,12] and Amaya *et al.*[13] are based upon the incorporation of fluorine atoms at positions C-2 and C-3 of sialic acid. These modifications result in formation of a covalent linkage within the neuraminidase active site and subsequent inactivation of the enzyme.

The aim of the present work is to translate the approach of Street *et al.* to the generation of deoxygenated and fluorinated sialic acid derivatives towards gaining a more detailed understanding of individual hydroxyl group contribution to transition-state stabilisation by influenza neuraminidases.[7,8] This is achievable by investigating the kinetic behaviour of the deoxygenated and fluorinated sialic acid derivatives towards neuraminidase, as well as gaining structural information by X-ray crystallographic studies of these derivatives in complex with neuraminidase.

1.2 Sialic acids

The generic term sialic acid is the name given to a group of more than 40 different variations of the two parent monosaccharides 3-deoxy-2-keto-*D*-glycero-*D*-galactononulosonic acid (KDN) (**1**) and 5-*N*-acetyl-3,5-dideoxy-2-keto-*D*-glycero-*D*-galactononulosonic acid (Neu5Ac) (**2**) originally isolated from salivary mucins (**Figure 1**).[14]

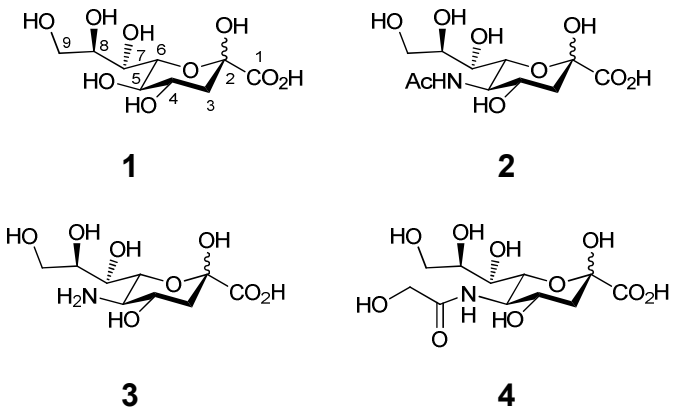

Figure 1 General structures of 3-deoxy-2-keto-*D*-glycero-*D*-galactononulosonic acid (KDN) (**1**), 5-*N*-acetyl-3,5-dideoxy-2-keto-*D*-glycero-*D*-galactononulosonic acid (Neu5Ac) (**2**), 5-*N*-amino-3,5-dideoxy-2-keto-*D*-glycero-*D*-galactononulosonic acid (Neu) (**3**), and 5-*N*-glycolylamido-3,5-dideoxy-2-keto-*D*-glycero-*D*-galacto-nonulosonic acid (Neu5Gc) (**4**).

All sialic acids are thought to be metabolically derived from the two parent monosaccharides KDN (**1**) and Neu5Ac (**2**) including modifications such as oxidation, single and multiple acetylations, sulfation and methylation.[1]

1.2.1 Nomenclature

The structural features common to all sialic acids are a 9-carbon backbone and a carboxylic acid at C-1 (pK_a ~ 2.2) making them negatively charged under physiological conditions.[15] The systematic names for sialic acids are too complicated for use in practice, so a uniform and simple nomenclature system is available. The root abbreviation KDN (**1**) and 5-*N*-amino-3,5-dideoxy-2-keto-*D*-glycero-*D*-galactononulosonic acid (Neu) (**3**) are then designated by letter codes (Ac = acetyl, Gc = glycolyl, Me = methyl, Lt = lactyl, S = sulfate), which are listed along with numbers indicating the location of the modification relative to the carbon backbone position (**Figure 1**). Thus, for example, the sialic acid 5-*N*-gycolylacetyl-3,5-dideoxy-2-keto-*D*-glycero-*D*-galacto-nonulosonic acid is named Neu5Gc (**4**).

1.2.2 Roles of sialic acids in vertebrate cells

Sialic acids are typically found at the outermost ends of N-linked glycans, O-linked glycans and glycosphingolipids, which easily interact with components of other cell surfaces, extracellular substances and effector molecules. In human biology, sialic acids play the dual role of either masking recognition sites or representing a biological target that allows recognition by a receptor protein, a lectin, thus being a ligand or counter-receptor.[16]

In vertebrate cells, KDN (**1**) and Neu5Ac (**2**) are biosynthetically derived through condensation of mannose-6-phosphate (Man-6-P) for KDN (**1**) or *N*-acetyl-*D*-mannosamine-6-phosphate (ManNAc-6-P) for Neu5Ac (**2**) with activated forms of pyruvate (e.g. phosphoenolpyruvate, PEP) and are believed to be the metabolic precursors of all other sialic acids (**Figure 2**).[1] Following dephosphorylation, the free Neu5Ac is activated by conversion to the nucleotide donor cytidine monophosphate sialic acid (CMP-Neu5Ac) and is pumped from the cytosol into the lumen of Golgi compartments by the action of a specific CMP Neu5Ac antiporter.

The transfer of sialic acids from CMP donors to newly synthesised glycoconjugates in the Golgi is catalysed by a family of linkage-specific sialyltransferases. Once these newly formed glycoconjugates are released in the cytosol, they can either be secreted from the cell via exocytosis, or are transported to the lysosomes via endosomes. Extracellular glycoconjugates are also transferred to the lysosomes by endosomes, where Neu5Ac is cleaved by the action of lysosomal sialidase. Once Neu5Ac is released into the lysosome, it is transported back into the cytosol by a specific exporter, which allows Neu5Ac to be either reutilized or degraded by pyruvate lyases into ManNAc and pyruvate.

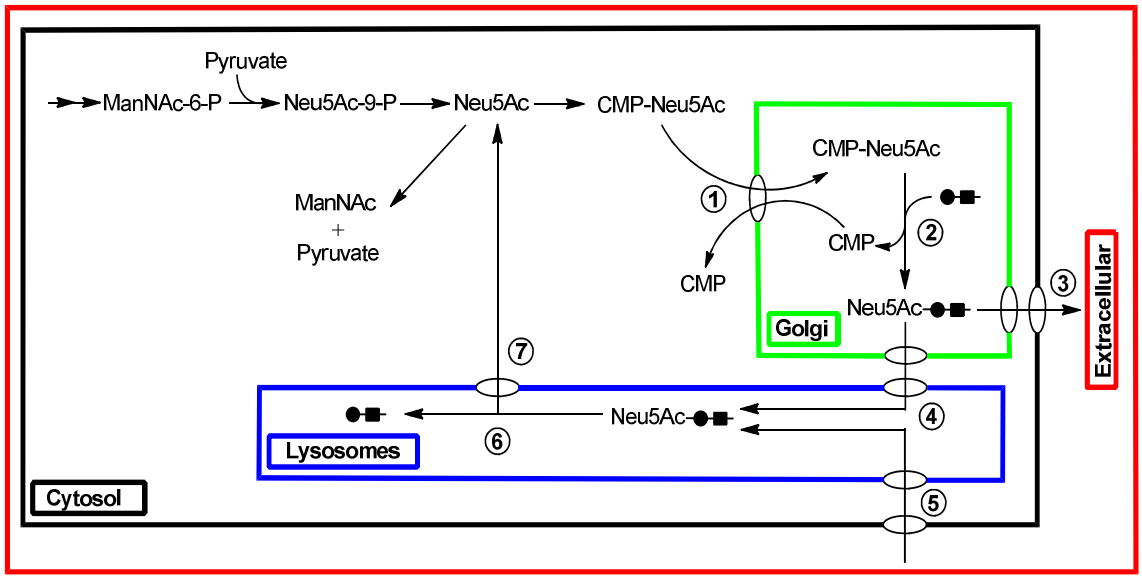

Figure 2 General pathways for biosynthesis, activation, transfer and eventual recycling of the common sialic acid Neu5Ac including CMP-Sia antiporter (1), sialyltransferases (2), exocytosis (3), endosomes (4), endocytosis (5), lysosomal sialidase (6) and sialic acid exporter (7) in vertebrate cells. (Adopted from Varki, A.)[1]

Many pathogens, for example viruses, bacteria and parasites have evolved two major strategies to rely on sialic acids in order to evade the host immune response, target and infect cells. Firstly, the pathogens cover through sialylation of external glycoconjugates, making it more likely for them to pass undetected through the host immune system, as the macrophages cannot detect the penultimate sugars and phagocytise the pathogens.[14] Secondly, some pathogens target specific sialic acid motifs on the host cell to aid the infection process.[17]

As a consequence of the important roles played by sialic acid and the enzymes responsible for hydrolysing these monosaccharides, the sialidases are of key interest as potential therapeutic interventions.

1.3 Sialidases

Sialidases are a superfamily of sialic acid-degrading enzymes (EC 3.2.1.18) widely found in higher eukaryotes and in a vast number of microbial pathogens.[18] In the glycoside hydrolase clan E (GH-E) of the Carbohydrate Active Enzymes Database (CAZy, http://www.cazy.org/), members of the sialidase superfamily have been classified according to their amino acid sequence similarities into the three distinct families of glycoside hydrolases comprising family 33 (GH 33) which includes most bacterial, simple eukaryotic and *trans*-sialidases, family GH 34 this includes viral sialidases and family GH 83 which contains the haemagglutinin-neuraminidases.[19]
Studies on viral[20], bacterial[21] and eukaryotic homologues[22] have shown that all sialidases share a six-bladed β-propeller topology and a highly conserved catalytic domain (**Figure 3**).

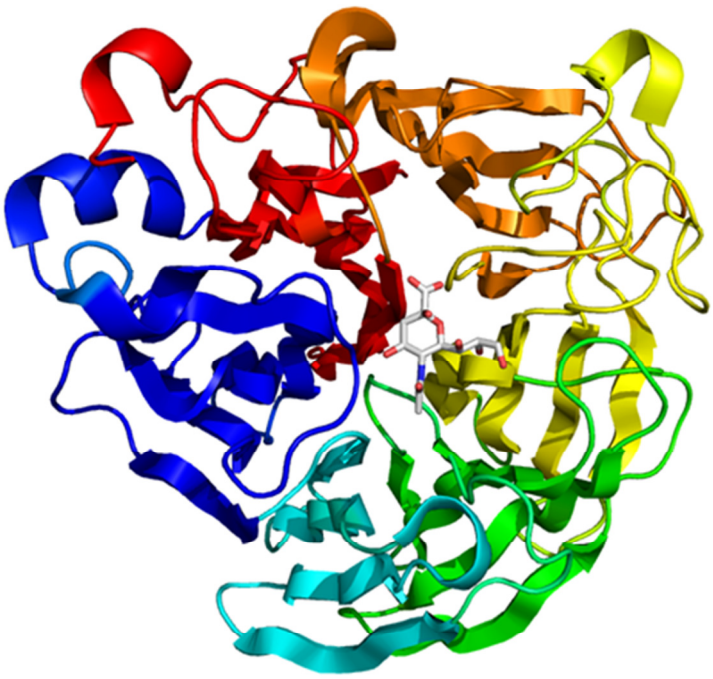

Figure 3 Six-bladed β-propeller topology of influenza neuraminidase N2 in complex with sialic acid (**2**). Generated with PyMOL[23] (PDB 2BAT).[24]

The fourth member of the GH-E clan is an *exo*-arabinanase that shares the six-bladed β propeller topology.[25] However, the catalytic mechanism is very different from that of sialidases.

1.3.1 Retaining glycoside hydrolases

The glycosidic bond is generally considered to be a very stable linkage within naturally occurring biopolymers, with the most prominent half-lives for spontaneous hydrolysis of cellulose and starch being in the range of 5 million years.[26] As such, enzymes hydrolysing these acetals have earned the reputation as some of the most proficient catalysts known.

Glycoside hydrolases hydrolyse the glycosidic bond with two possible stereochemical outcomes: inversion or retention of anomeric configuration.[2,27-29] Sialidases belonging to glycoside hydrolase families GH 33, GH 34 and GH 83 are known to operate with retention of anomeric configuration, hence for the purpose of this work we shall only focus on retaining glycoside hydrolases.

There are two proposed mechanisms for retaining glycoside hydrolases; both proceed through a double displacement mechanism. In the first mechanism, proposed by Koshland in 1953, one of the carboxylic groups acts as a general acid catalyst and protonates the glycosidic oxygen to promote glycosidic bond cleavage (**Scheme 1**).[2,30]

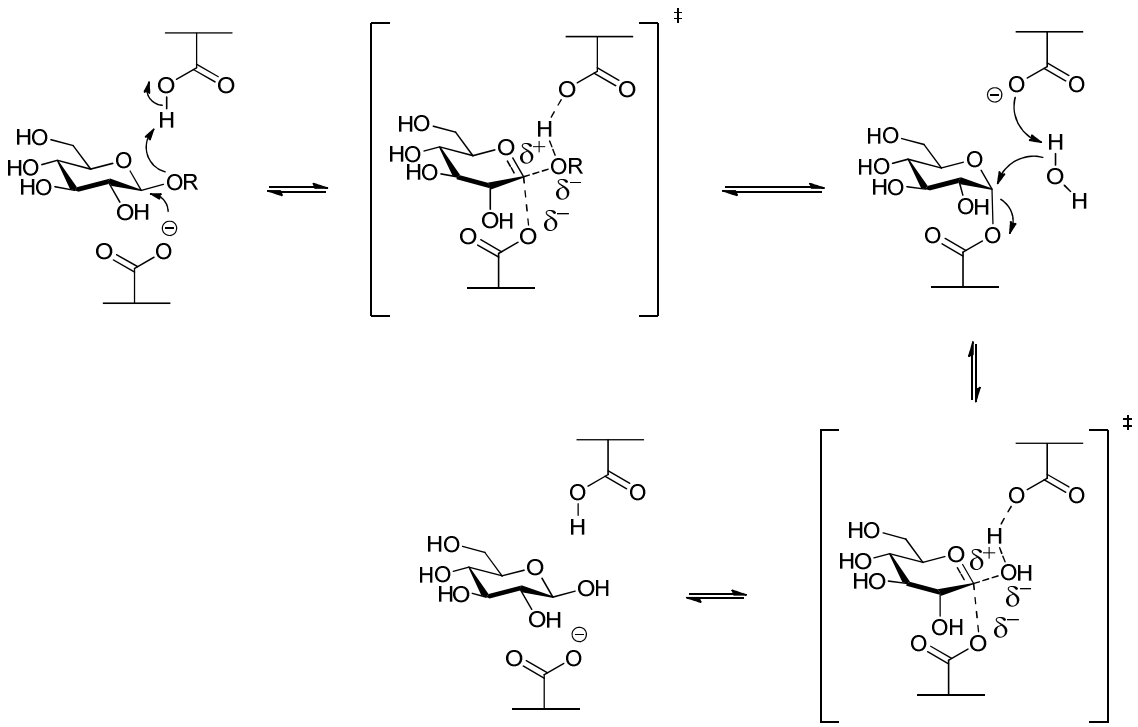

Scheme 1 Covalent glycosyl-enzyme intermediate mechanism for retaining glycoside hydrolases. (Taken from Zechel, D.L. *et al.*)[2]

The other carboxylic group functions as a nucleophile, forming a covalent glycosyl-enzyme intermediate at the anomeric position.

In the second step, the carboxylic side-chain group deprotonates an incoming water molecule, which then attacks at the anomeric centre and displaces the glycosyl-moiety. This mechanism claims the acid/base amino acid residue acting first as an acid catalyst (glycosylation) and second as a base catalyst (deglycosylation) with both steps involving transition-states with substantial oxocarbenium-ion character.

In contrast, the second mechanism for retaining glycoside hydrolases, proposed by Phillips in 1967, proceeds through a long-lived oxocarbenium-ion-pair intermediate rather than formation of a formal covalent glycosyl-enzyme linkage (**Scheme 2**).[31]

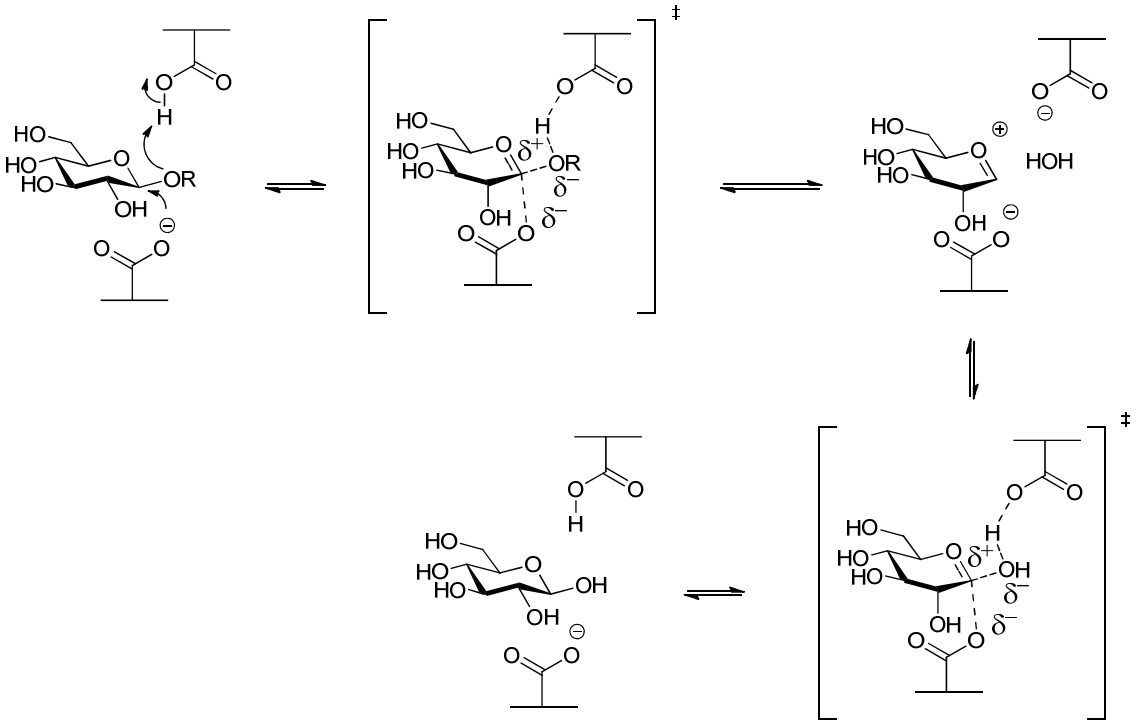

Scheme 2 Ion-pair intermediate mechanism for retaining glycoside hydrolases. (Taken from Zechel, D.L. *et al.*)[2]

The disclosure of the mechanisms for retaining glycoside hydrolases and the identification of the catalytic amino acid residues responsible has provided a rationale to intervene with their enzymatic function and led to the development of a number of potent and highly selective inhibitors.[32]

1.3.2 Inhibition of retaining glycoside hydrolases

In due consideration of the importance of glycoside hydrolases in many biological processes, the ability to moderate their enzymatic function is associated with numerous medical applications, ranging from treatment of type II diabetes[33] to antiviral[34-36] and cancer therapeutics.[37] Inhibitors of glycoside hydrolases can be classified as either reversible inhibitors or irreversible inactivators according to their mode of interaction with the enzyme.[38]

1.3.2.1 Reversible inhibitors

The majority of enzyme inhibitors operate through simple, reversible binding mechanisms with their target enzyme in a highly selective manner.[39] The formation of enzyme-inhibitor binary complexes can be quantified in familiar thermodynamic terms, such as an equilibrium dissociation constant for inhibition (K_i) and the Gibbs free energy of binding (ΔG_S).[40]

A general enzyme catalysed reaction starts with the reversible binding of substrate (*S*) to the free enzyme (*E*) to form the *E*•*S* complex, also commonly referred to as Michaelis complex, quantified by the dissociation constant K_S associated with the energetically favourable Gibbs free energy ΔG_S of realisation of the binding energy (**Scheme 3**).

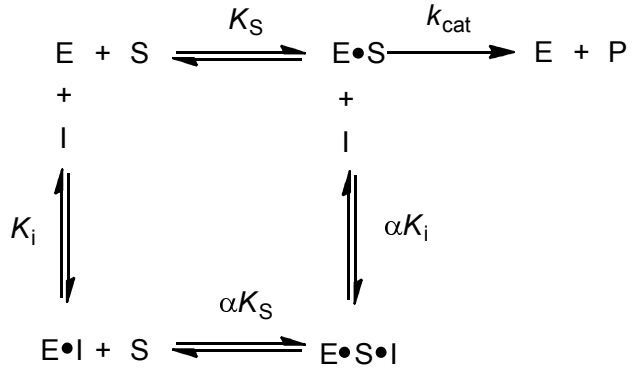

Scheme 3 Equilibrium scheme for enzyme turnover and the potential interactions of reversible inhibitors with enzyme. - Enzyme (*E*), substrate (*S*), inhibitor (*I*), substrate dissociation constant (K_S), Michaelis complexes (*E*•*S*) and (*E*•*I*), catalytic rate constant (k_{cat}), inhibitor (*I*), dissociation constant for inhibition/inactivation (K_i), ternary Michaelis complex (*E*•*S*•*I*) and product (*P*). (Taken from Copeland, R.A.)[40]

The *E•S* complex thus formed reacts through a series of chemical steps to the reaction product(s) (*P*), which are collectively defined by the first-order catalytic rate constant k_{cat} associated with the energetically unfavourable Gibbs free energy ($\Delta G^{‡}$) of the chemical steps of bond making and breaking The first mode of reversible inhibitor interaction is in which the inhibitor (*I*) binds to the free enzyme in direct competition with the substrate (competitive inhibitor) to form the *E•I* complex, defined by the dissociation constant K_i. The *E•I* complex could then react with substrate (*S*) to form the ternary *E•S•I* complex. However, the affinity of the *E•I* complex for substrate (*S*) may differ from the free enzyme (*E*), hence K_S must be modified by the constant α to describe the degree to which inhibitor binding effects the affinity of the enzyme (*E*) for substrate (*S*). Alternatively, the *E•S•I* complex can be formed by binding of inhibitor to the preformed *E•S* complex, defined by the modified dissociation constant αK_i. It is possible for the *E•S•I* complex formed to generate product(s), albeit at a reduced rate relative to the uninhibited reaction, which is referred to as partial inhibition. An inhibitor that binds exclusively to the free enzyme, for which $\alpha = \infty$, is said to be competitive because these inhibitors compete with the substrate for the pool of free enzyme molecules.

A reaction coordinate diagram for a chemical reaction to turn over the substrate (*S*) and the same reaction catalysed by an enzyme shows the Michaelis complex (*E•S*) at an energetically favourable Gibbs free energy. Together with the Gibbs energetically unfavourable high energy transition-state (*ES*‡) the dependence of the Gibbs free energy for k_{cat}/K_M ($\Delta G^{‡}_T$) on $\Delta G^{‡}$ and ΔG_S is illustrated (**Figure 4**).[41]

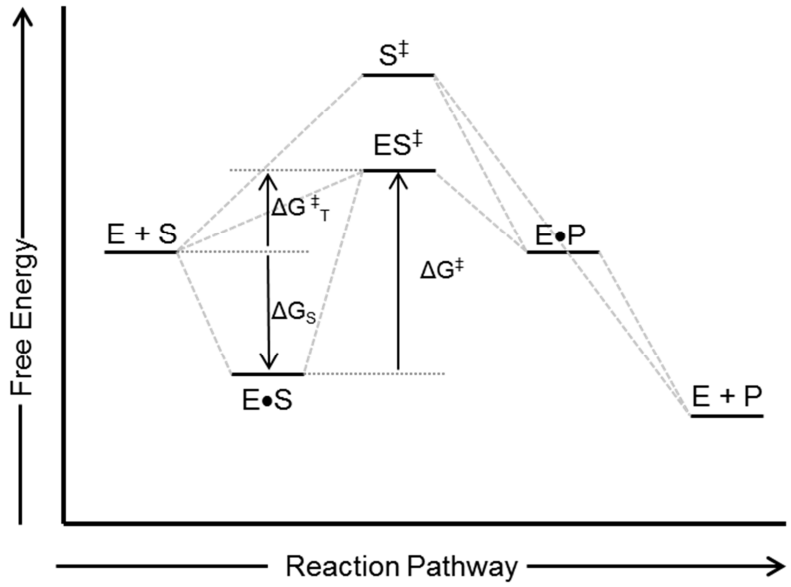

Figure 4 Reaction coordinate diagram for the reaction pathway of a chemical reaction and the same reaction catalysed by an enzyme. - Enzyme (*E*), substrate (*S*), Michaelis complex (*E•S*) and (*E•P*), transition-state ($ES^{‡}$), transition-state for the substrate ($S^{‡}$), Gibbs free energy of binding (ΔG_S), Gibbs free energy for k_{cat}/K_M ($\Delta G^{‡}_T$), Gibbs free energy of bond breaking and making ($\Delta G^{‡}$), and product (*P*). (Adopted from Copeland, R.A)[40]

1.3.2.2 Transition-state theory

The transition-state ($ES^{‡}$) represents the species with the highest energy formed during the enzyme catalysed cycle at which chemical bonds are in the process of being made and broken. This is in contrast to intermediates, whose bonds are fully formed and occupy troughs in a reaction coordinate diagram. Enzymes have evolved to form strong binding interactions with transition-states, which can be described by the apparent second-order rate constant k_{cat}/K_M and the proportional Gibbs free energy ($\Delta G^{‡}_T$) (**Scheme 4**).[42]

$$E + S \underset{}{\overset{k_{cat}/K_M}{\rightleftharpoons}} ES^{‡}$$

Scheme 4 Equilibrium scheme for transition-state formation. – Enzyme (*E*), substrate (*S*), apparent rate constant k_{cat}/K_M, and transition-state ($ES^{‡}$). (Adopted from Copeland, R.A)[40]

The transition-state ($ES^{‡}$) is an unstable structure which is poised between the chemical structures of the substrates and products.[43] The idea of the enzymatic transition-state was largely developed from the chemical rate theory by Eyring which allowed mathematical treatment using the thermodynamic and activated state concepts of the time.[44]

Transition-state theory relates the rate of a reaction to the difference in Gibbs free energy (ΔG) between the transition-state and the ground-state.[45] In terms of time, the smallest fraction of the catalytic cycle is spent in the transition-state with proposed lifetimes of 10^{-13} sec, equivalent to the time for a single bond vibration. A useful tool in the application of transition-state theory or in the analysis of structure-reactivity data is the Hammond postulate, which states that if there is an unstable intermediate on the reaction pathway, the transition-state for this reaction will resemble the structure of this intermediate.[42] This is a useful way of predicting the structure of the transition-state and for predicting the types of stabilisation it requires.[46]

Once a substrate (*S*) progresses from the Michaelis complex (*E*•*S*) to product (*P*), enzymes alter the electronic structure of the substrate by protonation, proton abstraction, electron transfer or interactions with Lewis acids and bases through sequential protein and substrate conformational changes resulting in a different Michaelis complex (*E*•*S*)'.[47] The summation of individually weak forces are brought to bear on the substrate and, combined, result in large forces capable of relocating bonding electrons to cause the breaking or formation of bonds, geometric distortion or hydrophobic partitioning.

Hydrogen bonds are the most common chemistry-promoting force between enzymes and substrates with an average bond distance from 2.6 to 3.1 Å.[48] At 3.1 Å, the hydrogen bond energy is weak, typically <1 Kcal/mol; however, short hydrogen bonds can contribute 4 – 6 Kcal/mol toward catalysis.[49] The strong dependence of hydrogen and ionic binding energy on bond distance, angle, solvent environment and relative pK_a values can be used to explain the increases in binding forces of the transition-state complex ($ES^{‡}$) relative to the Michaelis complex (*E*•*S*).

The catalytic site of an enzyme remains closed during the lifetime of the transition-state, preventing reactants from diffusing from the catalytic site, a definition of tight-binding at the transition-state.[50] A major energetic obstacle an enzyme has to overcome is to bind tightly only to the unstable transition-state structure, while avoiding comparative tight-binding to the substrate or products. The energetics of catalysis and binding a transition-state analogue with optimum binding energy are shown in the following reaction coordinate diagram (**Figure 5**).[47]

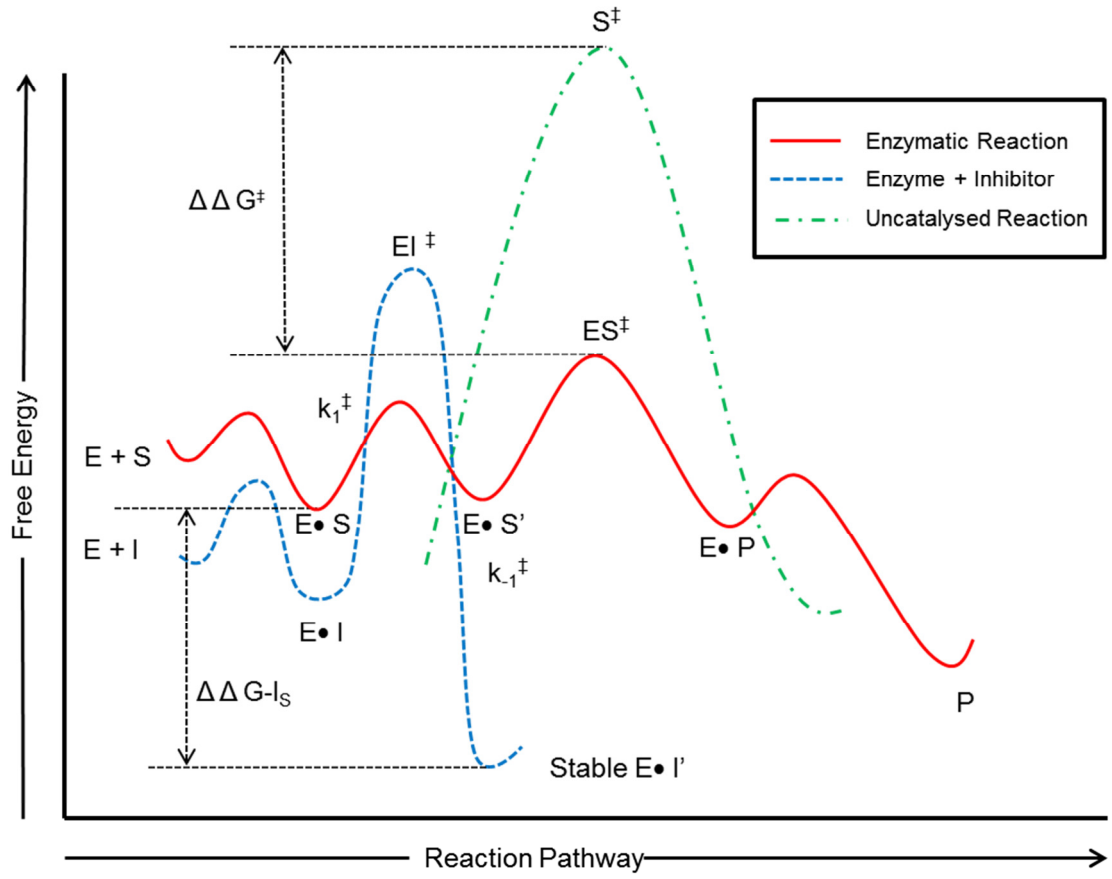

Figure 5 Reaction coordinate diagram of a catalysis and binding for an energetically perfect transition-state inhibitor (*I*). - Enzyme (*E*), substrate (*S*), Michaelis complexes (*E*•*S*) (*E*•S)' (*E*•*P*) (*E*•*I*) (*E*•*I*)', transition-states ($S^{‡}$) ($ES^{‡}$) ($EI^{‡}$), difference in Gibbs free energy of binding ($\Delta\Delta G^{‡}$), difference in Gibbs free energy for binding of the transition-state inhibitor and substrate ($\Delta\Delta G - I_S$), rate of onset for tight-binding inhibitors ($k_1^{‡}$), rate of escape for tight-binding inhibitors ($k_{-1}^{‡}$), and product (P). (Adopted from Schramm, V.L)[47]

The difference in Gibbs free energy of binding ($\Delta\Delta G^{‡}$) is the enzymatic efficiency compared to the uncatalysed reaction which equals $k_{enzyme}/k_{chemical}$ in terms of Gibbs free energy. The term $\Delta\Delta G - I_S$ describes the difference in Gibbs free energy of binding for a perfect transition-state inhibitor (*I*) and substrate (*S*).

The slow-onset inhibition common with transition-state inhibitors occurs after formation of a readily reversible (*E•I*) complex with the rate of onset for tight-binding inhibitors $k_1^{‡}$. It is noteworthy that the rate of escape $k_{-1}^{‡}$ has an unfavourable energetic barrier to escape from the stable (*E•I*)*'* complex.

A common mechanism in enzymatic catalysis is to generate a differential charge on the substrate between ground-state and transition-state, permitting electrostatic interactions to specifically stabilise the transition-state ($ES^{‡}$).[51]

However, an imperfect match between the enzyme (*E*) and the transition-state inhibitor is inevitable, mainly because it is impossible for stable compounds to mimic perfectly the non-equilibrium bond lengths of the transition-state. For the necessarily imperfect transition-state inhibitors, the $k_1^{‡}$ barrier corresponds to the time to fit the imperfect inhibitor into the lowest-energy structure.[52]

A common strategy, used in structure based drug design, is to mimic the assumed charge or the assumed geometry of the transition-state that is formed during the catalytic cycle of the enzyme. An example of a competitive inhibitor mimicking the transition-state charge would be Miglitol (**5**), which is prescribed towards type II diabetes.[53] This α-glycoside hydrolase inhibitor with the protonated endocyclic nitrogen at physiological pH imitates the oxocarbenium-ion present at the transition state in glycoside hydrolases. An inhibitor focusing on transition-state geometry is the anti-influenza therapeutic Oseltamivir (**6**). This influenza neuraminidase inhibitor mimics the half-chair conformation, which is commonly accepted to be the conformation adopted by the transition-state ($ES^{‡}$).[54]

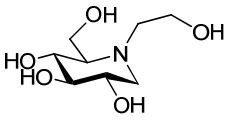

5

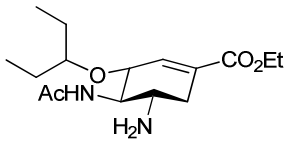

6

1.3.2.3 Irreversible inactivators

Compounds that interact with an enzyme molecule in such a way as to abolish enzyme function permanently are referred to as irreversible inactivators.[55] Enzyme inactivation generally occurs as a result of enzyme-based nucleophiles undergoing reaction with an electrophilic portion of the inactivator, leading to formation of a covalent bond between the enzyme and the inactivator. This covalent linkage either physically blocks substrate from entering the active or modifies an active site residue that is critical for catalysis, hence the activity of the enzyme is reduced irreversibly.

Two general mechanisms for irreversible enzyme inactivation are based on covalent modification of the enzyme, or of a critical cofactor or substrate of the enzyme reaction and are referred to as affinity labelling and mechanism-based inactivation.[56]

Affinity labels commonly incorporate an inherently reactive functional group that can covalently modify appropriate nucleophiles at any location within the enzyme. This lack of specificity in general makes affinity label therapeutics, also referred to as non-specific affinity label therapeutics, less acceptable as therapeutics. However, there are a number of examples of DNA-alkylating agents such as methanesulfonates and nitrosoureas that act as non-specific affinity labels, yet are still used clinically for the treatment of some forms of cancer.[40] In the case of non-specific affinity labelling, the rate constant k_{inact} for the single-step inactivation has units of a second-order rate constant ($M^{-1}s^{-1}$) to form the covalent enzyme inactivator complex (*E-I*) (**Scheme 5a**).[40]

As a result, quiescent affinity labels have been utilised containing a weak electrophile, which reversibly binds in the active site of the enzyme with some reasonable affinity (**Scheme 5b**). The electrophile in sensible concentration in solution does not react readily with nucleophiles but, in the case of already being bound within the solvent-shielded environment of the active site, the electrophile and the corresponding nucleophile is enough to form a covalent linkage. A clinical example of this class includes the β-lactam-containing antibiotics, which selectively modify the serine hydroxyl group of bacterial peptidoglycan transpeptidases to elicit their antibiotic activity.[40]

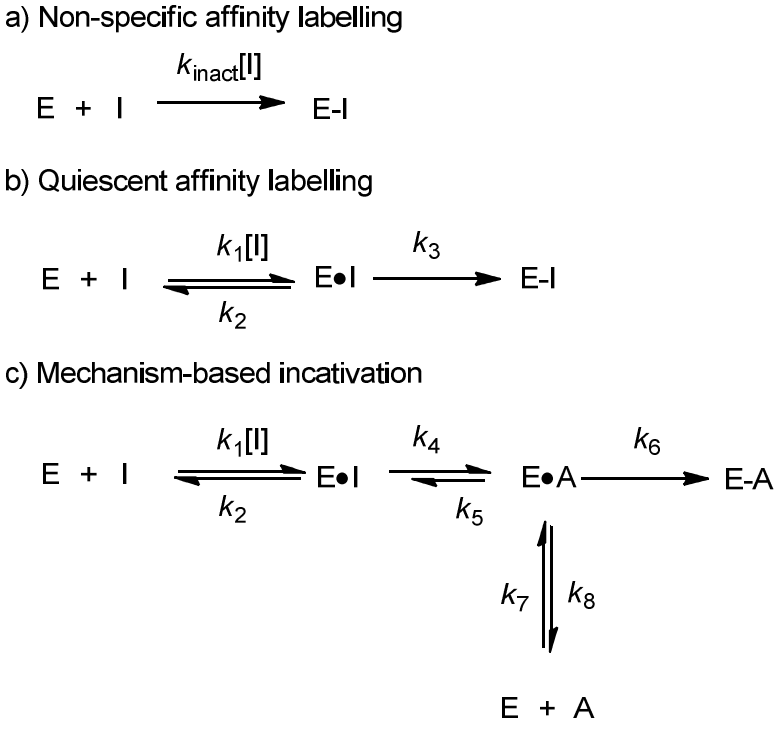

Scheme 5 Mechanisms of irreversible enzyme inactivation for enzyme (E), inactivator (I) and affinity label (A) in the case of a) Non-specific affinity labelling, b) quiescent affinity labelling and c) mechanism-based inactivation. (Taken from Copeland, R.A.)[40]

For quiescent affinity labels, the inactivation follows a two-step mechanism, involving binding of the inactivator to the enzyme (*E•I*), often under rapid equilibrium conditions, and subsequent covalent bond formation (**Scheme 5b**).[40]

In general, mechanism-based inactivators are chemically inert and require specific activation by the catalytic machinery of the enzyme into a species that can then act as an affinity label a transition-state analogue or a very tight-binding reversible inhibitor, prior to release from the active site.[57]

The inactivator is recognized by the enzyme as an alternative substrate that is acted upon by groups within the active site to catalytically generate an inhibitor, hence mechanism-based inactivators are competitive with the natural substrate of the enzyme and also commonly referred to as suicide substrates. Owing to their reliance on enzyme catalysis, mechanism-based inactivators generally display very high target specifity and inactivation can proceed either in a single step, or through a two-step mechanism (**Scheme 5c**).[40]

Whereas with quiescent affinity labels the second step involves the chemistry of covalent bond formation, the situation for mechanism-based inactivators is significantly more complicated.

Mechanism-based inactivators can bind in a reversible fashion to the enzyme to form an initial encounter complex (*E•I*), analogous to formation of *E•S* in the normal catalytic reaction of the enzyme. The bound complex is then chemically transformed by the catalytic machinery of the enzyme to form the affinity label A, defined by the forward equilibrium rate constant k_4. Hence, there is also the possibility of a reverse reaction going from (*E•A*) to (*E•I*), governed by the rate constant k_5.

Once the binary complex (*E•A*) has been formed, the affinity label can either react irreversibly with an enzyme nucleophile to a covalent species (*E-A*), or dissociate through a reversible process from the enzyme to form free enzyme (*E*) and the free affinity label (*A*).

1.3.2.4 Mechanism-based inactivators: Fluorinated glycosides

Mechanism-based inactivators target the catalytic nucleophile residue, which was shown to be of paramount importance to the activity of the enzyme and has been utilized in the development of new inactivators. Fluorinated glycosides have found much use a class of mechanism-based inactivators, owing to their mode of action specific to retaining glycoside hydrolases.

The activated 2-deoxy-2-fluoro glucoses (**7**) and (**8**), 5-fluoro glucose (**9**) and 2-deoxy-2,2-difluoro glycosides (**10**) belong to a specific class of mechanism-based inactivators of glucoside hydrolase activity.[9,10]

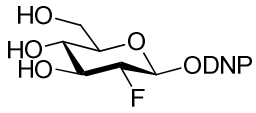

7

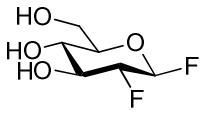

8

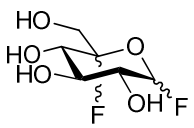

9

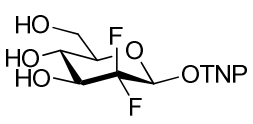

10

The 2-deoxy-2-fluoro substitution allows differentiation of glycosylation and deglycosylation rates involved in the catalytic mechanism in retaining glucoside hydrolases (**Scheme 1**).

The introduction of an electronegative fluorine atom in glucose causes an inductive effect on neighbouring charges and, if present at C-2 adjacent to the anomeric centre, leads to a destabilisation of the formation of positive charges at the anomeric centre in both glycosylation and deglycosylation transition-states. The destabilisation of the positive charge in the transition-state slows down the formation of the glycosyl-enzyme intermediate and its hydrolysis. The addition of an activated leaving group (LG) at position C-1 such as fluorine, 2,4-dinitrophenyl (DNP), or 2,4,6-trinitrophenyl (TNP) accelerates the glycosylation step, leading to the accumulation of the covalent glycosyl-enzyme intermediate whereby the enzyme is inactivated with observed lifetimes ranging from seconds to months (**Scheme 6**).[55]

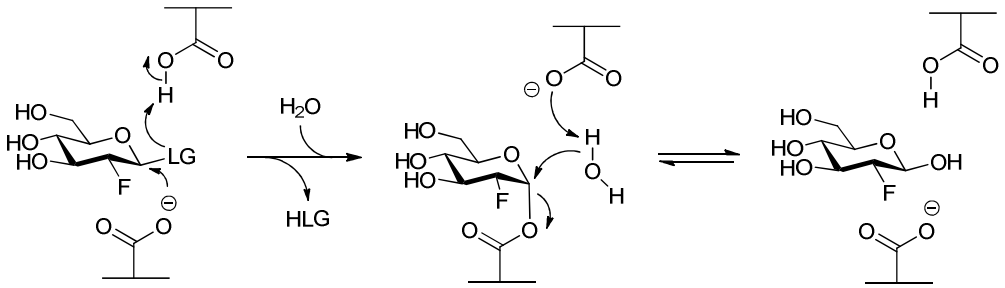

Scheme 6 General proposed mechanism of inactivation of retaining glycoside hydrolases by fluorinated-β-glycoside. - Leaving group (LG) and protonated leaving group (HLG). (Taken from Rempel, P.B. *et al.*)[55]

The enzyme is capable of reactivation through either hydrolysis of the covalent glycosyl-enzyme intermediate, or through trans-glycosylation onto a suitable acceptor substrate. As a consequence of the ability to recover enzyme activity, this class of inactivators is often referred to as very slow enzymatic substrates rather than true inactivators. However, for all practical purposes, the life-time of the trapped covalent glycosyl-enzyme intermediate are usually sufficiently long lived for enzyme inactivation.

Mechanism-based fluorinated glycoside inactivators were used by Withers and Aebersold to identify and label the catalytic nucleophile in retaining glycoside hydrolases through inactivation of the glycoside hydrolase.[56] Subsequent proteolysis, peptide localisation and sequencing by HPLC/MS using collision-induced fragmentation led to identify the label residue.

An example of identification of the catalytic nucleophile residue was performed by Watts *et al.* on *Trypanosoma cruzi* trans-sialidase leading to the identification of tyrosine as the catalytic nucleophile residue being responsible for the cleavage of anionic sialic acid residues.[11] The identification of the alternative tyrosine catalytic nucleophile residue instead of a carboxylic group, common in glycoside hydrolases, led to the development of novel mechanism-based fluorinated sialoside inactivators for neuraminidases. These novel inactivators have the promise of being a tool in drug discovery to tackle the pathogenic enzymes like influenza neuraminidase.[11]

1.4 Influenza virus

The influenza virus belongs to the *Orthomyxoviridae* family including six genera, *Influenza virus* A, *Influenza virus* B, *Influenza virus C*, *Isa virus*, *Thogota virus* and *Quarja virus* with a genome consisting of six to eight segments of single-strand RNA.[58] Due to the genetic capacity of the *Orthomyxoviridae* family to undergo reassortment within a specific genus, new virus strains can emerge that continue to elude the immune response and infect humans, poultry and livestock.[59] In terms of infection and mortality to humans, by far the most important virus from this family is influenza virus A.

The nomenclature of the different subtypes (HxNy) of influenza virus A relates to immunological specifications of the haemagglutinin (H) and neuraminidase (N) surface proteins. To date, sixteen different hemagglutinin subtypes (H1-H16) and nine neuraminidase subtypes (N1-N9) have been identified in a variety of hosts with wild water fowls as the native host and the ability to cross species barriers (**Figure 6**).[60,61]

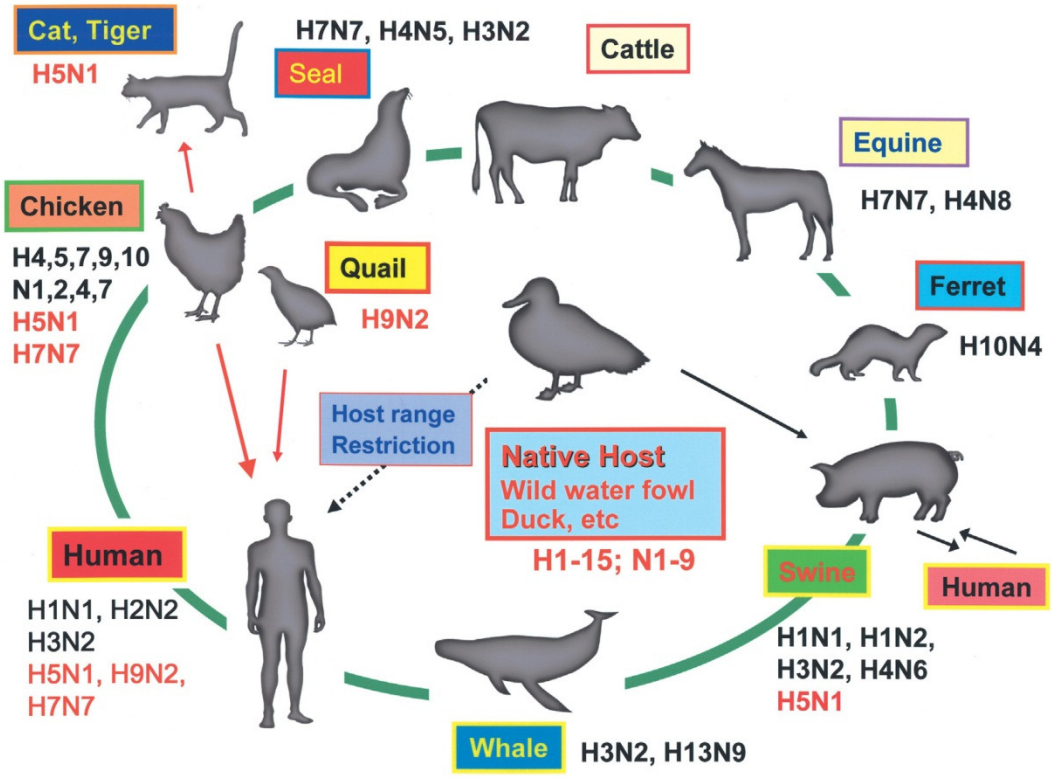

Figure 6 Range of hosts of influenza viruses (Taken from Suzuki,Y.)[61]

In 1980 the World Health Organisation introduced a new nomenclature system which is still in use to follow up on the diversity of influenza virus strains.[62] So, for example A/Wisconsin/67/2005/(H3N2) describes the type of influenza, the geographic origin, the isolate number, the year of isolation and the distinct haemagglutinin and neuraminidase subtype of the isolate. The large diversity of haemagglutinin and neuraminidase subtypes is the result of the two processes known as antigenic drift and antigenic shift.[63] Antigenic drift occurs during replication of the virus in the infected host cell by errors of polymerisation of the viral RNA with a rate of mutation of about 1 in 10^4 bases per replication, resulting in the formation of new serotypes which no longer can be targeted by antibodies.[64]

Antigenic shift is defined as the simultaneous infection of a host cell by at least two different strains of influenza virus, resulting in mixing and recombination of the genes of each strain during replication, forming a new strain of virus particles with new genetic material.

The continuous formation of virus particles with new genetic material enables the influenza virus continually to generate new subtypes, all with the potential to initiate a new pandemic.

Historically, the first well documented account of an influenza pandemic was what became known as the 'Spanish Flu' from 1918 till 1920, with an estimated death toll between 50 and 100 million people.[65] The next major outbreak of influenza virus A occurred in 1997, where a new strain, H5N1 commonly referred to as 'Bird Flu' emerged in the human population, never reaching pandemic status but still circulating with another outbreak in 2005.[66] However, the first pandemic of the 21st century was caused by an H1N1 strain originating from pigs, hence named 'Swine Flu' which had been endemic in pigs since 1918, when the virus crossed the species barrier to infect pigs and had remained there until recently crossing the species barrier back to humans again.[67]

1.4.1 Structure and life cycle of the influenza virus A

The influenza virus A particle is roughly spherical with a diameter of 80 – 120 nanometres, enveloped with a lipid bilayer and functions in combination with the two major surface glycoproteins haemagglutinin (H) and neuraminidase (N) (**Figure 7**).[68] The inner side of the lipid bilayer is lined by the non-structural proteins (NS1 and NS2) and the matrix protein (M1 and M2) of which M2 is forming ion channels. The RNA segments are packed with the 3 polymerase polypeptides PA, PB1 and PB2 in a helical form in the core of the viral particle (RNPs = RNA + nucleoprotein).[69]

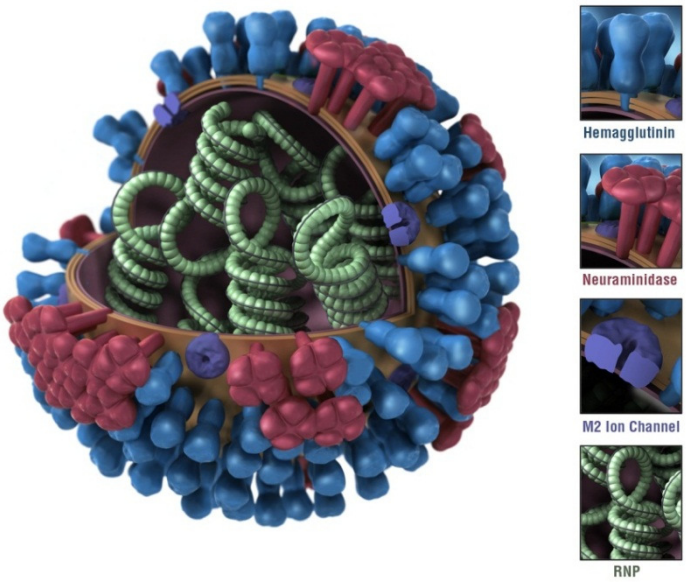

Figure 7 Cartoon illustration of an influenza virus particle. (Taken from Jordan, D.)[68]

In order to replicate in a host cell, the life cycle of the virus starts with binding of the viral particle surface glycoprotein haemagglutinin (H) to terminal sialic acid residues present on glycoproteins, glycolipids, or receptors located on the target cell surface (**Figure 8**).[70]

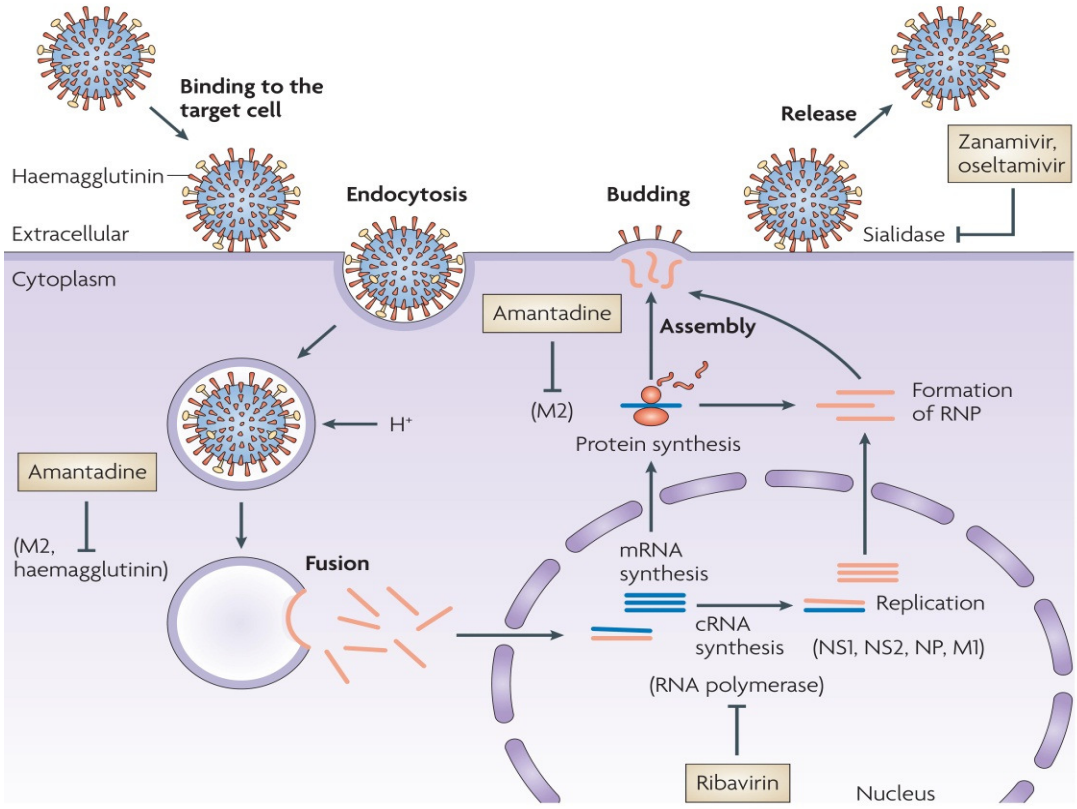

Figure 8 Schematic representation of the replication cycle of influenza virus A and targets for therapeutic intervention. (Taken from von Itzstein, M. with permission from the author)[70]

Once the new viral particle is formed, it first remains attached to the host cell membrane through binding of viral haemagglutinin protein to the terminal sialic acid residues present on cell surface glycoconjugates. If the new viral particle would remain on the cell surface, the host immune system would come into action and phagocytise the particle. The crucial role of viral neuraminidase at this late stage of viral replication is to hydrolyse the terminal sialic acid residues on the host cell surface in order to liberate the new viral particle, ready to infect other cells.

1.4.2 Therapeutic targets of influenza virus

The life cycle of influenza virus replication reveals key stages that have potential to act as therapeutic targets for inhibition of virus replication, such as the M2 ion-channels, RNA polymerase and sialidase (**Figure 8**).[70] The M2 ion-channels play a crucial role in the process of uncoating for the effective release of viral RNA into the host cytoplasm.[71] The RNA polymerase replicates viral RNA in the host cell and influenza neuraminidase facilitates the release of the new viral particles. Over the past decades all these key stages have been tackled in drug discovery efforts, resulting in several small-molecule approved therapeutics on the market.[70]

1.4.2.1 M2 ion-channel

The first synthetic compound to inhibit influenza virus replication was amantadine (Symmetrel®, Mantadix®) (**11**), which was postulated to block the interior channel within the tetrameric M2 helix bundle. Hence, amantadine stops the migration of H^+ ions from the cytosol into the inner virus particle, an important process for the viral uncoating to occur.[72]

The adamantamine derivatives amantadine (**11**)[73-75] and rimantadine (Flumadin®) (**12**)[76] have long been available for specific influenza virus A infection prophylaxis and therapy.

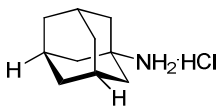

11

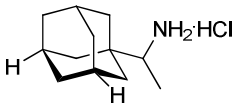

12

However, due to the rapid emergence of drug resistance, the ready transmissibility of drug-resistant viruses and particularly for amantadine, the occurrence of central nervous system side effects, they are no longer used as stand-alone therapeutics but still find use as a component of combination therapy.[77]

1.4.2.2 RNA transcription

Ribavirin (Virazole®) (**13**) was recognised as a broad-spectrum antiviral agent against the *Orthomyxoviridae* family and targets inosine 5`-monophosphate (IMP) dehydrogenase, a key enzyme involved in guanosine 3'-triposphate (GTP) and viral RNA synthesis. Ribavirin (**13**) is notable for not generating drug resistance and is active against both avian and human H5N1 influenza viruses.[78]

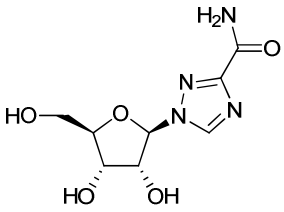

13

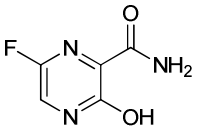

14

However, the use of ribavirin (**13**) is limited due to possible side effects in pregnant women and the dose-limiting toxicity of haemolytic anaemia.[79]
Another RNA transcription inhibitor showing promising results is the pyrazine derivative T-705 (Favipiravir) (**14**) which is currently in phase II clinical trials and has been postulated to be converted intracellularly to the triphosphate ribonucleotide and then inhibit influenza virus polymerase in a GTP competitive manner.[80]

Nevertheless, a small number of side effects in humans and no significant effects as commonly stand-alone therapy do not make it an auspicious candidate in drug discovery efforts towards the influenza virus, leaving influenza neuraminidase as the most viable target.[81].

1.4.2.3 Neuraminidase

Over the past few decades, vital structural and functional information on influenza neuraminidase has been gathered in order to elucidate the enzymes mode of action. Subsequently this information was used in the design of novel potent inhibitors with Zanamivir (**15**) and Oseltamivir (**6**) being the most prominent examples.[20,82] A more detailed structural and functional study of influenza neuraminidase will be the focus of this thesis.

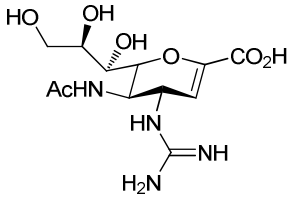

15

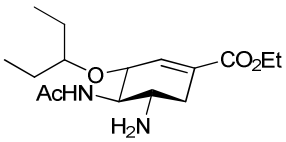

6

1.5 Influenza neuraminidase

Influenza neuraminidase (EC 3.2.1.18) is a glycoside hydrolase, cleaving terminal sialic acids from glycoconjugates. This cleavage facilitates infection by the virus in the upper respiratory tract and allows the liberation of the progeny viral particles from the host cell surface.[70]

X-ray crystallographic studies have identified key residues within the active site, which are conserved in neuraminidases across all influenza A and influenza B viruses and provide exciting opportunities for structure-based drug design.

The active site of influenza neuraminidase N2 consists of a tri-arginyl cluster of Arg118, Arg 292 and Arg371 which forms a salt bridge with the carboxylic group at C-1 on sialic acid (**2**), the Tyr406 which has been reported to act as the catalytic nucleophile, hydrogen bond interactions between Glu227 and Glu277 with the *N*-acetyl group as well as a catalytic water molecule (**Figure 9**).

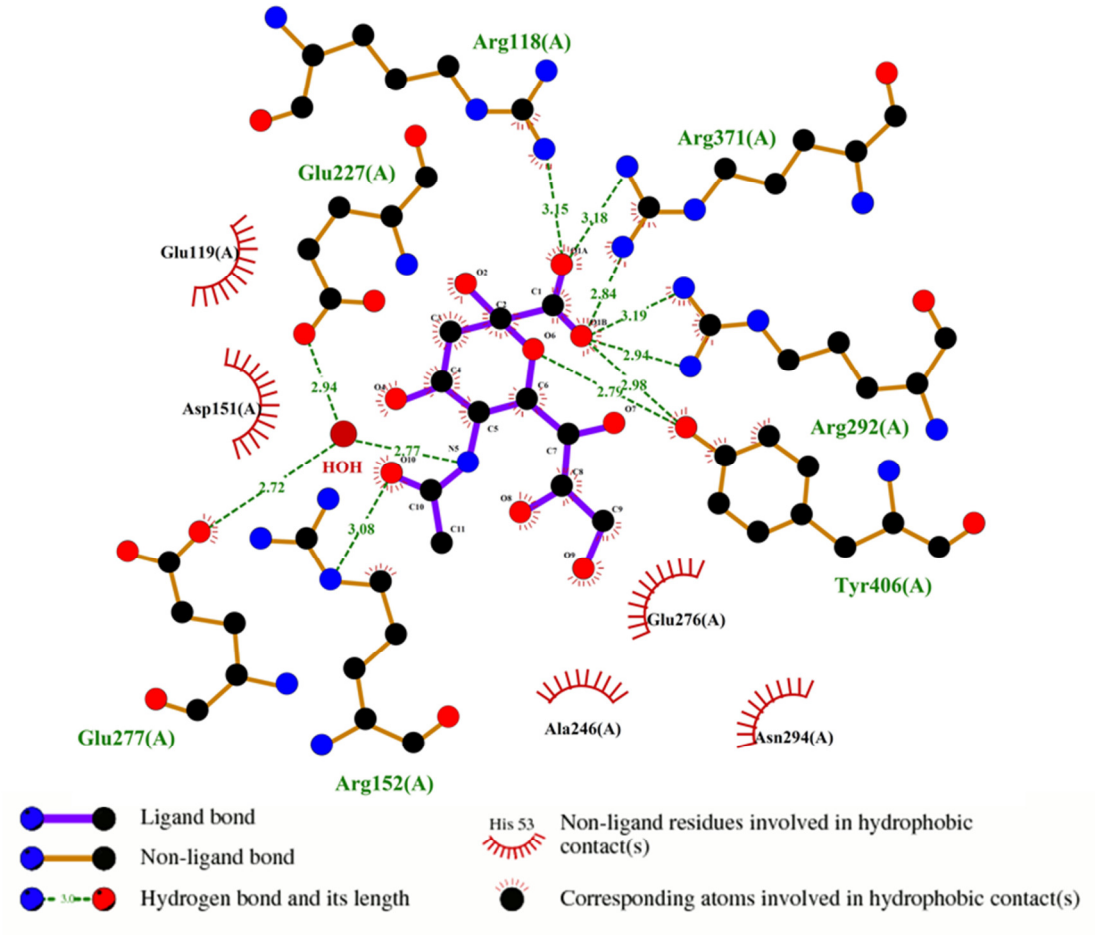

Figure 9 Interactions of sialic acid (**2**) with the residues present within the active site of influenza neuraminidase N2. Generated with LigPlot^{+} (PDB 2BAT).[83]

The description of the active site residues in conjunction with mechanistic considerations of general retaining glycoside hydrolases has previously been mentioned (Chapter 1.3.1) and led to two proposals for the catalytic mechanisms of influenza neuraminidases.

1.5.1 Proposed catalytic mechanisms

In analogy to general retaining glycoside hydrolases (see Chapter 1.3.1), there are two proposed mechanisms for neuraminidases, both proceeding by a double displacement mechanism involving three catalytic amino acids, namely aspartic acid, glutamic acid and tyrosine. The first proposed mechanism by Horenstein *et al.* proceeds through an initial distortion from a solution-dominant α-sialoside $^2C_5$ conformer into an α boat conformer upon binding, in order to form a salt bridge between the negatively charged carboxyl group of sialic acid and the highly conserved tri-arginyl cluster within the active site of neuraminidases (**Scheme 7**).[70,84]

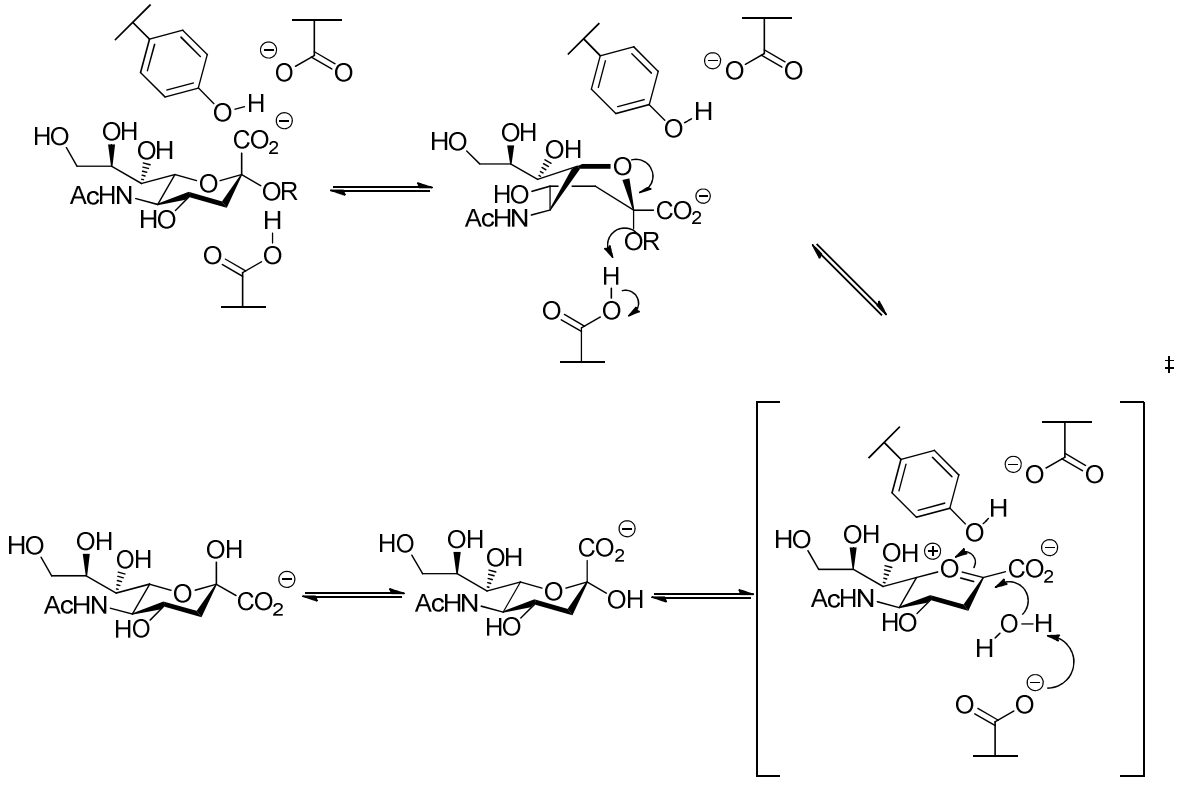

Scheme 7 Ion-pair intermediate mechanism for neuraminidases. R = glycoside. (Taken from von Itzstein, M.)[70]

The resulting conformational strain facilitates leaving of the protonated glycosidic oxygen and the formation of an oxocarbenium-ion intermediate, which has been identified by kinetic isotope effect measurements and modelling studies.[85,86]

Deprotonating a water molecule by an aspartic acid residue is activating a water molecule towards nucleophilic attack of the oxocarbenium-ion intermediate, forming an α sialic acid anomer, which then mutarotates to the thermodynamically favourable β anomer.

The identification of a tyrosine residue as the catalytic nucleophile in *Trypanosoma cruzi* trans-sialidase, as previously mentioned (Chapter 1.3.2.4) led to the proposal of a different catalytic mechanism for neuraminidases by Watts and Withers.[87] Following deprotonation of the hydroxyl group of the catalytic tyrosine residue by glutamic acid, the tyrosine can then act as a nucleophile, attacking the anomeric position C-2 of the sialic acid residue (**Scheme 8**).[70]

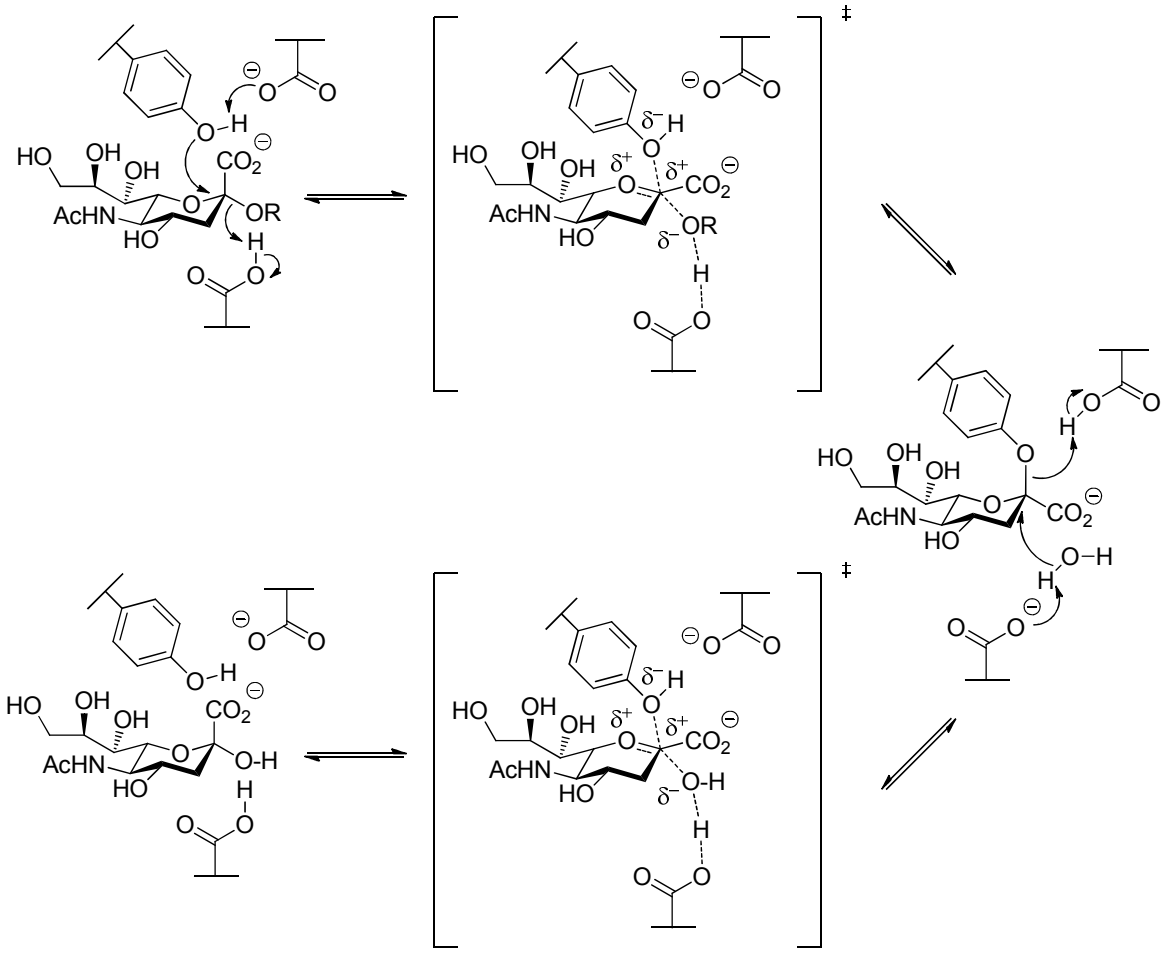

Scheme 8 Covalent glycosyl-enzyme intermediate mechanism for neuraminidases. R = glycoside. (Taken from von Itzstein, M.)[70,87]

Parallel to this action, the glycosidic oxygen is protonated by an aspartic acid residue activating it towards leaving and resulting in an oxocarbenium-ion transition-state, which with the tyrosine residue is leading to a covalent sialosyl-enzyme intermediate. This glycosylation step involves the cleavage of the sialic acid from the host cell membrane glycoconjugate.

However, in order to complete the catalytic cycle and to regain enzymatic activity, the deglycosylation step proceeds through deprotonating a water molecule by an aspartic acid residue, activating it towards nucleophilic attack on the sialosyl-enzyme intermediate. This nucleophilic attack leads to a second oxocarbenium-ion transition-state and results in bond cleavage between the sialic acid and the tyrosine residue under overall retention of configuration at the anomeric centre of the sialic acid.

The structural information and the proposed mechanisms proved valuable in the discovery and development of novel competitive inhibitors of influenza neuraminidase.

1.5.2 Competitive neuraminidase inhibitors as therapeutics

The first generation of competitive influenza neuraminidase inhibitors were targeted to mimic the oxocarbenium-ion species and its flattened conformation, which led to the idea of using 2-deoxy-2,3-didehydro-*N*-acetylneuraminic acid (DANA) (**16**) as a parent scaffold.

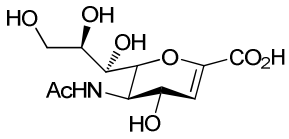

16

DANA (**16**) served as a starting point for structural based drug design as it gave potent inhibition of bacterial and mammalian neuraminidases[88] both *in vitro* and *in vivo* with a promising K_i of 4 µM against influenza neuraminidase N2 compared to a K_i of 1 mM with sialic acid (**2**), but DANA (**16**) lacked in specificity.[89]

1.5.2.1 Zanamivir

X-ray diffraction studies performed on DANA (**16**) in complex with influenza neuraminidase suggested that a cavity around the hydroxyl group at C-4 only present in viral neuraminidase, but absent in mammalian neuraminidase, could be used to achieve specificity.[90,91] Hence, introducing a large basic functionality at this position would benefit from interactions with neighbouring amino acid residues and could result in better inhibition.[90,91] The targeted molecule was identified as 4-*N*-amino-4-deoxy DANA (**17**) and was tested against influenza neuraminidase N2 showing a 100-fold improvement in the K_i compared to DANA (**16**).[70] The alternative introduction of a guanidino functional group to yield 4-guanidino DANA, better known as Zanamivir (**15**), gave a 10.000-fold improvement compared to the parent compound DANA (**16**) and a K_i of 0.2 nM.[70]

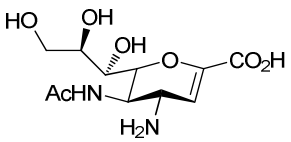

17

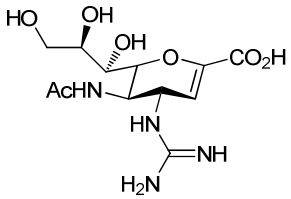

15

As predicted, X-ray crystal structures of Zanamivir (**15**) in complex with influenza neuraminidase N2 showed that the guanidino group at C-4 position occupies the cavity and forms hydrogen bonds with glutamic acid and several hydrophobic interactions with asparagine, methionine, isoleucine, and tyrosine amino acid residues (**Figure 10**).[86,92]

Due to the highly polar nature of Zanamivir (**15**) and therefore its low bioavailability (< 5%), it was developed as an inhaled formulation, delivering the drug directly to the lung, the main site of infection.

In 1999, following the success in clinical trials, Zanamivir (**15**) was approved by the US Food and Drug Administration (FDA) as the first neuraminidase targeting influenza inhibitor with the trade name Relenza®.[24,70]

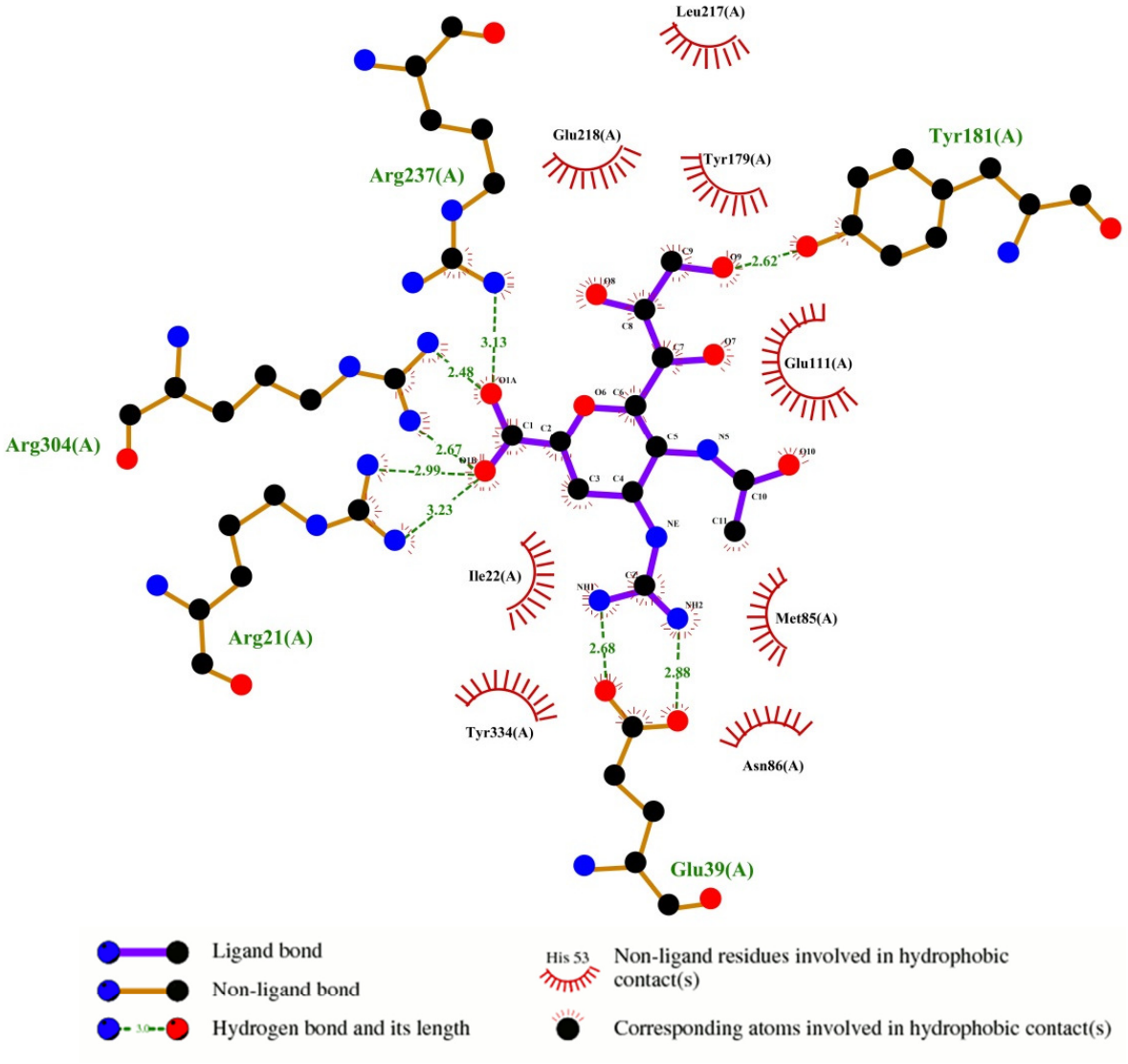

Figure 10 Interactions of Zanamivir (**15**) with the residues present within the active site of influenza neuraminidase N2. Generated with LigPlot^{+} (PDB 2F0Z).

Zanamivir (**15**) is very effective in the treatment of influenza viruses A and B and has shown low incidence of drug-induced resistance with only one case of resistance in an immunocompromised child reported in literature.[93-95]

The side effects of Zanamivir (**15**) treatment are very mild and largely confined to the airways (*e.g.* cough, nasal symptoms) but unfortunately the method of inhaled formulation cannot be employed to people with impaired lung capacity.[96]

1.5.2.2 Oseltamivir

The development of Zanamivir (**15**) provided a platform for further influenza neuraminidase inhibitors, with one aim being to increase hydrophobicity and potentially increase bioavailability without compromising inhibitory activity. The removal of the ring oxygen was considered to help increase hydrophobicity of the molecule and allow the development of cyclohexene analogues that mimic more closely the geometry of the oxocarbenium-ion species by changing the position of the alkene bond like compound (**18**).

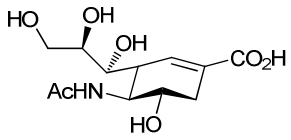

18

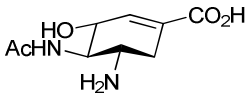

19

Compound (**18**) showed promising results against influenza neuraminidase N2 with an IC_{50} of 20 µM compared to a K_i of 4 µM with DANA (**16**).[97] In order to increase inhibitory activity further, the introduction of a hydroxyl group at C-6 instead of the glycerol side chain could pose an inductive electron-withdrawing effect on the double bond, similar to the highly polarised oxocarbenium-ion species, and could become a parent compound for the synthesis of ether analogues at the C-6 position. In addition, analogous to the introduction of an amino group during the development of Zanamivir (**15**), the introduction of an amino group at C-4 lead to compound (**19**) with an IC_{50} of 6.3 µM against influenza neuraminidase N2.[98] Extensive structure-activity studies with a range of alkyl group modifications at C-6 position were performed and the 3-pentyl side chain containing compound GS4071 (**20**) was found to be the most potent inhibitor against H1N1 with an IC_{50} of 1 nM.[99]

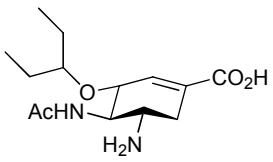

20

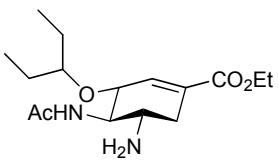

6

The oral bioavailability of the free acid was still found to be poor, hence the ethyl ester prodrug of GS4071 was formed to give the final compound Oseltamivir (**6**).

Oseltamivir (**6**) is readily converted to the active form *in vivo* by the action of endogenous liver esterase and was marketed as the second neuraminidase targeting influenza inhibitor with the trade name Tamiflu®.[100]

X-ray crystallographic studies of influenza neuraminidase N1 in complex with Oseltamivir (**6**) showed that the alkoxy side chain is involved in several hydrophobic contacts with Glu276, Glu277, Arg224, Arg292 and Asn294 in the space which was previously occupied by the glycerol side chain of sialic acid (**Figure 11**).[101]

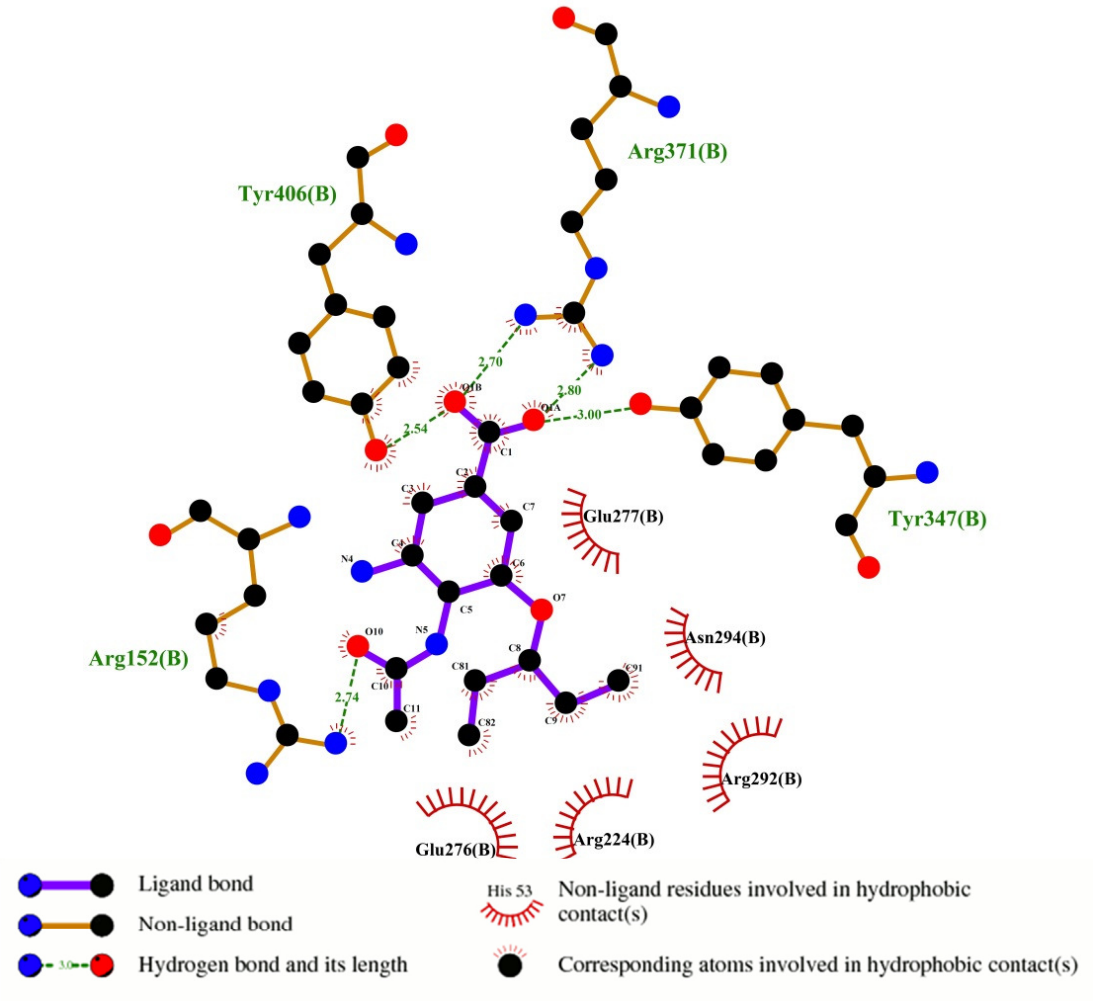

Figure 11 Interactions of Oseltamivir (**6**) with the residues present within the active site of influenza neuraminidase N1. Generated with LigPlot^{+} (PDB 2HU0).[101]

Oseltamivir (**6**) was found to exhibit high bioavailability when administered orally, produces very mild side effects and is currently stockpiled by countries around the world as the drug of choice against the influenza virus dominating over 90% of the world market.[102]

However, quite alarming is the number of mutant influenza viruses which have developed resistances towards Oseltamivir (**6**) and already circulate in the human population. One particular mutation was seen to pass from 0.4% resistance in the 2007-2008 flu season to virtually 100% in the following year.[4,103-107]

1.5.3 Point mutations conferring resistance towards current therapeutics

Reversible influenza neuraminidase inhibitors are strikingly similar in structure to their natural substrates and have been designed to target amino acid residues that are not essential for enzymatic activity. These non-essential amino acid residues are more likely to suffer point mutations, as these mutations do not compromise the ability of the enzyme to turnover the natural substrate. The number of mutant influenza viruses circulating in the human population is already alarming, affecting the inhibitor efficacy of Oseltamivir (**6**) and to a lesser extent Zanamivir (**15**) through five specific point mutations at positions Glu119, Arg152, Asp198, His274 or Arg292 (**Figure 12**).[77,108-113]

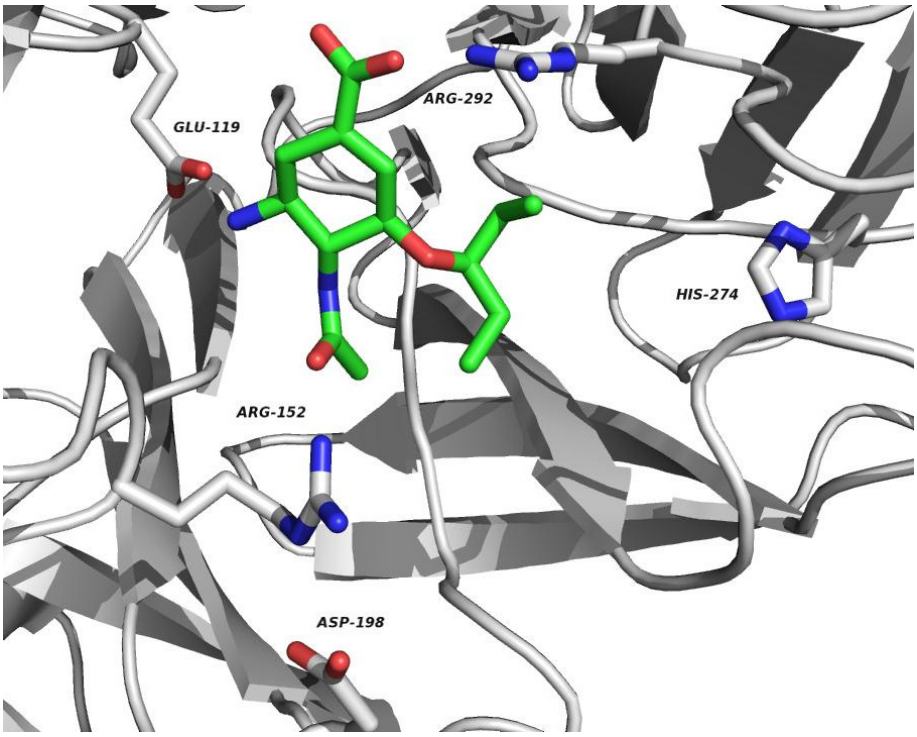

Figure 12 Point mutations of influenza neuraminidase known to induce drug resistance to Oseltamivir (**6**) shown on influenza neuraminidase N1 in complex with Oseltamivir (**6**). Amino acid residues are shown in stick representation. Generated with PyMOL (PDB 2HU0).[101]

Four different point mutations at residue Glu119 have been identified in several different strains of both influenza A and B viruses *in vivo*, these include the mutations Glu119Gly, Glu119Ala, Glu119Asp and Glu119Val. The mutation Glu119Val represents a clinically relevant mutant leading to Oseltamivir (**6**) resistance in the human strain A/Wuhan/359/1995/(H3N2). [114-117] The residue Glu119 interacts strongly with the basic nitrogen group at C-4 of Oseltamivir (**6**) and structural information suggests that diminished binding may be a consequence of an additional water molecule occupying the position previously occupied by the carboxylate of Glu119.[118]

The residue Arg152 is conserved in all influenza A and B viruses and forms a hydrogen bond to the *N*-acetyl group present at C-5 of the natural substrate sialic acid (**2**), Oseltamivir (**6**) and Zanamivir (**15**). The Arg152Lys mutant, first isolated from an immunocompromised child infected with influenza B virus and treated with Zanamivir (**15**) showed a very low enzyme activity (3 – 5% compared to the wild type enzyme) and was 1000-fold less sensitive to Zanamivir (**15**).[114]

The residue Asp198 interacts with Arg152, so altered interactions between Asp198 and Arg152 affect interactions of Arg152 with the *N*-acetyl group. The Asp198Glu mutant of B/Perth/211/2001 is known to confer cross resistance to Oseltamivir (**6**), Zanamivir (**15**) and Peramivir (**21**) and, as such, has proven to be useful for testing interactions around the *N*-acetyl group in novel influenza neuraminidase inhibitors being developed.[119]

Residue His274 interacts with Glu276 and the mutation His274Tyr affects the reorientation of Glu276 in order to form a salt link with Arg224.[4,120] This salt bridge is necessary to enable creation of the hydrophobic pocket necessary to accommodate the bulky hydrophobic pentenyl ether side chain in Oseltamivir (**6**) and Peramivir (**21**) (**Figure 11**).[121]

The residue Arg292 is one of the three highly conserved arginines that form part of the catalytic triad of influenza neuraminidase (**Figure 9**), hence enzymes mutated at this position all exhibit decreased catalytic activity relative to the wild type enzyme.[114] Detailed structural analysis of the Arg292Lys mutant revealed altered binding of the carboxylate group and the glycerol side-chain on the ligand, which would correlate with reduced enzyme activity as well as altered drug sensitivity. Further, this lysine residue is seen tor restrict Glu276 from moving, again required to accommodate the bulkier pentenyl ether group at Oseltamivir (**6**).[122,123]

Based on these results, it has been postulated that in terms of substrate architecture, inhibitors of a greater structural difference between inhibitor and natural substrate sialic acid (**2**), are more likely to induce the virus to mutate in order for it to maintain substrate binding, but decrease inhibitor binding. Hence, minimalist approach to drug design and mechanism-based inactivators would be less likely to generate viable mutants.[114]

1.5.4 Novel clinical candidates

Additional drug discovery efforts against the influenza virus are exceptionally well-motivated by the US Food and Drug Administration (FDA) which now provides a fast-track programme for the approval of potential future influenza neuraminidase inhibitors. Peramivir (**21**) and the dimeric derivatives of Zanamivir (**22**) are currently being evaluated in such fast-tracked clinical trials.[124]

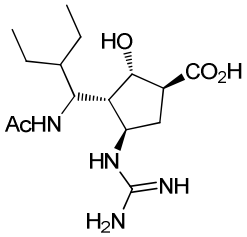

21

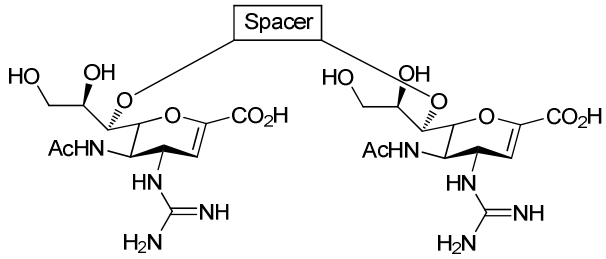

22

Peramivir (**21**) was designed to exploit the hydrophobic pocket observed with Oseltamivir (**6**) in complex with neuraminidase N1 (**Figure 11**) and has shown to be highly specific towards viral neuraminidase over bacterial and mammalian neuraminidases with *in vitro* and *in vivo* activities comparable to the activity of Zanamivir (**15**) and Oseltamivir (**6**).[124] In addition, the injectable formulation of Peramivir (**21**) might be of great value to patients who cannot readily take tablets and/or have a compromised lung capacity. However, quite alarming recent reports indicate that viruses resistant to Oseltamivir (**6**) may also be cross-resistant to Peramivir (**21**).[125-130]

The dimeric Zanamivir derivatives (**22**) with a carbamate linkage and a variety of hydrocarbon chains or benzylic spacers, have shown to be 100-fold more potent inhibitors than the parent compound Zanamivir (**15**) against influenza viruses H1N1 and H3N2, possibly due to aggregation of several viral particles and a subsequently more efficient auto immune response.[131] Furthermore, the dimeric Zanamivir derivatives (**22**) have proven to be long-lasting neuraminidase inhibitors with the potential to reduce the number of treatments required.[132,133] However, due to the highly polar nature and therefore low bio-availability, dimeric Zanamivir derivatives (**22**) are not considered to be a viable alternative in influenza treatment.

1.5.5 Mechanism-based inactivators as potential therapeutics

Mechanism-based inactivators of influenza neuraminidase are designed to target the covalently linked sialosyl-enzyme intermediate (**Scheme 8**), unlike the current influenza neuraminidase inhibitors Zanamivir (**15**) and Oseltamivir (**6**) which target the oxocarbenium-ion species (**Scheme 7**). It is anticipated that mechanism-based inactivators have the potential to be less susceptible to drug induced resistance in influenza neuraminidase as they target essential amino acid residues.

These essential amino acid residues are less likely to mutate as the influenza neuraminidase mutant is unable to turn over sialic acid, the natural substrate.[134-136]

The novel class of neuraminidase inhibitors based on 2,3-difluoro-sialic acid (**23**) were developed to attenuate glycosylation and deglycosylation rates in the catalytic cycle of neuraminidases and have previously been demonstrated in a number of studies on bacterial and trypanosomal neuraminidiases.[12]

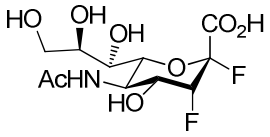

23

The introduction of a fluorine atom at C-3, adjacent to the anomeric position serves to destabilise the formation of a positive charge during the transition-state due to its electronegativity and is reducing the rate of glycosylation (k_1) and deglycosylation (k_2) (**Scheme 9**). A 'good leaving group' at the anomeric position C-2, such as fluorine, increases the rate of glycosylation, whereas deglycosylation remains unaffected, allowing the covalently linked sialosyl-enzyme intermediate to be kinetically accessible and accumulate to a high steady-state concentration, whereby the enzyme is inactivated.

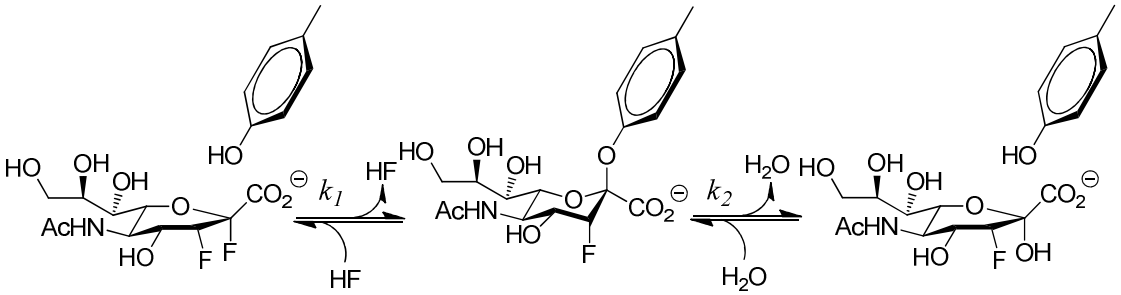

Scheme 9 The glycosylation (k_1) and deglycosylation (k_2) rate constants are attenuated by fluorine-containing mechanism-based inactivators. (Adopted from Watts, A. G. *et al.*)[12]

Recent unpublished work by the research groups of Dr. Andrew Watts and Prof. Stephen Withers has shown that influenza neuraminidase operates through a similar mechanism to bacterial and trypanosomal neuraminidase utilising a covalent sialosyl-enzyme intermediate and oxocarbenium-ion transition-states (**Scheme 8**), making 2,3-difluoro-sialic acid (**23**) viable as a parent compound to inhibit the action of influenza neuraminidase.

1.6 Aims and objectives

The binding of a ligand and its protein receptor based on intermolecular forces, such as ionic bonds, hydrogen bonds and Van der Waals forces, is fairly well documented but the relative contribution of each to both the overall binding interaction and to the specificity thereof are poorly understood.[7] Fersht *et al.* suggested that hydrophobic interactions contribute as the major driving force to association and that hydrogen-bonding interactions and salt-bridge formation primarily can be held responsible for specificity.[6]

In due consideration of the important role of carbohydrate/protein interactions (such as cell-cell recognition events), the large number of hydroxyl groups on carbohydrates may suggest that hydrogen-bonding interactions would be more important, particularly for monosaccharides that are completely buried in the active site of the protein.[6] In aqueous solution, water competes for hydrogen-bonding sites on both the carbohydrate and the protein making the binding energy a complex result of partially enthalpic differences, due to different hydrogen-bond geometry but largely a consequence of an increase in entropy associated with water release from the active site and the ligand into bulk water.[7]

X-ray crystallographic studies have proven to be a tremendously useful technique to derive information on carbohydrate/protein interactions, but provide little help to evaluate the contribution that individual hydrogen-bonding interactions towards transition-state stabilisation. Conservative modifications of the substrate such as deoxy and fluorodeoxy analogues that differ in their electronic properties and hydrogen-bonding capacity but may still be accepted by the enzyme, have proven to be a useful tool in the studies of individual hydroxyl group contribution to transition-state stabilisation, as has previously been demonstrated by Street *et al.* on glycogen phosphorylase.[8]

The proposed mechanism involving formation of a covalent sialosyl-enzyme intermediate (**Scheme 8**) applied to 2,3-difluoro-sialic acid (**23**) gives an energy profile with two high-energy transition-states and the covalent intermediate as a local energy minimum (**Graph 1**).

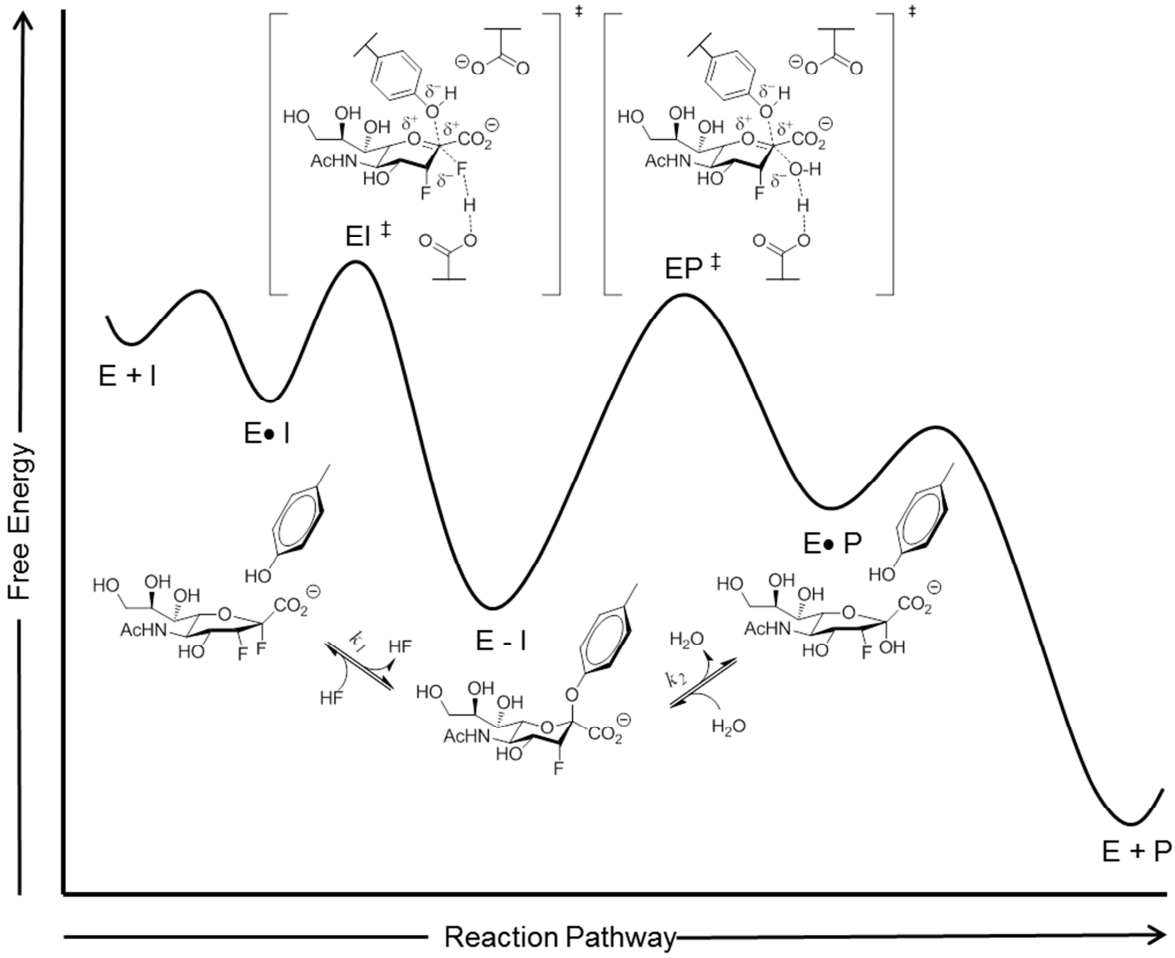

Graph 1 Reaction coordinate diagram representing the reaction pathway of 2,3-difluoro-sialic acid (**23**) and neuraminidase. Enzyme (*E*), inhibitor (*I*), product (*P*), Michaelis complexes (*E•I*) (*E•P*), transition-states ($EI^{‡}$) ($EP^{‡}$) and covalent intermediate (*E-I*).

Although the covalent sialosyl-enzyme intermediate is at a local energy minimum, this is not sufficient for complete inactivation and turnover of the intermediate at a greatly reduced rate is still observed.

The objective of this project is to translate the approach of Street *et al.* to the novel class of mechanism-based inactivators, based on 2,3-difluoro-sialic acid (**23**), in order to gain further information on the active site of influenza neuraminidase during the inactivation mechanism, both on the ground-state Michaelis complex (*E•I*) and at the transition-state($EI^{‡}$).[8]

We propose to achieve this through the synthesis of the novel monodeoxygenated 2,3-difluoro-sialic acid analogues (**24**) - (**27**), which are designed to function as mechanism-based inactivators of influenza neuraminidases.

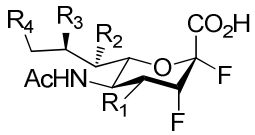

23 R_1, R_2, R_3, R_4 = OH

24 R_1 = H, R_2, R_3, R_4 = OH

25 R_2 = H, R_1, R_3, R_4 = OH

26 R_3 = H, R_1, R_2, R_4 = OH

27 R_4 = H, R_1, R_2, R_3 = OH

The systematic removal of each individual hydroxyl group allows dissection of individual hydroxyl group contribution towards transition-state stabilisation. It is anticipated that the monodeoxygenated 2,3-difluoro-sialic acid derivatives (**24**) - (**27**) will be useful to gain further information on the inactivation mechanism through X-ray protein crystal structures. Furthermore, biochemical evaluation of the kinetic behaviour of the monodeoxygenated 2,3-difluoro-sialic acid inactivators (**24**) - (**27**) towards influenza neuraminidase N9 will also give access to Michaelis-Menten kinetic parameters. We plan to determine key parameters for each monodeoxygenated 2,3-difluoro-sialic acid compound (**24**) to (**27**) such as the inactivation rate constant (k_{inact}) and the dissociation constant for the inactivator (K_i) through time-dependent inactivation of influenza neuraminidase N9 over a range of inactivator concentrations.

Based on these findings future projects are set up to utilise pharmacophores in order to optimise the 2,3-difluoro-sialic acid (**23**) parent compound as a potential therapeutic for the treatment of the influenza virus.

Chapter 2 - Synthesis of 4-deoxy-2,3-difluoro-sialic acid (24)

We began the synthesis of the putative mechanism-based influenza neuraminidase inactivator 4-deoxy-2,3-difluoro-sialic acid (**24**) by first studying known approaches towards the synthesis of 4-deoxy-sialic acid (**28**).

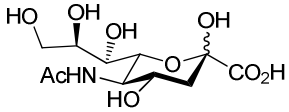

2

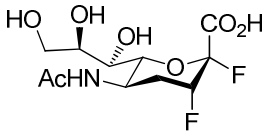

24

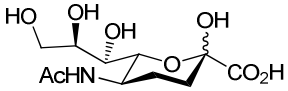

28

The synthesis of 4-deoxy-sialic acid (**28**) has been reported by Hagedorn and Brossmer which was accomplished via dehalogen hydrogenation of a C-4 iodo intermediate (Chapter 8.1.1).[137] However, this method was low yielding and as such was not considered appropriate for translation towards the synthesis of 4-deoxy-2,3-difluoro-sialic acid (**24**).[137] In a similar manner, the synthesis of 4-deoxy-sialic acid (**28**) was also accomplished by Baumberger and Vasella[138] who employed a 12-step sequence, which commenced with D-glucose. In an improved synthesis of 4-deoxy-sialic acid (**28**), performed by Estenne *et al.*[139] sialic acid (**2**) was used in an eight-step sequence. However, it was anticipated that applying either of these reported syntheses to the synthesis of 4-deoxy-2,3-difluoro-sialic acid (**24**) would require numerous synthetic steps with an anticipated low overall yield and, as such, neither approach was pursued any further.

A more encouraging synthesis has been reported by Ooi *et al.*, utilising the *per-O*-acetyl derivative (**29**) to generate the oxazoline (**30**), which following hydrogenation with palladium on charcoal yielded the *per-O*-acetyl-4-deoxy DANA (**31**) (**Scheme 10**).[140]

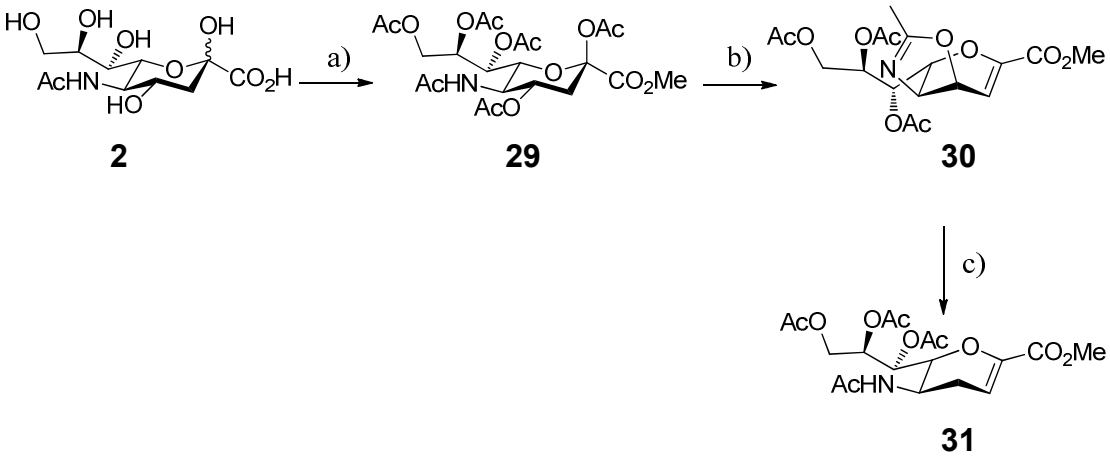

2 **29** **30** **31**

Scheme 10 Literature procedure for the synthesis of the 4-deoxy DANA derivative (**31**). a) (i) TFA, MeOH; (ii) Ac_2O, pyridine; b) TMSOTf, MeCN; (c) H_2/Pd.[140]

We envisaged that the *per-O*-acetyl-4-deoxy DANA derivative (**31**) could be a useful intermediate in the synthesis of 4-deoxy-2,3-difluoro-sialic acid (**24**) as a number of methods for the difluorination of glycals are reported in the literature.[141,142]

2.1 Attempted synthesis of 4-deoxy-2,3-difluoro-sialic acid (24) via the oxazoline (30)

2.1.1 Retrosynthetic analysis

The synthesis of 4-deoxy-2,3-difluoro-sialic acid (**24**) could be performed by difluorination of the 4-deoxy DANA derivative (**31**), based on a number of methods reported for the difluorination of unsaturated sialic acids deploying either a single step difluorination utilising F_2 or XeF_2 or deploying sequential introduction of fluorine at C-3 and then C-2 in two-steps (**Scheme 11**).[141,142]

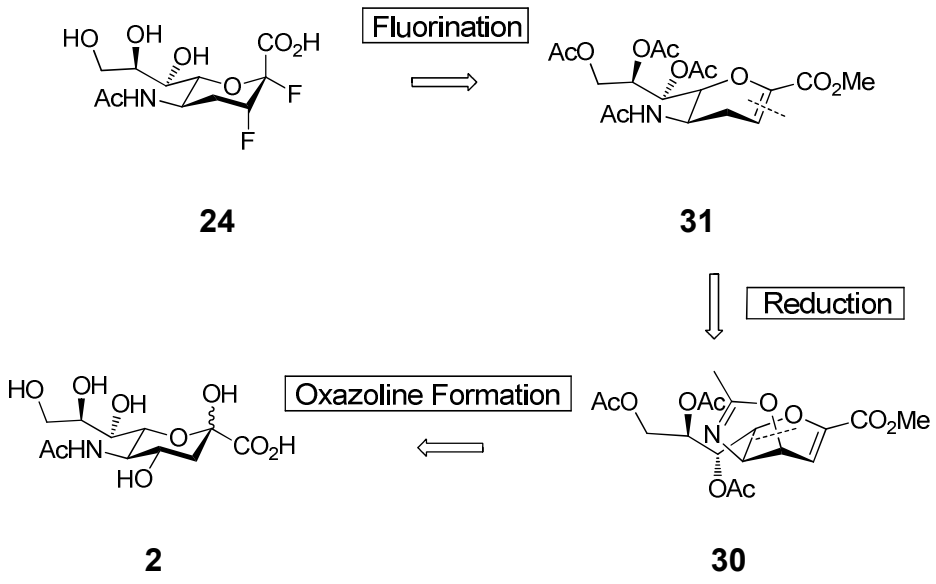

Scheme 11 Retrosynthetic strategy for the synthesis of 4-deoxy-2,3-difluoro-sialic acid (**24**) via the oxazoline (**30**).

However, as seen in the work previously performed by Nakajima *et al.* difluorination utilising F_2 afforded a mixture of isomers which were difficult to purify and gave a low overall yield.[141] As a result, we were prompted to consider a sequential two-step fluorination strategy.

Fluorination could be achieved utilising Selectfluor® (**33**) and previously performed mechanistic studies by Vincent *et al.* have shown that Selectfluor® (**33**) is reacting regioselective with glycals in a *syn* addition two-electron mechanism. In the case of sialic acid specific fluorination at the C-3 position and subsequent hydrolysis as previously shown by Burkart *et al.* then hydrolyses the trietylenediammonium moiety to give hemiketal (**34**) in 80% yield with a ratio of axial to equatorial fluorine of 3:1.[143] (**Scheme 12**).[144]

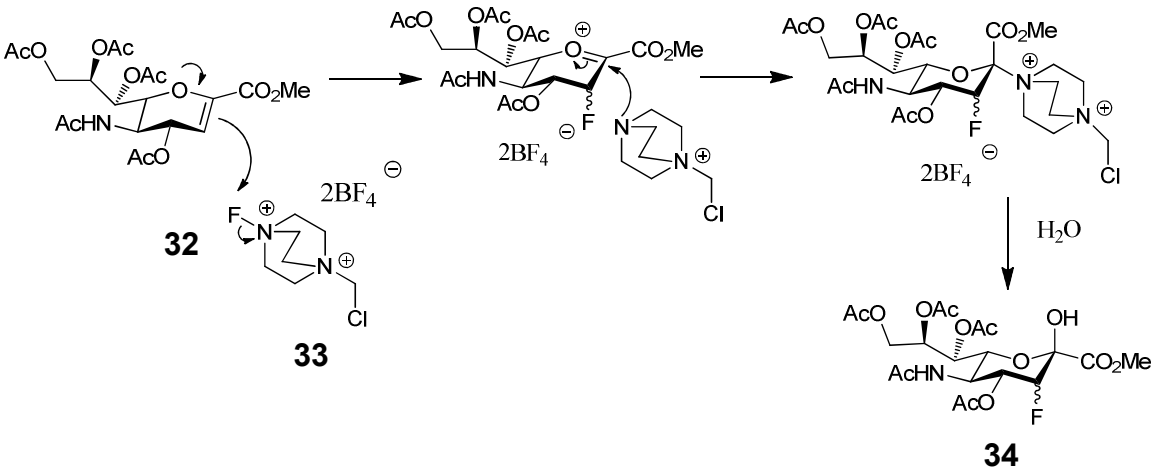

Scheme 12 Mechanism for the fluorination of DANA (**32**) with Selectfluor® (**33**). (DMF/H_2O, 50 ºC, 80%).[144]

In the case of the 4-deoxy DANA derivative (**31**) the resulting axial fluorine hemiketal could then be treated with (diethylamino)sulfur trifluoride (DAST) (**35**) in a nucleophilic fluorination step in accordance with the procedure reported by Watts and Withers to give the desired 4-deoxy-2,3-difluoro-sialic acid (**24**).[87]

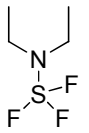

35

It then was intended to form 4-deoxy DANA derivative (**31**) according to the procedure previously accomplished by Ooi *et al.* in a reduction reaction of oxazoline (**30**) using hydrogen and palladium on charcoal (**Scheme 11**).[140] The desired oxazoline (**30**) could be yielded following the procedure which has previously been described by Schreiner *et al.* by treatment of *per*-*O*-acetyl-sialic acid (**29**) with trifluoromethanesulfonate (TMSOTf).[145]

2.1.2 Formation of oxazoline (30)

The formation of oxazoline (**30**) was accomplished according to Schreiner *et al.* starting with the esterification of sialic acid (**2**), using trifluoroacetic acid (TFA) in MeOH at room temperature and subsequent acetylation of the sialic acid methyl ester with acetic anhydride (Ac_2O) in pyridine gave the *per*-*O*-acetyl derivative (**29**) (**Scheme 13**).[145]

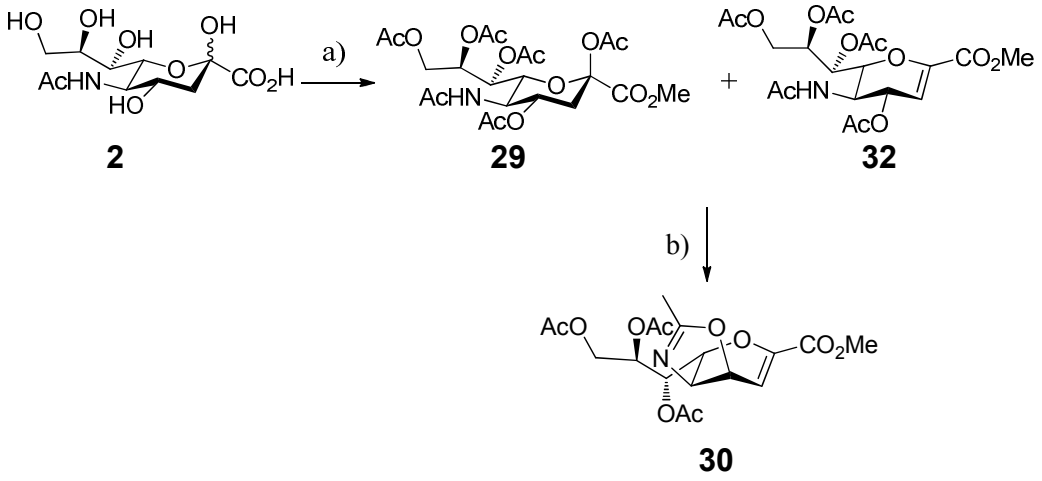

2 **29** **32** **30**

Scheme 13 Synthesis of oxazoline (**30**). a) (i) TFA, MeOH, r.t., O/N; (ii) Ac_2O, pyridine, r.t., 3 days; b) TMSOTf, MeCN, 50 ºC, O/N, 76% (over 3 steps).

Analysis of the crude reaction mixture from this step showed an inseparable mixture of the desired *per*-*O*-acetyl compound (**29**), as well as the *per*-*O*-acetyl DANA compound (**32**) and oxazoline (**30**) in a ratio of 5:1:2.

The proposed mechanism for the formation of oxazoline (**30**) proceeds by activation of the anomeric acetyl group with trifluoromethanesulfonate (TMSOTf), which triggers a *trans*-diaxial elimination, forming the *per*-*O*-acetyl DANA (**32**) (**Scheme 14**). The proposed mechanism for the formation of oxazoline (**30**) commences by activation of the C-4 acetyl group of *per*-*O*-acetyl DANA (**32**) by TMSOTf, which then can be displaced by nucleophilic attack of the oxygen present at the *N*-acetyl group in position C-5 to give oxazoline (**30**).

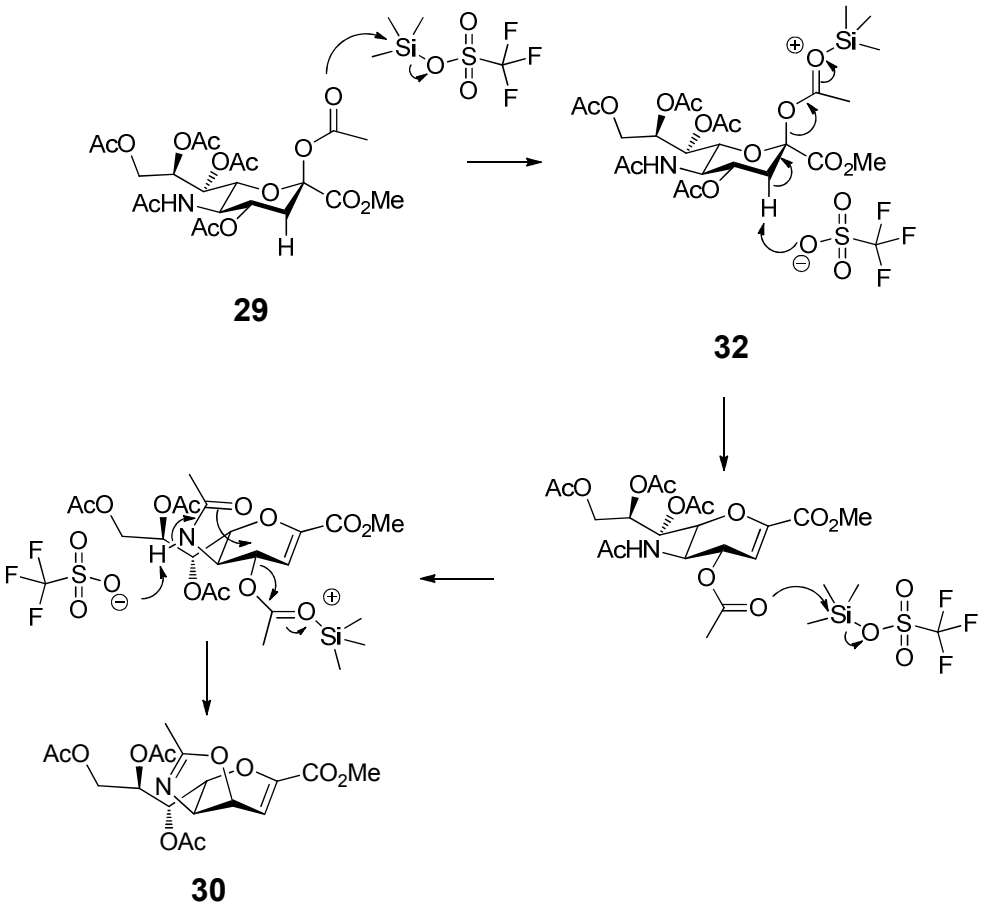

Scheme 14 Mechanism for the formation of oxazoline (**30**). TMSOTf, MeCN, 50 ºC, O/N.

The *per-O*-acetyl DANA (**32**) intermediate has already been identified to be part of the mixture from the acetylation step, hence it was proposed that the crude mixture could be used for conversion to the desired product (**30**).
Therefore, following the acetylation, the crude mixture was purified by filtration through a silica plug and treated with TMSOTf and acetonitrile (MeCN) to give the oxazoline (**30**) in 76% yield starting from sialic acid (**2**).

2.1.3 Attempted synthesis of *per-O*-acetyl-4-deoxy DANA (31)

The formation of the 4-deoxy DANA derivative (**31**) was then attempted according to the literature procedure by Ooi *et al.* utilising 10% Pd/C in 1,4-dioxane for 4 hours at room temperature.[140] However, reaction of oxazoline (**30**) under these conditions only gave unreacted starting material (**Table 1, entry 1)**.

Table 1 Different conditions used for the synthesis of 4-deoxy DANA derivative (**31**). **Condition A**: H_2, 10% Pd/C (0.2 eq.), 1,4-dioxane; **Condition B**: H_2, 5% Pd/C (0.2 eq.), 1,4-dioxane; **Condition C**: H_2, 10% Pd/C (0.2 eq.), THF; **Condition D**: H_2, 10% Pd/C (0.2 eq.), MeOH.

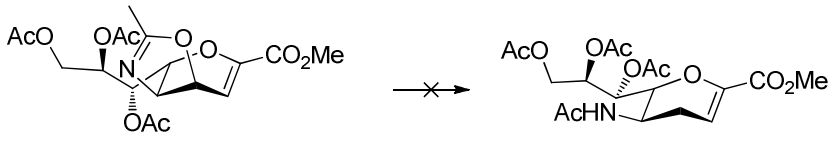

30 **31**

Entry	Condition	Time	T [°C]	Product	Yield (%), Ratio
1	A	4 h	r.t.	**30**	67
2	A	14 h	r.t.	**30**	n.d.
3	A	19 h	r.t.	**30 + 36**	3:1
4	B	17 h	r.t.	**30 + 36**	5:1
5	C	15 h	4	**30**	n.d.
6	C	15 h	r.t.	**36**	n.d.
7	D	5 h	r.t.	**36**	n.d.
8	D	3 h	4	**30 + 36**	9:1

n.d. = not determined

Subsequently increasing the reaction time to 14 hours in 1,4-dioxane at room temperature also failed to yield the desired product and again only starting material (**30**) was recovered (**Table 1, entry 2**). Finally, extending the reaction time to 19 hours (**Table 1, entry 3**) resulted in mixture of starting material (**30**) and over-reduced compound (**36**) in a ratio of 3:1 being formed.

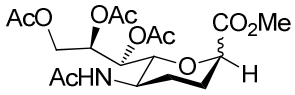

36

The formation of the over-reduced derivative (**36**) then prompted us to investigate the use of alternative catalysts as well as reducing the loading of palladium on charcoal. Unfortunately, reduction with 5% Pd/C for 17 hours (**Table 1, entry 4**) was also found to give a mixture of starting material (**30**) and fully reduced compound (**36**) in a ratio of 5:1. Furthermore, changing the solvent to THF (**Table 1, entry 5 and 6**) or methanol (**Table 1, entry 7 and 8**) and employing a variety of reaction temperatures and reaction times also failed to improve the reaction, with only over reduced derivative (**36**) or starting material (**30**) ever being observed.

Given the problem of over-reduction of oxazoline (**30**), it was considered that by performing the introduction of fluorine at position C-3 prior to the reduction step at position C-4 these difficulties could be overcome.

2.2 Attempted synthesis of 4-deoxy-2,3-difluoro-sialic acid (24) via the 3-fluoro-oxazoline (37)

We then set out to synthesise was the novel 3-fluoro-oxazoline derivative (**37**). This molecule, to our knowledge, has never been synthesised before and we envisaged that it could be a useful intermediate towards the synthesis of 4-deoxy-2,3-difluoro-sialic acid (**24**).

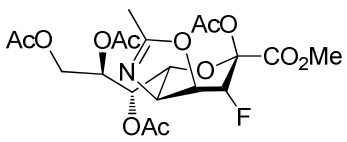

37

2.2.1 Retrosynthetic analysis

We considered that the 4-deoxy-2,3-difluoro-sialic acid (**24**) could be produced by fluorination of the 4-deoxy-3-fluoro-sialic acid hemiketal (**38**) employing the method previously described by Watts and Withers utilising (diethylamino)sulfur trifluoride (DAST) (**Scheme 15**).[87]

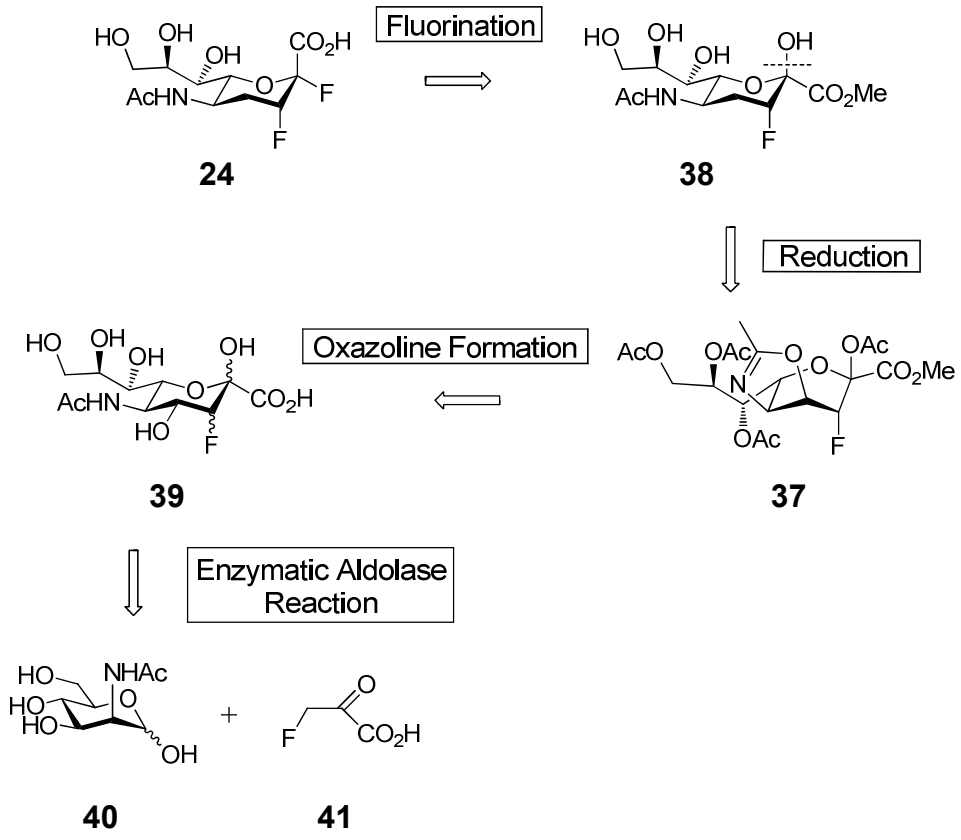

Scheme 15 Retrosynthetic strategy for the synthesis of 4-deoxy-2,3-difluoro-sialic acid (**24**) via the 3-fluoro-oxazoline (**37**).

We anticipated that the synthesis of the 4-deoxy-3-fluoro-sialic acid hemiketal (**38**) could be achieved through reduction of 3-fluoro-oxazoline derivative (**37**) using hydrogen and palladium on charcoal, based on the methods previously deployed (Chapter 2.1.3) but avoiding over-reduction. The 3-fluoro-oxazoline derivative (**37**) could be yielded following the procedure described by Schreiner *et al.* utilising 3-fluoro-sialic acid (**39**).[145]

The formation of 3-fluorosialic acid (**39**) has previously been demonstrated by Watts and Withers performing an enzymatic aldolase reaction of 2-*N*-acetyl-*D*-mannosamine (**40**) and β-fluoropyruvic acid (**41**).[87] It was intended to obtain the desired axial 3-fluoro-sialic acid (**39**) exclusively in highest possible yield by the enzymatic aldolase approach of Watts and Withers.[87]

2.2.2 Synthesis of 3-fluoro-sialic acid (39)

The first step in the synthesis of 4-deoxy-2,3-difluoro-sialic acid (**24**) involved the formation of 3-fluoro-sialic acid (**39**), which has previously been described by Watts and Withers using an enzymatic aldolase reaction (**Scheme 16**).[87] According to this procedure, 2-*N*-acetyl-*D*-mannosamine (**40**) and β-fluoropyruvic acid (**41**) were subjected to Neu5Ac aldolase in aqueous solution at room temperature for five days.

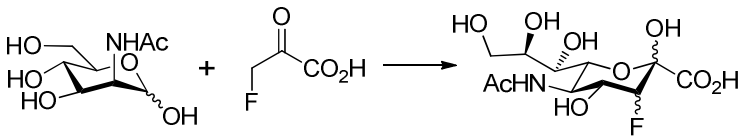

40 **41** **39**

Scheme 16 Formation of 3-fluoro-sialic acid (**39**). Neu5Ac aldolase, H_2O, r.t., 5 days.

The Neu5Ac aldolase catalysed aldol reaction can be performed at a pH range of 6 to 9 and at an optimum temperature of 37 ºC. Neu5Ac aldolase is tolerant towards slight modifications to the pyruvate donor such as the presence of a fluorine atom at the β carbon, although a large reduction in the rate of enzymatic turnover is observed.

During the synthesis of 3-fluoro-sialic acid (**39**) the reaction was monitored by the disappearing ^{19}F NMR signal corresponding to β-fluoropyruvic acid (**41**) at δ -229.1 ppm and the appearing signals corresponding to formation of β-3-axial-fluoro-sialic acid (**42**) at δ -208.1 ppm and the β-3-equatorial-fluoro-sialic acid (**43**) at -199.2 ppm (**Figure 13**).

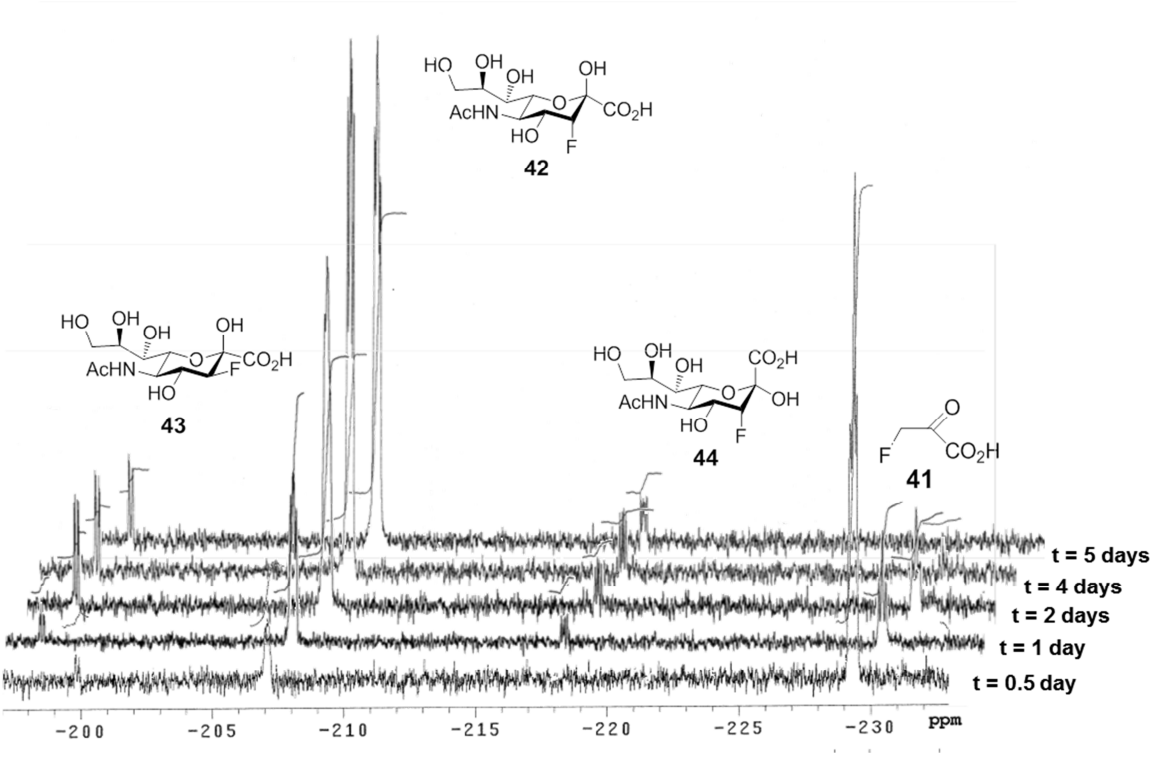

Figure 13 ^{19}F NMR of the aldolase reaction, showing the consumption of β-fluoropyruvic acid (**41**) and the formation of three different 3-fluoro-sialic acid isomers (**42**), (**43**) and (**44**).

At δ -217.7 ppm the formation of the epimer of the desired product (**42**) the α-3-axial-fluoro-sialic acid (**44**) could be observed. The reaction mixture was purified by ion-exchange column chromatography (formate form) from unreacted 2-*N*-acetyl-*D*-mannosamine (**40**) to afford the 3-fluoro-sialic acid isomers (**42**), (**43**) and (**44**).

The aldolase-catalysed reaction of 2-*N*-acetyl-*D*-mannosamine (**40**) and β-fluoropyruvic acid (**41**) is known to result in mixtures of isomers as non-natural substrates are used for the enzymatic conversion. A possible explanation might be given in consideration of the enzyme-catalysed mechanism proposed by Lin *et al.* (**Scheme 17**).[146] This mechanism proceeds via formation of an enamine between a lysine (Lys) residue in the active site of the aldolase and β-fluoropyruvic acid (**41**).[146-148] At this stage cis/trans isomerisation of the enamine adduct can occur with its ratio directing the formation of axial or equatorial fluorine at position C-3.

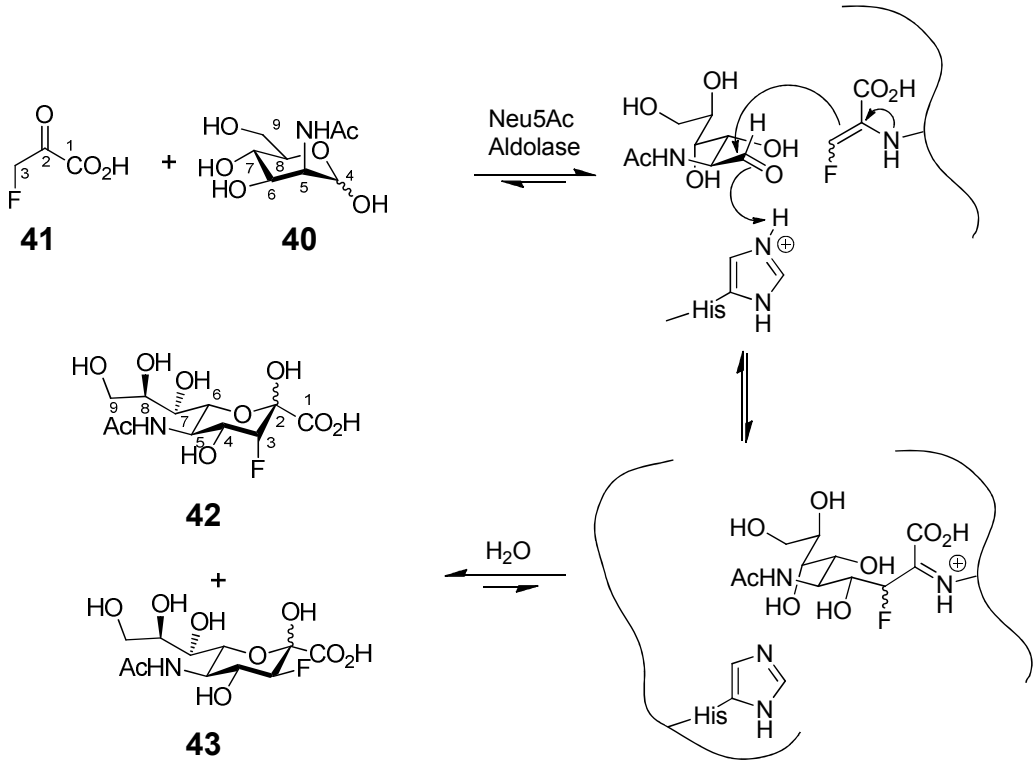

Scheme 17 Mechanism for the Neu5Ac aldolase-catalysed aldol reaction between 2-*N*-acetyl-*D*-mannosamine (**40**) and β-fluoropyruvic acid (**41**). The numbering of the carbon backbone is indicated corresponding to the final 3-fluoro-sialic acid isomers (**42**) and (**43**).[147]

Subsequently the aldehyde group of the acyclic form of 2-*N*-acetyl-*D*-mannosamine (**40**) is activated by a histidine (His) residue in the active site of the aldolase. A new carbon-carbon bond between the activated aldehyde and the preformed β-fluoropyruvic acid enamine is then formed.

The resulting iminium cation is hydrolysed to release the catalytic lysine residue of the aldolase and also generates the carbohydrate moiety in an acyclic form. The hydrolysed acyclic aldehyde is then cyclised to form the 3-fluoro-sialic acid isomers (**42**) and (**43**).

The ratio of the fluorine atom at C-3 in axial (**42**) or equatorial orientation (**43**) has been reported to be dependent on the stoichiometric ratio between β-fluoropyruvic acid (**41**) and 2-*N*-acetyl-*D*-mannosamine (**40**).[149]

The reason for this correlation is still not fully understood, however an experimental study by Beliczey *et al.* together with experimental data has determined that a ratio of 1:2 of (**41**) to (**40**) results in the isomer with an axial fluorine atom at C-3 (**42**) being the predominant isomer in 90%.[149]

As well as accepting alterations on the pyruvic acid moiety, aldolase also accepts a number of modifications on the hexose moiety at C-7, C-8 and C-9 (numbered according to the carbon backbone of the final product (**Scheme 17**). We considered that this might be of interest for the synthesis of some subsequent monodeoxygenated 2,3-difluorosialic acid derivatives (**25**), (**26**) and (**27**).

2.2.3 Attempted synthesis of 3-fluoro-oxazoline (37)

Following the enzyme-catalysed aldolase reaction, the crude residue was esterified using trifluoroacetic acid (TFA) in methanol to give 3-fluoro-sialic acid methyl ester (**44**) (**Scheme 18**).

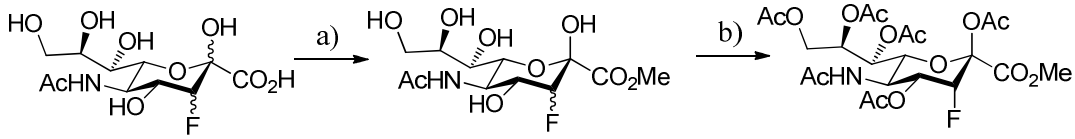

39 **44** **45**

Scheme 18 Synthesis of *per-O*-acetyl-3-fluoro-sialic acid (**45**). a) TFA, MeOH, r.t., O/N; b) Ac_2O, pyridine, DMAP, r.t., 17 h, 72% (starting from β-fluoropyruvic acid (**41**)).

Due to its highly polar nature, the 3-fluoro-sialic acid methyl ester (**44**) was not purified and isolated at this stage. However, subsequent acetylation with acetic anhydride in pyridine gave the *per-O*-acetyl-3-fluoro-sialic acid (**45**) after silica column chromatography in 72% yield.

Following the procedure of Schreiner *et al.* the formation of 3-fluoro-oxazoline (**37**) was attempted by treatment of *per-O*-acetyl-3-fluorosialic acid (**45**) with trimethylsilyl trifluoromethanesulfonate (TMSOTf) in acetonitrile (MeCN) at 50 °C overnight (**Scheme 19**).[145]

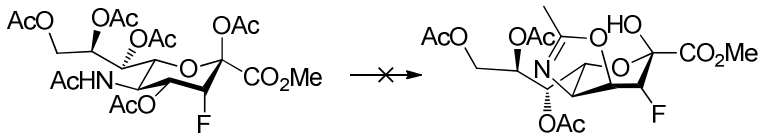

45 **37**

Scheme 19 Attempted synthesis of 3-fluoro-oxazoline (**37**). TMSOTf, MeCN, 50 ºC, O/N.

However, the reaction failed under the conditions applied and only starting material was isolated. In consideration of the mechanism to form the oxazoline, which has previously been shown (**Scheme 14**), the formation of a DANA-like intermediate seems to be crucial for oxazoline formation as it results in allylic activation of the acetyl group at position C-4. In addition, the introduction of a fluorine atom at position C-3 with its electron-withdrawing effect prevents activation and subsequent nucleophilic substitution of the acetyl group at position C-4. Hence, the introduction of a fluorine atom at position C-3, as intended prevents the formation of a DANA-like intermediate but undesirably also averts oxazoline formation.

As a result, the synthetic strategy was re-assessed and it was decided to investigate an alternative class of reactions for the formation of 4-deoxy-2,3-difluoro-sialic acid (**24**) with the Barton-McCombie deoxygenation being amongst the most common methods for the removal of hydroxyl groups in synthetic chemistry.[150,151]

2.3 Synthesis of 4-deoxy-2,3-difluoro-sialic acid (24) via the C-4 Barton-McCombie deoxygenation

It was anticipated that, the previously synthesised 3-fluoro-sialic acid methyl ester (**44**) via a selective protection protocol to form a C-4 xanthate (**46**) and subsequent C-4 Barton-McCombie deoxygenation, could provide a feasible route to form 4-deoxy-2,3-difluoro-sialic acid (**24**).

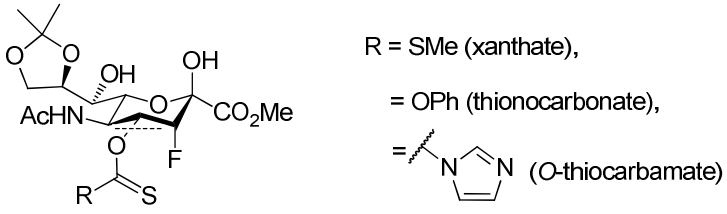

46

2.3.1 Retrosynthetic analysis

The formation of 4-deoxy-2,3-difluoro-sialic acid (**24**) could proceed via a fluorination step with (diethylamino)sulfur trifluoride (DAST) following the procedure reported by Watts and Withers but utilising the 4-deoxy-3-fluoro-sialic acid hemiketal (**38**) (**Scheme 20**).[87]

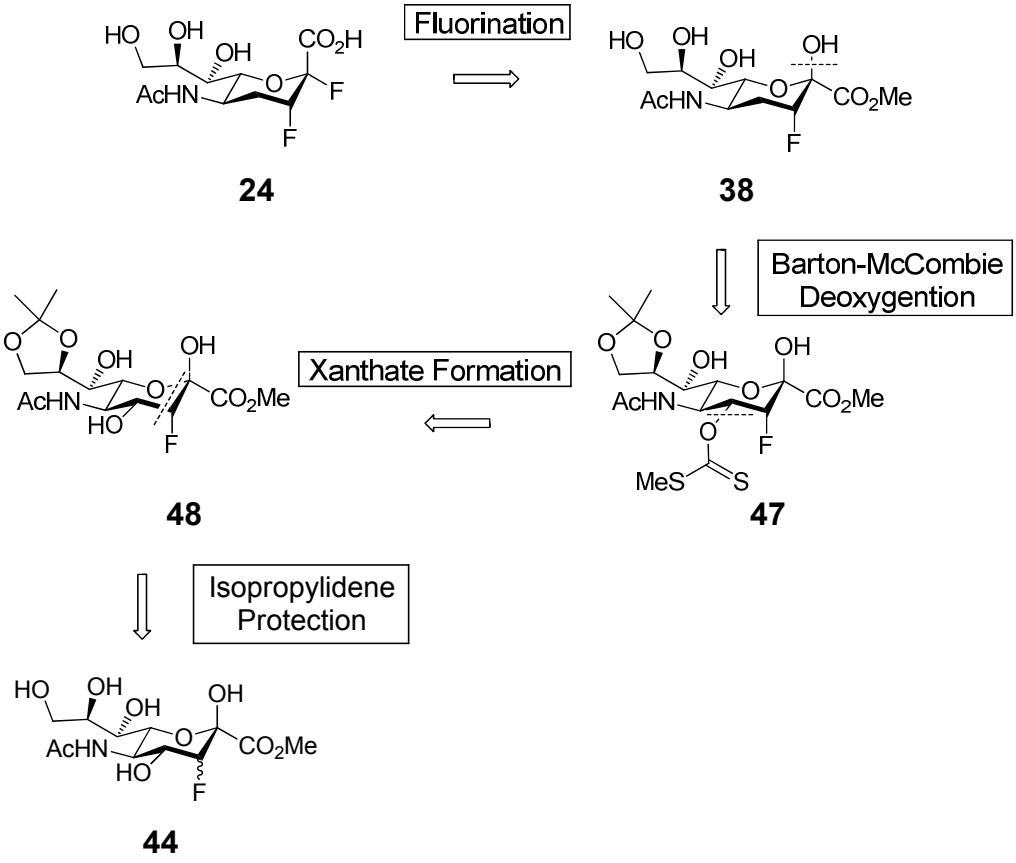

Scheme 20 Retrosynthetic strategy for the synthesis of 4-deoxy-2,3-difluoro-sialic acid (**24**) via the C-4 xanthate (**47**).

As such, formation of 4-deoxy-3-fluoro-sialic acid hemiketal (**38**) could be accomplished by Barton-McCombie deoxygenation with Bu_3SnH on a C-4 xanthate (**47**).[150,152] It was predicted that formation of the C-4 xanthate (**47**) could be attempted on 3-fluoro-8,9-*O*-isopropylidene-sialic acid methyl ester (**48**) without further protection steps.

This strategy is based upon the assumption that following activation, the most nucleophilic hydroxyl group in 3-fluoro-8,9-*O*-isopropylidene-sialic acid methyl ester (**48**) would be at C-4 position.

The 3-fluoro-8,9-*O*-isopropylidene-sialic acid methyl ester (**48**) could be yielded according to the procedure of Ogura *et al.* utilising TFA in methanol and 2,2'-dimethoxypropane on 3-fluoro-sialic acid (**39**).[153] The formation of 3-fluoro-sialic acid (**39**) could be performed employing an enzymatic aldolase reaction of 2-*N*-acetyl-*D*-mannosamine (**40**) and β-fluoropyruvic acid (**41**) as previously accomplished (Chapter 2.2.2).[87]

2.3.2 Formation of 4-deoxy-3-fluoro-8,9-*O*-isopropylidene-sialic acid methyl ester (50)

The 3-fluorosialic acid methyl ester (**44**) was treated with 2,2'-dimethoxypropane and catalytic amounts of *p*-toluenesulfonic acid (*p*-TSA) in acetone according to the procedure of Ogura *et al.* to give the 3-fluoro-8,9-*O*-isopropylidene-sialic acid methyl ester (**48**) in 71% yield from β-fluoropyruvic acid (**41**) (**Scheme 21**).[153]

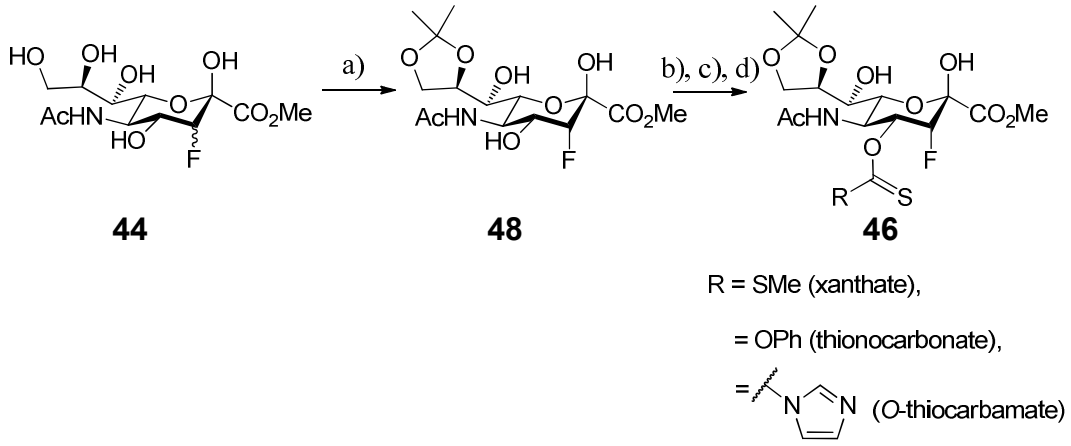

44 **48** **46**

Scheme 21 Synthesis of the C-4 xanthate (**46**). a) 2,2'-Dimethoxypropane, *p*-TSA, acetone, r.t., O/N, 71% (starting from β-fluoropyruvic acid (**41**)); b) CS_2, CH_3I; c) Phenyl chlorothionoformate; d) 1,1'-Thiocarbonyldiimidazole.

Although acceptable, it was considered that the yield of 71% could potentially be improved upon. As such, an alternative method to introduce the isopropylidene protecting group utilising 2-methoxypropene was attempted. However, this reaction failed to improve the yield of the desired product (**48**) and so was not investigated further.

The Barton-McCombie protocol consists of first transforming an alcohol into a xanthate, thionocarbonate or *O*-thiocarbamate followed by treatment with tributyltin hydride under radical conditions to yield the deoxygenated product. The driving force for the Barton-McCombie deoxygenation is the formation of the energetically favoured sulfur-tin bond. A possible mechanism for the Barton-McCombie deoxygenation involves the steps of initiation (**Scheme 22a**) with azobisisobutyronitrile (AIBN) as a radical carrier, which then is attacked (**Scheme 22b**) by sulfur of xanthates, thionocarbonates or *O*-thiocarbamates.

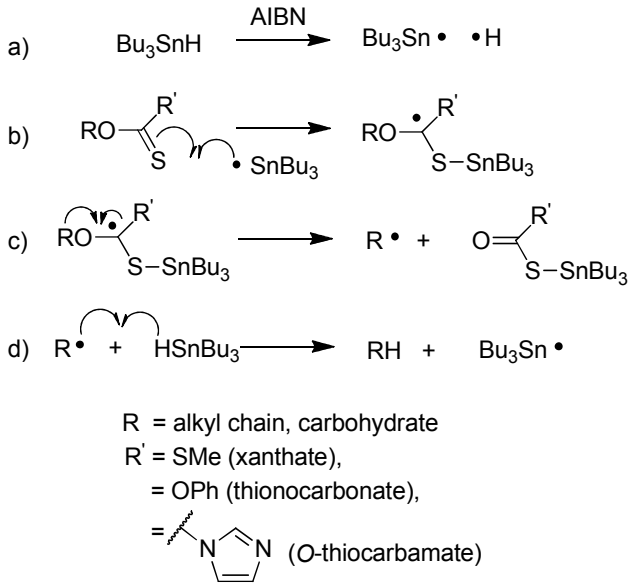

Scheme 22 A mechanism for the Barton-McCombie deoxygention.[151]

Subsequent β – cleavage (**Scheme 22c**) and finally hydrogen radical transfer from tributyltin hydride (**Scheme 22d**) gives the deoxygenated product and the radical carrier tributyl tin.

The commonly used radical initiator azobisisobutyronitrile (AIBN) is no longer commercially accessible, due to its explosive property, but there are alternatives such as azobiscyanocyclohexane or the peroxides 2,2-bis(*tert*-butylperoxy)-butane and (2,5-bis(*tert*-butylperoxy)-2,5-dimethylhexane), also known as Luperox® 101, which are available.

According to the procedure of Barton *et al.* methyl xanthates can be introduced under basic conditions through the addition of carbon disulfide and iodomethane.[154] For the synthesis of the C-4 xanthate (**46**), the risk of elimination of methyl xanthates under basic conditions and the lack of selectivity to introduce methyl xanthates at position C-4 with other hydroxyl groups present prompted us to consider thionocarbonates and *O*-thiocarbamates.

As alternatives to methyl xanthates, thionocarbonates and *O*-thiocarbamates can be introduced under essentially neutral conditions from *O*-phenyl chlorothionoformate and 1,1'-thiocarbonyldiimidazole respectively. As well, thionocarbonates and *O*-thiocarbamates can react at lower temperatures for the radical deoxygenation and have been used successfully to deoxygenate sialic acid derivatives.[155]

As such, 3-fluoro-8,9-*O*-isopropylidene-sialic acid methyl ester (**48**) was treated with phenyl chlorothionoformate in pyridine and dichloromethane to give 3-fluoro-8,9-*O*-isopropylidene-4-*O*-(phenoxy)thiocarbonyl-sialic acid methyl ester (**49**) in 76% yield (**Scheme 23**).

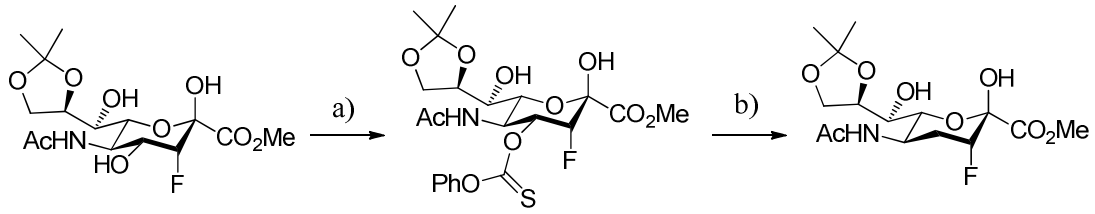

Scheme 23 Synthesis of 4-deoxy-3-fluoro-8,9-*O*-isopropylidene-sialic acid methyl ester (**50**). a) Phenyl chlorothionoformate, CH_2Cl_2/pyridine, - 40 ºC → r.t., 4 h, 76% (**49**); b) 2,2-Bis(*tert*-butylperoxy)-butane, Bu_3SnH, 1,4-dioxane, 100 ºC, 4 h, 81% (**50**).

In order to probe the optimal conditions for the Barton-McCombie deoxygenation, the thionocarbonate (**49**) was used as the model substrate, while radical initiator, radical carriers, solvents and temperatures were varied in an effort to generate 4-deoxy-3-fluoro-8,9-*O*-isopropylidene-sialic acid methyl ester (**50**) in the highest possible yield.

In the first set of reactions (**Table 2, entry 1 - 3**) according to Lopez *et al.* bis(tributyltin) oxide was used to generate tributyltin hydride in situ (**Scheme 24**).[151]

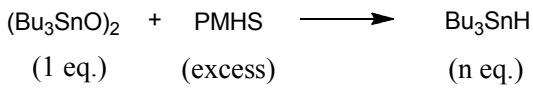

Scheme 24 In situ formation of Bu_3SnH. Toluene, 80 °C, 4 h, without n-BuOH n = 1, with n-BuOH n = 2.

This has the advantage of low costs and longer storage stability over tributyltin hydride. In this procedure poly(methylhydrosiloxane) (PMHS) and *n*-butanol in toluene are used in order to generate two equivalents of tributyltin hydride.
The 4-*O*-(phenoxy)thiocarbonyl derivative (**49**) was subjected to bis(tributyltin) oxide, n-BuOH and azobiscyanocyclohexane in toluene at 80 °C overnight as previously described by Lopez *et al.* (**Table 2, entry 1**).[151] However, under these conditions only starting material (**49**) was recovered largely owing to the low solubility of the compound. To overcome the problem of solubility the reaction was repeated using DMF as a co-solvent (**Table 2, entry 2**), but no reaction was observed. In an attempt to generate desired product (**50**), the solution of 3-fluoro-8,9-*O*-isopropylidene-4-*O*-(phenoxy)thiocarbonyl-sialic acid methyl ester (**49**) was degassed and molecular sieves was added (**Table 2, entry 3**). Nevertheless, decomposition of the starting material (**49**) could be observed through formation of a highly polar side product. As a consequence, a different strategy not involving toxic tributyltin derivatives was pursued. Tributyltin hydride is a versatile reagent for organic synthesis, however the undesirable toxicity[140] stimulated the development of alternatives for tributyltin hydride such as silanes,[156] dialkyl phosphate,[151] hydrophosphorous acid together with its salts[146] and recent developments also involve tetrabutylammonium peroxydisulfate and formate ion.[157]

Table 2 Overview of the different conditions used for the synthesis of 4-deoxy-3-fluoro-8,9-*O*-isopropylidene-sialic acid methyl ester (**50**). **Condition A**: $(Bu_3Sn)_2O$ (0.037 eq.), PMHS (5 eq.), *n*-BuOH (5.5 eq.), azobiscyanocyclohexane (0.15 eq.), toluene; **Condition B**: $(Bu_3Sn)_2O$ (0.037 eq.), PMHS (5 eq.), *n*-BuOH (5.5 eq.), azobiscyanocyclohexane (0.15 eq.), toluene/DMF; **Condition C**: $(Bu_3Sn)_2O$ (0.037 eq.), PMHS (5 eq.), *n*-BuOH (5.5 eq.), azobiscyanocyclohexane (0.15 eq.), toluene/DMF, solution was degassed and molecular sieves added; **Condition D**: $(Bu_4N)_2S_2O_8$ (3 eq.), $NaHCO_3$ (6 eq.), DMF; **Condition E**: $(Bu_4N)_2S_2O_8$ (3 eq.), $NaHCO_3$ (6 eq.), DMF, solution was degassed and molecular sieves added; **Condition F**: Bu_3SnH (2 eq.), azobiscyanocyclohexane (0.3 eq.), toluene; **Condition G**: Bu_3SnH (2 eq.), azobiscyanocyclohexane (0.3 eq.), toluene, the solution was heated under reflux with Dean Stark apparatus for 2 hours prior to radical reaction; **Condition H**: Bu_3SnH (3.7 eq.), 50% 2,2-bis(*tert*-butylperoxy)-butane solution (0.45 eq.), 1,4-dioxane.

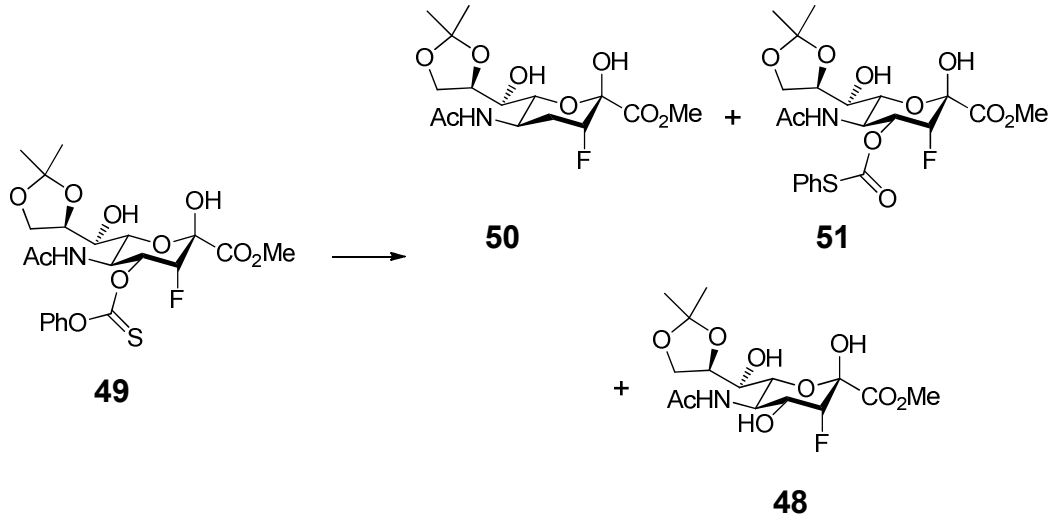

Entry	Condition	Time	T [°C]	Product	Yield (%)[a]
1	A	O/N	80	**49**	n.d.
2	B	O/N	80	**49**	n.d.
3	C	3.5 h	90	dec.	n.d.
4	D	2.5 h	60	dec.	n.d.
5	E	1 d	60	**50**	17
6	E	5 h	70	**50**	24
7	F	23 h	80	dec.	n.d.
8	G	1 d	120	**50**	24
9	H	4 h	100	**50**	81

[a] Isolated yields after silica chromatography, dec. = decomposition, n.d. = not determined.

It has been reported by Park *et al.* (**Table 2, entry 4 - 6**) that tetrabutylammonium peroxydisulfate and sodium formate can be used in a facile Barton-McCombie deoxygenation.[157] A reported mechanism utilising tetrabutylammonium peroxydisulfate and sodium formate suggests that a carbon dioxide radical anion ($CO_2^{\bullet -}$) is initially formed (**Scheme 25a**).[157] Subsequent sulfur attack on the carbon dioxide radical anion (**Scheme 25b**), β – cleavage (**Scheme 25c**), and hydrogen radical transfer from DMF or HCO_2^- (**Scheme 25d**) gives the deoxygenated product.[157]

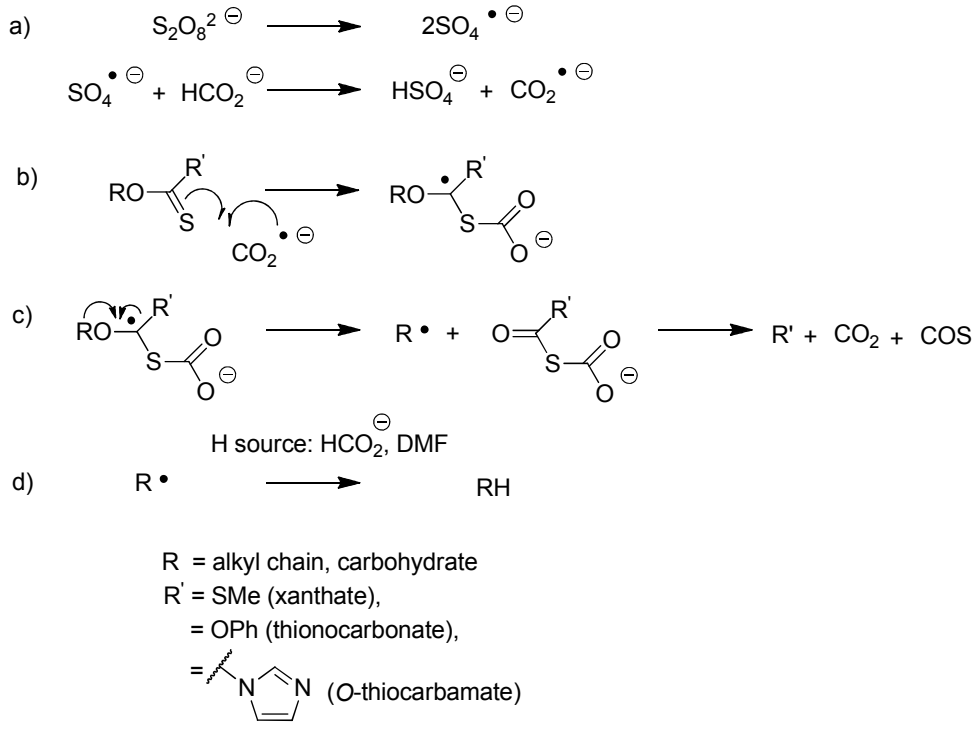

Scheme 25 Reported mechanism for the deoxygenation of alcohols with $(Bu_4N)_2S_2O_8$ and HCO_2Na.[157]

The 4-*O*-(phenoxy)thiocarbonyl derivative (**49**) was subjected to tetrabutylammonium peroxydisulfate and sodium formate in DMF at 60 °C for two and a half hours as previously described by Park *et al.* (**Table 2, entry 4**).[157] An aqueous work up in order to remove the polar reagents was then performed. However, an undesired side reaction gave a highly polar product that under these conditions could not be isolated.

To overcome the formation of side products, the solution was degassed and molecular sieves were added. After silica column chromatography (EtOAc:MeOH, 85:15) the desired product (**50**) was obtained in 17% yield (**Table 2, entry 5**).[157] In addition to desired product (**50**), starting material (**49**) as well as the hydrolysed compound (**48**) could be isolated and polar decomposed material in the aqueous phase could be observed.[158,159] Several attempts to improve the yield under the same conditions could only be optimised to give a yield of 24% (**Table 2, entry 6**).

In an attempt to improve the yield for the deoxygenation reaction, the 4-*O*-(phenoxy)thiocarbonyl derivative (**49**) was subjected to the general Barton-McCombie protocol utilising tributyltin hydride in toluene under reflux conditions (**Table 2, entry 7 - 9**). However, (**Table 2, entry 7**) only formation of a highly polar product could be seen. Hence, in order to eliminate side reactions correlating with water, it was concluded to perform an azeotropic Dean-Stark distillation prior to the Barton-McCombie reaction, which gave desired product (**50**) in 24% yield (**Table 2, entry 8**). The major side product under these conditions could be identified as the sulphur-oxygen exchanged carbonate (**51**). This rearrangement reaction of thionocarbonates under Barton-McCombie conditions to give *O*-thiocarbonyl (**51**) has previously been described by Powers and Tarbell.[160] Hence, in an effort to optimise the yield, shorter reaction times were chosen and moreover, to resolve solubility issues the solvent was changed from toluene to 1,4-dioxane.

The 3-fluoro-8,9-*O*-isopropylidene-4-*O*-(phenoxy)thiocarbonyl-sialic acid methyl ester (**49**) was next subjected to radical Barton-McCombie conditions using 2,2-bis(*tert*-butylperoxy)-butane as a radical initiator and the radical carrier tributyltin hydride under reflux conditions in 1,4-dioxane to give the 4-deoxy-3-fluoro-8,9-*O*-isopropylidene-sialic acid methyl ester (**50**) in 81% yield (**Table 2, entry 9**).[150]

2.3.3 Synthesis of 4-deoxy-3-fluoro hemiketal (53)

We next set out to perform a selective deacetylation at the anomeric position of the 4-deoxy-3-fluoro-8,9-*O*-isopropylidene-sialic acid methyl ester (**50**). As a consequence, the 4-deoxy-3-fluoro-8,9-*O*-isopropylidene-sialic acid methyl ester (**50**) was subjected to 80% acetic acid according to the procedure of Anazawa *et al.* to remove the isopropylidene protection group. Subsequent global acetylation with acetic anhydride in pyridine gave the *per*-*O*-acetyl-4-deoxy-3-fluoro-sialic acid methyl ester (**52**) in 76% yield (**Scheme 26**).[161]

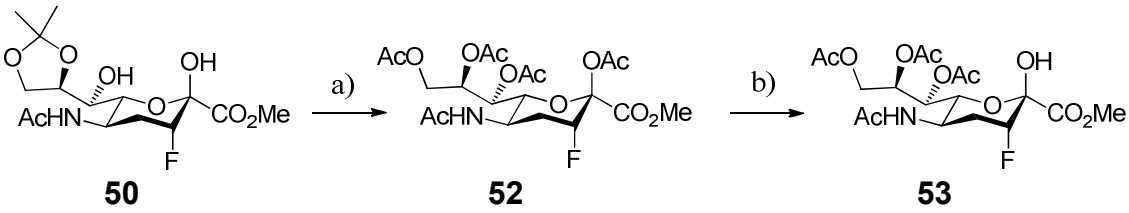

Scheme 26 Synthesis of 7,8,9-tri-*O*-acetyl-4-deoxy-3-fluoro-sialic acid methyl ester (**53**). a) (i) 80% AcOH/H_2O, 60 °C, 2 h; (ii) Ac_2O, DMAP, pyridine, r.t., O/N, 76% (over 2 steps) (**52**); b) Hydrazine acetate, CH_2Cl_2/MeOH, 4 °C, O/N, 51% (**53**).

The *per*-*O*-acetyl-4-deoxy-3-fluoro-sialic acid methyl ester (**52**) was then selectively deprotected at position C-2 utilizing hydrazine acetate in dichloromethane and MeOH, affording the hemiketal (**53**) in 51% yield. The higher reactivity of the anomeric acetal relative to the other hydroxyl groups in conjunction with hydrazine acetate, as a weak nucleophile, makes the deacetylation reaction selective for the anomeric position.[162] However, hydrazine acetate is highly hygroscopic and additional water molecules can act as alternative nucleophiles to hydrazine in the reaction, leading to further deacetylation. Despite numerous attempts, like re-crystallisation or pre-drying of hydrazine acetate, the moderate yield could not be improved.

2.3.4 Formation of 4-deoxy-2,3-difluoro-sialic acid (24)con

The fluorination of position C-2 of sialic acid hemiketal (**54**) utilising DAST to give 2,3-difluoro-sialic acid (**55**) has previously been performed by Watts and Withers (**Scheme 27**).[87]

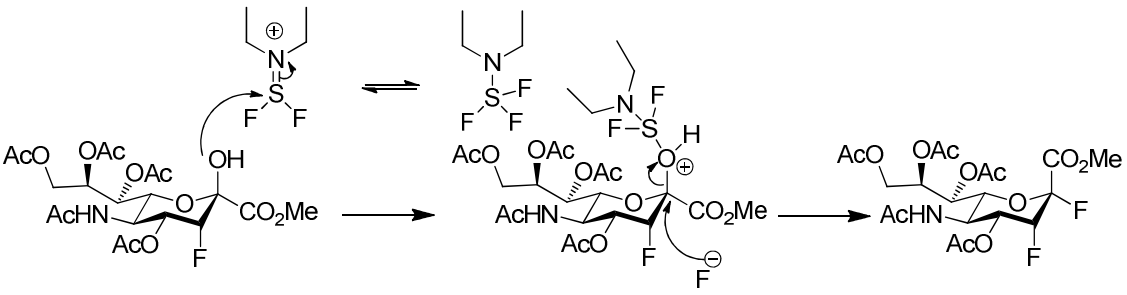

54 **55**

Scheme 27 Mechanism for the fluorination of hemiketal (**54**) using DAST. CH_2Cl_2 - 30 ºC, 30 min., 45%.[87]

The fluorination of hemiketal (**54**) was reported to proceed through a nucleophilic attack on the sulfonium ion by the anomeric hydroxyl of the hemiketal (**54**). Subsequently, this activation increases the leaving group ability of the anomeric hydroxyl group, which then undergoes S_N2 displacement by a fluoride with inversion of configuration at C-2 and affords the fluorinated product (**55**).[163]

Following the procedure of Watts and Withers the hemiketal (**53**) was then fluorinated by treatment with DAST in dichloromethane at - 40 °C → - 10 °C (**Scheme 28**).[87]

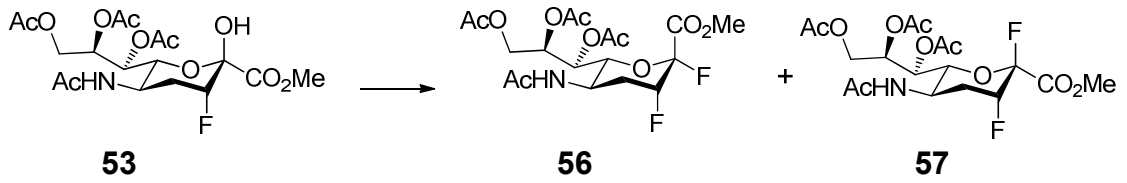

53 **56** **57**

Scheme 28 Formation of 4-deoxy-2,3-difluoro-sialic acid methyl ester (**56**) and (**57**). DAST, CH_2Cl_2, - 40 ºC → - 10 ºC, 1 hr, 45% (**56**) and 30% (**57**).

However, after silica column chromatography, two compounds, characterised by different R_f, different chemical shift and multiplicity in ^{19}F NMR but identical molecular mass, were obtained.

Identification of the two compounds by analysis of ^{19}F NMR coupling constants was not possible as the coupling constants between F-2 and F-3 were ambiguous for the identification of the anomers. As such, we utilised X-ray crystallographic analysis of the less polar compound to confirm the axial fluorine atom at position C-2 labelled F1 in the X-ray structure (**Figure 14**).

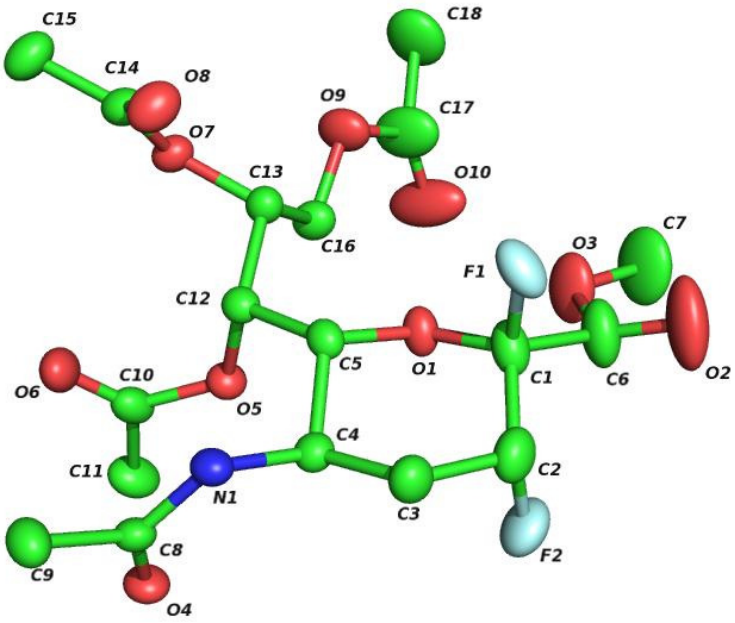

Figure 14 X-ray crystallographic structure of C-2 axial fluorine *per-O*-acetyl-4-deoxy-2,3-difluoro-sialic acid methyl ester (**57**).

Concluding from the X-ray crystallographic structure the desired α-anomer (**56**) was isolated in 45% and the β-anomer (**57**) in 30%.

An explanation for the formation of the two isomers might be given in consideration of a proposed mechanism for the fluorination of hemiketal (**53**), which proceeds by a nucleophilic attack of the anomeric hydroxyl of the hemiketal (**53**) on the sulfonium ion (**Scheme 29**).

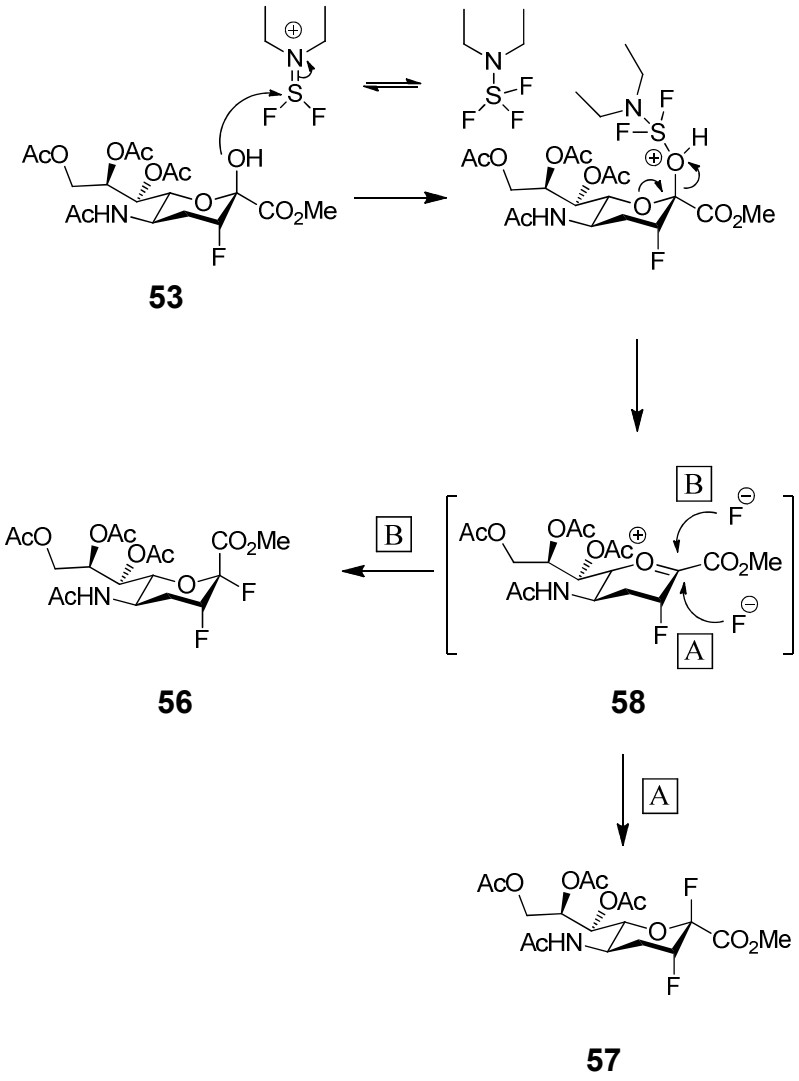

Scheme 29 Proposed mechanism for the formation of the two 2,3-difluoro-sialic acid methyl ester anomers (**56**) and (**57**).

This increase in the leaving group ability of the anomeric hydroxyl group then results in the formation of an oxocarbenium-ion (**58**). Once the oxocarbenium-ion is formed, the fluoride ion can then attack either the *re*-face to form the β-anomer (**57**) (path A), or the *si*-face to form the desired α-anomer (**56**) (path B).

In addition, the stereochemical outcome of the fluorination reaction of hemiketal (**53**) might be due to a competing nucleophilic substitution S_N1 character, forming a stable oxocarbenium-ion (**58**) (**Scheme 29**) over a S_N2 nucleophilic substitution reaction (**Scheme 27**).

In addition, the flat geometric predisposition of the oxocarbenium-ion (**58**) and steric hindrance of the glycerol side chain might preferentially enhance path B over path A but not enough to make it completely stereoselective.[164]
Subsequently, the *per-O*-acetyl-α-4-deoxy-2,3-difluoro-sialic acid methyl ester (**56**) was globally deacetylated following Zemplén conditions using sodium in methanol at room temperature.[165] Finally, saponification of the crude with 0.5M sodium hydroxide solution in water and subsequent silica column chromatography gave the target compound 4-deoxy-2,3-difluoro-sialic acid (**24**) in 52% yield (**Scheme 30**).

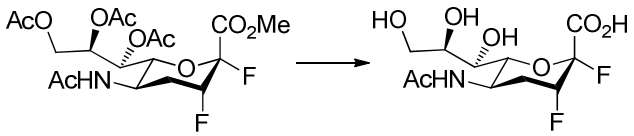

56 **24**

Scheme 30 Formation of 4-deoxy-2,3-difluoro-sialic acid (**24**). (i) NaOMe, MeOH, r.t., 3 h; (ii) 0.5M NaOH, H_2O, r.t, 30 min., 52% (over 2 steps).

The total synthesis from β-fluoropyruvic acid (**41**) to 4-deoxy-2,3-difluoro-sialic acid (**24**) was achieved in 11 steps, with an overall yield of 4%.

Chapter 3 - Synthesis of 7-deoxy-2,3-difluoro-sialic acid (25)

For the synthesis of the putative mechanism-based influenza neuraminidase inactivator 7-deoxy-2,3-difluoro-sialic acid (**25**) we intended to utilise the synthesis of 4-deoxy-2,3-difluoro-sialic acid (**24**) (Chapter 2.3).

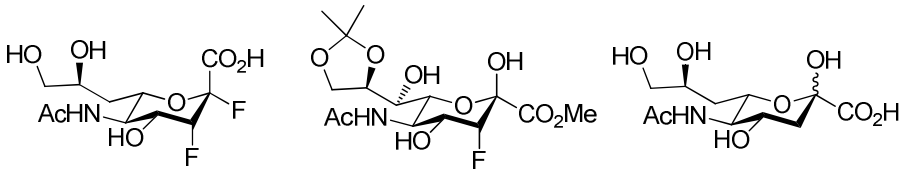

25 **48** **59**

We also considered known approaches towards the synthesis of 7-deoxy derivative (**59**), including a study performed by Miyazaki *et al.* utilising sialic acid (**2**) in a Barton-McCombie protocol via a C-7 *O*-thiocarbamate derivative.[155] Hence, it was concluded that the previously successfully synthesised 3-fluoro-8,9-*O*-isopropylidene-sialic acid methyl ester (**48**) could be used as a common intermediate towards the synthesis of the C-7 xanthate (**60**). This intermediate could be part of a viable route towards the synthesis of 7-deoxy-2,3-difluoro-sialic acid (**25**).

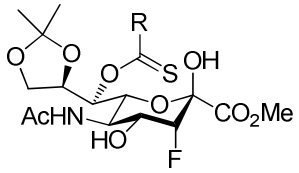

60

R = alkyl chain, carbohydrate
R' = SMe (xanthate),
= OPh (thionocarbonate),
=  (*O*-thiocarbamate)

3.1 Retrosynthetic analysis

We considered it likely that the 7-deoxy-2,3-difluoro-sialic acid (**25**) could be produced from hemiketal (**61**) by fluorination with DAST in a similar manner to that used for the synthesis of 4-deoxy-2,3-difluoro-sialic acid (**24**) (Chapter 2.3.4) (**Scheme 31**).

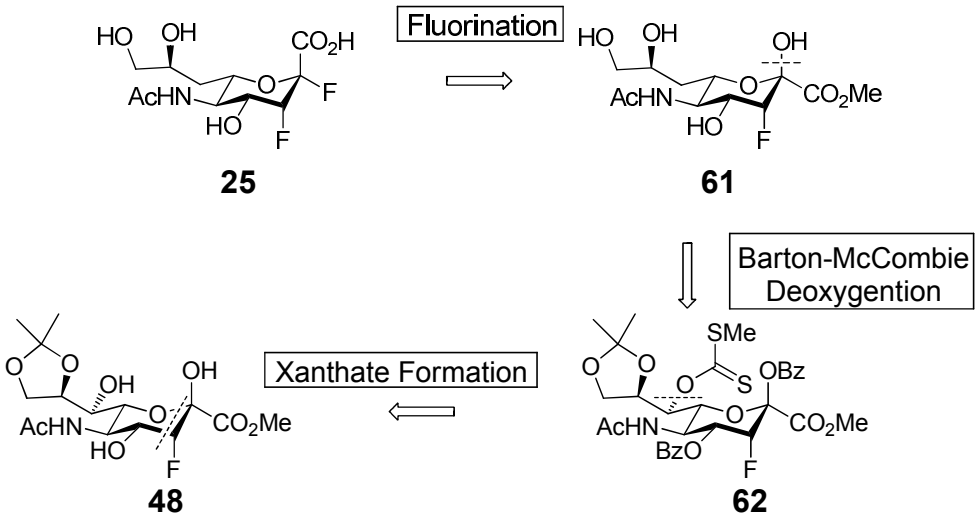

Scheme 31 Retrosynthetic strategy for the synthesis of 7-deoxy-2,3-difluoro-sialic acid (**25**) via the C-7 xanthate (**62**).

The formation of 7-deoxy-3-fluoro-sialic acid hemiketal (**61**) could be accomplished by performing a Barton-McCombie deoxygenation on the C-7 xanthate (**62**) with tributyltin hydride.[150]

It was predicted that formation of the C-7 xanthate (**62**) could be attempted on 3-fluoro-8,9-*O*-isopropylidene-sialic acid methyl ester (**48**) deploying a selective protection protocol. This selective protection protocol is based upon differential nucleophilicity of hydroxyl groups present at 3-fluoro-8,9-*O*-isopropylidene-sialic acid methyl ester (**48**) after activation.

As such, it was concluded that the hydroxyl group present at C-7 position based on nucleophilicity differences along with steric hindrances could be the least reactive hydroxyl group. A benzoyl protecting group seemed to be most applicable for the selective protection protocol to protect the hydroxyl groups at position C-2 and C-4.

Furthermore, it was intended that after the Barton-McCombie deoxygenation the benzoyl protecting group would enable selective deprotection at position C-2 using hydrazine acetate to form the hemiketal (**61**).

The formation of 3-fluoro-8,9-*O*-isopropylidene-sialic acid methyl ester (**48**) could be yielded utilising TFA in methanol and 2,2'-dimethoxypropane on 3-fluoro-sialic acid (**39**) as previously accomplished (Chapter 2.3.2).

3.2 Synthesis of 2,4-di-*O*-benzoyl-7-deoxy-3-fluoro-8,9-*O*-isopropylidene-sialic acid methyl ester (68)

The 3-fluoro-8,9-*O*-isopropylidene-sialic acid methyl ester (**48**) was treated with benzoyl chloride in a mixture of dichloromethane/pyridine, which after standard work up and silica column chromatography afforded a mixture of 2,4-di-*O*-benzoyl-3-fluoro-8,9-*O*-isopropylidene-sialic acid methyl ester (**63**) in 54% and 2,4,7-tri-*O*-benzoyl-3-fluoro-8,9-*O*-isopropylidene-sialic acid methyl ester (**64**) in 18% yield respectively (**Scheme 32**).

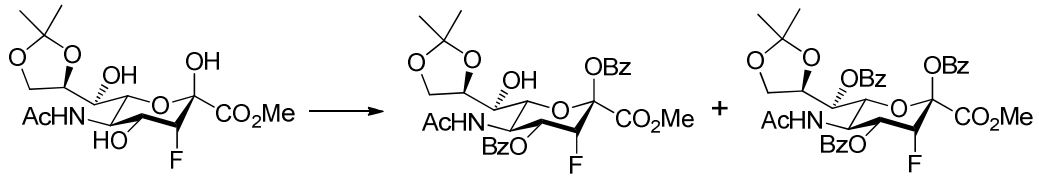

48 **63** **64**

Scheme 32 Formation of 2,4-di-*O*-benzoyl-3-fluoro-8,9-*O*-isopropylidene-sialic acid methyl ester (**63**) and 2,4,7-tri-*O*-benzoyl-3-fluoro-8,9-*O*-isopropylidene-sialic acid methyl ester (**64**). Benzoyl chloride, CH_2Cl_2/pyridine, - 40 °C → -20 °C, 1.5 h, 54% (**63**) and 18% (**64**).

The synthesis of *O*-thionocarbonate at C-7 position utilising phenyl chlorothionoformate under conditions previously deployed on the synthesis of 4-*O*-(phenoxy)thiocarbonyl-sialic acid methyl ester (**49**) (Chapter 2.3.2) gave an inseparable mixture of starting material (**63**), desired product (**65**) and the previously observed sulphur-oxygen exchanged rearrangement (**66**) according to Powers *et al.* in a ratio of 1:2:2 (**Scheme 33**).[160]

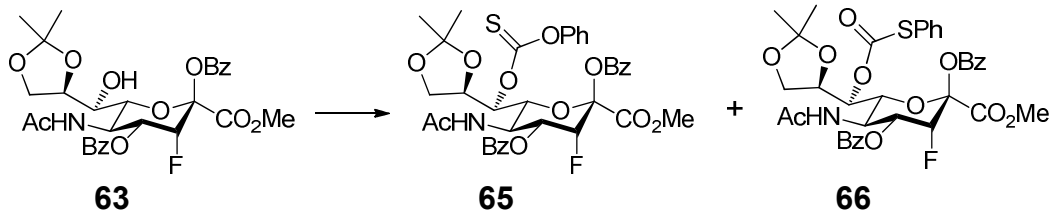

63 **65** **66**

Scheme 33 Attempted synthesis of 2,4-di-*O*-benzoyl-3-fluoro-8,9-*O*-isopropylidene-7-*O*-(phenoxy)thiocarbonyl-sialic acid methyl ester (**65**). Phenyl chlorothionoformate, CH_2Cl_2/pyridine, r.t., O/N.

Furthermore, changing the solvent to pyridine and employing a variety of reaction temperatures (such as - 40 °C and 0 °C), together with attempts to degas the solution failed to improve the reaction and gave the known mixture in comparable ratios.

Given the problem of forming an inseparable mixture, it was considered that utilising a thiocarbamate following the protocol of Miyazaki *et al.* these difficulties could be overcome. The thiocarbamate was anticipated to give better yields in the following Barton-McCombie deoxygenation, as the deoxygenation reaction itself requires lower temperatures and the risk of side reactions with forming the sulphur-oxygen exchanged side product is considerable lower.[154]

The 2,4-di-*O*-benzoyl-3-fluoro-8,9-*O*-isopropylidene-sialic acid methyl ester (**65**) was treated with 1,1'-thiocarbonyldiimidazole in anhydrous dichloromethane to give after silica column chromatography the 3-fluoro-8,9-*O*-isopropylidene-7-*O*-thiocarbamate-sialic acid derivative (**67**) in 95% yield (**Scheme 34**).[155]

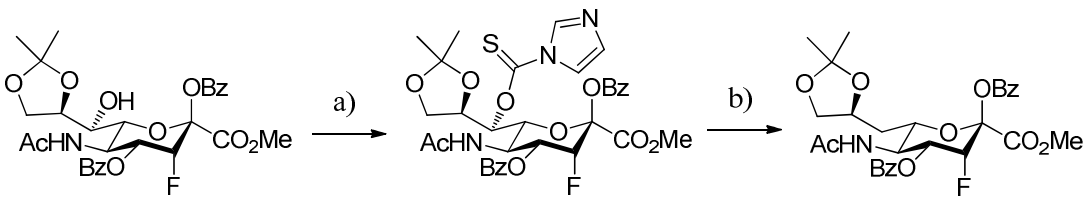

65 **67** **68**

Scheme 34 Synthesis of 7-deoxy-3-fluoro-8,9-*O*-isopropylidene-sialic derivative (**68**). a) 1,1'-Thiocarbonyldiimidazole, CH_2Cl_2, 40 °C, 20 h, 95% (**67**) b) Luperox® 101, Bu_3SnH, 1,4-dioxane, 100 °C, 4 h, 89% (**68**).

The 3-fluoro-8,9-*O*-isopropylidene-7-*O*-thiocarbamate-sialic acid derivative (**67**) was then subjected to Barton-McCombie deoxygenation conditions using Luperox® 101 as a radical initiator and the radical carrier tributyltin hydride under reflux conditions in 1,4-dioxane to give 7-deoxy-3-fluoro-8,9-*O*-isopropylidene-sialic acid methyl ester (**68**) in 89% yield (**Scheme 34**). The radical initiator Luperox® 101 was used as the previous deployed 2,2-bis(*tert*-butylperoxy)-butane radical initiator was no longer commercially available and Luperox® 101, as an alternative, gave advantages in terms of cost and longer stability over other radical initiators available.

3.3 Formation of 7-deoxy-3-fluoro hemiketal (71)

The anomeric deprotection of 2,4-di-*O*-benzoyl-7-deoxy-3-fluoro-8,9-*O*-isopropylidene-sialic acid methyl ester (**68**) with hydrazine acetate in a solvent mixture of dichloromethane and methanol was attempted (**Scheme 35**).

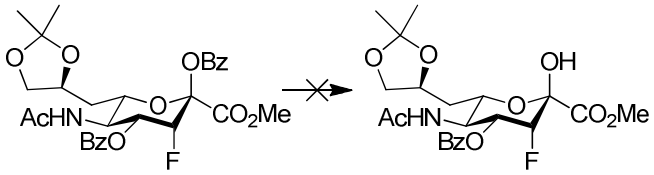

68 **69**

Scheme 35 Attempted formation of 4-*O*-benzoyl-7-deoxy-3-fluoro-8,9-*O*-isopropylidene-sialic acid methyl ester (**69**). Hydrazine acetate, CH_2Cl_2/MeOH, 4 °C, O/N.

However, numerous reaction conditions were tried including increasing the temperature from 4 °C to 40 °C and the use of more equivalents of hydrazine acetate failed to give desired product but resulted in decomposition of starting material (**68**). In addition, the use of a stronger nucleophile hydrazine hydrate and different work up methods to remove excess of hydrazine were performed with acidic or copper sulfate washes. Nevertheless, the reaction conditions applied were found to give starting material (**68**) and polar side product formation.

The unsuccessful selective anomeric deprotection of 2,4-di-*O*-benzoyl-7-deoxy-3-fluoro-8,9-*O*-isopropylidene-sialic acid methyl ester (**68**) prompted us to investigate an alternative synthetic strategy involving global deprotection and subsequent acetylation to finally perform anomeric deprotection on an anomeric acetate, as previously performed on the *per*-*O*-acetyl-4-deoxy-3-fluoro-sialic acid methyl ester (**52**) (Chapter 2.3.3).

The 2,4-di-*O*-benzoyl-7-deoxy-3-fluoro-8,9-*O*-isopropylidene-sialic acid methyl ester (**68**) was subjected to sodium in methanol according to the previously deployed method (Chapter 2.3.3) following Zemplén conditions (**Scheme 36**).[165] The crude mixture was then treated with 80% acetic acid following the procedure of Anazawa *et al.*[161] (Chapter 2.3.3) and finally, globally acetylated with acetic anhydride in pyridine to give the *per*-*O*-acetyl-7-deoxy-3-fluoro-sialic acid methyl ester (**70**) in 83% yield over 3 steps (**Scheme 36**).

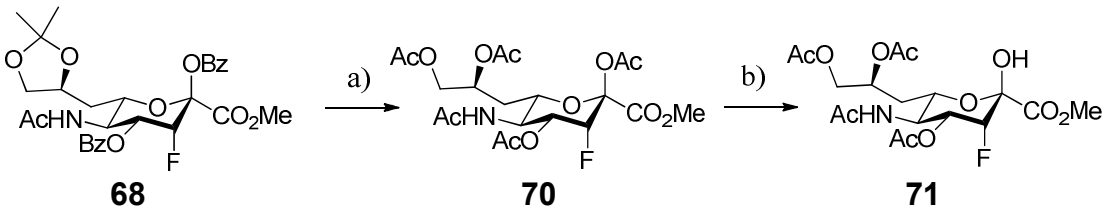

68 **70** **71**

Scheme 36 Synthesis of 4,8,9-tri-*O*-acetyl-7-deoxy-3-fluoro-sialic acid methyl ester (**71**). a) (i) NaOMe, MeOH, 40 °C, 36 h; (ii) 80% AcOH/H_2O, 60 °C, 2 h; (iii) Ac_2O, DMAP, pyridine, r.t., O/N, 83% (over 3 steps) (**70**); b) Hydrazine acetate, CH_2Cl_2/MeOH, 4 °C, O/N, 84% (**71**).

The *per*-*O*-acetyl-7-deoxy-3-fluoro-sialic acid methyl ester (**70**) was then deprotected at position C-2 using hydrazine acetate in a solvent mixture of dichloromethane and methanol at 4 °C following the method previously deployed on *per*-*O*-acetyl-4-deoxy-3-fluoro-sialic acid methyl ester (**52**) (Chapter 2.3.3) to afford the hemiketal (**71**) in 84% yield (**Scheme 36**).

3.4 Synthesis of 7-deoxy-2,3-difluoro-sialic acid (25)

The hemiketal (**71**) was then treated with DAST in dichloromethane at - 40 °C → - 10 °C according to the methodology previously deployed on hemiketal (**53**) (Chapter 2.3.4) to afford a mixture of α- and β-fluoride anomers (**72**) (**Scheme 37**).

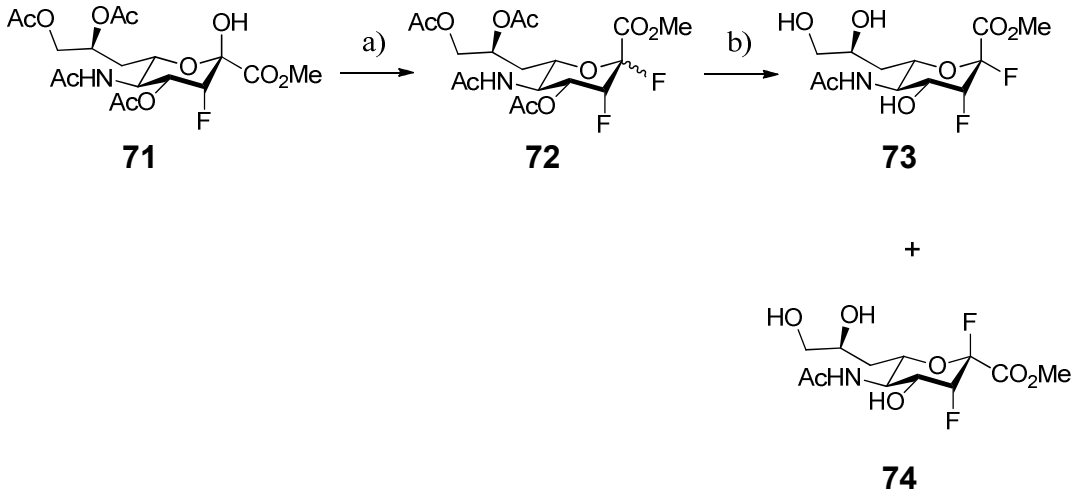

71 **72** **73** **74**

Scheme 37 Synthesis of 7-deoxy-2,3-difluoro-sialic acid methyl ester anomers (**73**) and (**74**). a) DAST, CH_2Cl_2, - 40 ºC → - 10 ºC, 1 hr; b) NaOMe, MeOH, r.t., 3 h, 41% (over 2 steps) (**73**), 20% (over 2 steps) (**74**).

The formation of a mixture of anomers is in compliance with results previously observed on hemiketal (**53**) (Chapter 2.3.4). The correct molecular weight was confirmed by mass spectrometry but, despite exhaustive solvent combinations in silica column chromatography the α- and β-anomers (**72**) could not be purified by at this stage, as the two anomers coeluted.

It was considered, that separation might be possible following deacetylation of the anomeric mixture. As such, the α-/β-mixture (**72**) was deacetylated using sodium in methanol at room temperature following Zemplén conditions.[165]

Subsequent purification by silica column chromatography gave the desired α isomer (**73**) pure in 41% yield and the β isomer (**74**) in 20%, over the 2 steps.

Finally, ester saponification of the 7-deoxy-2,3-difluoro-sialic acid methyl ester (**73**) with 0.5M sodium hydroxide solution in water at room temperature gave then the desired 7-deoxy-2,3-difluoro-sialic acid (**25**) in 49% yield (**Scheme** 38).

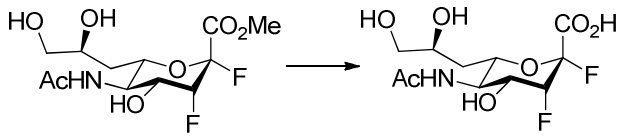

73 **25**

Scheme 38 Formation of 7-deoxy-2,3-difluoro-sialic (**25**). 0.5M NaOH, H_2O, r.t, 45 min., 49%.

The total synthesis from β-fluoropyruvic acid (**41**) to 7-deoxy-2,3-difluoro-sialic acid (**25**) was achieved in 13 steps, with an overall yield of about 5%.

Chapter 4 - Synthesis of 8-deoxy-2,3-difluoro-sialic acid (26)

The synthesis of the putative mechanism-based influenza neuraminidase inactivator 8-deoxy-2,3-difluoro-sialic acid (**26**) was deployed in consideration of the previously accomplished syntheses of 4-deoxy-2,3-difluoro-sialic acid (**24**) (Chapter 2.3) and 7-deoxy-2,3-difluoro-sialic acid (**25**) (Chapter 3).

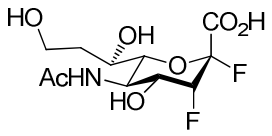

26

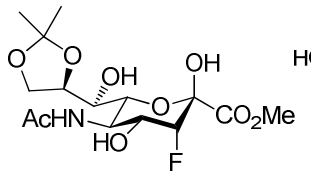

48

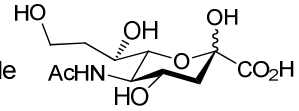

75

We also considered known approaches towards the synthesis of the 8-deoxy derivative (**75**), which was achieved following Barton-McCombie deoxygenation of a C-8 *O*-thionocarbonate by Miyazaki *et al.*[155] This approach could be used as a proof of principle for the Barton-McCombie deoxygenation strategy. It was intended again to utilise the 3-fluoro-8,9-*O*-isopropylidene-sialic acid methyl ester (**48**), the common intermediate of the succeeding syntheses of C-7 and C-4 xanthate to develop a feasible approach via the C-8 xanthate (**76**) towards the synthesis of 8-deoxy-2,3-difluoro-sialic acid (**26**).

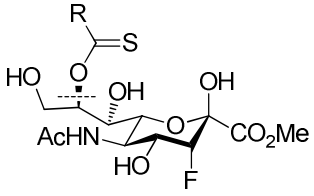

76

R = SMe (xanthate),

= OPh (thionocarbonate),

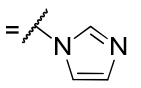
(*O*-thiocarbamate)

4.1 Retrosynthetic analysis

Given the successful hemiketal fluorination with DAST in the synthesis of 4-deoxy-2,3-difluoro-sialic acid (**24**) and 7-deoxy-2,3-difluoro-sialic acid (**25**), we considered a similar approach to perform the synthesis of 8-deoxy-2,3-difluoro-sialic acid (**26**) from the hemiketal (**78**) (**Scheme 39**).

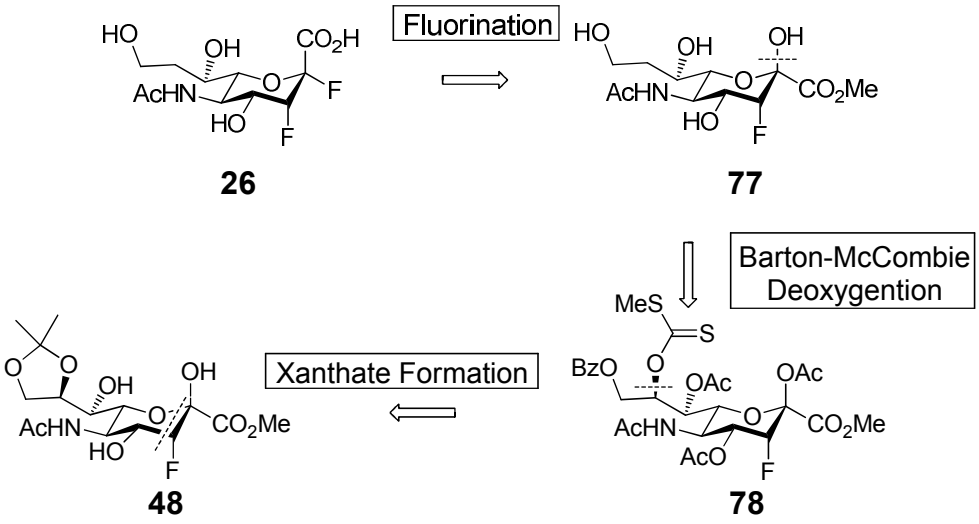

Scheme 39 Retrosynthetic strategy for the synthesis of 8-deoxy-2,3-difluoro-sialic acid (**26**) via the C-8 xanthate (**78**).

It was concluded that the 8-deoxy-3-fluoro-sialic acid hemiketal (**77**) could be achieved through Barton-McCombie deoxygenation of the xanthate (**78**). The xanthate (**78**) could be accessible from the previously formed 3-fluoro-8,9-*O*-isopropylidene-sialic acid methyl ester (**48**) through a series of standard protecting group manipulations.

It was anticipated that acetylation at position C-2, C-4 and C-7 of the common intermediate 3-fluoro-8,9-*O*-isopropylidene-sialic acid methyl ester (**48**) following isopropylidene deprotection according to the procedure of Anazawa *et al.* would permit subsequent selective protection of the hydroxyl group at position C-9 over the hydroxyl group at position C-8, using for example a benzoate protecting group.[161]

4.2 Synthesis of C-8 xanthate (84)

The common intermediate 3-fluoro-8,9-*O*-isopropylidene-sialic acid methyl ester (**48**) was achieved as mentioned previously (Chapter 2.3.2). Subsequent acetylation by treatment with acetic anhydride in pyridine gave 2,4,7-tri-*O*-acetyl-3-fluoro-8,9-*O*-isopropylidene-sialic acid methyl ester (**79**) in 91% yield from the 8,9-*O*-isopropylidene-sialic acid derivative (**48**) (**Scheme 40**).

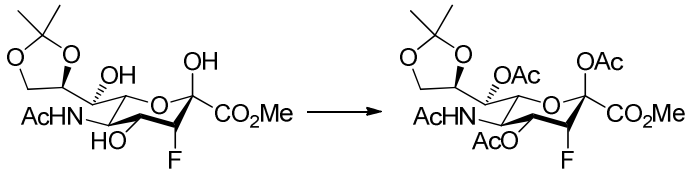

48 **79**

Scheme 40 Formation of 2,4,7-tri-*O*-acetyl-3-fluoro-8,9-*O*-isopropylidene-sialic acid methyl ester (**79**). Ac_2O, pyridine, r.t., 7 days, 91%.

In an attempt to shorten reaction times, catalytic amounts of DMAP were added to the reaction mixture but the reaction failed as formation of isopropylidene-deprotected side product was observed.

Next, the 2,4,7-tri-*O*-acetyl-3-fluoro-8,9-*O*-isopropylidene-sialic acid methyl ester (**79**), was treated with 80% acetic acid according to the procedure of Anazawa *et al.* (**Scheme 41**).[161]

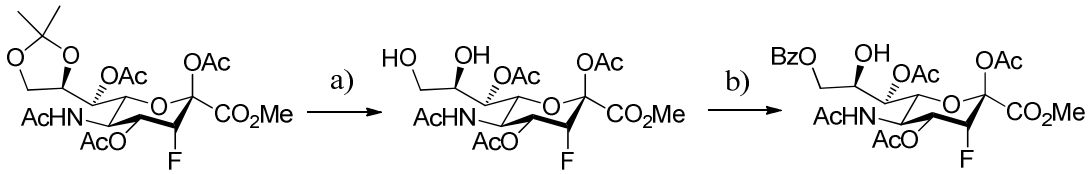

79 **80** **81**

Scheme 41 Synthesis of 2,4,7-tri-*O*-acetyl-9-*O*-benzoyl-3-fluoro-sialic acid methyl ester (**81**). a) 80% AcOH/H_2O, 60 °C, 2 h; b) Benzoyl chloride, pyridine, r.t., O/N, 70% (over 2 steps).

An aqueous work up following the acidic hydrolysis failed as the desired product 2,4,7-tri-*O*-acetyl-3-fluoro-sialic acid methyl ester (**80**) did decompose and was found to accumulate in the aqueous phase.

Acetyl group migration under acidic conditions was known to occur and together with further deacetylation might be an explanation for the difficulties envisaged in the purification of 2,4,7-tri-*O*-acetyl-3-fluoro-sialic acid methyl ester (**80**).[161,166,167]

Hence, following isopropylidene deprotection, the crude mixture was treated with benzoyl chloride in pyridine at room temperature to give the selective C-9 benzoyl-protected derivative (**81**) in 70% over the two steps (**Scheme 41**).

Considering our previous success of introducing the C-7 *O*-thiocarbamate in the synthesis of 7-deoxy-2,3-difluoro-sialic acid (**25**) (Chapter 3.2), we applied the use of this group in the synthesis of 8-deoxy-2,3-difluoro-sialic acid (**26**). Consequently, the 2,4,7-tri-*O*-acetyl-9-*O*-benzoyl-3-fluoro-sialic acid methyl ester (**81**) was subjected to 1,1'-thiocarbonyldiimidazole in anhydrous dichloromethane (**Scheme 42**).

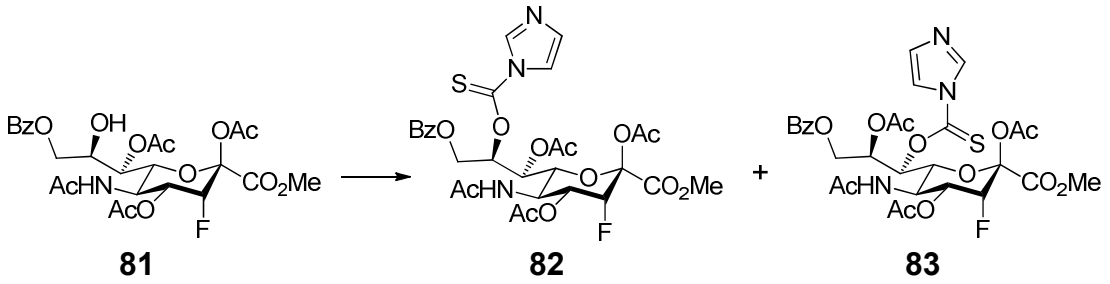

Scheme 42 Attempted formation of 2,4,7-tri-*O*-acetyl-9-*O*-benzoyl-3-fluoro-8-*O*-thiocarbamate-sialic acid methyl ester (**82**). 1,1'-Thiocarbonyldiimidazole, CH_2Cl_2, 40 °C, 24 h.

Following aqueous work up and silica column chromatography, analysis by mass spectrometry confirmed the formation of a species with the correct molecular weight. However, analysis of the ^{1}H NMR spectrum indicated the product was a mixture of C-8 (**82**) and C-7 *O*-thiocarbamate (**83**) in a ratio of 1:1. Despite exhaustive solvent combinations in silica column chromatography the mixture of C-8 (**82**) and C-7 *O*-thiocarbamate (**83**) could not be purified. It was concluded that formation of the mixture of thiocarbamates at C-7 and C-8 might be due to acetyl migration under the conditions applied.

In an attempt to overcome the problem of acetyl migration we anticipated that formation of the C-8 thionocarbonate could be less susceptible to acetyl migration, as shorter reaction times and lower temperatures are required. Hence, the 2,4,7-tri-*O*-acetyl-9-*O*-benzoyl-3-fluoro-sialic acid methyl ester (**81**) was treated with phenyl chlorothionoformate in pyridine at 0 °C affording, after silica column chromatography, the 2,4,7-tri-*O*-acetyl-9-*O*-benzoyl-3-fluoro-8-*O*-(phenoxy)thiocarbonyl-sialic acid methyl ester (**84**) in 84% yield (**Scheme 43**).

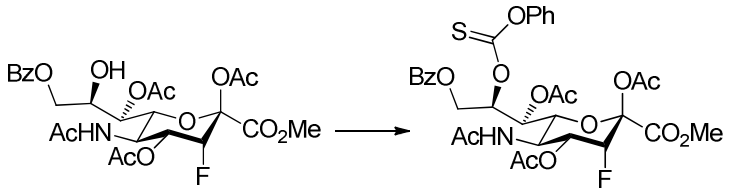

81 **84**

Scheme 43 Formation of 2,4,7-tri-*O*-acetyl-9-*O*-benzoyl-3-fluoro-8-*O*-(phenoxy)thiocarbonyl-sialic acid methyl ester (**84**). Phenyl chlorothionoformate, pyridine, 0 ºC → r.t., 15 h, 84%.

4.3 Formation of 8-deoxy-3-fluoro hemiketal (86)

The 2,4,7-tri-*O*-acetyl-9-*O*-benzoyl-3-fluoro-8-*O*-(phenoxy)thiocarbonylsialic acid methyl ester (**84**) was then subjected to Barton-McCombie conditions using Luperox® 101 as a radical initiator and the radical carrier tributyltin hydride under reflux conditions in 1,4-dioxane to give according to the methodology previously deployed on 7-*O*-thiocarbamate-sialic acid methyl ester (**67**) (Chapter 3.2) the 8-deoxy-3-fluoro-sialic acid derivative (**85**) in 80% yield (**Scheme 44**).

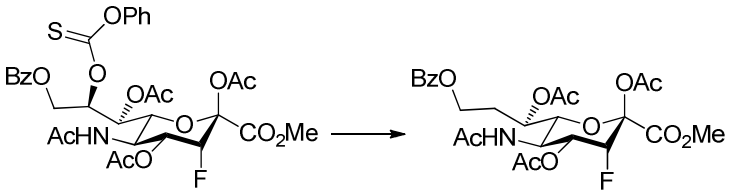

84 **85**

Scheme 44 Synthesis of 8-deoxy-3-fluoro-sialic acid derivative (**85**). Luperox® 101, Bu_3SnH, 1,4-dioxane, 100 ºC, 4 h, 80%.

Subsequent anomeric deprotection of the 2,4,7-tri-*O*-acetyl-9-*O*-benzoyl-8-deoxy-3-fluoro-sialic acid methyl ester (**85**) employing the method using hydrazine acetate in dichloromethane and methanol at 4 °C as previously described on *per*-*O*-acetyl-4-deoxy-3-fluoro-sialic acid methyl ester (**52**) (Chapter 2.3.3) to give the hemiketal (**86**) in 83% yield (**Scheme 45**).

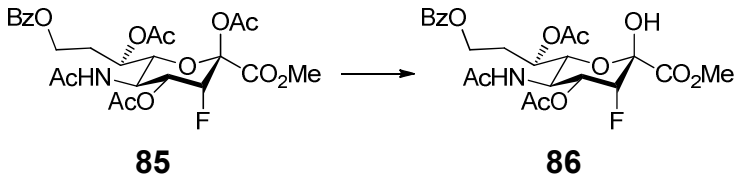

85 **86**

Scheme 45 Formation of 4,7-di-*O*-acetyl-9-*O*-benzoyl-8-deoxy-3-fluoro-sialic acid methyl ester (**86**). Hydrazine acetate, CH_2Cl_2/MeOH, 4 °C, O/N, 83%.

4.4 Synthesis of 8-deoxy-2,3-difluoro-sialic acid (26)

The hemiketal (**86**) was then treated with DAST in dichloromethane at - 40 °C → - 10 °C according to the methodology previously deployed on hemiketal (**53**) (Chapter 2.3.4) to afford a mixture of α- and β-fluoride anomers (**87**) (**Scheme 46**).

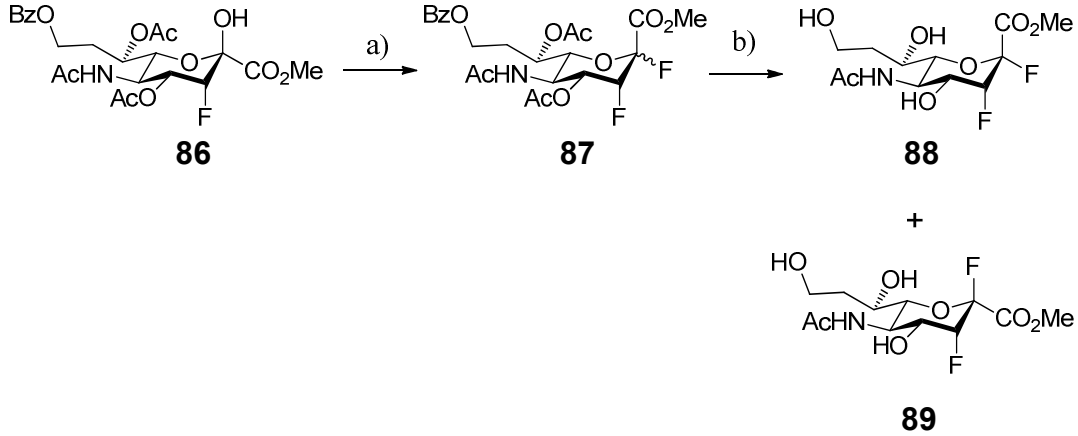

86 **87** **88**

89

Scheme 46 Synthesis of 8-deoxy-2,3-difluoro-sialic acid methyl ester anomers (**88**) and (**89**). a) DAST, CH_2Cl_2, - 40 ºC → - 10 ºC, 1 hr; b) (i) NaOMe, MeOH, r.t., O/N; (ii) TFA, MeOH, r.t., O/N, 25% (over 3 steps) (**88**), 11% (over 3 steps) (**89**).

The formation of a mixture of anomers is in compliance with results observed on hemiketal (**53**) (Chapter 2.3.4). The correct molecular weight was confirmed by mass spectrometry but, despite exhaustive solvent combinations in silica column chromatography the α-/β-mixture (**87**) could not be purified by at this stage, as the two anomers coeluted.

It was considered, that separation might be possible following deacetylation of the anomeric mixture as previously demonstrated on the α-/β-mixture (**72**) (Chapter 3.4). As such, the α-/β-mixture (**87**) was deacetylated using sodium in methanol at room temperature following Zemplén conditions.[165]

However, applying Zemplén conditions resulted in formation of a polar side product.[165] The suspected de-esterification generated a highly polar mixture α- and β-fluoride anomers, impossible to purify by C18 reverse phase column chromatography. Hence, subsequent esterification using trifluoroacetic acid in methanol was attempted, followed by silica column chromatography to give the desired α anomer (**88**) in 25% and the β anomer (**89**) in 11% yield respectively over the 3 steps.

Finally, ester saponification of the desired anomer 8-deoxy-2,3-difluoro-sialic acid methyl ester (**88**) with 0.5M sodium hydroxide solution in water and subsequent silica column chromatography gave the desired 8-deoxy-2,3-difluoro-sialic acid (**26**) in 22% yield (**Scheme 47**).

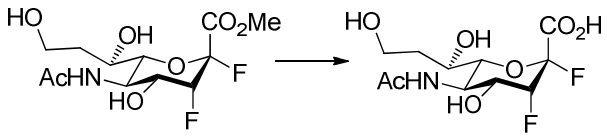

88 **26**

Scheme 47 Formation of 8-deoxy-2,3-difluoro-sialic (**26**). 0.5M NaOH, H_2O, r.t, 45 min., 22%.

The total synthesis from β-fluoropyruvic acid (**41**) to 8-deoxy-2,3-difluoro-sialic acid (**26**) was achieved in 12 steps, with an overall yield of 2%.

Chapter 5 - Synthesis of 9-deoxy-2,3-difluoro-sialic acid (27)

In order to synthesise the putative mechanism-based influenza neuraminidase inactivator 9-deoxy-2,3-difluoro-sialic acid (**27**), we considered known approaches towards the synthesis of 9-deoxy-sialic acid (**90**).

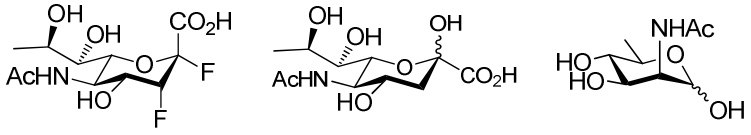

27 **90** **91**

A study performed by Miyazaki *et al.* proceeded via a C-9 *O*-thionocarbonate derivative, which after Barton-McCombie deoxygenation gave the 9-deoxy-sialic acid derivative in 39% yield. The Barton-McCombie deoxygenation is known to give low yields at position C-9 of sialic acid.[154] Therefore, it was anticipated to achieve better results utilising 2-*N*-acetyl-6-deoxy-*D*-mannosamine (**91**) in an enzymatic aldolase reaction, which has previously been pointed out (Chapter 2.2.2) to give 9-deoxy-3-difluoro-sialic acid (**92**) (**Scheme 48**).

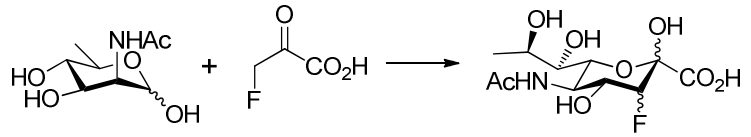

91 **41** **92**

Scheme 48 Proposed formation of 9-deoxy-3-fluoro-sialic acid (**92**). Neu5Ac aldolase, H_2O, r.t..

As such, the synthesis of 2-*N*-acetyl-6-deoxy-*D*-mannosamine (**91**) has previously been accomplished by Bucchini *et al.* starting from 2-*N*-acetyl-*D*-mannosamine (**40**).[168] 2-*N*-acetyl-*D*-mannosamine (**40**) itself is a cheap starting material and the formation of 2-*N*-acetyl-6-deoxy-*D*-mannosamine (**91**) in highest possible yields could be a vigorous route towards the synthesis of 9-deoxy-2,3-difluorosialic acid (**27**).

5.1 Attempted synthesis of 9-deoxy-2,3-difluoro-sialic acid (27) via the 2-*N*-acetyl-6-deoxy-*D*-mannosamine (91)

5.1.1 Retrosynthetic analysis

We considered it likely that the 9-deoxy-2,3-difluorosialic acid (**27**) could be produced from hemiketal (**93**) by fluorination with DAST in a similar manner to that used for the synthesis of 4-deoxy-2,3-difluoro-sialic acid (**24**) (Chapter 2.3.4) (**Scheme 49**).

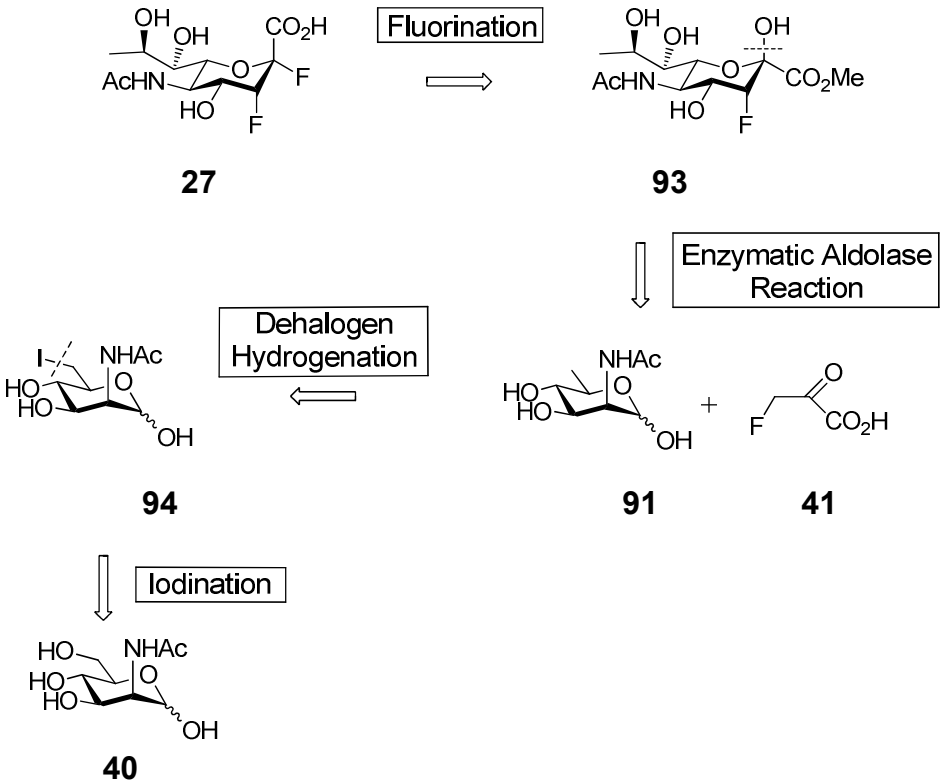

Scheme 49 Retrosynthetic strategy for the synthesis of 9-deoxy-2,3-difluoro-sialic acid (**27**) via the 2-*N*-acetyl-6-deoxy-*D*-mannosamine (**91**).

The 9-deoxy-3-fluoro-sialic acid hemiketal (**93**) could be achieved in an enzymatic aldolase reaction of 2-*N*-acetyl-6-deoxy-*D*-mannosamine (**91**) and β-fluoropyruvic acid (**41**), according to the method employed by Watts and Withers.[87] The 2-*N*-acetyl-6-deoxy-*D*-mannosamine (**91**) could be yielded utilising the C-6 iodo derivative (**94**) in a dehalogen hydrogenation reaction following the previously accomplished synthesis of Bucchini *et al*.[168]
The formation of the C-6 iodo derivative (**94**) could be achieved, after activation of the C-6 position in 2-*N*-acetyl-*D*-mannosamine with sodium iodide (**40**).

5.1.2 Synthesis of *per-O*-acetyl-2-*N*-acetyl-6-iodo-*D*-mannosamine (96)

The 2-*N*-acetyl-*D*-mannosamine (**40**) was treated with *p*-toluenesulfonyl chloride in pyridine at 0 °C and subsequently acetylated with acetic anhydride in pyridine overnight to give the *per-O*-acetyl-*N*-acetyl-6-tosyl-*D*-mannosamine (**95**) following the procedure of Saxon *et al.*[169] and Buchini *et al.*[168] in 48% over the 2 steps (**Scheme 50**).

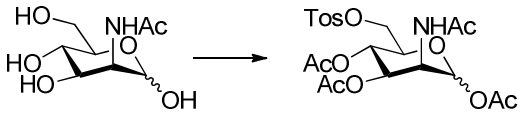

40 **95**

Scheme 50 Synthesis of *per-O*-acetyl-2-*N*-acetyl-6-tosyl-*D*-mannosamine (**95**). (i) 4-Toluenesulfonyl chloride, pyridine, 0 °C, 7 h; (ii) Ac_2O, pyridine, r.t., O/N, 48% (over 2 steps).

The low yield might be due to impure starting material 2-*N*-acetyl-*D*-mannosamine (**40**), which had been recovered from previously performed enzymatic aldolase reactions of 2-*N*-acetyl-*D*-mannosamine (**40**) with β-fluoropyruvic acid (**41**) (Chapter 2.2.2).

The *per*-*O*-acetyl-2-*N*-acetyl-6-tosyl-*D*-mannosamine (**95**) was then subjected to potassium iodide in butanone to give *per*-*O*-acetyl-2-*N*-acetyl-6-iodo-*D*-mannosamine (**96**) according to the procedure by Horita *et al.* after silica column chromatography in 50% yield (**Scheme 51**).[170]

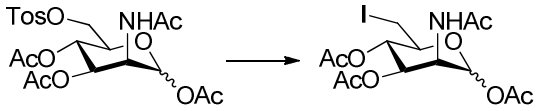

95 **96**

Scheme 51 Formation of *per*-*O*-acetyl-2-*N*-acetyl-6-iodo-*D*-mannosamine (**96**). KI, butanone, 90 °C, 18 h, O/N, 50%.

Although acceptable, it was considered that the yield of 50% could potentially be improved upon. As such, alternative methods to introduce the iodine by testing a number of iodide sources and employing a number of solvents and temperatures were attempted (**Table 3**).

Table 3 Different conditions used for the formation of *per*-*O*-acetyl-2-*N*-acetyl-6-iodo-*D*-mannosamine (**96**). **Condition A**: NaI (2 eq.), DMF; **Condition B**: KI (2 eq.), DMF; **Condition C**: KI (2 eq.), butanone; **Condition D**: CsI (2 eq.), butanone.

95 **96**

Entry	Condition	Time	T [°C]	Product	Yield (%)[a]
1	A	18 h	80	**96**	30
2	B	24 h	70	**96**	44
3	C	24 h	r.t.	**95**	n.d.
4	C	17 h	70	**96**	44
5	C	36 h	90	**96**	40
6	C	18 h	90	**96**	50
7	D	23 h	70	**96**	39

[a] Isolated yields after silica chromatography. n.d. = not determined.

The *per*-*O*-acetyl-2-*N*-acetyl-6-tosyl-*D*-mannosamine (**95**) was treated with sodium iodide in dimethylformamide at 80 °C (**Table 3, entry 1**) and gave desired product (**96**) in 30% yield, but also resulted in formation of a highly polar side product that could not be isolated under the conditions applied. Therefore, the alternative iodide source potassium iodide was investigated under similar conditions but at 70 °C (**Table 3, entry 2**) and gave more encouraging yield of 44%. Difficulties in removing the solvent DMF and subsequent purification were tried to be resolved by changing the solvent to butanone instead (**Table 3, entry 3 to 7**). The best yield for the transformation of *per*-*O*-acetyl-2-*N*-acetyl-6-tosyl-*D*-mannosamine (**95**) to the 6-iodo derivative (**96**) was achieved utilising potassium iodide in butanone at 90 °C in 50% yield respectively (**Table 3, entry 6**). Despite, numerous alternative reaction conditions, such as using caesium iodide (**Table 3, entry 7**) no better yields could be achieved.

In all reactions performed starting material *per*-*O*-acetyl-2-*N*-acetyl-6-tosyl-*D*-mannosamine (**95**) was recovered. However, longer reaction times in order to push the reaction to completion resulted in decomposition of the product and afforded lower yields. The expected elimination product (**97**), which also could have been used for the synthesis of 2-*N*-acetyl-6-deoxy-*D*-mannosamine (**91**), was not observed.

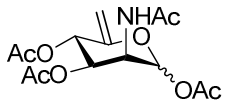

97

5.1.3 Attempted synthesis of 2-*N*-acetyl-6-deoxy-*D*-mannosamine (91)

The *per*-*O*-acetyl-2-*N*-acetyl-6-iodo-*D*-mannosamine (**96**) was then subjected to Barton-McCombie conditions using Luperox® 101 as a radical initiator and the radical carrier tributyltin hydride under reflux conditions in 1,4 dioxane as previously employed (Chapter 3.2) to give the *per*-*O*-acetyl-2-*N*-acetyl-6-deoxy-*D*-mannosamine (**98**) in 70% yield (**Scheme 52**).

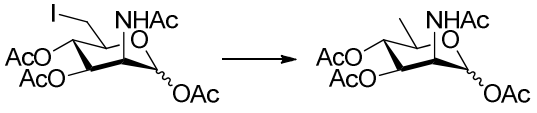

96 **98**

Scheme 52 Synthesis of *per*-*O*-acetyl-2-*N*-acetyl-6-deoxy-*D*-mannosamine (**98**). Luperox® 101, Bu_3SnH, 1,4-dioxane, 100 ºC, 4 h, 70%.

The *per*-*O*-acetyl-2-*N*-acetyl-6-deoxy-*D*-mannosamine (**98**) was then deacetylated using sodium in methanol following Zemplén conditions (**Table 4**).[165] The conditions applied generated, due to epimerisation of the 2-*N*-acetyl group at basic conditions, an inseparable mixture of 2-*N*-acetyl-*D*-mannosamine and 2-*N*-acetyl-*D*-glucosamine (**99**) together with their corresponding mixture of anomers (**Table 4, entry 1**).

Table 4 Different conditions used for the synthesis of 2-*N*-acetyl-6-deoxy-*D*-mannosamine (**91**). **Condition A**: NaOMe (0.3 eq.), MeOH;[165] **Condition B**: AcCl (0.1 eq.), MeOH;[171] **Condition C**: Molecular sieves 4 Å, MeOH.[172]

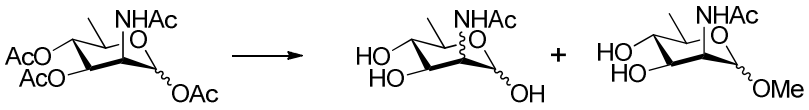

98 **99** **100**

Entry	Condition	Time	T [°C]	Product	Yield (%)
1	A	5 h	0	**99**	n.d.
2	B	21 h	4	**100**	n.d.
3	C	72 h	r.t.	**98**	n.d.

n.d. = not determined

The deacetylation following Zemplén[165] conditions has previously been performed by Buchini *et al.*[168] on *per*-*O*-acetyl-2-*N*-acetyl-6-azido-*D*-mannosamine (**101**), but translation towards the synthesis of 2-*N*-acetyl-6-deoxy-*D*-mannosamine (**91**) could not be accomplished.[168]

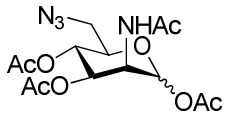

101

We investigated known approaches for the deprotection of acetyl groups such as acidic conditions utilising acetyl chloride in methanol (**Table 4, entry 2**), but these acidic conditions enhanced the formation of the methyl glycoside 2-*N*-acetyl-6-deoxy-*D*-mannosamine (**100**).[171]

We also examined milder basic conditions deploying the use of molecular sieves 4 Å in methanol (**Table 4, entry 3**), but only starting material (**98**) together with similar side reactions as previously reported using Zemplén conditions (**Table 4, entry 1**) were observed.[165,172]

Given the difficulties using acetyl protecting groups at the anomeric position of 2-*N*-acetyl-*D*-mannosamine, we were prompted to use alternative anomeric protecting groups.

A synthesis performed by Liu *et al.* afforded allyl 2-*N*-acetyl-3,4-di-*O*-acetyl-2-deoxy-6-*O*-tolylsulfonyl-α-*D*-mannopyranoside (**103**) using an allyl anomeric protecting group. This known approach could be useful to accomplish the synthesis of 2-*N*-acetyl-6-deoxy-*D*-mannosamine (**91**) (**Scheme 53**).[173]

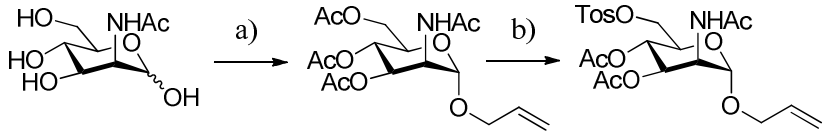

40 **102** **103**

Scheme 53 Literature protocol for the synthesis of allyl 2-*N*-acetyl-3,4-di-*O*-acetyl-2-deoxy-6-*O*-tolylsulfonyl-*α*-mannopyranoside (**103**). a) (i) Ac_2O, pyridine, r.t., O/N; (ii) Allyl alcohol, $BF_3 \bullet OEt_2$, CH_3NO_2, 40 °C, 3 h, 36% (over 2 steps) (**102**); b) (i) NaOMe, MeOH, r.t., 3 h; (ii) TosCl, pyridine, 0 °C, 7 h; (iii) Ac_2O, pyridine, r.t., O/N, 36% (over 3 steps) (**103**).[173]

The 2-*N*-acetyl-*D*-mannosamine (**40**) was acetylated using acetic anhydride in pyridine at room temperature overnight and subsequently treated with borontrifluoride dietherate in nitromethane at 40 °C for 3 hours to give allyl *per*-*O*-acetyl-2-*N*-acetyl-*D*-mannosamine (**102**) in 36% over the 2 steps.

The allyl *per*-*O*-acetyl-2-*N*-acetyl-*D*-mannosamine (**102**) was deprotected using sodium in methanol following Zemplén conditions and then subjected to *p*-toluenesulfonyl chloride in pyridine at 0 °C. Subsequent acetylation with acetic anhydride in pyridine overnight gave the allyl *per*-*O*-acetyl-2-*N*-acetyl-6-tosyl-*D*-mannosamine (**103**) in 36% yield over the 3 steps.[165] Reassessing the number of steps and taking into account the moderate yields obtained, the formation of 2-*N*-acetyl-6-deoxy-*D*-mannosamine (**91**) following this approach seemed not viable.

Therefore, a different approach by Liu *et al.* was pursued to form benzyl 2-*N*-acetyl-α-*D*-mannopyranoside (**104**).

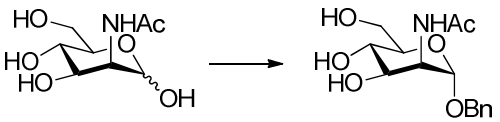

40 **104**

Scheme 54 Literature protocol for the synthesis of benzyl 2-*N*-acetyl-α-*D*-mannopyranoside (**102**). (i) Ac_2O, pyridine, r.t., O/N; (ii) BnOH, $BF_3 \bullet OEt_2$, CH_3NO_2, 80 °C, 3 h; (iii) NaOMe, MeOH, r.t., 1.5 h, 48% (over 3 steps).[173]

The 2-*N*-acetyl-*D*-mannosamine (**40**) was acetylated using acetic anhydride in pyridine at room temperature overnight (**Scheme 54**). The crude residue was then benzyl protected at the anomeric position using borontrifluoride dietherate, followed by acetyl deprotection using Zemplén conditions to give benzyl 2-*N*-acetyl-α-*D*-mannopyranoside (**104**) in 48% over the 3 steps (**Scheme 54**).[165]

The benzyl 2-*N*-acetyl-α-*D*-mannopyranoside (**104**) was subjected to iodine, triphenylphosphine and imidazole following an encouraging method developed by Garegg and Samuelsson to convert primary hydroxyl groups into an iodo group in the presence of secondary hydroxyl groups on carbohydrates (**Scheme 55**).[174-176]

The proposed mechanism of Garegg and Samuelsson's method proceeds via a phosphor-imidazolium cation a), which subsequently activates the primary hydroxyl group b) as a phosphonium oxide (**Scheme 55**). This activated hydroxyl group is then replaced by iodine in a nucleophilic substitution c).

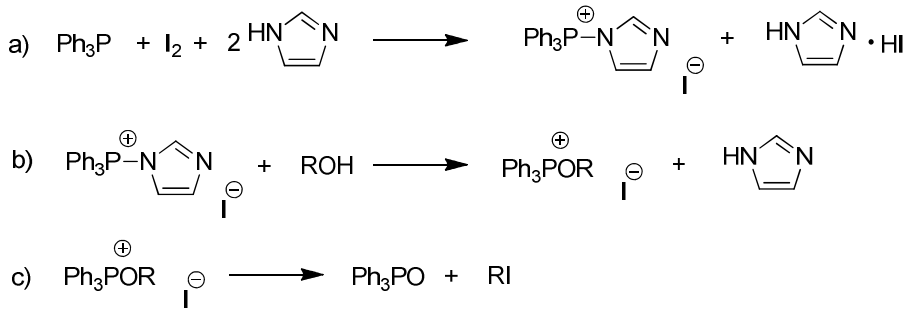

Scheme 55 Proposed mechanism for the conversion of primary hydroxyl groups into iodo groups in carbohydrates.[176]

Due to limited solubility of benzyl 2-*N*-acetyl-α-*D*-mannopyranoside (**104**) in toluene, nitromethane as a co-solvent was added. However, the reaction resulted in the formation of a highly polar side product (**Scheme 56**).

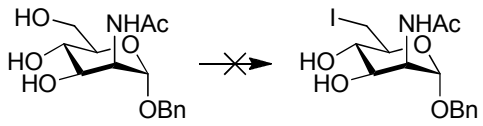

104 **105**

Scheme 56 Protocol of Garegg and Samuelsson to form benzyl 2-*N*-acetyl-6-iodo-α-*D*-mannopyranoside (**105**).[176] I_2, Ph_3P, imidazole, toluene/MeCN, 90 °C, 2 h.

In order to resolve the difficulties in the one step Garegg and Samuelsson process, the primary hydroxyl group at position C-6 was first converted into a tosyl group, using *p*-toluenesulfonyl chloride in pyridine at 0 °C to give benzyl 6-*O*-tolylsulfonyl-α-*D*-mannopyranoside derivative (**Scheme 57**). Subsequently, the tosyl group at position C-6 was treated with sodium iodide in acetone to give benzyl 2-*N*-acetyl-6-iodo-α-*D*-mannopyranoside (**103**) in 52% yield over the 2 steps (**Scheme 57**).

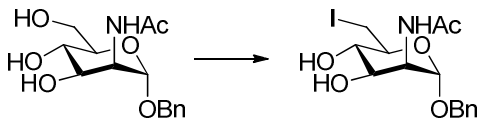

104 **105**

Scheme 57 Formation of benzyl 2-*N*-acetyl-6-iodo-*α*-*D*-mannopyranoside (**105**). (i) TosCl, pyridine, 0 ºC → r.t., 6 h; (ii) NaI, acetone, 50 ºC, 32 h, 52% (over 2 steps).

It was anticipated that hydrogenation of benzyl 2-acetyl-6-iodo-α-*D*-mannopyranoside (**105**) would remove the iodine at position C-6 as well as the benzyl protection group at the anomeric C-1 position to generate 2-*N*-acetyl-6-deoxy-*D*-mannosamine (**91**) and a number of hydrogenation conditions were examined (**Table 5**).

Table 5 Different conditions used for the synthesis of 2-*N*-acetyl-6-deoxy-*D*-mannosamine (**91**). **Condition A**: $Pd(OH)_2$/C, MeOH/H_2O; **Condition B**: Pd/C, THF/AcOH.

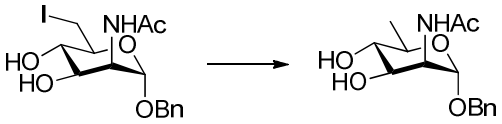

105 **106**

Entry	Condition	Time	T [°C]	Product
1	A	4 d	r.t.	**106**
2	A[a]	17 h	r.t.	**106**
3	A	17 h	40	**106**
4	B	17 h	40	**106**

[a] Condition A but hydrogenation was performed at 6 bar.

A number of hydrogenation protocols including alternative palladium catalysts, such as $Pd(OH)_2$ and solvent systems such as methanol/water and tetrahydrofuran/acetic acid together with raising the reaction temperature and hydrogen gas pressure only resulted in the isolation of benzyl 2-*N*-acetyl-6-deoxy-α-*D*-mannopyranoside (**106**) (**Table 5, entry 1 to 4**).

Hence, the removal of the benzyl protecting group at the anomeric position could not be accomplished.

Given the difficulties we encountered towards the synthesis of 2-*N*-acetyl-6-deoxy-*D*-mannosamine (**91**) we re-evaluated our synthetic strategy and concluded to focus our studies on methods to form 9-iodo-3-fluoro-sialic acid (**107**).

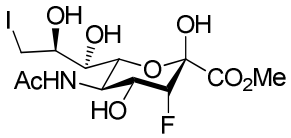

107

5.2 Synthesis of 9-deoxy-2,3-difluoro-sialic acid (27) via the 3-fluoro-9-iodo-sialic acid methyl ester (107)

5.2.1 Retrosynthetic analysis

Given the successful hemiketal fluorination with DAST in the synthesis of 4-deoxy-2,3-difluoro-sialic acid (**24**), 7-deoxy-2,3-difluoro-sialic acid (**25**) and 8-deoxy-2,3-difluoro-sialic acid (**26**), we considered a similar approach to perform the synthesis of 9-deoxy-2,3-difluoro-sialic acid (**27**) from the hemiketal (**108**) (**Scheme 58**).

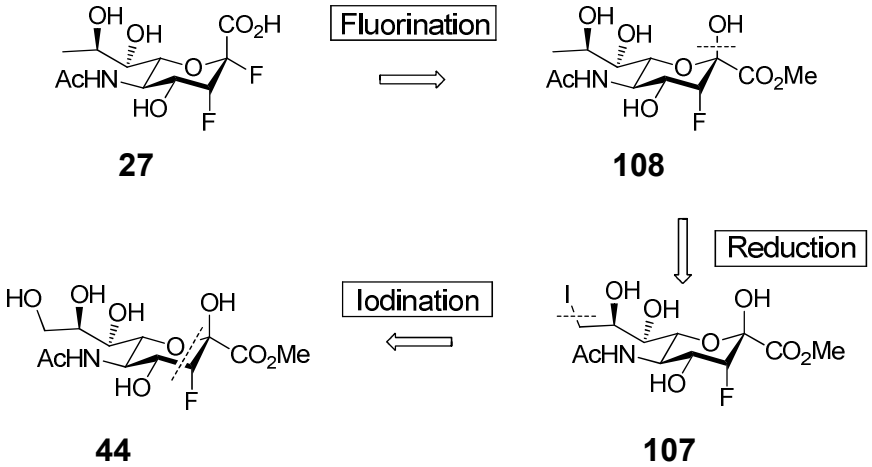

27 **108**

44 **107**

Scheme 58 Retrosynthetic strategy for the synthesis of 9-deoxy-2,3-difluoro-sialic acid (**27**) via the C-9 iodo-sialic acid (**107**).

The 9-deoxy-3-fluoro-sialic acid hemiketal (**108**) itself could be formed in a reduction reaction deploying dehalogen hydrogenation from 3-fluoro-9-iodo-sialic acid (**107**). It was anticipated that formation of 3-fluoro-9-iodo-sialic acid (**107**) could be achieved through a series of standard protecting group manipulations based upon the differential nucleophilicity of primary over secondary hydroxyl groups present in 3-fluoro-sialic acid methyl ester (**44**).
The synthesis of 3-fluoro-sialic acid methyl ester (**44**) using an enzymatic aldolase reaction of 2-*N*-acetyl-*D*-mannosamine (**40**) and β-fluoropyruvic acid (**41**) has previously been accomplished (Chapter 2.2.3).

5.2.2 Synthesis of 9-iodo-3-fluoro-sialic acid methyl ester (107)

The 3-fluoro-sialic acid methyl ester (**44**) was subjected to the previously employed method using iodine, triphenylphosphine and imidazole according to the method of Garegg and Samuelsson (Chapter 5.1.3) to form 3-fluoro-9-iodo-sialic acid (**107**) (**Scheme 59**).[176]

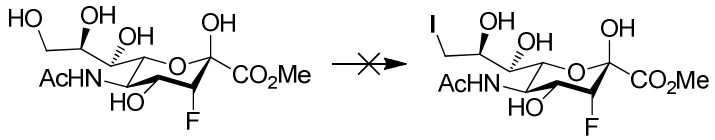

44 **107**

Scheme 59 Attempted formation of 3-fluoro-9-iodo-sialic acid methyl ester (**107**). I_2, Ph_3P, imidazole, toluene/MeCN, 90 °C, 2 h.

However, solubility issues of the starting material (**44**) and purification difficulties of triphenylphosphine oxide, which have previously been encountered on benzyl 2-*N*-acetyl-α-*D*-mannopyranoside (**104**) (Chapter 5.1.3) failed to give desired product (**107**).
To overcome the problems of the one-step Garegg and Samuelsson method, stepwise series of standard protecting group manipulations of the hydroxyl group at position C-9 with mesyl, tosyl or trityl followed by acetylation of position C-2, C-4, C-7 and C-8 with a subsequent nucleophilic substitution at position C-9 with iodine was attempted (**Scheme 60**).

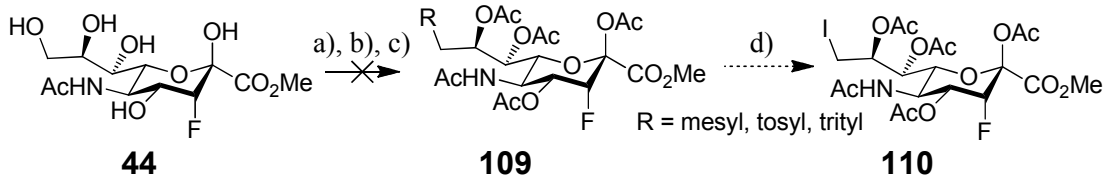

Scheme 60 Proposed synthesis of *per-O*-acetyl-3-fluoro-9-iodo-sialic acid methyl ester (**110**). a) (i) MesCl, pyridine, - 20 °C; (ii) Ac_2O, pyridine, r.t.; b) (i) TosCl, pyridine, 0 °C; (ii) Ac_2O, pyridine, r.t.; c) (i) Trityl chloride, pyridine, - 20 °C; (ii) Ac_2O, pyridine, r.t.; d) KI, butanone, 90 °C;

However, the conditions applied resulted in elimination of the protection group present at position C-9. A strategy based on a series of standard protecting group manipulations of the primary hydroxyl group at position C-9 such as silyl groups, followed by acetylation of position C-2, C-4, C-7 and C-8 with subsequent deprotection of position C-9 was considered to involve too many steps and was not attempted.

A known method deployed by Schreiner *et al.* subjected sialic acid methyl ester methyl glycoside (**111**) to thiophosgene and *p*-cresol to form a cyclic 8,9-*O*-carbonothioate derivative (**112**), which was then opened with iodomethane to give the C-9 iodo compound (**113**). Subsequently, the C-9 iodo compound (**113**) was treated with tributyltin hydride to give a 4,7,9-trideoxy derivative. It was anticipated that this approach could provide a vigorous method and could be used for the synthesis of 9-deoxy-2,3-difluoro-sialic acid (**27**) (**Scheme 61**).[177]

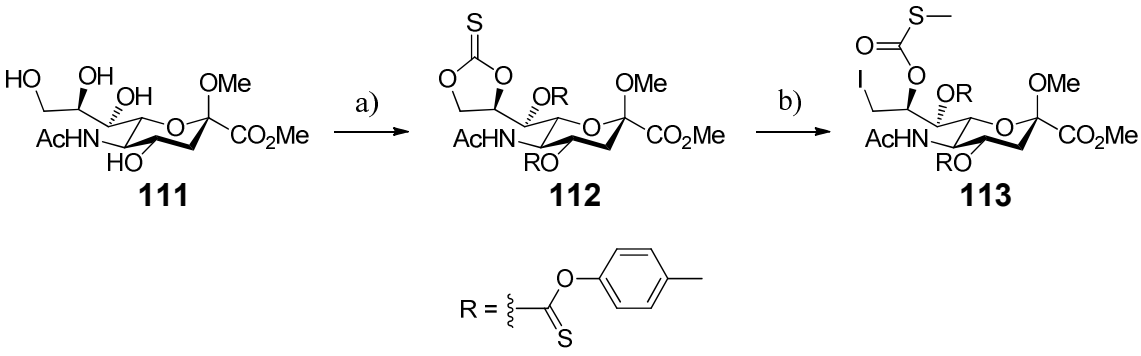

Scheme 61 Literature protocol for the synthesis 9-iodo-8-*O*-methylthiocarbonyl-sialic acid methyl ester (**113**). a) (i) $CSCl_2$, DMAP, CH_2Cl_2, - 45 °C; (ii) *p*-Cresol, 68% (**112**); b) CH_3I, 56 °C, O/N, 57% (**113**).[177]

The 2,4,7-tri-*O*-benzoyl-3-fluoro-8,9-*O*-isopropylidene-sialic acid methyl ester (**64**), a side product formed in the synthesis of 7-deoxy-2,3-difluoro-sialic acid (**25**) (Chapter 3.2), following isopropylidene deprotection could be used to generate a cyclic carbonothioate. Therefore, the 2,4,7-tri-*O*-benzoyl-3-fluoro-8,9-*O*-isopropylidene-sialic acid methyl ester (**64**) was subjected to acetic acid as previously deployed (Chapter 2.3.3) (**Scheme 62**).[161]

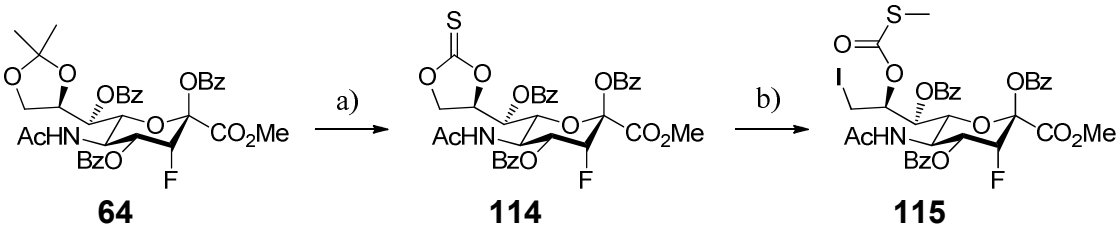

64 **114** **115**

Scheme 62 Synthesis of 2,4,7-tri-*O*-benzoyl-3-fluoro-9-iodo-8-*O*-methylthiocarbonyl-sialic acid methyl ester (**115**). a) (i) 80% AcOH/H_2O, 60 °C, 2 h; (ii) 1,1'-Thiocarbonyldiimidazole, CH_2Cl_2, 40 °C, 2 d, 81% (over 2 steps) (**114**); b) CH_3I, 56 °C, 20 h, 95% (**115**).

Next, the crude mixture was treated with thiophosgene according to the procedure of Schreiner *et al.* to form the cyclic 8,9-*O*-carbonothioate (**114**) but no desired product could be isolated.[177]

However, reaction of the crude mixture with 1,1'-thiocarbonyldiimidazole in anhydrous dichloromethane gave the desired 2,4,7-tri-*O*-benzoyl-8,9-*O*-carbonothioate-3-fluoro-sialic acid methyl ester (**114**) in 81% yield over the 2 steps (**Scheme 62**).

The 2,4,7-tri-*O*-benzoyl-8,9-*O*-carbonothioate-3-fluoro-sialic acid methyl ester (**114**) was then subjected to freshly distilled iodomethane at 56 °C overnight as previously deployed by Schreiner *et al.* to give the 9-iodo-8-*O*-methylthiocarbonyl-sialic acid derivative (**115**) in 95% yield.

5.2.3 Formation of 9-deoxy-3-fluoro hemiketal (118)

The 9-iodo-8-*O*-methylthiocarbonyl-sialic acid derivative (**115**) was then subjected to Barton-McCombie deoxygenation conditions using Luperox® 101 as a radical initiator and the radical carrier tributyltin hydride under reflux conditions in 1,4-dioxane as previously deployed on 7-*O*-thiocarbamate-sialic acid methyl ester (**68**) (Chapter3.2) to give the 9-deoxy-3-fluoro-8-*O*-methylthiocarbonyl-sialic acid derivative (**114**) in 98% yield (**Scheme 63**).

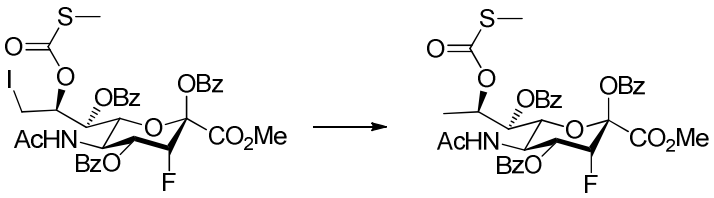

115 **116**

Scheme 63 Synthesis of 2,4,7-tri-*O*-benzoyl-9-deoxy-3-fluoro-8-*O*-methylthiocarbonyl-sialic acid methyl ester (**116**). Luperox® 101, Bu_3SnH, 1,4-dioxane, 100 °C, 4 h, 98%.

The 9-deoxy-3-fluoro-8-*O*-methylthiocarbonyl-sialic acid derivative (**114**) was then globally deprotected using sodium in methanol according to Zemplén conditions and subsequently acetylated utilising acetic anhydride in pyridine to give the *per*-*O*-acetyl-9-deoxy-3-fluoro-sialic acid methyl ester (**117**) (**Scheme 64**) in 77% yield over the 2 steps.[165]

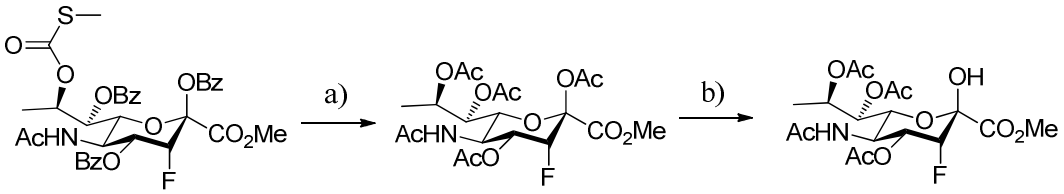

116 **117** **118**

Scheme 64 Formation of 4,7,8-tri-*O*-acetyl-9-deoxy-3-fluoro-sialic acid methyl ester (**118**). a) (i) NaOMe, MeOH, r.t., O/N; (ii) Ac_2O, DMAP, pyridine, r.t., O/N, 77% (over 2 steps) (**117**); b) Hydrazine acetate, CH_2Cl_2/MeOH, 4 °C, O/N, 68% (**118**).

Finally, the *per*-*O*-acetyl-9-deoxy-3-fluoro-sialic acid methyl ester (**117**) was deprotected at position C-2 with hydrazine acetate in dichloromethane and methanol at 4 °C as previously described on *per*-*O*-acetyl-4-deoxy-3-fluoro-sialic acid methyl ester (**52**) (Chapter 2.3.3) to afford hemiketal (**118**).

5.2.4 Synthesis of 9-deoxy-2,3-difluoro-sialic acid (27)

The hemiketal (**118**) was then treated with DAST in dichloromethane at - 40 °C → - 10 °C according to the methodology previously deployed on hemiketal (**53**) (Chapter 2.3.4) to afford a mixture of α- and β-fluoride anomers (**Scheme 65**).

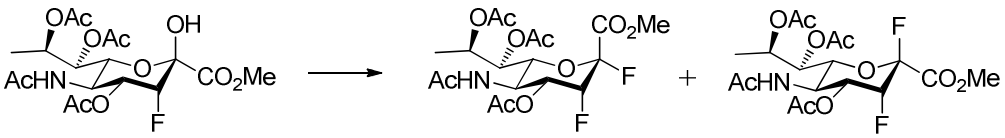

118 **119** **120**

Scheme 65 Synthesis of 9-deoxy-2,3-difluoro-sialic acid methyl ester anomers (**119**) and (**120**). DAST, CH_2Cl_2, - 40 ºC → - 10 ºC, 1 hr, 38% (**119**), 38% (**120**).

The formation of a mixture of anomers is in agreement with results previously observed on hemiketal (Chapter 2.3.4). The mixture of anomers was purified by silica column chromatography and gave the anomers in a ratio of 1:1 in 38% yields respectively.

The *per-O*-acetyl-9-deoxy-α-2,3-difluoro-sialic acid methyl ester (**119**) was then globally deacetylated using sodium in methanol at room temperature following Zemplén conditions. Finally, ester saponification of the crude residue with 0.5M sodium hydroxide solution in water gave the desired 9-deoxy-2,3-difluoro-sialic acid (**27**) after column chromatography in 99% over the 2 steps (**Scheme 66**).[165]

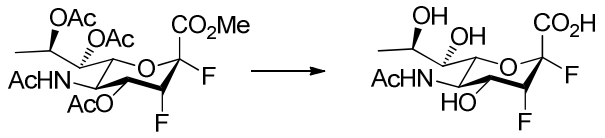

119 **27**

Scheme 66 Formation of 9-deoxy-2,3-difluoro-sialic acid (**27**). (i) NaOMe, MeOH, r.t., 3 h; (ii) 0.5M NaOH, H_2O, r.t, 30 min., 99% (over 2 steps).

The total synthesis from β-fluoropyruvic acid (**41**) to 9-deoxy-2,3-difluoro-sialic acid (**27**) was achieved in 14 steps, with an overall yield of 9%.

Chapter 6 - Kinetic analysis of inactivation of influenza neuraminidase by monodeoxygenated 2,3-difluoro-sialic acids

6.1 Preface

A general mechanism for inactivation of influenza neuraminidase by mechanism-based inactivators can be expressed by the following scheme with K_i being the dissociation constant of inhibition/inactivation and (*E-I*) being the covalent sialosyl-enzyme intermediate (**Scheme 67**).

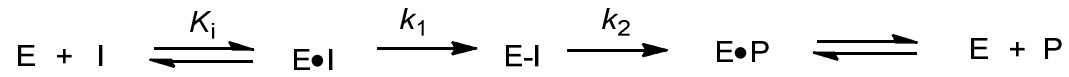

Scheme 67 Equilibrium scheme for mechanism-based inactivators with enzyme. - Enzyme (*E*), inactivator (*I*), Michaelis complex (*E•I*) and *(E•P*), rate of glycosylation (k_1), rate of deglycosylation (k_2), dissociation constant for inhibition/inactivation (K_i) and product (*P*).

Recent unpublished work by the research groups of Dr. Andrew Watts and Prof. Stephen Withers has shown that 2,3-difluoro-sialic acid (**23**) attenuates the rate of glycosylation (k_1) and deglycosylation (k_2) of influenza neuraminidase, allowing the covalently linked sialosyl-enzyme intermediate (*E-I*) to be kinetically accessible and accumulate to a high steady-state concentration, whereby the enzyme is inactivated. We proposed that on influenza neuraminidase the putative mechanism-based inactivators (**24**) - (**27**) operate through a similar mechanism.

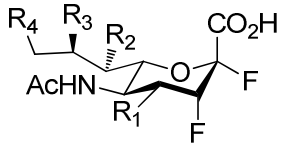

23 R_1, R_2, R_3, R_4 = OH

24 R_1 = H, R_2, R_3, R_4 = OH

25 R_2 = H, R_1, R_3, R_4 = OH

26 R_3 = H, R_1, R_2, R_4 = OH

27 R_4 = H, R_1, R_2, R_3 = OH

This chapter will first discuss inactivation kinetics of influenza G70C/H1N9/wt. by the monodeoxygenated 2,3-difluoro-sialic acid putative inactivators (**24**) - (**27**). The time-dependent inactivation study of influenza neuraminidase N9 G70C was based on a previous inactivation study performed on *Trypanosoma rangeli* with 2,3-difluoro-sialic acid (**23**) by Watts and Withers.[12]

Furthermore, the monodeoxygenated 2,3-difluoro-sialic acid putative inactivators (**24**) - (**27**) have been evaluated in IC_{50} measurements against a panel of influenza viruses including wild types (wt.) and Oseltamivir (**6**) resistant mutants by our collaborators and the results will be discussed.[178]

Finally, plaque reduction assays as the first stage of *in* vivo assays were performed on the 4-deoxy-2,3-difluoro-sialic acid (**24**) and the 8-deoxy-2,3-difluoro-sialic acid (**26**) by our collaborators and the results will be analysed in this chapter.

6.2 Time-dependent inactivation of wild type influenza neuraminidase N9 G70C by monodeoxygenated 2,3-difluoro-sialic acids

Influenza neuraminidase G70C/H1N9/wt. was chosen for inactivation kinetics as this strain has previously been utilised in enzyme inhibition kinetics by Blick *et al.,*[118] which in conjunction with extensive X-ray crystal structures on G70C/H1N9/wt. allows interpretation of inactivation kinetics on a physical basis.[128]

An assay measuring the time-dependent fluorescent intensity of the hydrolysed 4-methylumbelliferone from the substrate 2′-(4-methylumbelliferyl) α-*D*-*N*-acetylneuraminic acid (**121**) by influenza neuraminidase G70C/H1N9/wt. at different monodeoxygenated 2,3-difluoro-sialic acid inactivator (**24**) - (**27**) concentrations has to be developed.

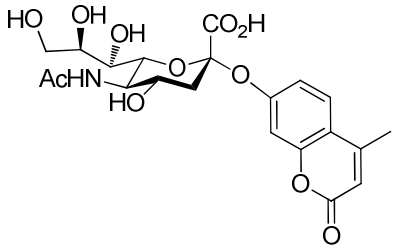

121

A reduction in the fluorescence intensity correlates with the association of the inactivator to the enzyme, which results in a slower rate of the enzyme processing the substrate and less 4-methylumbelliferone being released. A time-dependent inactivation assay investigating the inactivation of *Trypanosoma cruzi* trans-sialidase by 2,3-difluoro-sialic acid (**23**) based on the reduction of the fluorescent intensity has previously been performed by Buchini *et al*.[168]

In general, the time-dependent inactivation assay of influenza neuraminidase 70C/H1N9/wt., which was kindly provided by Dr. Jennifer McKimm-Breschkin (Materials Science and Engineering, CSIRO, Australia), was performed at 37 °C in 1 mM NaOAc buffer pH 5.5, 0.1 mM $CaCl_2$ and 0.2 mM 2′-(4-methylumbelliferyl) α-*D*-*N*-acetylneuraminic acid (**121**) in duplicate on a 96 well plate. The fluorescence intensity of the hydrolysed 4-methylumbelliferone was monitored over 30 minutes following addition of the substrate 2′-(4-methylumbelliferyl) α-*D*-*N*-acetylneuraminic acid (**121**), using an excitation wavelength of 355 nm and an emission wavelength of 460 nm for 6 different incubation time-points at 5 different concentrations of inactivator. The measured activity with no inactivator gave the maximum activity, and was set to 100%. The activities obtained for the different concentrations of inactivator were correlated to this maximum activity to give the residual activities.

6.2.1 Time-dependent inactivation of wild type influenza neuraminidase N9 G70C by 4-deoxy-2,3-difluoro-sialic acid (24)

Time-dependent inactivation studies of influenza neuraminidase G70C/H1N9/wt. were performed utilising the general inactivation assay in 5 different concentrations of the putative mechanism-based inactivator 4-deoxy-2,3-difluoro-sialic acid (**24**).

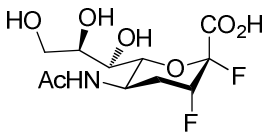

24

As such, concentrations of 200, 100, 50, 25 and 10 nM of inactivator (**24**) and incubation times of 5, 10, 15, 25, 35 and 50 minutes were deployed and the residual activities were plotted *versus* time (**Graph 2**).

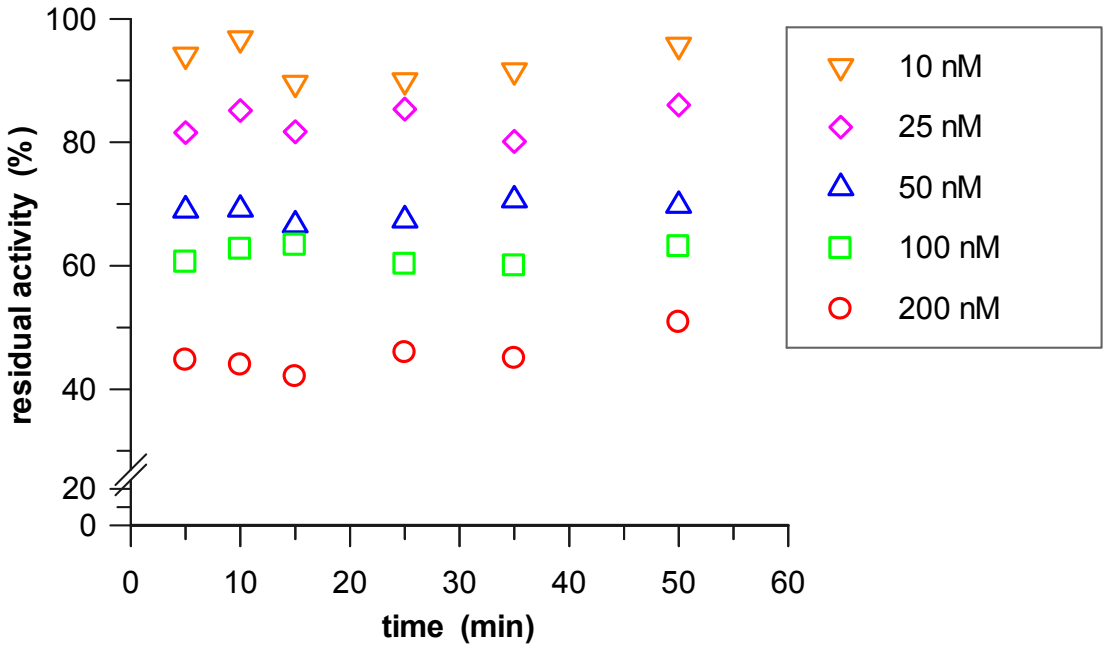

Graph 2 Residual activity of wild type neuraminidase N9 G70C with inactivator 4-deoxy-2,3-difluoro-sialic acid (**24**) *versus* time (unpublished results).

It can clearly be seen from (**Graph 2**) that increasing the concentration of 4-deoxy-2,3-difluoro-sialic acid (**24**) inactivator results in a decrease of residual activity. However, it can also be seen that the residual activity remains constant at incubation time-points from 5 to 35 minutes, indicating no time-dependent inactivation. A similar result has been observed for inactivation kinetics on α-glycosidases and 5-fluoro-α-glycosyl fluorides performed by Howard *et al*, which gave fast glycosylation on a time scale shorter than the assay time.[179] Based on inactivation kinetics of *Trypanosoma rangeli* neuraminidase with 2,3-difluoro-sialic acid (**23**), which also showed fast turnover and have previously been performed by Watts *et al.,*[12] it was concluded that the rate of 4-deoxy-2,3-difluoro-sialic acid (**24**) inactivator glycosylation (k_1) by influenza neuraminidase G70C/H1N9/wt. to form the sialosyl-enzyme intermediate takes place faster than the assay time.

A number of methods have been reported to reduce the rate of intermediate formation. These include using lower inhibitor concentrations (which could also result in increased ratio of reactivation), reducing the temperature of the assay, use of a competitive inhibitor during inactivation (in case of influenza neuraminidase with a competitive inhibitor like DANA), or stopped-flow kinetic experiments.[12]

It can also be seen, that after incubation of 50 minutes increasing residual activities were observed, indicating reactivation (**Graph 2**). This reactivation might represent fast deglycosylation (k_2) of the 4-deoxy-2,3-difluoro-sialic acid (**24**) inactivator.

Since the 4-deoxy-2,3-difluoro-sialic acid (**24**) inactivator did not display time-dependent inactivation characteristics, but steady-state characteristics we investigated the properties of the inactivator as a competitive inhibitor obeying Michaelis-Menten parameters to calculate IC_{50} values.[179] Hence, the mean residual activities at incubation time-points from 5 to 35 minutes including their standard errors were re-plotted against the inactivator concentration, [**24**], using GraFit 5.0.13 (**Graph 3**).[180]

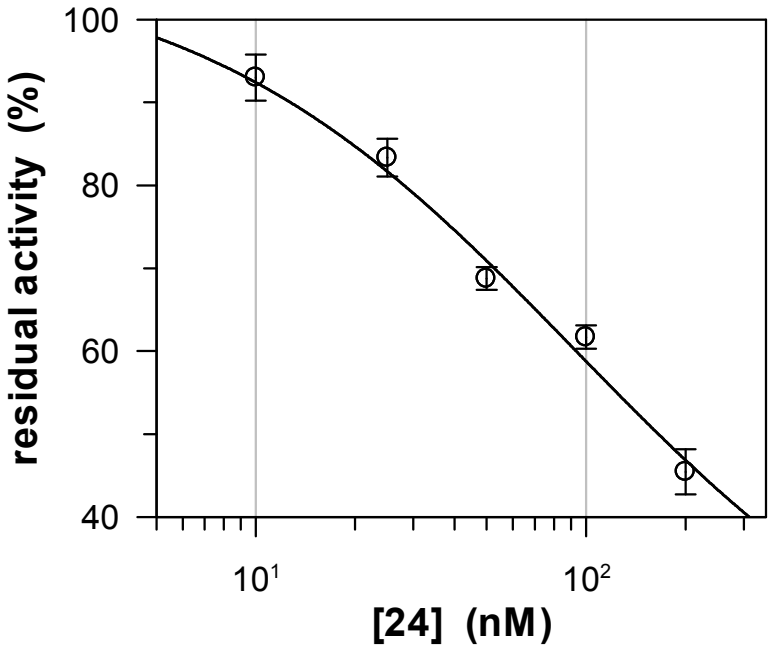

Graph 3 Residual activity of wild type neuraminidase N9 G70C *versus* concentration of inactivator 4-deoxy-2,3-difluoro-sialic acid (**24**) (unpublished results).

The inhibition data was then fitted to the non-linear 4 parameter equation (**Equation 1**) to give the parameters for y range, slope factor, background and for the inhibition of influenza neuraminidase G70C/H1N9/wt. by 4-deoxy-2,3-difluoro-sialic acid (**24**) an encouraging IC_{50} value of 92 $\pm$ 71 nM (**Table 6**).

$$y = \frac{Range}{1 + \left(\frac{x}{\mathrm{IC}_{50}}\right)^{S}} + Background$$

Equation 1 Four parameter equation for the calculation of IC_{50} values. The range is the fitted uninhibited value minus the background, and *S* is a slope factor. Equation fulfilled if *y* falls with increasing *x*.

Table 6 Non-linear fit of the inhibition data of 4-deoxy-2,3-difluoro-sialic acid (**24**) on G70C/H1N9/wt. to four parameter equation (**Equation 1**).

	Value	Std. error
y range	93.6650	53.9331
IC_{50}	91.9577	71.2254
Slope factor	0.7583	0.6975
Background	13.4222	38.7926

6.2.2 Time-dependent inactivation of wild type influenza neuraminidase N9 G70C by 7-deoxy-2,3-difluoro-sialic acid (25)

Time-dependent inactivation studies of influenza neuraminidase G70C/H1N9/wt. were performed utilising the general inactivation assay in 5 different concentrations of the putative mechanism-based inactivator 7-deoxy-2,3-difluoro-sialic acid (**25**).

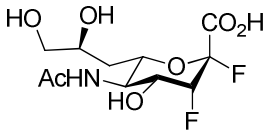

25

As such, concentrations of 50, 25, 10, 5 and 1 µM of inactivator (**25**) and incubation times of 5, 10, 15, 25, 35 and 50 minutes were deployed and the residual activities were plotted *versus* time (**Graph 4**).

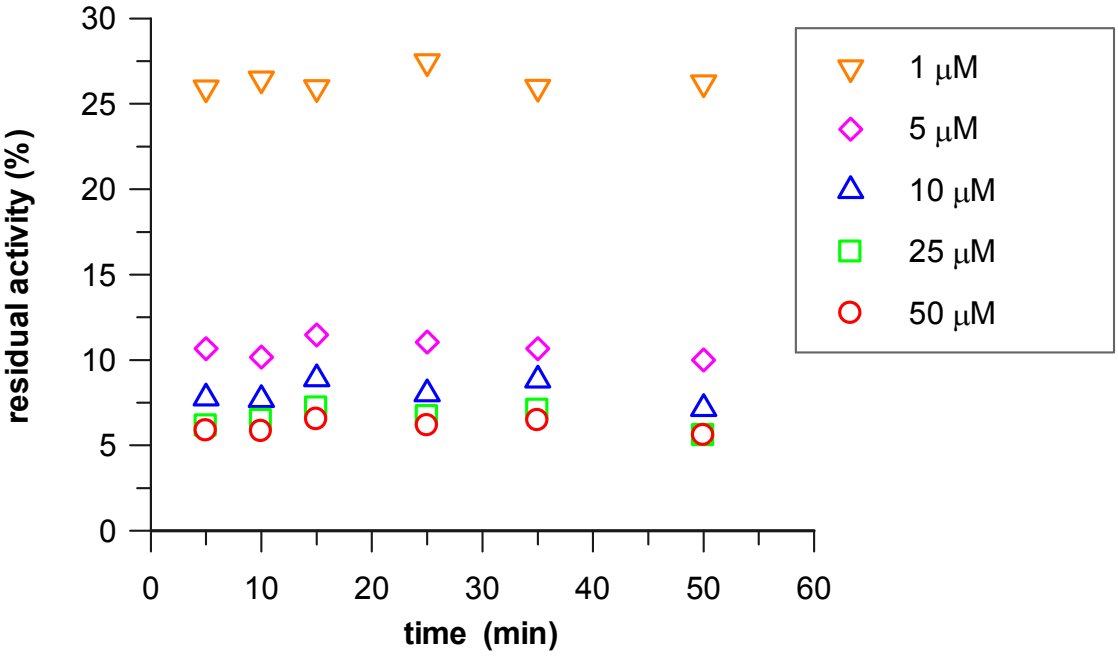

Graph 4 Residual activity of wild type neuraminidase N9 G70C with inactivator 7-deoxy-2,3-difluoro-sialic acid (**25**) *versus* time (unpublished results).

It can clearly be seen from (**Graph 4**) that increasing the concentration of 7-deoxy-2,3-difluoro-sialic acid (**25**) inactivator results in a decrease of residual activity.

It also can be seen that the residual activity remains constant for the incubation time points from 5 to 50 minutes (**Graph 4**). This lack of time-dependent inactivation is similar to the inactivation behaviour of 4-deoxy-2,3-difluoro-sialic acid (**24**) (Chapter 6.2.1) and as previously proposed can be due to the fast rate of glycosylation (k_1), on a time scale shorter than the assay time.[179]

In contrast to inactivation kinetics of 4-deoxy-2,3-difluoro-sialic acid (**24**), the 7-deoxy-2,3-difluoro-sialic acid (**25**) showed no reactivation after 50 minutes, which might indicate a slow deglycosylation (k_2) and an accumulation of high steady-state concentration of the covalent intermediate, whereby the enzyme is inactivated (**Graph 4**).

Unfortunately, the inactivation assay for the range of concentrations of inactivator 7-deoxy-2,3-difluoro-sialic acid (**25**) gave residual activities lower than 30%. Hence, it was not possible to determine an IC_{50} value for the inactivation of 7-deoxy-2,3-difluoro-sialic acid (**25**) on influenza neuraminidase G70C H1N9.

6.2.3 Time-dependent inactivation of wild type influenza neuraminidase N9 G70C by 8-deoxy-2,3-difluoro-sialic acid (26)

Time-dependent inactivation studies of influenza neuraminidase G70C/H1N9/wt. were performed utilising the general inactivation assay in 4 different concentrations of the putative mechanism-based inactivator 8-deoxy-2,3-difluoro-sialic acid (**26**).

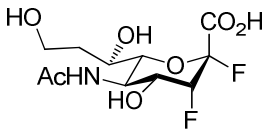

26

As such, concentrations of 50, 25, 10 and 1 µM of inactivator (**26**) and incubation times of 5, 10, 15, 25 and 35 were deployed and the residual activities were plotted *versus* time (**Graph 5**).

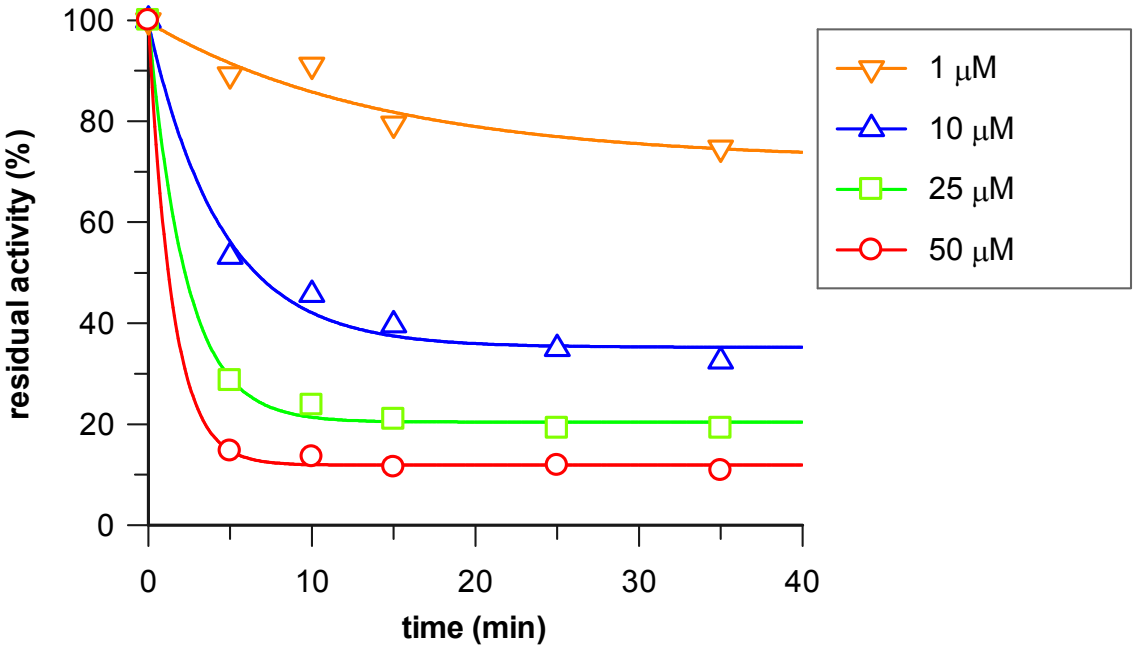

Graph 5 Residual activity of wild type neuraminidase N9 G70C with inactivator 8-deoxy-2,3-difluoro-sialic acid (**26**) *versus* time (unpublished results).

A clear time-dependent inactivation of wild type influenza neuraminidase N9 G70C by 8-deoxy-2,3-difluoro-sialic acid (**26**) was seen (**Graph 5**), which could be consistent with a kinetic model whereby the rate of deglycosylation (k_2) is significantly slower than the rate of glycosylation (k_1) for high inactivator concentrations.[168] However, particularly at lower inactivator concentrations, the inactivation was not complete and steady-state characteristics can be observed (**Graph 5**), which could be due more rapid rates of deglycosylation (k_2).

This steady-state allows determination of an apparent dissociation constant for inhibition/inactivation K_i' (**Equation 2**) which takes the form of the Michaelis-Menten expression for K_M.

$$K_i' = \frac{K_i}{(1 + \frac{k_1}{k_2})}$$

Equation 2 Equation for the apparent dissociation constant for inhibition/inactivation K_i' in steady-state conditions with dissociation constant of inhibition/inactivation K_i, the rate of glycosylation k_1 and the rate of deglycosylation k_2.

The residual activity plotted *versus* time (**Graph 5**) was used to calculate first order rate constants for each concentration of inactivator 8-deoxy-2,3-difluorosialic acid (**26**) by fitting a single exponential decay with offset (**Equation 3**) to the measured residual activities (**Table 7**) using GraFit 5.0.13.[180] The single exponential decay with offset was chosen as the experimental data retained a steady-state with a discrete residual activity.

$$y = A_0 e^{-kt} + offset$$

Equation 3 Single exponential decay that decays to a non-zero value.

The rate constants calculated (**Table 7**) were then used to generate the Lineweaver-Burk plot with the inverse of rate constants *versus* the inverse of the inactivator (**26**) concentrations (**Graph 6**).[181]

Table 7 Results of single exponential curve fitting with offset to residual activities over time for each concentration of 8-deoxy-2,3-difluorosialic acid (**26**).

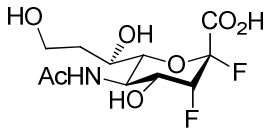

26

	50 μM (X1)		25 μM (X2)		10 μM (X3)	
	Value	Std. error	Value	Std. error	Value	Std. error
Initial value	88.1126	1.2659	79.5657	1.9659	64.2365	3.9324
Rate constant	0.6828	0.0837	0.4405	0.0443	0.2239	0.0354
Offset	11.8862	0.5745	20.4026	0.9287	35.2395	2.1834

	1 μM (X5)	
	Value	Std. error
Initial value	27.4192	7.1426
Rate constant	0.0698	0.0438
Offset	72.1606	7.1943

$$\frac{1}{V} = \frac{K_i}{V_m\,[\text{Inhibitor}]} + \frac{1}{V_m}$$

Equation 4 Lineweaver-Burk equation for Michaelis-Menten kinetics with reaction rate V, dissociation constant of inhibition/inactivation K_i, maximum reaction rate V_m and inhibitor concentration [inhibitor].

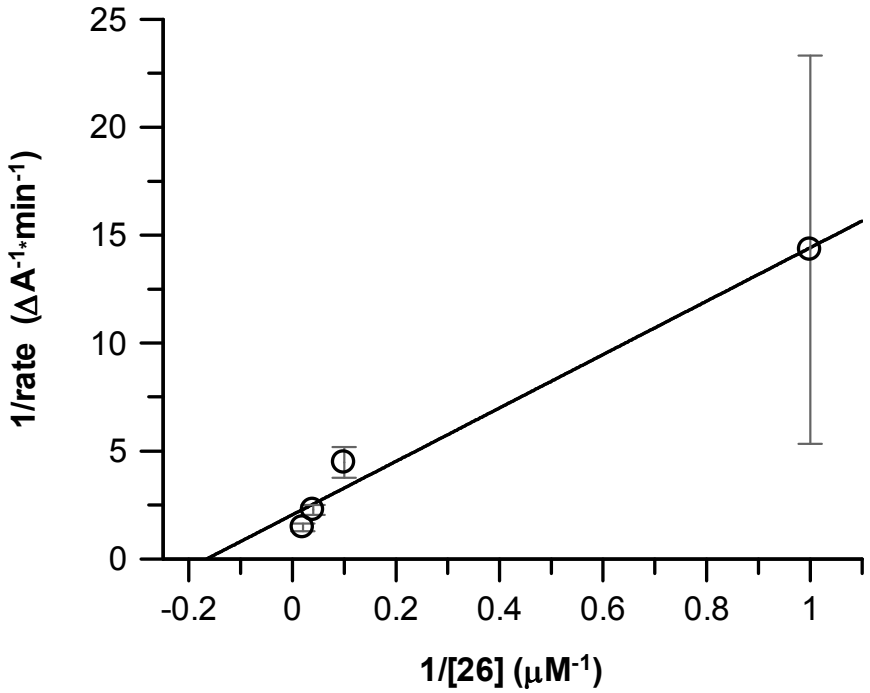

Graph 6 Lineweaver-Burk plot of wild type influenza neuraminidase N9 G70C with inactivator 8-deoxy-2,3-difluoro-sialic acid (**26**). The intercept at the *x* axis gives the inverse of K_i, the intercept at the *y* axis the inverse of V_m and a gradient of K_i/V_m.

The apparent dissociation constant for inhibition/inactivation K_i' was then readily determined through linear regression of the Lineweaver-Burk plot (**Graph 6**) with the intercept at the *x* axis giving the inverse of K_i' (**Table 8**). The K_i' of 8-deoxy-2,3-difluoro-sialic acid (**26**) on influenza neuraminidase G70C/H1N9/wt. was determined as 6.1 $\pm$ 1.99 µM.

Table 8 Linear regression of the Lineweaver-Burk plot (**Graph 6**).

	Value	Std. error
a (intercept)	2.0432	0.6372
b (gradient)	12.3747	1.2668
Correlation coefficient	0.9897	

6.2.4 Time-dependent inactivation of wild type influenza neuraminidase N9 G70C by 9-deoxy-2,3-difluoro-sialic acid (27)

Time-dependent inactivation studies of influenza neuraminidase G70C/H1N9/wt. were performed utilising the general inactivation assay in 5 different concentrations of the putative mechanism-based inactivator 9-deoxy-2,3-difluoro-sialic acid (**27**).

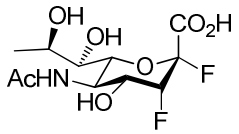

27

As such, concentrations of 25, 10, 5, 2 and 1 µM of inactivator (**27**) and incubation times of 5, 10, 15, 25 and 35 were deployed and the residual activities were plotted *versus* time (**Graph 7**).

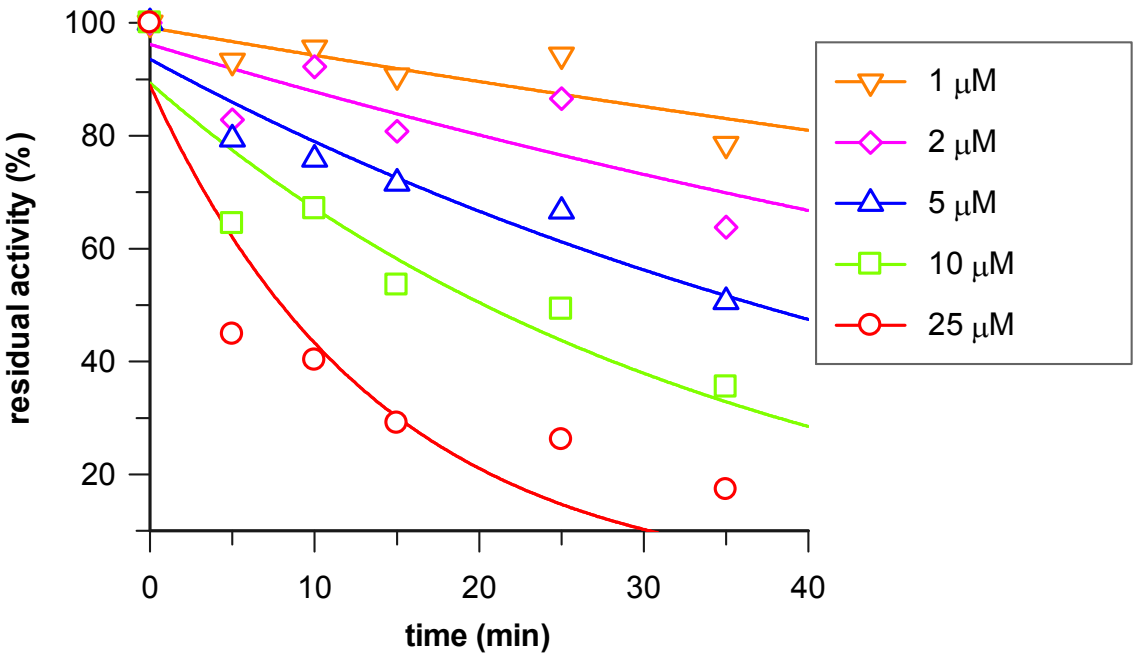

Graph 7 Residual activity of wild type neuraminidase N9 G70C with inactivator 9-deoxy-2,3-difluoro-sialic acid (**27**) *versus* time (unpublished results).

A clear time-dependent inactivation of wild type influenza neuraminidase N9 G70C by 9-deoxy-2,3-difluoro-sialic acid (**27**) was seen and an increase in the concentration of inactivator (**27**) resulted in a decrease of residual activity (**Graph 7**). It also can be seen that the inactivation did not reach a discrete residual activity after 35 minutes, indicating a slower rate of glycosylation (k_1). However, it was proposed that the residual activities might level off to a discrete standard to give steady-state characteristics. This steady-state allows determination of an apparent dissociation constant for inhibition/inactivation K_i' (**Equation 2**) which takes the form of the Michaelis-Menten expression for K_M.

The residual activity plotted *versus* time (**Graph 7**) was used to calculate first order rate constants for each concentration of inactivator 9-deoxy-2,3-difluoro-sialic acid (**27**) by fitting a single exponential decay without offset (**Equation 5**) to the measured residual activities (**Table 9**) using GraFit 5.0.13.[180] The single exponential decay without offset was chosen as the inactivator expressed slow-binding kinetics with proposed steady-state characteristics, but experimental conditions applied did not allow determination of the discrete residual activity offset.

$$y = A_0 e^{-kt}$$

Equation 5 Single exponential decay without offset.

The rate constants calculated (**Table 9**) were then used to generate the Lineweaver-Burk plot with the inverse of rate constants *versus* the inverse of the [**27**] (**Graph 8**).[181]

Table 9 Results of single exponential curve fitting without offset to residual activities over time for each concentration of 9-deoxy-2,3-difluorosialic acid (**27**).

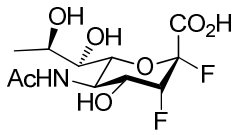

27

	25 μM (X1)		10 μM (X2)		5 μM (X3)	
	Value	Std. error	Value	Std. error	Value	Std. error
Initial value	88.8962	11.5054	89.3275	7.1433	93.5438	4.0750
Rate constant	0.0720	0.0187	0.0286	0.0064	0.0170	0.0029

	2 μM (X4)		1 μM (X5)	
	Value	Std. error	Value	Std. error
Initial value	27.4192	7.1426	27.4192	7.1426
Rate constant	0.0698	0.0438	0.0698	0.0438

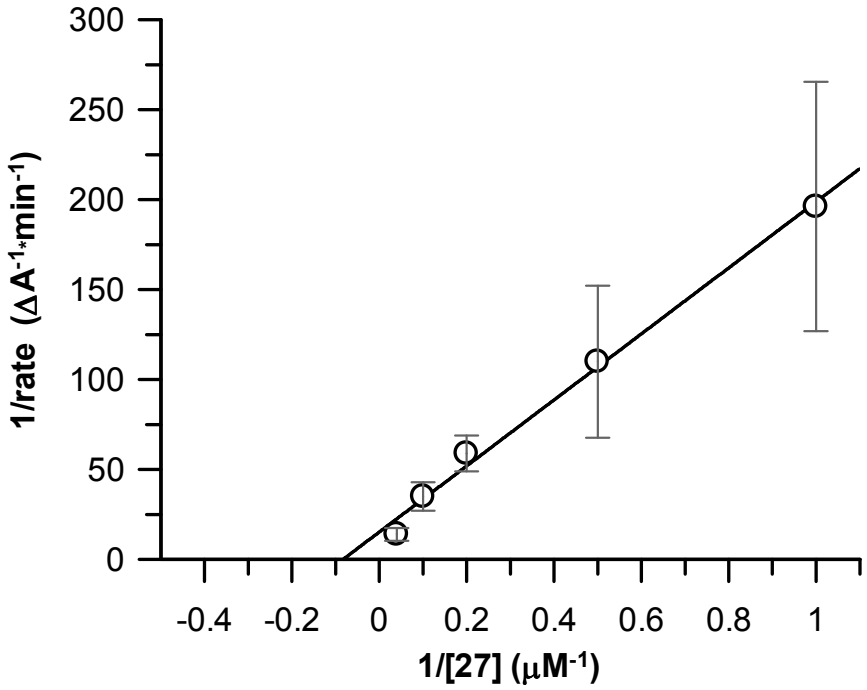

Graph 8 Lineweaver-Burk plot of wild type neuraminidase N9 G70C with 9-deoxy-2,3-difluoro-sialic acid (**27**). The intercept at the x axis gives the inverse of K_i, the intercept at the y axis the inverse of V_m and a gradient of K_i/V_m.

The apparent dissociation constant for inhibition/inactivation K_i' was then readily determined through linear regression of the Lineweaver-Burk plot (**Graph 8**) with the intercept at the *x* axis giving the inverse of K_i' (**Table 10**). The K_i' of 9-deoxy-2,3-difluoro-sialic acid (**27**) on influenza neuraminidase G70C/H1N9/wt. was determined as 12.1 $\pm$ 1.96 µM.

Table 10 Linear regression of the Lineweaver-Burk plot (**Graph 8**).

	Value	Std. error
a (intercept)	15.1856	4.4157
b (gradient)	183.5423	8.6537
Correlation coefficient	0.9967	

The preliminary inactivation results of wild type influenza neuraminidase N9 G70C gave K_i' values in the low µM range for 8-deoxy-2,3-difluoro-sialic acid (**26**) and 9-deoxy-2,3-difluoro-sialic acid (**27**) and an encouraging IC_{50} value in the low nM range for 4-deoxy-2,3-difluoro-sialic acid (**24**).

However, the ambiguous properties for the rate of glycosylation (k_1) and deglycosylation (k_2) of wild type influenza neuraminidase N9 G70C by the monodeoxygenated 2,3-difluoro-sialic acid inactivators (**24**) - (**27**) prompted us to further investigate the time-dependent inactivation and reactivation. In addition to time-dependant inactivation of influenza neuraminidase N9 G70C, a panel of influenza viruses also will be explored.

6.3 Inhibitory studies of monodeoxygenated 2,3-difluoro-sialic acids against a panel of influenza viruses

In addition to time-dependant inactivation of influenza neuraminidase N9 G70C, the inactivation of a panel of influenza viruses also will be explored to begin to examine whether neuraminidase inhibition is consistent across a range of serotypes. This set of experiments was performed by our collaborator Sue Barrett, Molecular and Health Technologies, CSIRO, Australia. A description of the influenza strains and mutants tested will be given in the summary. Since the efficacy of the mechanism-based 2,3-difluoro-sialic acid inactivators (**24**) - (**27**) is dependent on the combination of rate of glycosylation (k_1) and deglycosylation (k_2) the IC_{50} measurements were executed in two different experimental modes.[54] Experiments with no pre-incubation and experiments with pre-incubation of inactivator and influenza neuraminidase for 30 minutes prior to addition of the substrate 2′-(4-methylumbelliferyl) α-*D*-N-acetylneuraminic acid (**121**) were performed.[182]

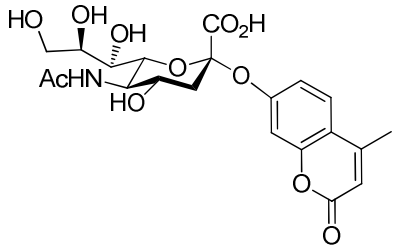

121

The experiment with no pre-incubation is used to follow the rate of glycosylation (k_1) of the inactivator with the influenza neuraminidase over a 60 minutes period.

On the other hand, the experiment with pre-incubation prior to the addition of substrate (**121**), allows the examination of further association processes, such as conformational changes of the enzyme and gives qualitative information concerning the rate of deglycosylation (k_2) of the inactivator-influenza neuraminidase complex.

To clarify: The inactivator IC_{50} kinetic assay was performed by our collaborators (Molecular and Health Technologies, CSIRO, Australia), while the analysis and interpretation of the results obtained was performed by the author.

6.3.1 IC_{50} analysis of monodeoxygenated 2,3-difluoro-sialic acids against a panel of influenza viruses

The 2,3-difluoro-sialic acid derivative (**23**) has previously been identified by Watts *et al.* (unpublished results) to be a time-dependent mechanism-based inactivator of influenza neuraminidases (unpublished results), also referred to as slow binding inactivator.

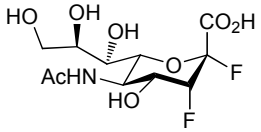

23

The loss of the slow-binding characteristics often correlates with resistances towards influenza neuraminidases.[183-186] However, as as we previously described only the 8-deoxy-2,3-difluoro-sialic acid (**26**) and 9-deoxy-2,3-difluoro-sialic acid (**27**) inactivator gave time-dependent inactivation characteristics whereas time-dependent inactivation could not be observed for the 4-deoxy-2,3-difluoro-sialic acid (**24**) and the 7-deoxy-2,3-difluoro-sialic acid (**25**) (Chapter 6.2). To further investigate this behaviour on an extensive panel of influenza neuraminidase a novel influenza neuraminidase inactivator IC_{50} kinetic assay was developed.[54]

In general, the inactivator IC_{50} kinetic assay without pre-incubation was performed on a variety of influenza neuraminidases with a series of dilutions of inactivator and the fluorescence intensity was monitored in 10 minute intervals for 60 minutes after addition of substrate (**121**).

The inactivator IC_{50} kinetic assay with pre-incubation was performed with 30 minutes pre-incubation of influenza neuraminidase with inactivator prior to the addition of substrate (**121**). Subsequently, the fluorescence intensity was monitored in 10 minute intervals for 60 minutes.

The inactivator IC_{50} kinetic assay without pre-incubation of 2,3-difluoro-sialic acid (**23**) showed a decrease in the IC_{50} values over time in the range of 1 µM across the panel of influenza neuraminidases tested, indicating slow-binding characteristics (**Graph 9a**).

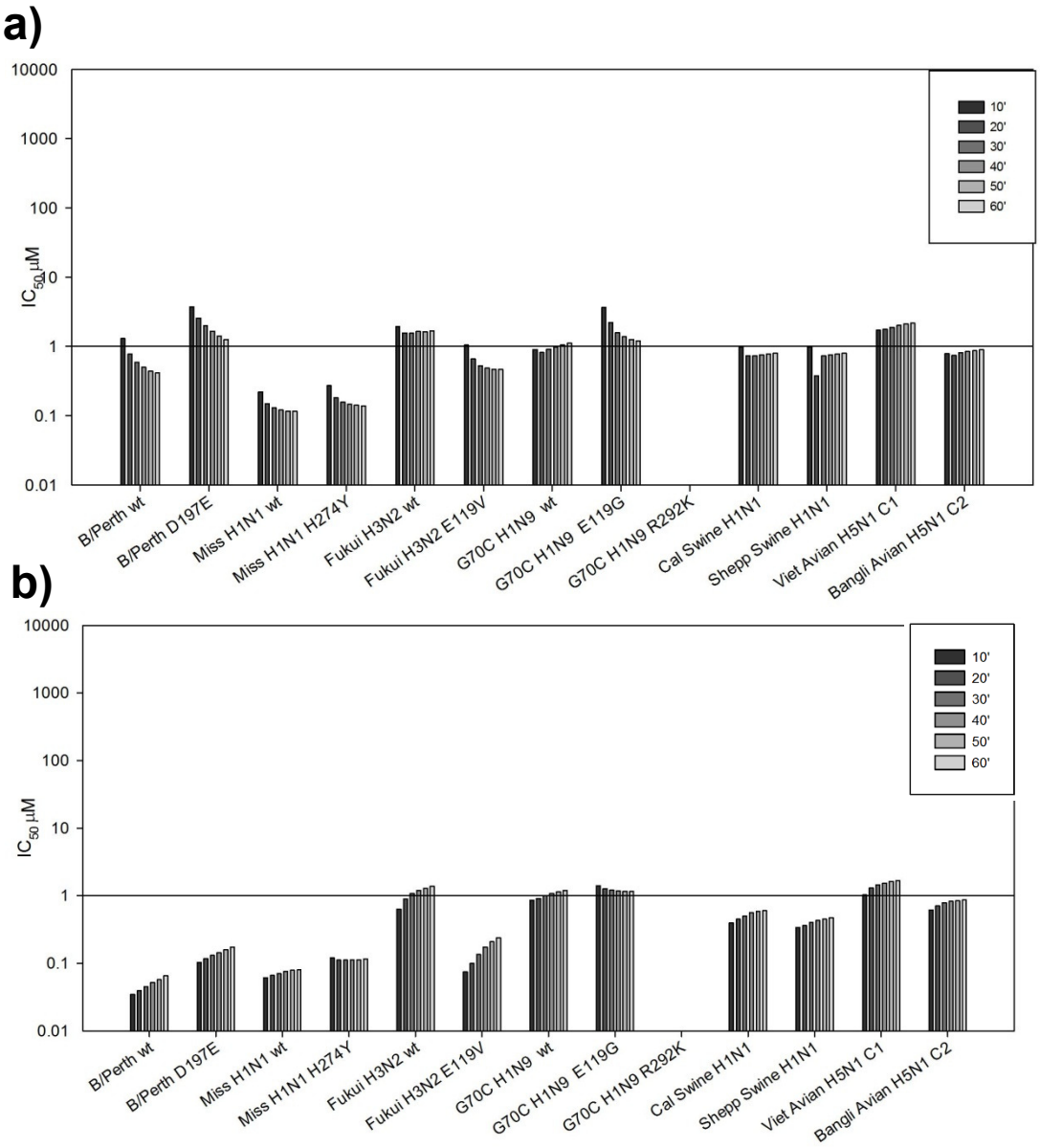

Graph 9 Values for IC_{50} kinetic evaluation of 2,3-difluoro-sialic acid (**23**) on wild type (wt.) and mutant influenza neuraminidases. a) Without pre-incubation; b) with pre-incubation (unpublished results).

However, on **Fukui H3N2 wt.**, **G70C H1N9 wt.**, **Cal. Swine H1N1**, **Shepp. Swine H1N1**, **Viet. Avian H1N5** and **Bangli. Avian H1N5** increasing IC_{50} values over time were seen, correlating to slow inactivator dissociation (**Graph 9a**).

In general, the inactivator IC_{50} kinetic assay with pre-incubation of the 2,3-difluoro-sialic acid (**23**) showed lower IC_{50} values than the kinetic assay without pre-incubation (**Graph9b**). However, the inactivator IC_{50} kinetic assay with pre-incubation showed an increase in fluorescence intensity on the influenza neuraminidase strains tested, which could correlate to higher substrate turnover and might indicate a slow dissociation of the inactivator (**Graph 9b**). Remarkably, the influenza strains **Miss H1N1 H274Y** and **G70C H1N9 E119G** showed a constant IC_{50} value over the time measured, indicating no inactivator dissociation (**Graph 9b**).

The inactivator IC_{50} kinetic assay without pre-incubation of 4-deoxy-2,3-difluoro-sialic acid (**24**) gave better absolute IC_{50} values on **B/Perth wt.**, **B/Perth D197E**, **Miss H1N1 wt.** and **Miss H1N1 H274Y** than the parent compound 2,3-difluoro-sialic acid (**23**) (**Graph 10a**).

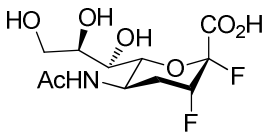

24

However, all other influenza strains tested showed increasing IC_{50} values over time correlating to slow inactivator dissociation (**Graph 10a**). The IC_{50} values obtained for **G70C H1N9 wt.** is in compliance with the results previously obtained in time-dependent inactivation experiments of 4-deoxy-2,3-difluoro-sialic acid (**24**) (Chapter 6.2.1) with a measured IC_{50} value of 92±71 nM and reactivation after 50 minutes. An increase in absolute IC_{50} values could correlate to higher substrate turnover and indicates a slow dissociation of the inactivator.

The inactivator IC_{50} kinetic assay with pre-incubation of 4-deoxy-2,3-difluoro-sialic acid (**24**) showed increasing IC_{50} values over time correlating to slow inactivator dissociation, across the panel of influenza neuraminidases tested (**Graph 10a**).

However, the inactivator IC_{50} kinetic assay with pre-incubation on **G70C H1N9 R292K** showed a decrease in IC_{50} values, correlating to slow-binding characteristics.

a)

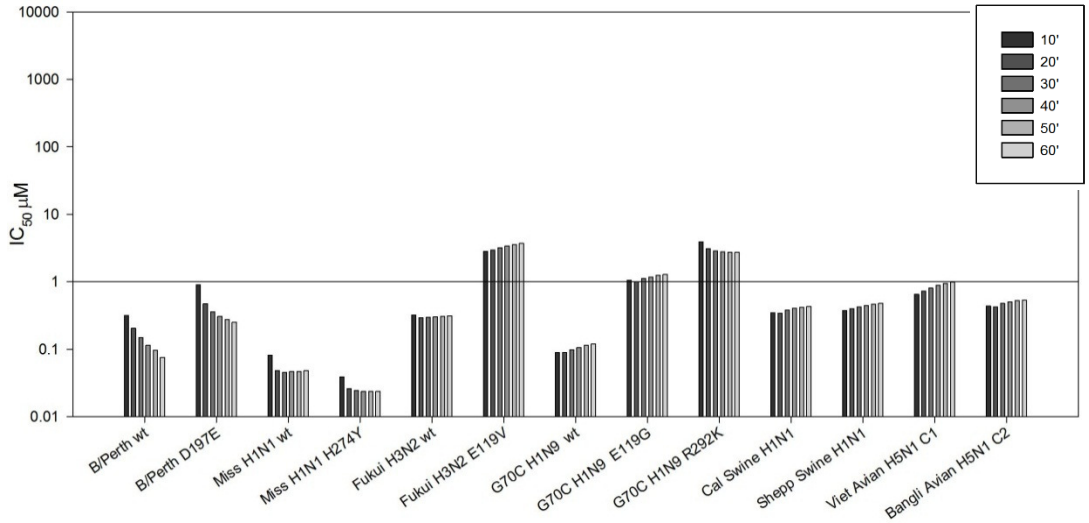

b)

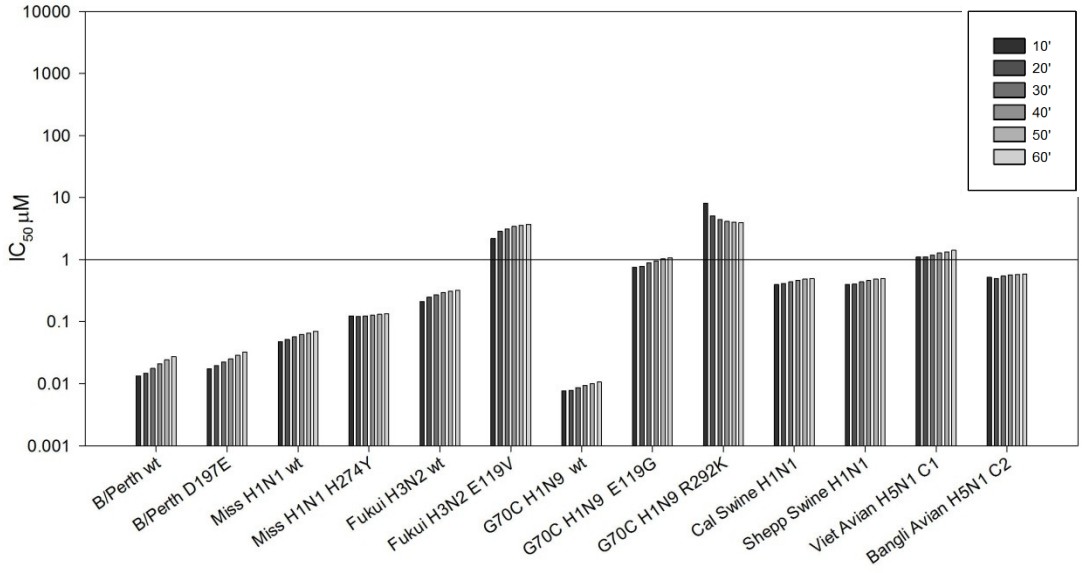

Graph 10 Values for IC_{50} kinetic evaluation of 4-deoxy-2,3-difluoro-sialic acid (**24**) on wild type (wt.) and mutant influenza neuraminidases. a) Without pre-incubation; b) with pre-incubation (unpublished results).

The inactivator IC_{50} kinetic assay without pre-incubation of 7-deoxy-2,3-difluoro-sialic acid (25) was performed on a reduced panel of influenza strains (**Graph 11a**).

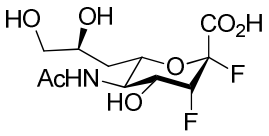

25

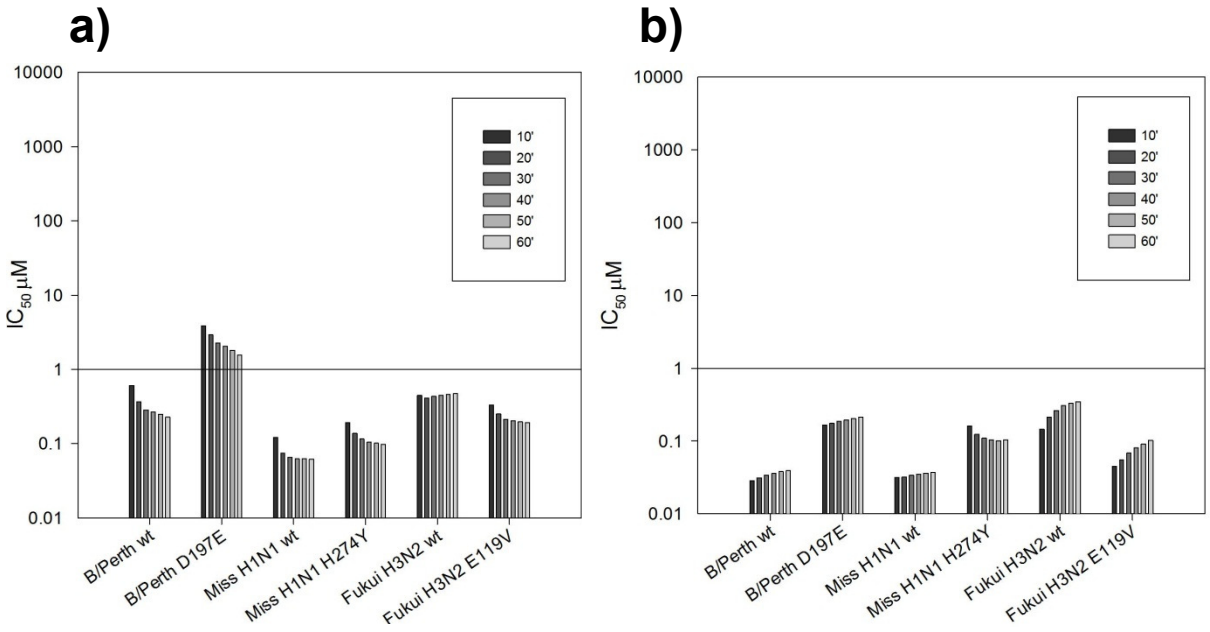

Graph 11 Values for IC_{50} kinetic evaluation of 7-deoxy-2,3-difluoro-sialic acid (**25**) on wild type (wt.) and mutant influenza neuraminidases. a) Without pre-incubation; b) with pre-incubation (unpublished results).

However, the 7-deoxy-2,3-difluoro-sialic acid (**25**) in the kinetic assay showed a decrease in the IC_{50} values over time correlating to slow-binding characteristics, but not on **Fukui H3N2 wt.** where an increase in the IC_{50} values over time could be seen (**Graph 11a**).

The IC_{50} kinetic assay with pre-incubation of 7-deoxy-2,3-difluoro-sialic acid (**25**) performed on a reduced panel of influenza strains, showed slow inactivator dissociation characteristics, but not on **Miss H1N1 H274Y** where slow binding was observed (**Graph 11b**).

The inactivator IC_{50} kinetic assay without pre-incubation of 8-deoxy-2,3-difluoro-sialic acid (**26**) gave a consistent decrease in IC_{50} values in the range of 50 µM throughout the extensive panel of influenza neuraminidases tested, correlating to slow binding (**Graph 12a**).

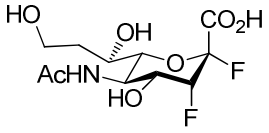

26

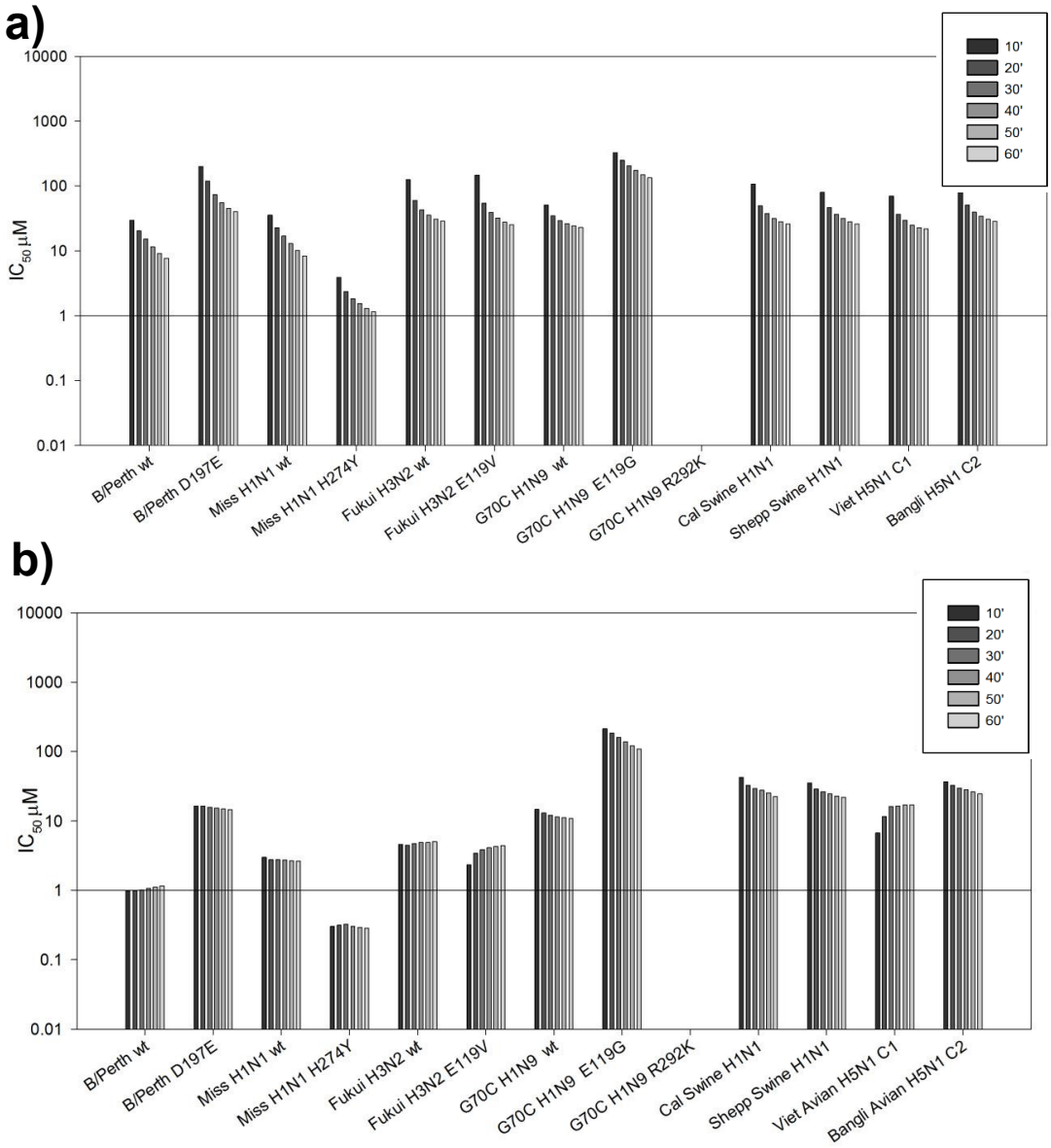

Graph 12 Values for IC_{50} kinetic evaluation of 8-deoxy-2,3-difluoro-sialic acid (**26**) on wild type (wt.) and mutant influenza neuraminidases. a) Without pre-incubation; b) with pre-incubation (unpublished results).

The IC_{50} kinetic assay with pre-incubation of 8-deoxy-2,3-difluoro-sialic acid (**26**) showed slow-binding characteristics on the influenza strains tested, but with the exception of **B/Perth wt., Fukui H3N2 E119V** and **Viet Avian H1N5 C1** where slow dissociation could be seen (**Graph 12b**).

The slow decrease in IC_{50} values of 8-deoxy-2,3-difluoro-sialic acid (**26**) obtained for **G70C H1N9 wt.** is in compliance with the results previously obtained in time-dependent inactivation experiments (Chapter 6.2.3).

The inactivator IC_{50} kinetic assay without pre-incubation of 9-deoxy-2,3-difluoro-sialic acid (**27**) showed consistent decrease in IC_{50} values in the range of 10 to 100 µM throughout the extensive panel of influenza neuraminidases tested, correlating to slow binding (**Graph 13a**)

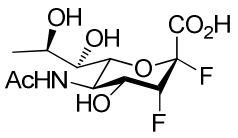

27

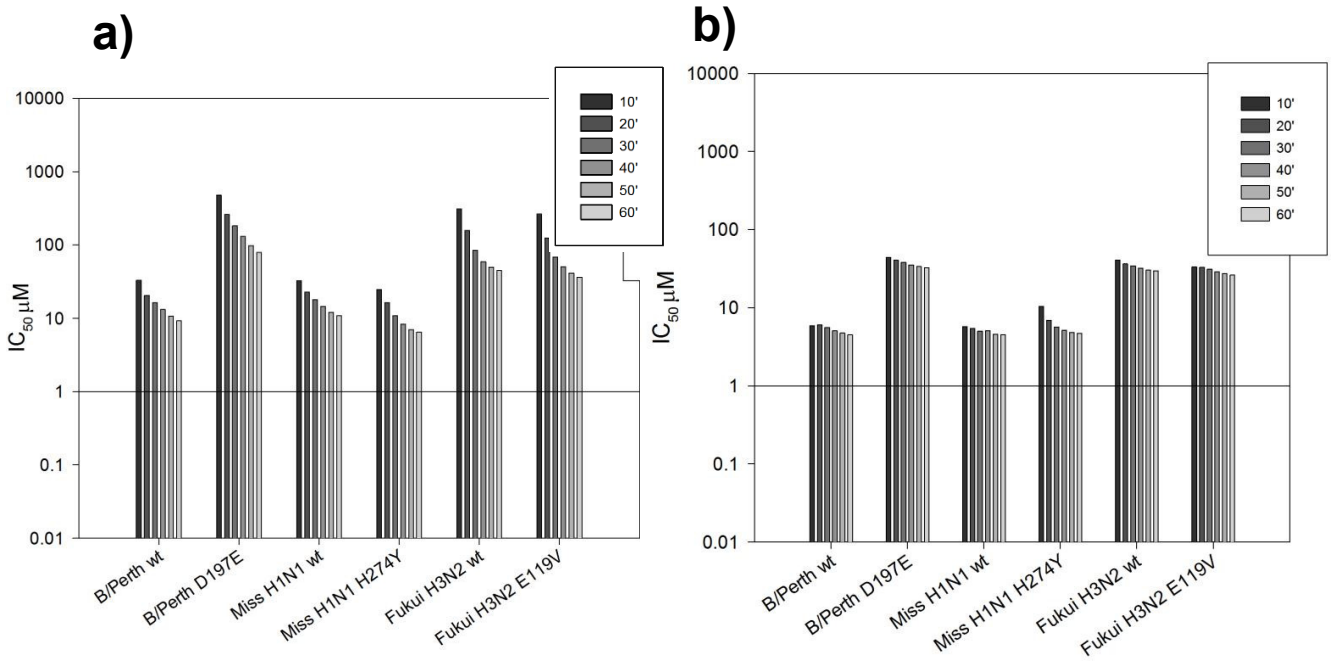

Graph 13 Values for IC_{50} kinetic evaluation of 9-deoxy-2,3-difluoro-sialic acid (**27**) on wild type (wt.) and mutant influenza neuraminidases. a) Without pre-incubation; b) with pre-incubation (unpublished results).

The inactivator IC_{50} kinetic assay with pre-incubation of the 9-deoxy-2,3-difluoro-sialic acid (**27**) still showed slow-binding characteristics, which could be due to the fact that reactivation might only occur after the time-span measured in this assay (**Graph 13b**).

In summary, the IC_{50} values without pre-incubation of monodeoxygenated 2,3-difluoro-sialic acid inactivators (**24**) - (**27**) against a panel of influenza neuraminidases after 60 minutes are compared to the IC_{50} values of activated Oseltamivir (**6**), Zanamivir (**15**) and the parent compound 2,3-difluoro-sialic acid (**23**) (**Table 11**).

The 4-deoxy-2,3-difluoro-sialic acid (**24**) inactivator gave very encouraging IC_{50} values in nM range, but mainly against Flu B (**Table 11, entry 1 and 2**) and H1N1 (**Table 11, entry 3 and 4**). Above all, 4-deoxy-2,3-difluoro-sialic acid (**24**) displayed better IC_{50} values than Oseltamivir (**6**) against Flu B with a slow dissociation from all viruses, wild types and mutants.

The Flu B mutant **FluB/Perth/D197E** (**Table 11, entry 2**) is useful for looking at interactions around the C-5 *N*-acetyl group and displayed cross resistance to Oseltamivir (**6**). The mutation gave comparable effects on the front-line influenza neuraminidase inhibitor therapeutics Oseltamivir (**6**), Zanamivir (**15**) and on all 2,3-difluoro-sialic acid inactivators.

The mutant **Miss/H1N1/H274Y** (**Table 11, entry 4**) displayed specific resistance towards Oseltamivir (**6**) with a 300 fold worse binding to Oseltamivir (**6**). However, there was hardly any effect on the 2,3-difluoro-sialic acid inactivators with the 8-deoxy-2,3-difluoro-sialic acid (**26**) and 9-deoxy-2,3-difluoro-sialic acid (**27**) inactivators giving an improved IC_{50} value compared to the wild type (**Table 11, entry 3**).

The IC_{50} value for the 4-deoxy-2,3-difluoro-sialic acid (**24**) on **Fukui/H3N2/wt.** (**Table 11, entry 5**) was encouragingly better than the parent compound 2,3-difluoro-sialic acid (**23**). However, as expected on **Fukui/H3N2/E119V** an Oseltamivir resistant mutant (**Table 11, entry 6**), which is used to look at interactions at position C-4 of the inactivator, the 4-deoxy-2,3-difluoro-sialic acid (**24**) gave a 10-fold reduction in binding.

Mutations of the arginine residue in **G70C/H1N9/R292K** with Arg292 being part of the catalytic arginine triade have dramatic effects on Oseltamivir (**6**) with slowing down the binding 10.000-fold (**Table 11, entry 8**).[187]

Comparable effects were also demonstrated on Zanamivir (**15**) and 4-deoxy-2,3-difluoro-sialic acid (**24**) with a 20-fold increase of the IC_{50} values.

Table 11 IC_{50} values obtained for the monodeoxygenated 2,3-difluoro-sialic acid inactivators (**24**) to (**27**) on a panel of influenza neuraminidases without pre-incubation given in µM (unpublished results).

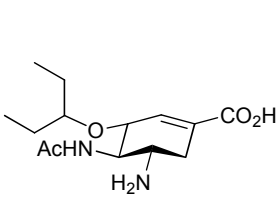

6

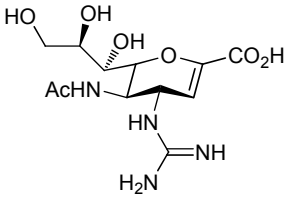

15

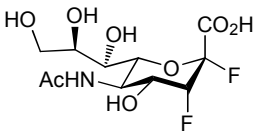

23

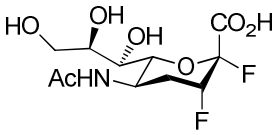

24

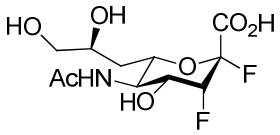

25

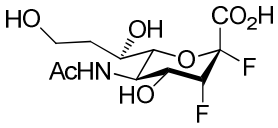

26

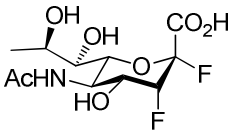

27

Entry	Neuraminidase	**6**	**15**	**23**	**24**	**25**	**26**	**27**
1	**FluB/Perth/wt**	0.14	0.17	0.41	0.075	0.23	7.60	9.20
2	**FluB/Perth/D197E**	0.66	0.43	1.26	0.25	1.50	40.1	79.1
3	**Miss/H1N1/wt**	0.007	0.008	0.12	0.048	0.06	8.30	10.8
4	**Miss/H1N1/H274Y**	2.35	0.006	0.14	0.024	0.10	1.10	6.40
5	**Fukui/H3N2/wt**	0.005	0.032	1.67	0.31	0.47	28.7	44.6
6	**Fukui/H3N2/E119V**	0.21	0.052	0.46	3.70	0.19	25.1	36.3
7	**G70C/H1N9/wt**	0.004	0.006	1.10	0.12	n.a.	23.1	n.a.
8	**G70C/H1N9/E119G**	0.005	0.82	1.20	1.28	n.a.	132.6	n.a.
8	**G70C/H1N9/R292K**	30.1	0.11	n.a.	2.72	n.a.	n.a.	n.a.
9	**Cal Swine/H1N1**	0.020	0.012	0.79	0.43	n.a.	25.8	n.a.
10	**Shepp/Swine/H1N1**	0.007	0.006	0.79	0.47	n.a.	25.8	n.a.
11	**Viet Avian/H5N1/C1**	0.004	0.012	2.17	0.99	n.a.	21.7	n.a.
12	**Bangli Avian/H5N1/C2**	0.021	0.011	0.89	0.54	n.a.	28.2	n.a.

= better IC_{50} values than Oseltamivir (**6**), = better IC_{50} values than Zanamivir (**15**), n.a. = not available.

In general the inactivators 8-deoxy-2,3-difluoro-sialic acid (**26**) and 9-deoxy-2,3-difluoro-sialic acid (**27**) displayed poor inactivation against all influenza strains tested. The poor inhibition results might point out the important role of OH-8 and OH-9 towards transition-state stabilisation.

In summary, the second set of experiments with a 30 minutes pre-incubation prior to the addition of substrate (**121**) gave the same trends of inhibition, but slightly better absolute IC_{50} values than the experiments without pre-incubation (**Table 12**).

In contrast to the experiment without pre-incubation the 2,3-difluoro-sialic acid (**23**), 4-deoxy-2,3-difluoro-sialic acid (**24**) and 7-deoxy-2,3-difluoro-sialic acid (**25**) obtained better inhibition than Oseltamivir (**6**) and Zanamivir (**15**) against Flu B (**Table 12, entry 1 and entry 2**).

In addition the 4-deoxy-2,3-difluoro-sialic acid (**24**) gave a 10-fold better IC_{50} value on **G70C/H1N9/wt.** compared to the experiment without pre-incubation and ended up to be 100-fold better than the parent 2,3-difluoro-sialic acid (**23**) (**Table 12, entry 7**).

In conclusion, although the 4-deoxy-2,3-difluoro-sialic acid (**24**) and 7-deoxy-2,3-difluoro-sialic acid (**25**) achieved promising IC_{50} values on Flu B neuraminidases, the IC_{50} values of the monodeoxygenated 2,3-difluoro-sialic acid inactivators (**24**) - (**27**) vary greatly across the panel of influenza neuraminidases (**Table 12**). Together with the inconclusive inactivation results of Oseltamivir (**6**) and Zanamivir (**15**) (**Table 12**), the preservation of potency of anti-viral drugs against a number of influenza neuraminidases could be seen as a major hurdle.[188]

Table 12 IC_{50} values obtained for the monodeoxygenated 2,3-difluoro-sialic acid inactivators (**24**) to (**27**) on a panel of influenza neuraminidases with 30 minutes pre-incubation given in µM (unpublished results).

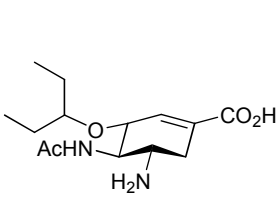

6

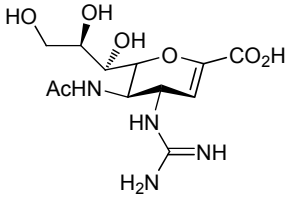

15

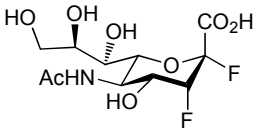

23

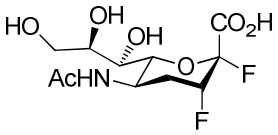

24

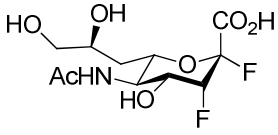

25

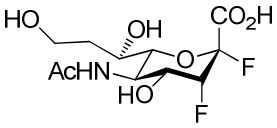

26

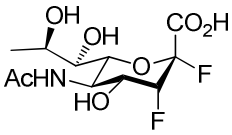

27

Entry	Neuraminidase	**6**	**15**	**23**	**24**	**25**	**26**	**27**
1	**FluB/Perth/wt**	0.10	0.090	0.070	0.030	0.040	1.20	4.50
2	**FluB/Perth/D197E**	0.71	0.26	0.17	0.030	0.21	14.5	32.2
3	**Miss/H1N1/wt**	0.003	0.002	0.080	0.070	0.037	2.60	4.50
4	**Miss/H1N1/H274Y**	2.44	0.002	0.12	0.13	0.10	0.30	4.70
5	**Fukui/H3N2/wt**	0.002	0.004	1.38	0.32	0.34	5.0	29.5
6	**Fukui/H3N2/E119V**	0.26	0.003	0.24	3.67	0.10	4.40	26.0
7	**G70C/H1N9/wt**	0.003	0.003	1.19	0.010	n.a.	10.9	n.a.
8	**G70C/H1N9/E119G**	0.003	0.68	1.15	1.05	n.a.	107.9	n.a.
8	**G70C/H1N9/R292K**	24.7	0.095	n.a.	3.88	n.a.	n.a.	n.a.
9	**Cal Swine/H1N1**	0.005	0.001	0.60	0.49	n.a.	22.4	n.a.
10	**Shepp/Swine/H1N1**	0.005	0.001	0.47	0.49	n.a.	22.0	n.a.
11	**Viet Avian/H5N1/C1**	0.001	0.003	1.66	1.40	n.a.	17.0	n.a.
12	**Bangli Avian/H5N1/C2**	0.020	0.001	0.86	0.58	n.a.	24.5	n.a.

= better IC_{50} values than Oseltamivir (**6**), = better IC_{50} values than Zanamivir (**15**), n.a. = not available.

Our collaborators then investigated the inactivation behaviour of 4-deoxy-2,3-difluoro-sialic acid (**24**) and 8-deoxy-2,3-difluoro-sialic acid (**26**) under conditions more closely related to humans by utilising a plaque reduction assay and the results obtained will be discussed next.

6.3.2 Plaque reduction assay of 4-deoxy-2,3-difluoro-sialic acid (24) and 8-deoxy-2,3-difluoro-sialic acid (26) on Miss/H1N1

In the plaque assay, each infectious virus particle multiplies under conditions that result in a localized area of infected cells or 'plaque'. The plaques are revealed either as areas of dead/destroyed cells detected by general cellular stains or as areas of infected cells detected by immuno-staining. As such, the plaque reduction assay is the first stage of *in* vivo assays and can be performed to get an IC_{50} value that is closer related to the IC_{50} values expected in humans.[189] The 4-deoxy-2,3-difluoro-sialic acid (**24**) and the 8-deoxy-2,3-difluoro-sialic acid (**26**) were tested by our collaborators (Molecular and Health Technologies, CSIRO, Australia) in a plaque reduction assay on Miss/H1N1/wt. (**Figure 15**).[190]

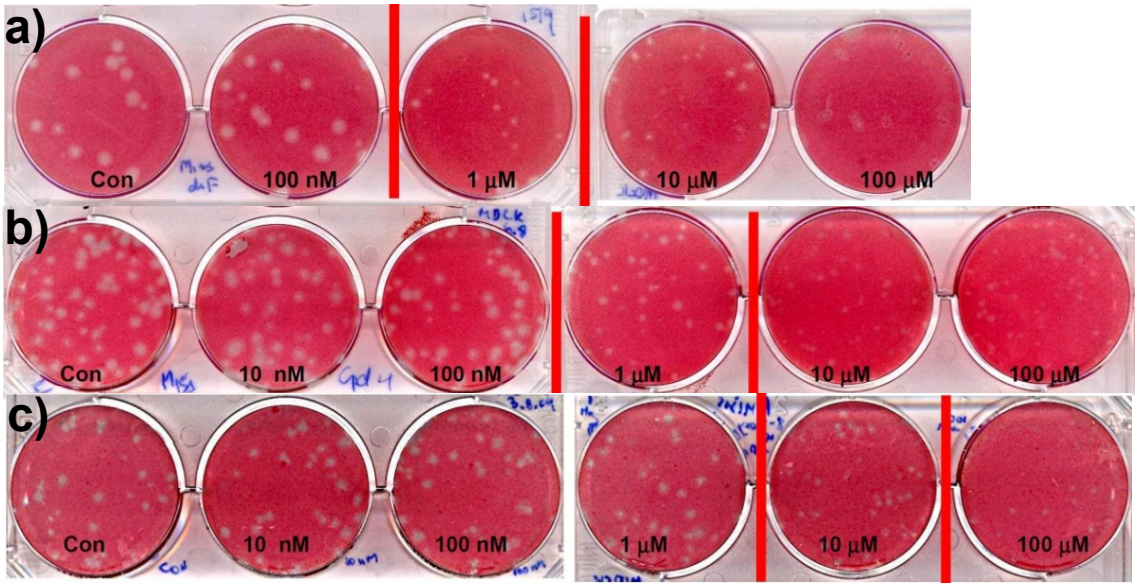

Figure 15 Plaque reduction assay of Miss/H1N1/wt. with the red lines showing the endpoint on reduction in plaque size of a) 2,3-difluoro-sialic acid (**23**), b) 4-deoxy-2,3-difluoro-sialic acid (**24**) and c) 8-deoxy-2,3-difluoro-sialic acid (**26**) (unpublished results).

The 2,3-difluoro-sialic acid (**23**) with a neuraminidase inhibitor IC_{50} of 80 nM as well as the 4-deoxy-2,3-difluoro-sialic acid (**24**) with an IC_{50} of 70 nM against Miss/H1N1/wt. (**Table 12, entry 3**) gave about a 10-fold worse IC_{50} in the plaque reduction assay, reflecting faster turnover. Similar results were seen with 8-deoxy-2,3-difluoro-sialic acid (**26**), which showed a neuraminidase inhibitor IC_{50} of 2.6 µM and in the plaque reduction assay an IC_{50} of about 10 µM.

We then set out to understand the effects of inactivation on a physical basis. Hence, X-ray crystal structures of wild type influenza neuraminidase N9 G70C in complex with the monodeoxygenated 2,3-difluoro-sialic acid inactivators (**24**) - (**27**) were performed.

Chapter 7 - Analysis of structural studies performed on monodeoxygenated 2,3-difluoro-sialic acids in complex with influenza neuraminidase N9

7.1 Preface

Having successfully observed differences between the rate of glycosylation (k_1) and deglycosylation (k_2) during inactivation of influenza neuraminidases with our series of monodeoxygenated 2,3-difluoro-sialic acid inactivators (**24**) - (**27**), we wished to develop a further understanding of their effects upon inactivation on a physical basis (**Scheme 68**).

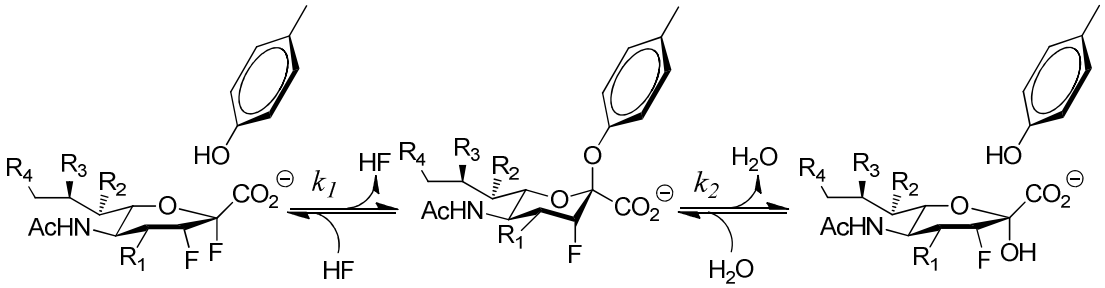

24 R_1 = H, R_2, R_3, R_4 = OH

25 R_2 = H, R_1, R_3, R_4 = OH

26 R_3 = H, R_1, R_2, R_4 = OH

27 R_4 = H, R_1, R_2, R_3 = OH

Scheme 68 The glycosylation (k_1) and deglycosylation (k_2) rate constants associated with the mechanism-based inactivators (**24**) - (**27**).

We considered that analysis of the X-ray crystal structures of the trapped covalent sialosyl-enzyme reaction intermediates could give further information on the mechanism of inactivation of influenza neuraminidases by monodeoxygenated 2,3-difluoro-sialic acid inactivators (**24**) - (**27**) on influenza neuraminidase. This chapter will first discuss ready available X-ray crystal structures of the active site of influenza neuraminidase N9 in complex with sialic acid (**2**) considering the position of the hydroxyl group targeted in the deoxygenation of 2,3-difluoro-sialic acid (**23**). Following, the X-ray crystallographic structure of the covalent complex of influenza neuraminidase N9 with the monodeoxygenated 2,3-difluoro-sialic acid inactivators (**24**) - (**27**) will be discussed. It was anticipated that comparing structures determined on inactivators (**24**) - (**27**) with the structures generated from previous studies performed on sialic acid (**2**) and DANA (**16**) might give further insight into the mechanism through which monodeoxygenated 2,3-difluoro-sialic acid inactivators (**24**) - (**27**) are processed by influenza neuraminidases.

The X-ray cyrstal structure of the covalent sialosyl-enzyme intermediate has previously been shown by Watts *et al.* on *Trypanosoma rangeli* in complex with 2,3-difluoro-sialic acid (**23**) and by Resende on influenza neuraminidase N9 in complex with 7-*N*,*N*-diethylamino-2,3-difluoro-sialic acid (**122**) (unpublished work).[12,164]

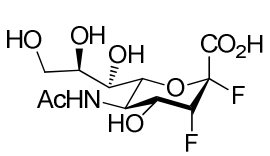

23

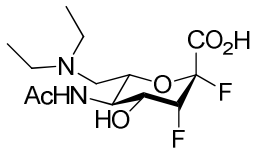

122

The X-ray crystal structures of 2,3-difluoro-sialic acid (**23**) (**Figure 16a**) and 7-*N*,*N*-diethylamino-2,3-difluoro-sialic acid (**122**) (**Figure 16b**) have both confirmed the existence of the covalently linked sialosyl-enzyme intermediate by observing clear electron density alongside the proposed covalent bond.

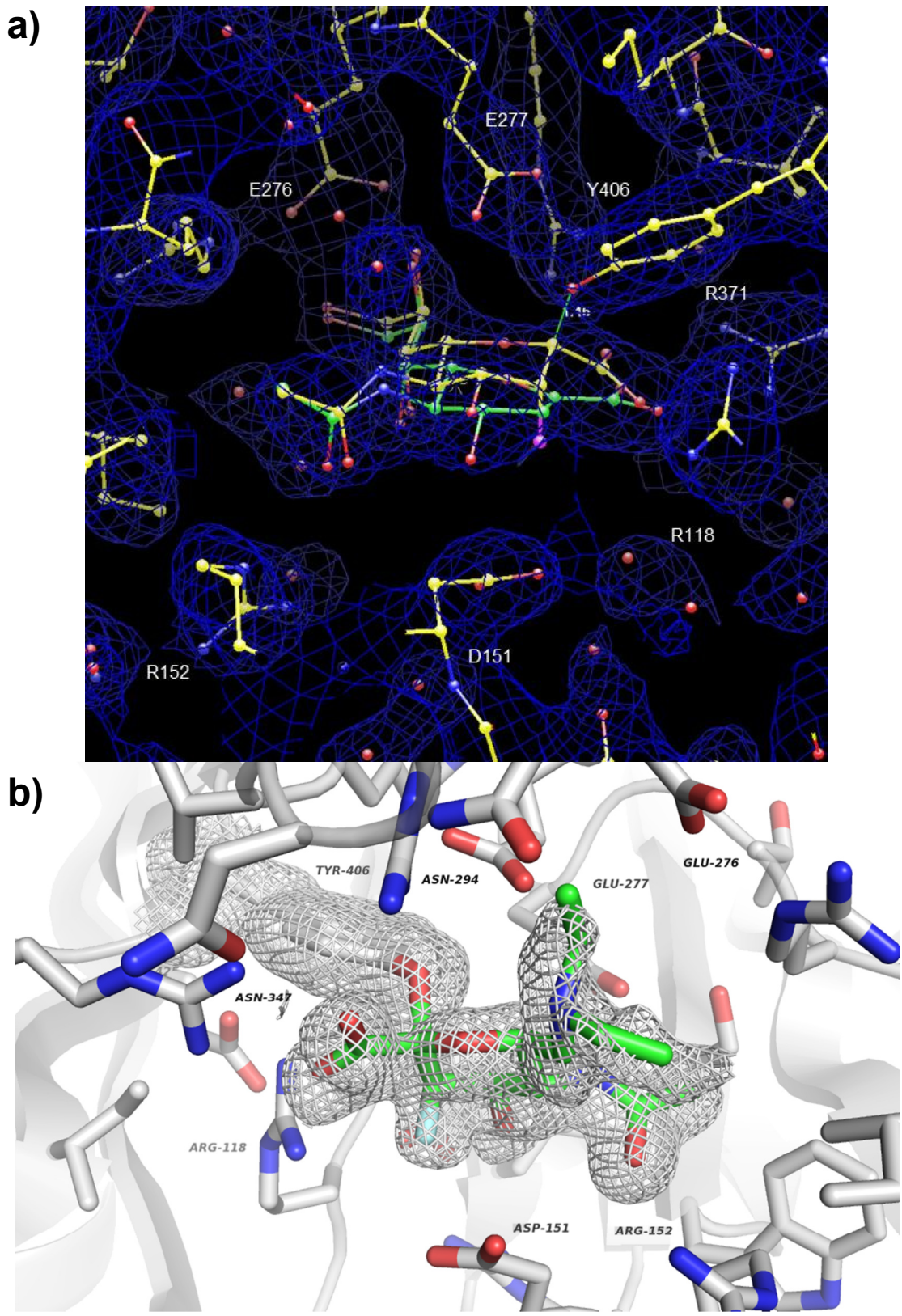

Figure 16 X-ray crystal structures of influenza neuraminidase N9 displaying electron density alongside the covalently linked sialosyl-enzyme intermediate in complex with a) 2,3-difluoro-sialic acid (**23**). The structure is shown with population of the DANA-like compound given in green; b) 7-*N*,*N*-diethylamino-2,3-difluoro-sialic acid (**122**) (unpublished results).

The refined model of 2,3-difluoro-sialic acid (**23**) (**Figure 16a**) showed in dual occupancy a covalently linked sialosyl-enzyme intermediate of the 2,3-difluoro-sialic acid (**23**) and a DANA-like compound (shown in green). The covalently linked sialosyl-enzyme intermediate was identified through a clear rotation of the carboxyl group compared to 2,3-difluoro-sialic acid (**23**) and the loss of the fluorine atom at position C-2 of 2,3-difluoro-sialic acid (**23**).

The distance of ~ 1.4 Å between the oxygen of the residue Tyr406 and position C-2 of the inactivator with electron density alongside the putative covalent bond indicates covalent binding (**Figure 16a**).

The second ligand in the active site of influenza neuraminidase N9 with an occurrence of 60% could correspond to a flattened ring conformation consistent with a DANA-like elimination product (**Figure 16a**, shown in green).

In a study performed by Burmeister *et al.* the natural sialic acid (**2**) turnover in Flu B neuraminidase showed DANA (**16**).[192] This formation of DANA (**16**) proceeds via simple proton elimination. However, on 2,3-difluoro-sialic acid (**23**) the formation of a of a DANA-like derivative would need a redox elimination mechanism. At present, no mechanism for the formation of the DANA-like elimination product has yet been proposed and it remains unclear if influenza neuraminidases processes 2,3-difluoro-sialic acid (**23**) through an alternative metabolic mechanism. Other explanations could also involve the formation of the DANA-like elimination product as part of the crystallisation conditions used, or the DANA (**16**) compound might be a side product formed in the synthesis and remained an impurity throughout. The uncertainty of the DANA-like elimination product formation needs to be addressed and is part of future synthetic and protein crystallographic strategies.

To clarify: The influenza neuraminidase N9 used for crystallisation studies was provided by Dr. Jennifer McKimm-Breschkin (Materials Science and Engineering, CSIRO, Australia). All protein crystallisation, X-ray crystallographic studies and refinements were performed by Dr. Victor Streltsov at the Australian Synchrotron MX-2 (Livestock Industries, CSIRO Australia). The PDB coordinates (unpublished work) used in this chapter were provided by Dr. Victor Streltsov, but the analysis and interpretation of the results obtained are performed by the author.

7.2 The C-4 position

In the active site of influenza neuraminidase N9, the amino acid residues Tyr406, Glu119 and Asp151 have been identified as being crucial for catalysis, and are all located within a pocket of 4 Å radius around the oxygen of the C-4 hydroxyl group of sialic acid (**2**) (**Figure 17**).

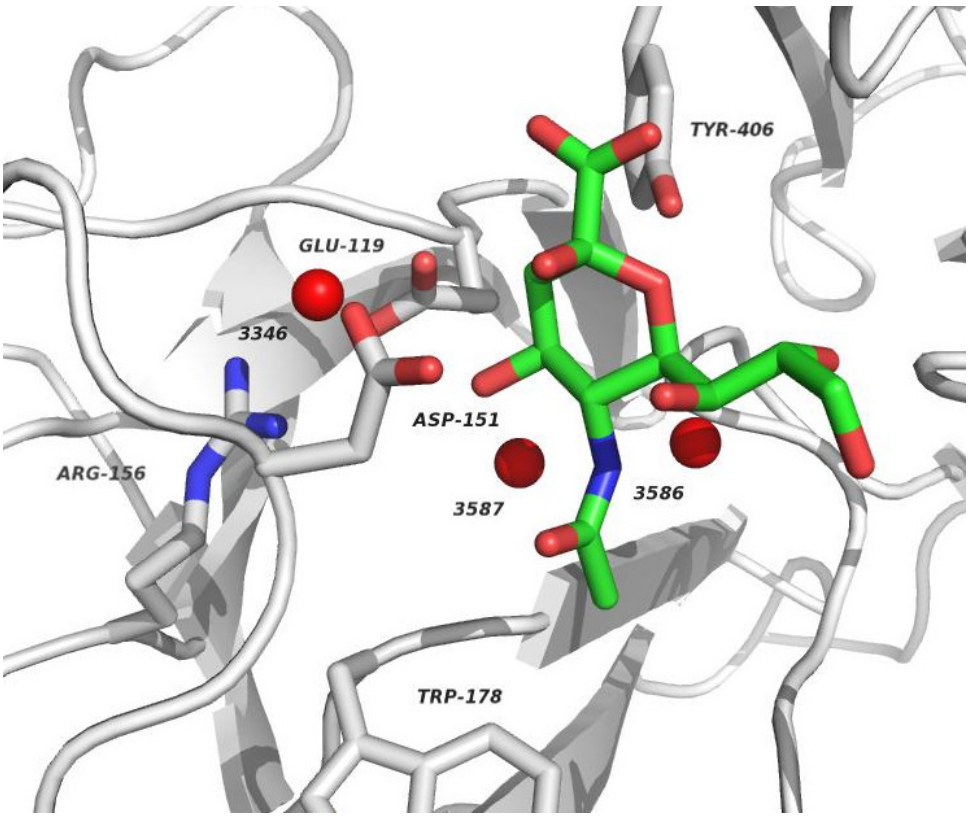

Figure 17 Key amino acid residues and water molecules located within a 4 Å radius of the oxygen at position C-4 of sialic acid (**2**) in the active site of influenza neuraminidase N9. Amino acid residues are shown in stick representation and water molecules in spherical representation. Generated with PyMOL (PDB 1MWE).[191]

In addition to the three catalytic residues (Tyr406, Glu119 and Asp151) two further amino acid residues (Arg156 and Trp178) and three water molecules are also found to lie within the 4 Å pocket around the OH-4 group. Since water molecules can play a crucial role in transition-state stabilisation through hydrogen bond interactions and/or entropic effects, the presence of water molecules could have an effect on the overall neuraminidase activity and so will be considered as part of our analysis.

In general, influenza neuraminidases are known to be particularly tolerant towards modifications at position C-4 of sialic acid (**2**). As previously demonstrated by Zanamivir (**15**), interactions at position C-4 with amino acid residues in the active site of influenza neuraminidase are of major interest and the introduction of a large basic functionality like a guanidino substituent at this position did result in better inhibition of influenza neuraminidase.[90,91]

However, the 4-deoxy-2,3-difluoro-sialic acid (**24**) inactivator gave comparable or better IC_{50} values than the parent 2,3-difluoro-sialic acid (**23**) on the influenza neuraminidase strains tested (Chapter 6.3.1).

Crystals of influenza neuraminidase N9 in complex with 4-deoxy-2,3-difluoro-sialic acid (**24**) were obtained by co-crystallisation. Diffraction data were collected from a single crystal that diffracted to 1.9 Å and refinement was performed with REFMAC 5.5.0110 on 3710 atoms (**Figure 18**).

The refined model showed in dual population a covalently linked sialosyl-enzyme intermediate of the 4-deoxy-2,3-difluoro-sialic acid (**24**) and a DANA-like compound (shown in purple). The covalently linked sialosyl-enzyme intermediate was identified through a clear rotation of the carboxyl group compared to 4-deoxy-2,3-difluoro-sialic acid (**24**) and the loss of the fluorine atom at position C-2 of 4-deoxy-2,3-difluoro-sialic acid (**24**). Together with the distance of ~ 1.4 Å between the oxygen of the residue Tyr406 and position C-2 of the inactivator with electron density alongside the putative covalent bond indicates covalent binding (**Figure 19**).

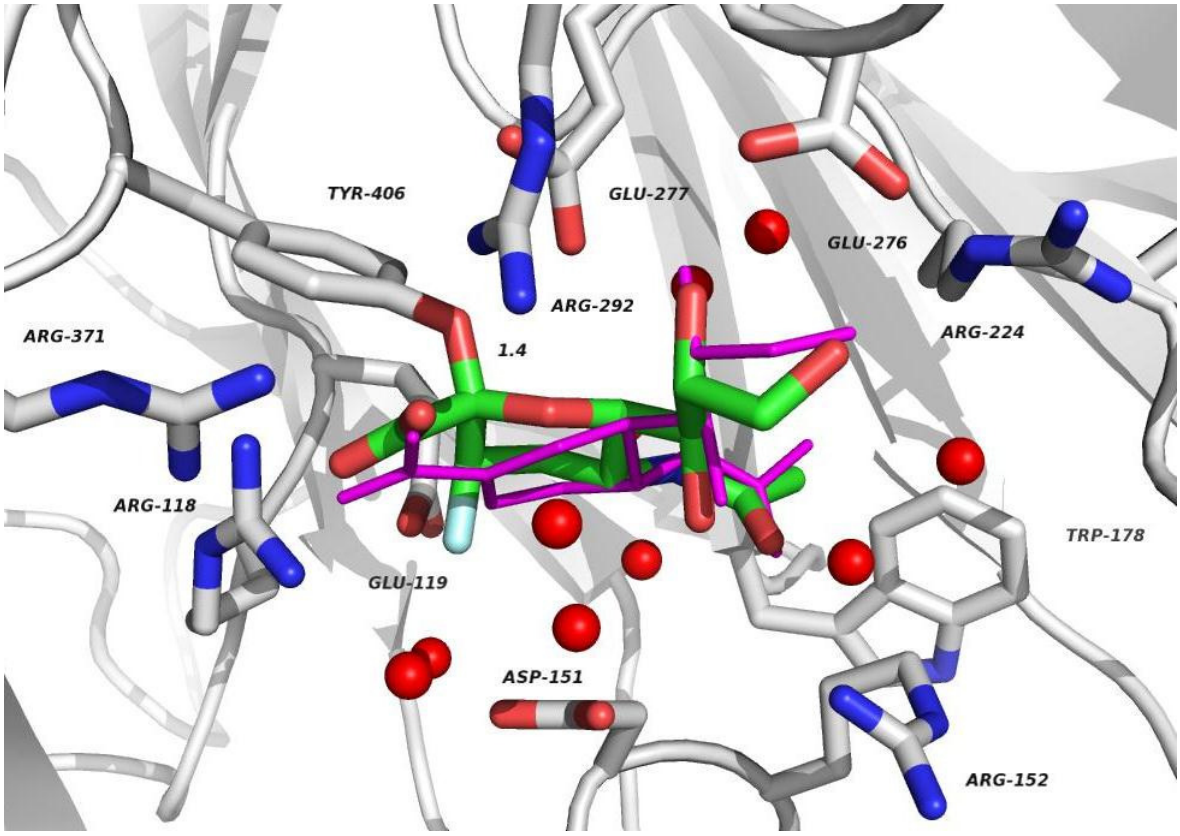

Figure 18 Key amino acid residues and water molecules located within a 4 Å radius of the covalently bound β-4-deoxy-3-fluoro-sialosyl moiety in the active site of influenza neuraminidase N9. Amino acid residues are shown in stick representation and water molecules in spherical representation. The structure is shown with population of the DANA-like compound given in purple. Generated with PyMOL (unpublished work).

The second ligand in the active site of influenza neuraminidase N9 with an occurrence of 80% could correspond to a DANA-like elimination product (**Figure 18**, shown in purple and **Figure 19**, shown in green). The second structure shows a flattened ring conformation consistent with DANA.

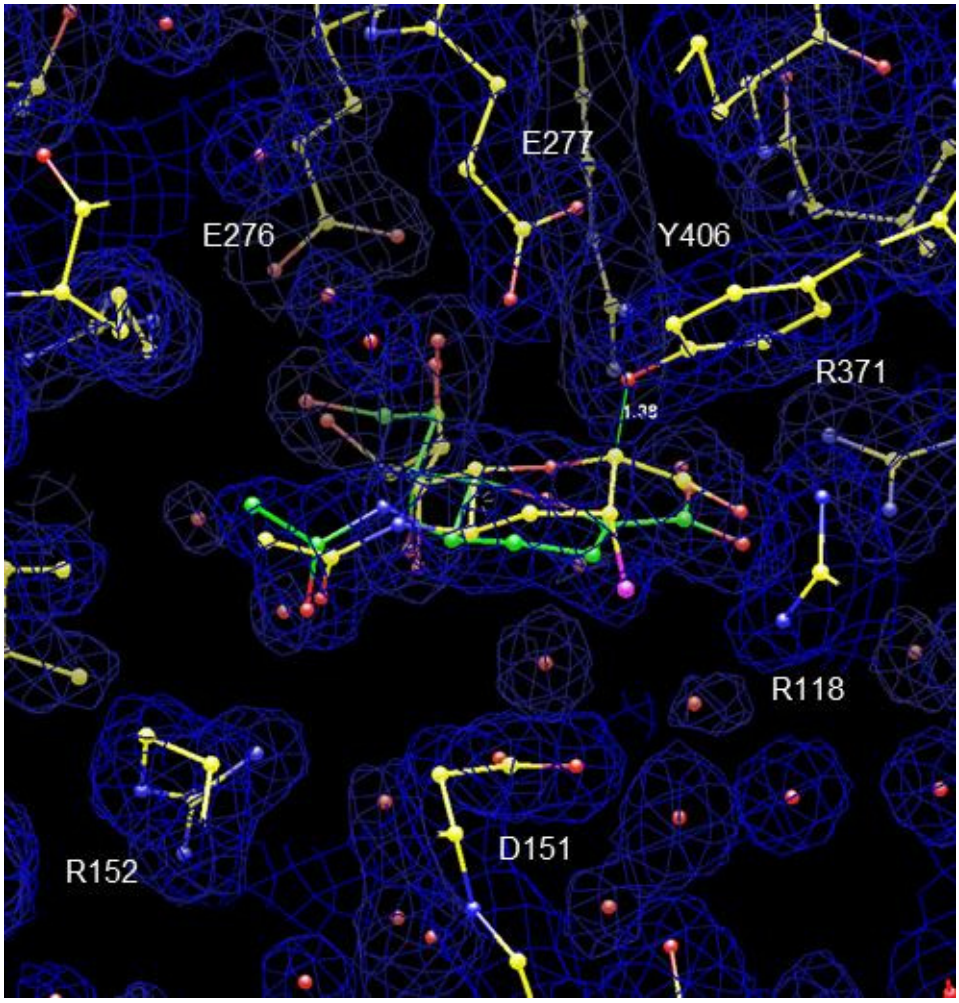

Figure 19 X-ray crystal structure of influenza neuraminidase N9 displaying electron density alongside the covalently linked sialosyl-enzyme intermediate of 4-deoxy-2,3-difluoro-sialic acid (**24**). The structure is shown with population of the DANA-like compound given in green (unpublished results).

The X-ray crystal structure obtained from influenza neuraminidase N9 in complex with 4-deoxy-2,3-difluoro-sialic acid (**24**) was superimposed with the structure of influenza neuraminidase N9 in complex with sialic acid (**2**) to investigate any conformational changes to the inactivator or active site residues of influenza neuraminidase (**Figure 20**). The alignment tool in PyMOL was used on 362 atoms of the backbone and gave a root-mean-square deviation (RMSD) of 0.103.

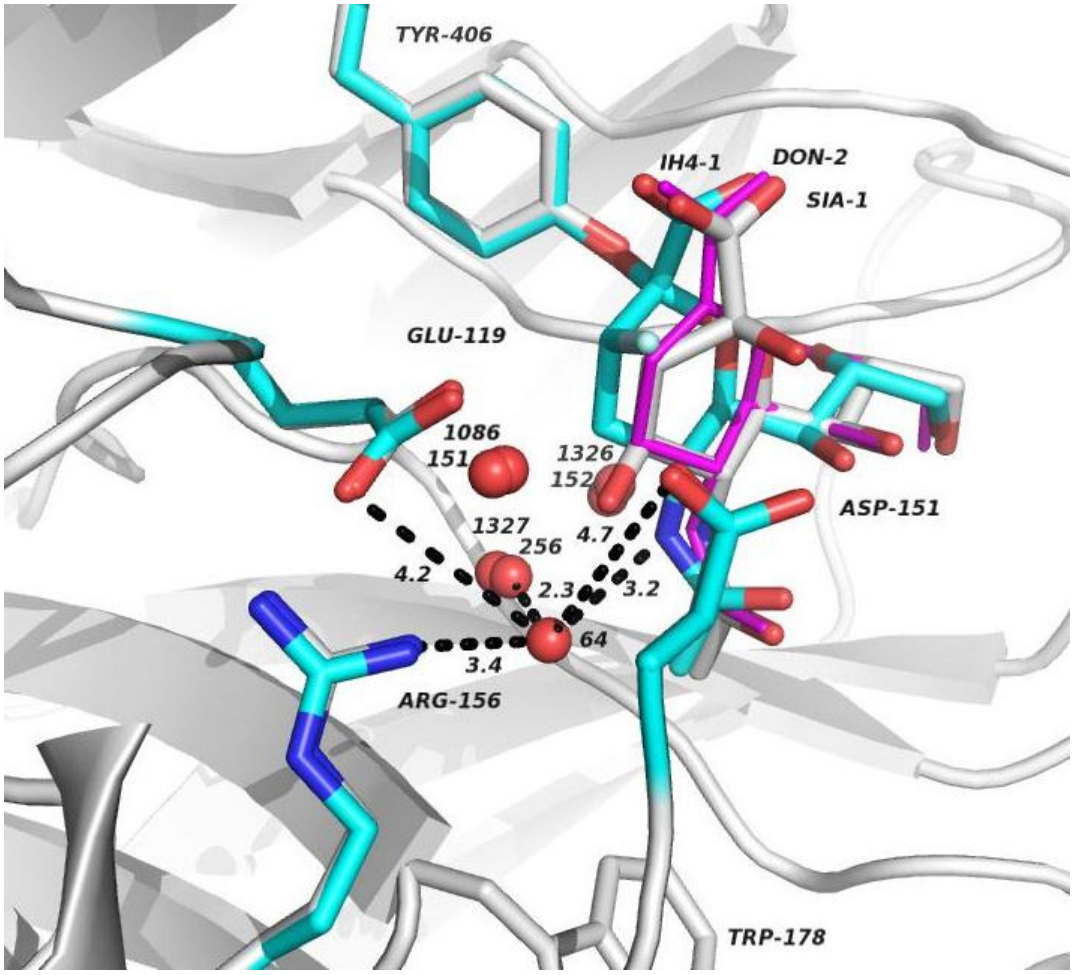

Figure 20 Superimposition of the active site of influenza neuraminidases N9 in complex with sialic acid (**2**) (SIA-1, grey) and β-4-deoxy-3-fluoro-sialosyl moiety (IH4-1, blue), The structure is shown with population of the DANA-like compound given in purple. Key amino acid residues and water molecules located within a 4 Å radius of the oxygen at position C-4 of sialic acid (**2**) in the active site of influenza neuraminidase N9. Amino acid residues are shown in stick representation and water molecules in spherical representation. Generated with PyMOL (PDB 1MWE, grey) (unpublished work).[191]

The superimposition of the two X-ray crystal structure sets on influenza neuraminidase N9 demonstrated highly conserved active site amino acid residues and a twisted ring distortion of the covalently linked β-4-deoxy-3-fluoro-sialosyl moiety was observed. The removal of the OH-4 group results in reorientation of the C-5 *N*-acetyl group and the glycerol side chain. Furthermore, the three water molecules close to the Glu119 residue appear to be congruent in the active site of influenza neuraminidase N9 (**Figure 20**).

However, one additional water molecule could be seen within a 4 Å radius of the oxygen at position C-4 of sialic acid (**2**). The additional water molecule could be in the range of hydrogen-bonding interactions with the C-5 *N*-acetyl group, the catalytic amino acid residues Arg156 and other water molecules. This additional water molecule could be an explanation for the behaviour of 4-deoxy-2,3-difluoro-sialic acid (**24**) in inactivation kinetics with better IC_{50} values than the parent inactivator 2,3-difluoro-sialic acid (**23**), as previously demonstrated (Chapter 6.3.1). To further investigate the role of this water molecule for catalysis, computer aided hydration free energy calculations could be performed, however this is beyond the scope of this project.[193] The role of water molecules towards the inactivation mechanism in influenza neuraminidase is ambiguous, but has recently been targeted in novel drug discovery efforts.[194,195]

The X-ray crystal structure obtained from influenza neuraminidase N9 in complex with 4-deoxy-2,3-difluoro-sialic acid (**24**) was superimposed with the structure of influenza neuraminidase N9 in complex with DANA (**16**), which as a competitive transition-state analogue inhibitor could be used to elucidate the behaviour of the 4-deoxy-2,3-difluoro-sialic acid (**24**) in the enzymatic catalytic cycle of influenza neuraminidase (**Figure 21**).

The superimposition of the two X-ray crystal structure sets on influenza neuraminidase N9 using the alignment tool in PyMOL on 365 atoms of the backbone gave a root-mean-square deviation (RMSD) of 0.107. The alignment showed that the position of the DANA-like ligand obtained in the X-ray crystal structure on 4-deoxy-2,3-difluoro-sialic acid (**24**) closely mimics the position of DANA (**16**) in the structure obtained of its complex with influenza neuraminidase N9.

The previously described additional water molecule was seen again within a pocket of 4 Å radius of the oxygen at position C-4 of DANA (**16**) and could be in the range of hydrogen-bonding interactions with the C-5 *N*-acetyl group, the catalytic amino acid residues Arg156 and other water molecules and might reinforce the role of this water molecule for catalysis.

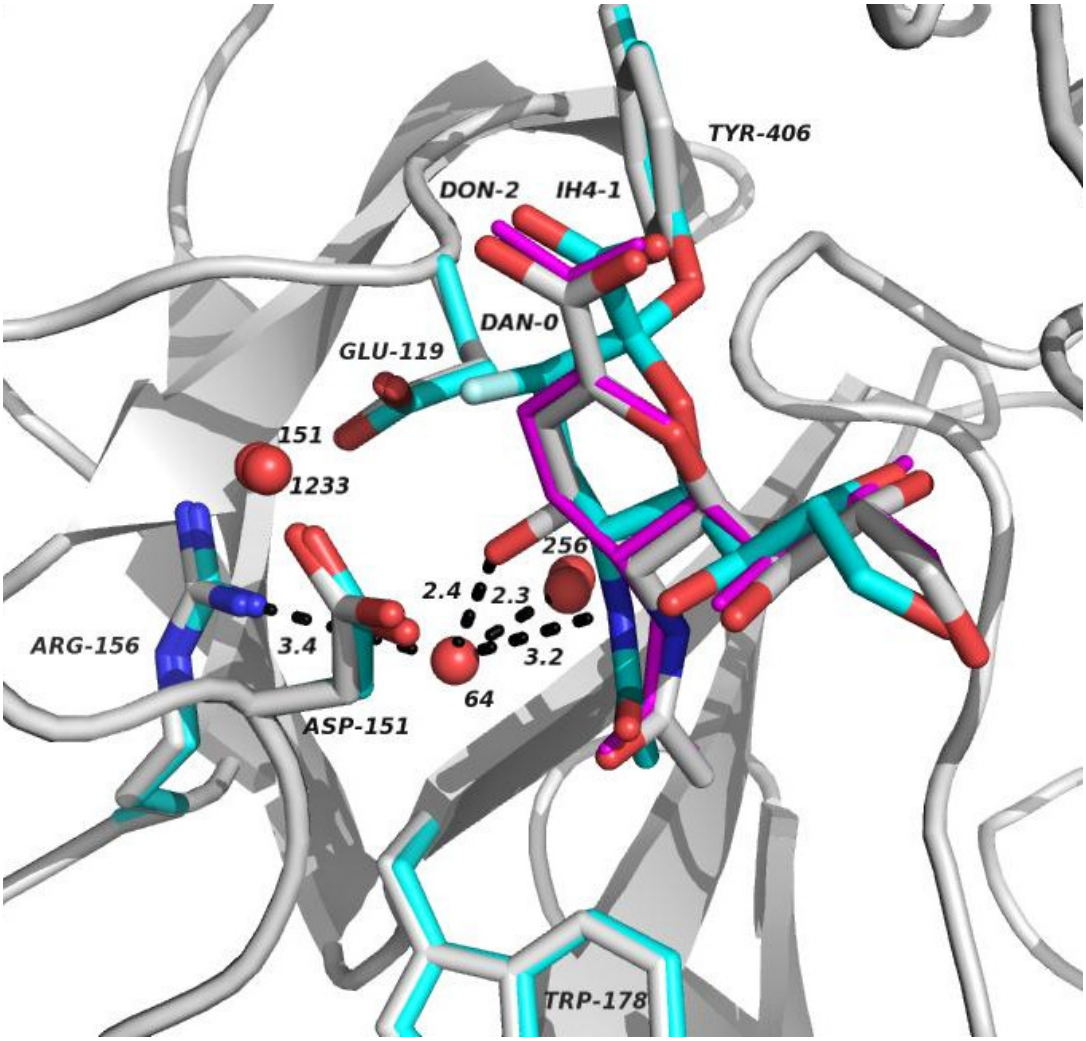

Figure 21 Superimposition of the active site of influenza neuraminidases N9 in complex with DANA (**16**) (DAN-0, grey) and β-4-deoxy-3-fluoro-sialosyl moiety (IH4-1, blue). The structure is shown with population of the DANA-like compound given in purple Key amino acid residues and water molecules located within a 4 Å radius of the oxygen at position C-4 of DANA (**16**) in the active site of influenza neuraminidase N9. Amino acid residues are shown in stick representation and water molecules in spherical representation. Generated with PyMOL (PDB 1F8B, grey) (unpublished work).[196]

7.3 The C-7 position

In the active site of influenza neuraminidase N9, the catalytic amino acid residues Asp151 and Arg152 are located in a pocket within a 4 Å radius around the oxygen of the C-7 hydroxyl group of sialic acid (**2**) (**Figure 22**).

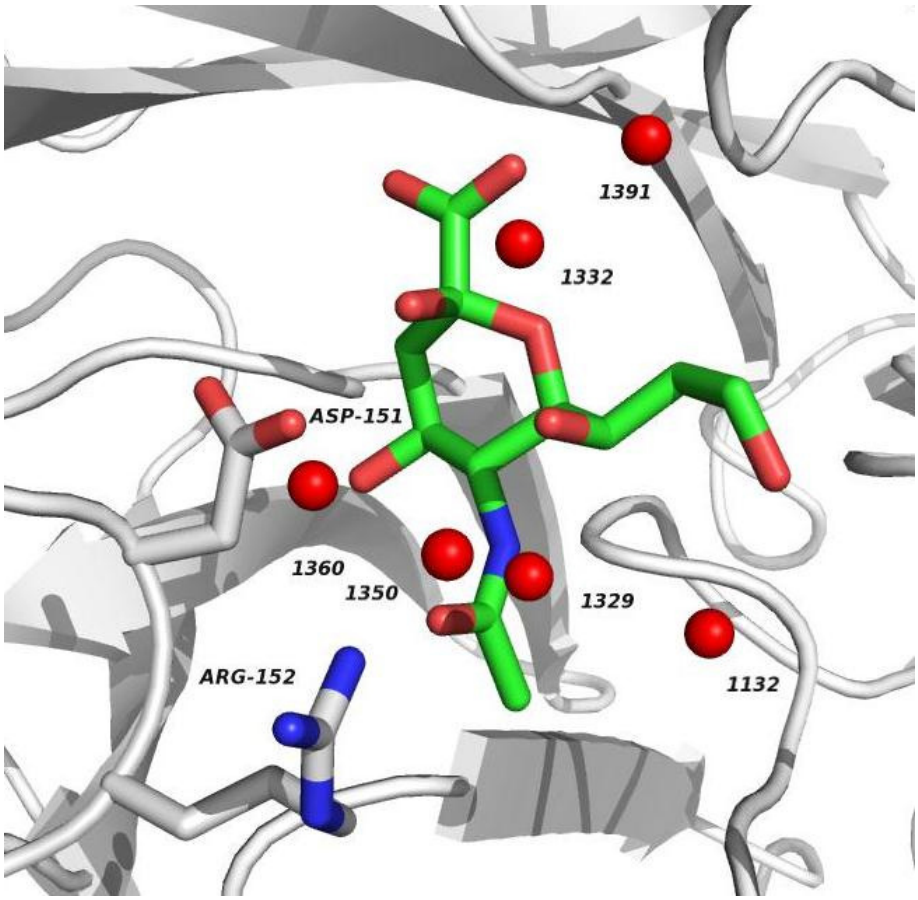

Figure 22 Key amino acid residues and water molecules located within a 4 Å radius of the oxygen at position C-7 of sialic acid (**2**) in the active site of influenza neuraminidase N9. Amino acid residues are shown in stick representation and water molecules in spherical representation. Generated with PyMOL (PDB 1MWE).[191]

In addition to the two catalytic residues (Asp151 and Arg152) six water molecules are also found to lie within the 4 Å pocket around the OH-7 group.
Of the five hydroxyl groups present in sialic acid (**2**) the hydroxyl group at position C-7 is considered to contribute least towards non-covalent interactions, as previously demonstrated in X-ray crystallographic structures of influenza neuraminidase N2 in complex with sialic acid (**2**) (**Figure 9**) (Chapter 1.5).

In support of this observation, studies performed by Macdonald *et al.* it have shown that derivatives of Zanamivir (**15**) functionalised at the position C-7 with an aminohexyl carbamate retain good activity against all influenza virus strains tested, while dimeric derivatives of Zanamivir (**22**) (Chapter 1.5.4) exhibit increased potencies attributed to bivalent binding to multiple neuraminidase enzymes.[131,197,198]

As a consequence, position C-7 is interesting in terms of transition-state stabilisation as well as on information of the active site of influenza neuraminidase during the inactivation mechanism with 7-deoxy-2,3-difluoro-sialic acid (**25**).

Crystals of 7-deoxy-2,3-difluoro-sialic acid (**25**) in complex with Influenza neuraminidase N9 were obtained by co-crystallisation. Diffraction data were collected from a single crystal that diffracted to 1.8 Å and refinement was performed with REFMAC 5.6.0100 on 3786 atoms (**Figure 23**).

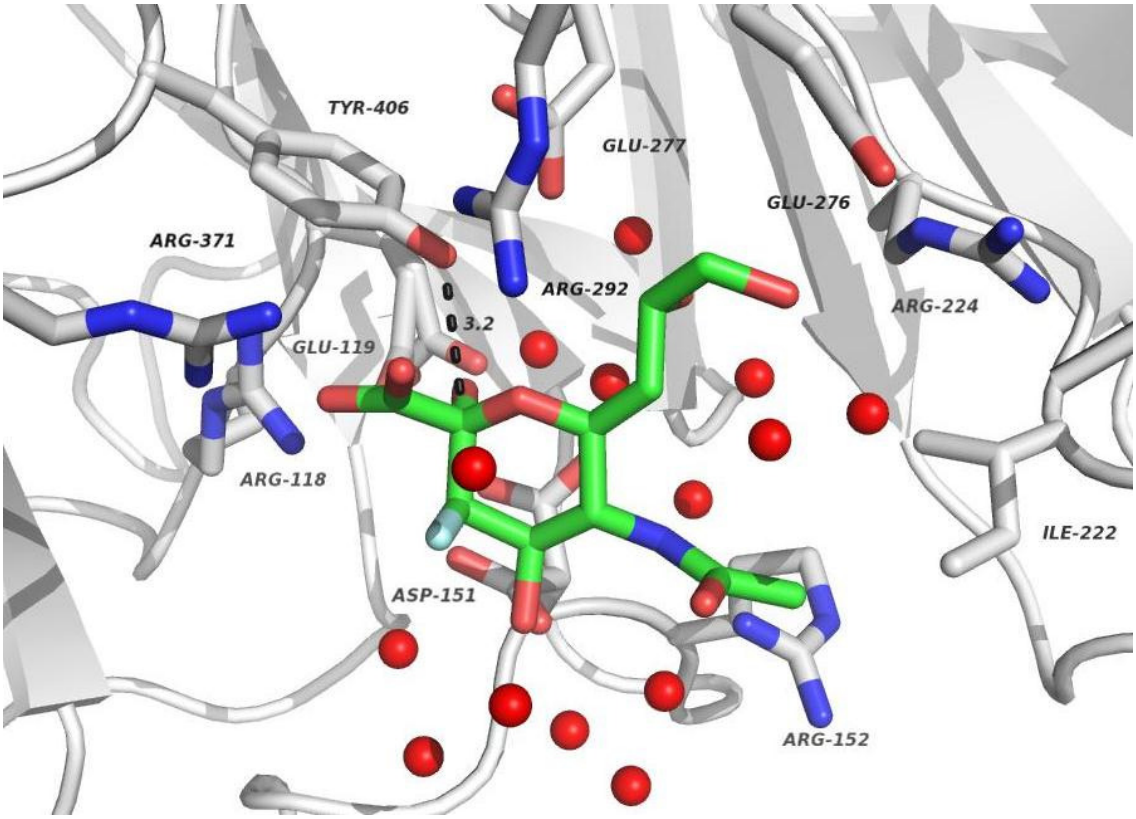

Figure 23 Key amino acid residues and water molecules located within a 4 Å radius of the 7-deoxy-2,3-difluoro-sialic acid (**25**) in the active site of influenza neuraminidase N9. Amino acid residues are shown in stick representation and water molecules in spherical representation. Generated with PyMOL (unpublished work).

Surprisingly, the refined model showed no evidence of covalent binding of the 7-deoxy-sialic acid derivative, but an axial group at the anomeric position and the sialic acid moiety was seen in a twisted orientation in the active site of influenza neuraminidase N9 (**Figure 23**). This result might be explained by considering the mechanism of inactivation (**Scheme 69**).

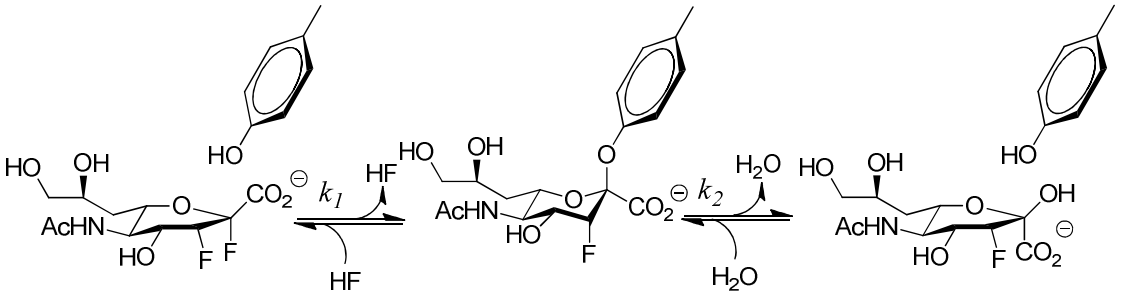

25 **123** **124**

Scheme 69 The glycosylation (k_1) and deglycosylation (k_2) rate constants associated with the mechanism-based inactivator 7-deoxy-2,3-difluoro-sialic acid (**25**).

The time frame in the co-crystallisation method might not have been appropriate to trap the covalently linked sialosyl-enzyme intermediate, but resulted in the isolation of the hydrolysed 3-fluoro-sialic acid (**124**). In an attempt to prove our hypothesis about the hydrolysed 3-fluoro-sialic acid (**124**), co-crystallisation of influenza neuraminidase N9 with the synthetically prepared 3-fluoro-sialic acid (**124**) was performed, however no binding could be observed. Impurity concerns of the 7-deoxy-2,3-difluoro-sialic acid (**25**) with β-2,3-difluoro-sialic acid derivative (**125**) were addressed in extensive ^{19}F NMR analysis. Together with attempted co-crystallisation of influenza neuraminidase N9 with synthetically prepared β-2,3-difluoro-sialic acid (**125**), which showed no binding, it was confirmed that the structure in the refined model is not the β-2,3-difluoro-sialic acid derivative (**125**).

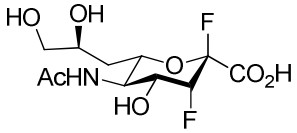

125

As a consequence, an alternative crystallisation method in order to shorten the time frame for the crystallisation was used, in which the 7-deoxy-2,3-difluoro-sialic acid (**25**) was soaked for 15 minutes at 4 °C with a preformed crystal of influenza neuraminidase N9. Diffraction data were collected from a single crystal that diffracted to 2.0 Å and refinement utilising REFMAC 5.6.0100 on 3805 atoms (**Figure 24**).

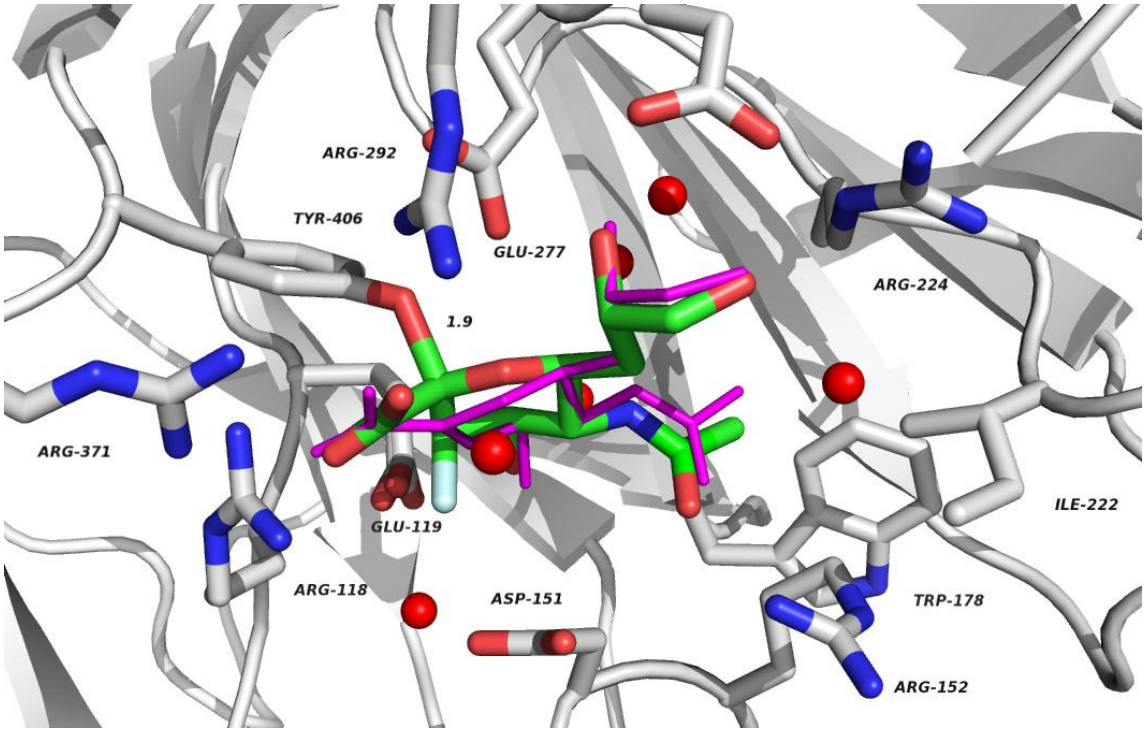

Figure 24 Key amino acid residues and water molecules located within a 4 Å radius of the covalently bound β-7-deoxy-3-fluoro-sialosyl moiety in the active site of influenza neuraminidase N9. Amino acid residues are shown in stick representation and water molecules in spherical representation. The structure is shown with population of the DANA-like compound given in purple. Generated with PyMOL (unpublished work).

The refined model showed in dual population a putative covalently linked sialosyl-enzyme intermediate of the 7-deoxy-2,3-difluoro-sialic acid (**25**) and a DANA-like compound (shown in purple). The covalently linked sialosyl-enzyme intermediate could be identified through a clear rotation of the carboxyl group compared to 7-deoxy-2,3-difluoro-sialic acid (**25**) and the loss of the fluorine atom at position C-2 of 7-deoxy-2,3-difluoro-sialic acid (**25**) Together with the distance of ~ 1.9 Å between the oxygen of the residue Tyr406 and position C-2 of the inactivator could be assumed.

Unfortunately, the final proof of the covalent intermediate was not possible as the electron density map has not been provided.

The second ligand in the active site of influenza neuraminidase N9 with an occurrence of 75% could correspond to a DANA-like elimination product (**Figure 24**). The second structure shows a flattened ring conformation consistent with DANA and has previously been demonstrated on X-ray structures with 4-deoxy-2,3-difluoro-sialic acid (**24**) (Chapter 7.2).

To investigate conformational changes on the inactivator and the active site of influenza neuraminidase the X-ray, the crystal structure obtained on influenza neuraminidase N9 in complex with 7-deoxy-2,3-difluoro-sialic acid (**25**) was superimposed with the structure of influenza neuraminidase N9 in complex with sialic acid (**2**) (**Figure 25**).

The alignment tool in PyMOL was used on 356 atoms of the backbone and gave a root-mean-square deviation (RMSD) of 0.107. The superimposition showed, a twisted ring distortion of the putative covalently linked β-7-deoxy-3-fluoro-sialosyl moiety, as it was previously demonstrated on 4-deoxy-2,3-difluoro-sialic acid (**24**).

The removal of the OH-7 group did not cause any reorientation of the glycerol side chain as the superimposed crystal structures exhibit congruent characteristics.

Out of six water molecules present in the crystal structure of influenza neuraminidase N9 in complex with sialic acid (**2**) three seem to be congruent with the water molecules in the crystal structure obtained on influenza neuraminidase N9 in complex with 7-deoxy-2,3-difluoro-sialic acid (**25**) (**Figure 25**). The water molecules might play a role in the mechanism of inactivation on influenza neuraminidase, but a clear catalytic function of the water molecules within a pocket of 4 Å radius of the oxygen at position C-7 of sialic acid (**2**) in the active site of influenza neuraminidase N9 could not be identified.

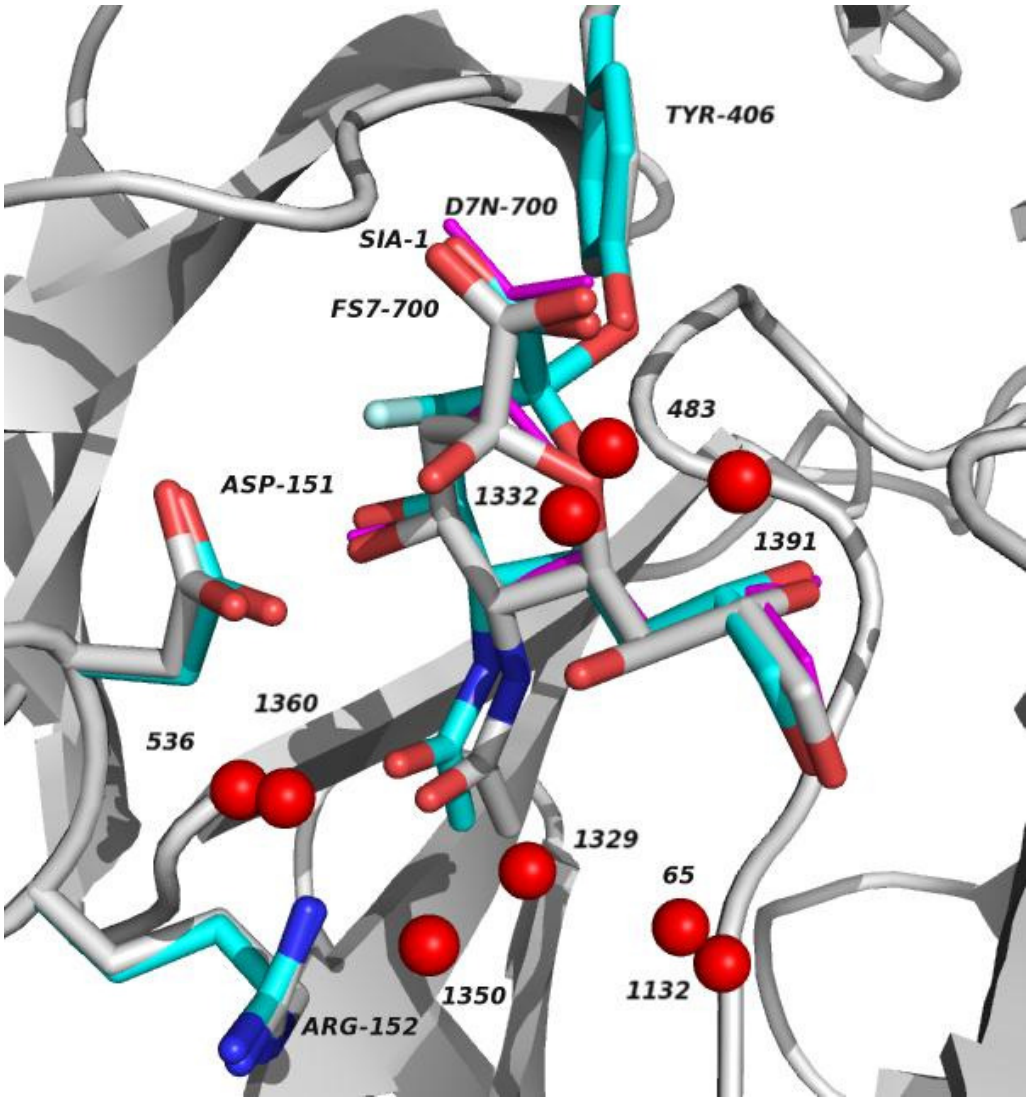

Figure 25 Superimposition of the active site of influenza neuraminidases N9 in complex with sialic acid (**2**) (SIA-1, grey) and β-7-deoxy-3-fluoro-sialosyl moiety (FS7-700, blue). The structure is shown with population of the DANA-like compound given in purple. Key amino acid residues and water molecules located within a 4 Å radius of the oxygen at position C-7 of sialic acid (**2**) in the active site of influenza neuraminidase N9. Amino acid residues are shown in stick representation and water molecules in spherical representation. Generated with PyMOL (PDB 1MWE, grey).[191]

Finally, the X-ray crystal structure obtained from influenza neuraminidase N9 in complex with 7-deoxy-2,3-difluoro-sialic acid (**25**) was superimposed with the structure of influenza neuraminidase N9 in complex with DANA (**16**), which as a competitive transition-state analogue inhibitor could be used to elucidate the behaviour of the 7-deoxy-2,3-difluoro-sialic acid (**25**) in the enzymatic catalytic cycle of influenza neuraminidase (**Figure 26**).

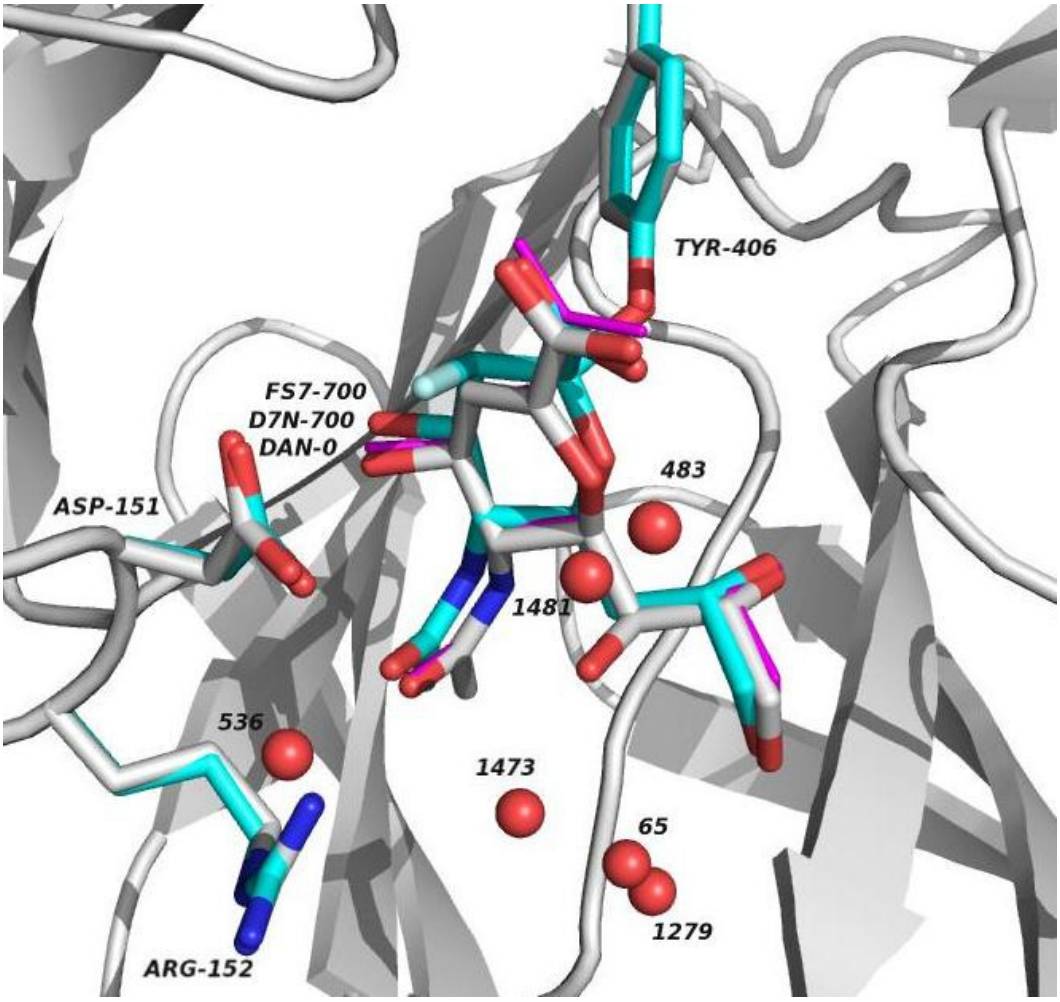

Figure 26 Superimposition of the active site of influenza neuraminidases N9 in complex with DANA (**16**) (DAN-0, grey) and β-7-deoxy-3-fluoro-sialosyl moiety (FS7-700, blue). The structure is shown with population of the DANA-like compound given in purple. Key amino acid residues and water molecules located within a 4 Å radius of the oxygen at position C-7 of DANA (**16**) in the active site of influenza neuraminidase N9. Amino acid residues are shown in stick representation and water molecules in spherical representation. Generated with PyMOL (PDB 1F8B, grey) (unpublished work).[196]

The alignment tool in PyMOL was used on 344 atoms of the backbone to give a root-mean-square deviation (RMSD) of 0.112.

The superimposition showed a ring distortion of the putative covalently linked β-7-deoxy-3-fluoro-sialosyl moiety. However, the distortion of the ring is not as pronounced and might show a related configuration of the refined model obtained with DANA (**16**). This ambiguity with regards to the inactivation mechanism of 7-deoxy-2,3-difluoro-sialic acid (**25**) needs to be addressed and is part of future synthetic and protein crystallographic strategies.

7.4 The C-8 position

In the active site of influenza neuraminidase N9, the catalytic amino acid residues Arg292, Glu277 and Tyr406 are located in a pocket within a 4 Å radius around the oxygen of the C-8 hydroxyl group of sialic acid (**2**) (**Figure 27**).

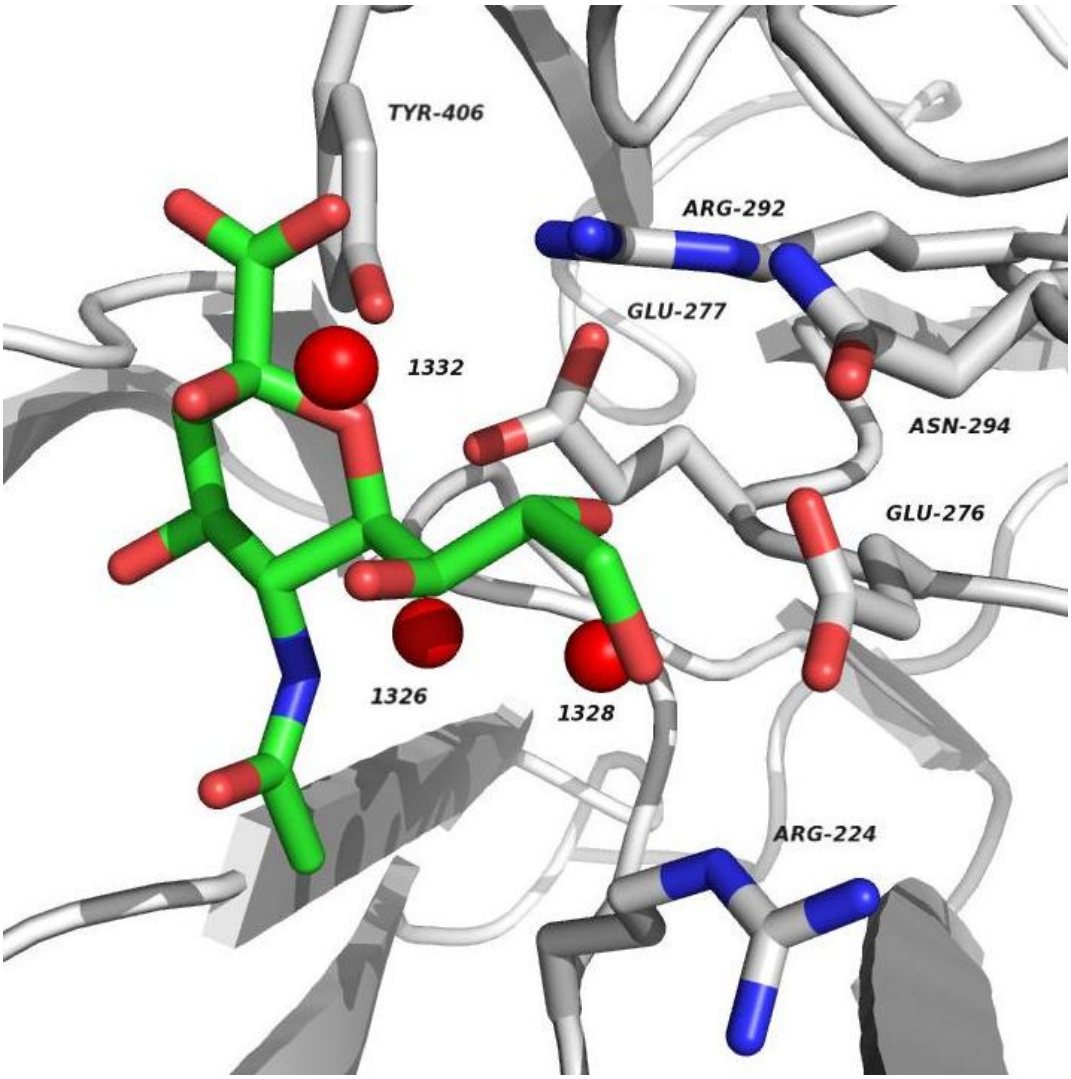

Figure 27 Key amino acid residues and water molecules located within a 4 Å radius of the oxygen at position C-8 of sialic acid (**2**) in the active site of influenza neuraminidase N9. Amino acid residues are shown in stick representation and water molecules in spherical representation. Generated with PyMOL (PDB 1MWE).[191]

In addition to the three catalytic residues three other amino acid residues (Arg224, Asn294 and Glu276) and three water molecules are also found to lie within the 4 Å pocket around the OH-8 group.

The position C-8 has many important non-covalent interactions within the active site of influenza neuraminidase which has previously been demonstrated on influenza neuraminidase N2 in complex with sialic acid (**2**) (**Figure 9**).

Due to its multiple sites of possible non-covalent interactions, the position C-8 of sialic acid (**2**) has been heavily targeted in the development of novel influenza neuraminidase inhibitors.

One of the most prominent examples in influenza neuraminidase inhibitor drug design was the introduction of a pentenyl ether side chain instead of the glycerol side chain which lead to the development of Oseltamivir (**6**) (Chapter 1.5.2.2).[99] Hence, it was anticipated that X-ray crystal structures of influenza neuraminidase N9 in complex with 8-deoxy-2,3-difluoro-sialic acid (**26**) could be useful to develop some understanding of the active site of influenza neuraminidase during the mechanism of inactivation on a physical basis.

Crystals of influenza neuraminidase N9 in complex with 8-deoxy-2,3-difluoro-sialic acid (**26**) were obtained by co-crystallisation. Diffraction data were collected from a single crystal that diffracted to 1.85 Å and refinement was achieved using REFMAC 5.5.0110 on 3797 atoms (**Figure 28**).

The refined model showed in dual population a covalently linked sialosyl-enzyme intermediate of the 8-deoxy-2,3-difluoro-sialic acid (**26**) and a DANA-like compound (shown in purple). The covalently linked sialosyl-enzyme intermediate was identified through a clear rotation of the carboxyl group compared to 8-deoxy-2,3-difluoro-sialic acid (**26**) and the loss of the fluorine atom at position C-2 of 8-deoxy-2,3-difluoro-sialic acid (**26**) (**Figure 28**).

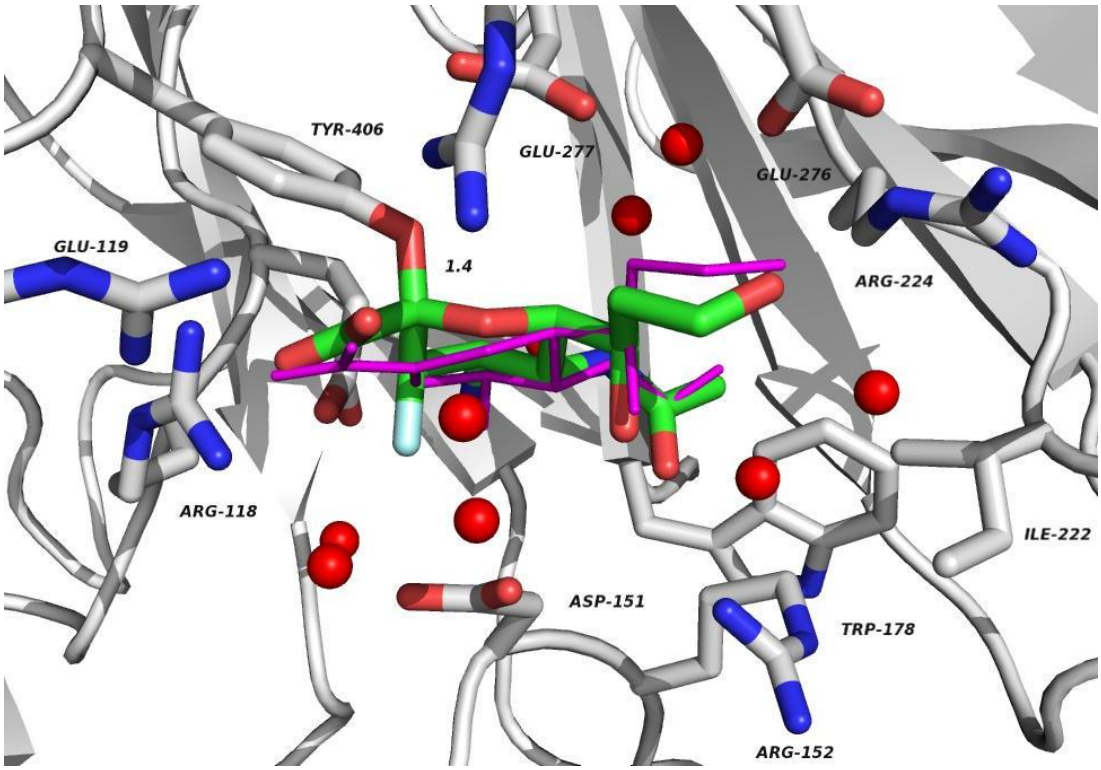

Figure 28 Key amino acid residues and water molecules located within a 4 Å radius of the covalently bound β-8-deoxy-3-fluoro-sialosyl moiety in the active site of influenza neuraminidase N9. Amino acid residues are shown in stick representation and water molecules in spherical representation. The structure is shown with population of the DANA-like compound given in purple. Generated with PyMOL (unpublished work).

Together with the distance of ~ 1.4 Å between the oxygen of the residue Tyr406 and position C-2 of the inactivator with electron density alongside the putative covalent bond indicates covalent binding (**Figure 29**).

The second ligand in the active site of influenza neuraminidase N9 with an occurrence of 60% could correspond to a DANA-like elimination product (**Figure 28**, shown in purple and **Figure 29**, shown in green). The second structure shows a flattened ring conformation consistent with DANA.

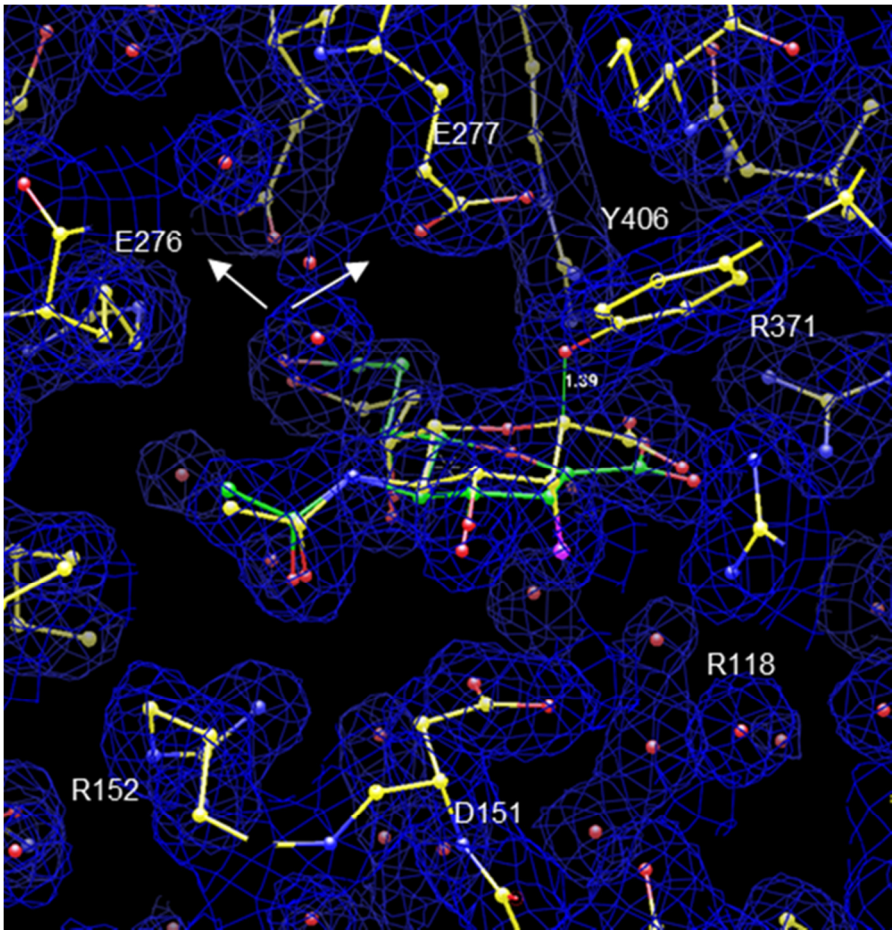

Figure 29 X-ray crystal structure of influenza neuraminidase N9 displaying electron density alongside the covalently linked sialosyl-enzyme intermediate of 8-deoxy-2,3-difluoro-sialic acid (**26**). The structure is shown with population of the DANA-like compound given in green (unpublished results).

The X-ray crystal structure obtained from influenza neuraminidase N9 in complex with 8-deoxy-2,3-difluoro-sialic acid (**26**) was superimposed with the structure of influenza neuraminidase N9 in complex with sialic acid (**2**) to investigate any conformational changes to the inactivator or active site residues of influenza neuraminidase (**Figure 30**).

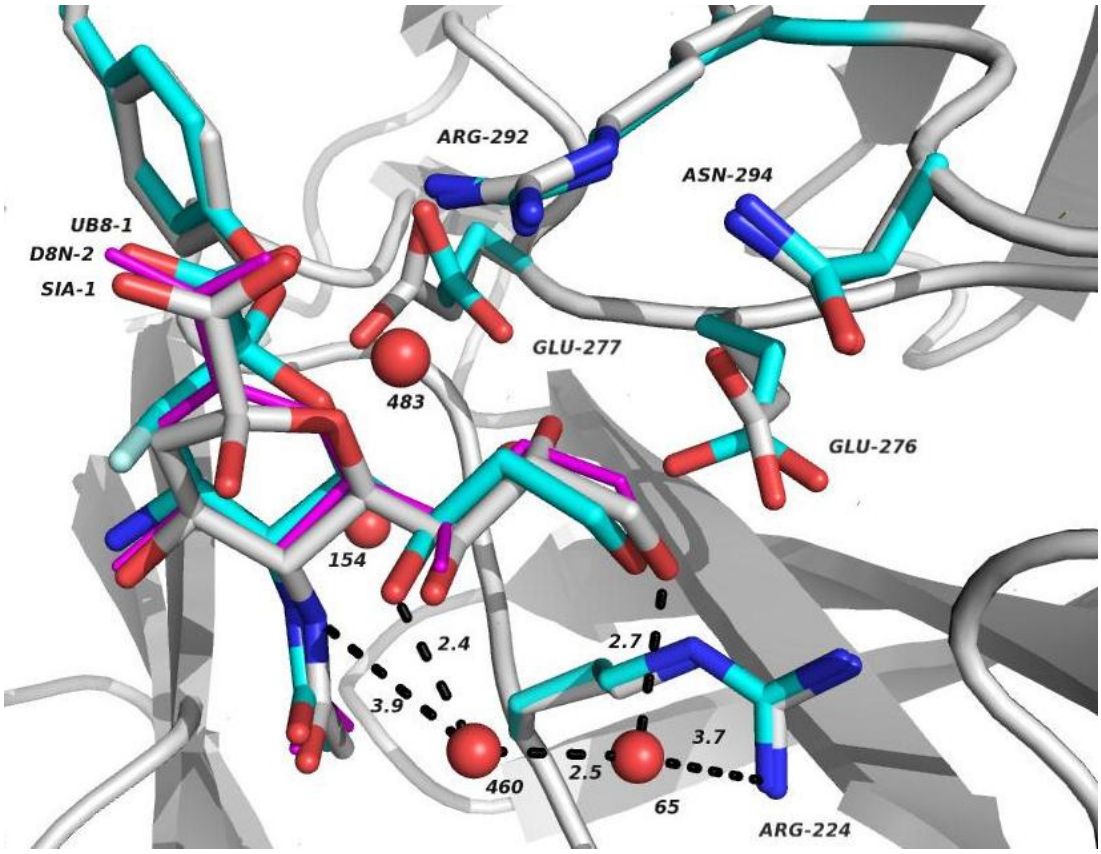

Figure 30 Superimposition of the active site of influenza neuraminidases N9 in complex with sialic acid (**2**) (SIA-1, grey) and β-8-deoxy-3-fluoro-sialosyl moiety (UB-8-1, blue). The structure is shown with population of the DANA-like compound given in purple. Key amino acid residues and water molecules located within a 4 Å radius of the oxygen at position C-8 of sialic acid (**2**) in the active site of influenza neuraminidase N9. Amino acid residues are shown in stick representation and water molecules in spherical representation. Generated with PyMOL (PDB 1MWE, grey).[191]

The alignment tool in PyMOL was used on 369 atoms of the backbone and gave a root-mean-square deviation (RMSD) of 0.101.

The superimposition of the two X-ray crystal structure sets on influenza neuraminidase N9 demonstrated highly conserved active site amino acid residues and a twisted ring distortion of the covalently linked β-8-deoxy-3-fluoro-sialosyl moiety, as it was previously shown on 4-deoxy-2,3-difluoro-sialic acid (**24**) was observed. However, an upwards displacement of the covalently bound β-8-deoxy-3-fluoro-sialosyl moiety could be seen and the loss of hydrogen-bonding interaction at position C-8 might correlate with a rotation of the residues Glu276 and Glu277.

However, one additional water molecule could be seen within a 4 Å radius of the oxygen at position C-8 of sialic acid (**2**). The additional water molecule could be in the range of hydrogen-bonding interactions with the C-5 *N*-acetyl group over another water molecule and the catalytic amino acid residues Arg224. This additional water molecule could be an explanation for the behaviour of 8-deoxy-2,3-difluoro-sialic acid (**26**) in inactivation kinetics with worse IC_{50} values than the parent inactivator 2,3-difluoro-sialic acid (**23**), as previously demonstrated (Chapter 6.3.1). To further investigate the role of this water molecule for catalysis, computer aided hydration free energy calculations could be performed, however this is beyond the scope of this project.[193]

Finally, the X-ray crystal structure obtained from influenza neuraminidase N9 in complex with 8-deoxy-2,3-difluoro-sialic acid (**26**) was superimposed with the structure of influenza neuraminidase N9 in complex with DANA (**16**), which as a competitive transition-state analogue inhibitor could be used to elucidate the behaviour of the 8-deoxy-2,3-difluoro-sialic acid (**26**) in the enzymatic catalytic cycle of influenza neuraminidase (**Figure 31**).

The alignment tool in PyMOL was used on 365 atoms of the backbone to give a root-mean-square deviation (RMSD) of 0.111. The superimposition showed a twisted ring distortion of the covalently linked β-8-deoxy-3-fluoro-sialosyl moiety, which has previously been observed on 4-deoxy-2,3-difluoro-sialic acid (**24**). Remarkably, the glycerol side chain in 8-deoxy-2,3-difluoro-sialic acid (**26**) is rotated towards the additional water molecule, which might reinforce the role of this water molecule for catalysis

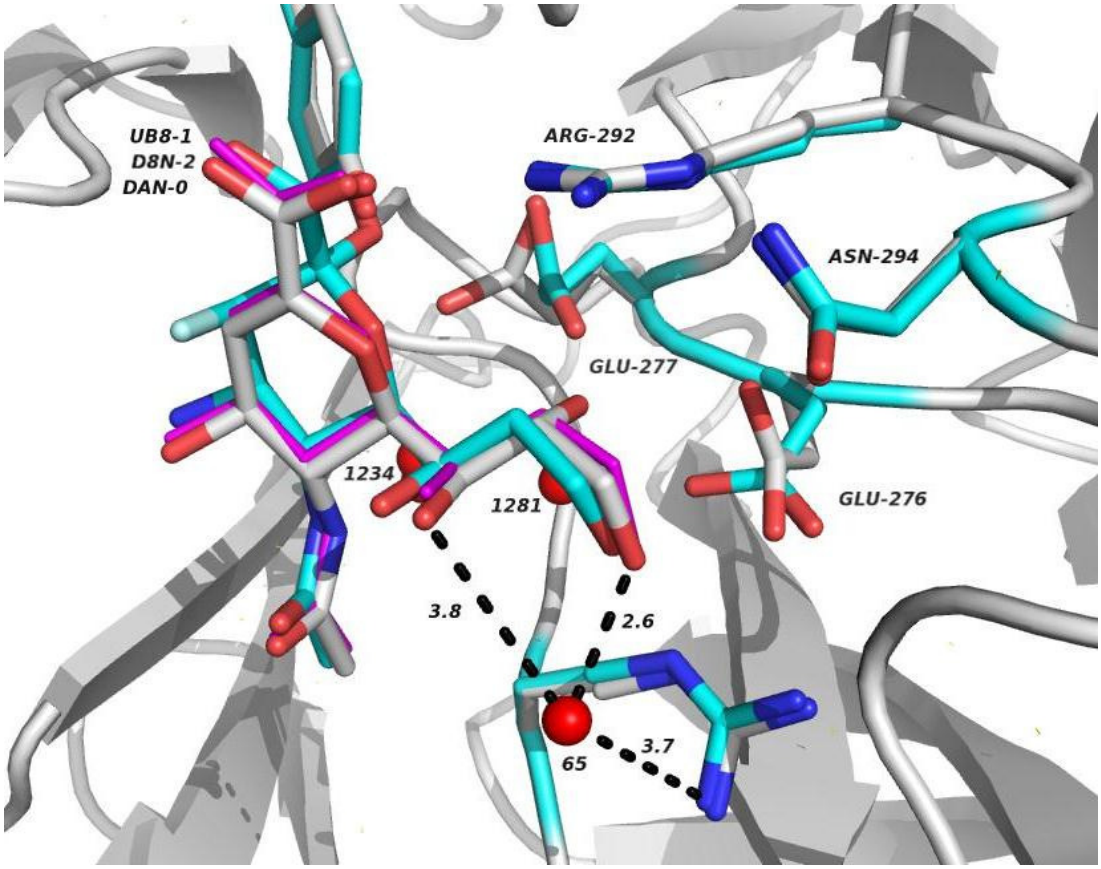

Figure 31 Superimposition of the active site of influenza neuraminidases N9 in complex with DANA (**16**) (DAN-0, grey) and β-8-deoxy-3-fluoro-sialosyl moiety (UB8-1, blue). The structure is shown with population of the DANA-like compound given in purple. Key amino acid residues and water molecules located within a 4 Å radius of the oxygen at position C-8 of DANA (**16**) in the active site of influenza neuraminidase N9. Amino acid residues are shown in stick representation and water molecules in spherical representation. Generated with PyMOL (PDB 1F8B, grey) (unpublished work).[196]

7.5 The C-9 position

In the active site of influenza neuraminidase N9, the catalytic amino acid residues Arg224, Ala 246, Glu276 and Asn294 are located in a pocket within a 4 Å radius around the oxygen of the C-9 hydroxyl group of sialic acid (**2**) (**Figure 32**).

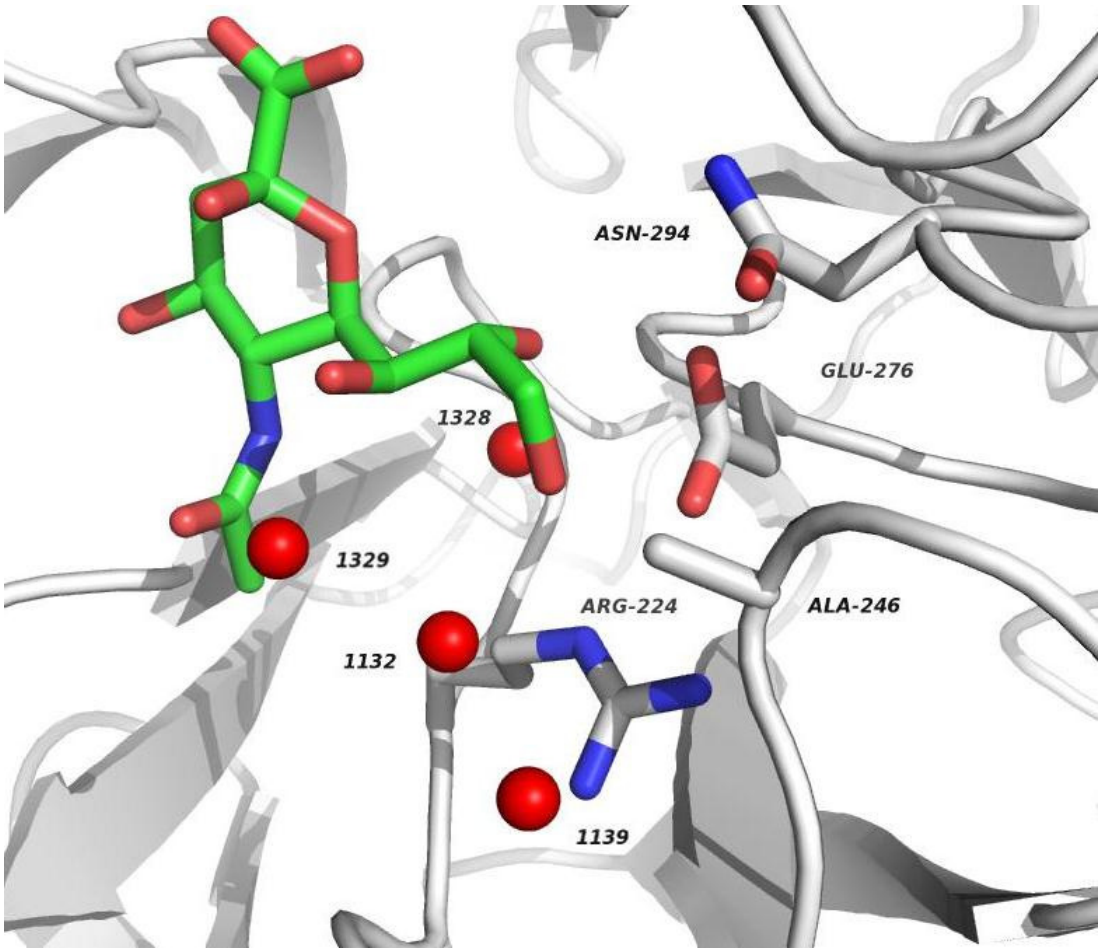

Figure 32 Key amino acid residues and water molecules located within a 4 Å radius of the oxygen at position C-9 of sialic acid (**2**) in the active site of influenza neuraminidase N9. Amino acid residues are shown in stick representation and water molecules in spherical representation. Generated with PyMOL (PDB 1MWE).[191]

In addition, four water molecules are also found to lie within the 4 Å pocket around the OH-9 group.

Position C-9 in sialic acid plays a crucial role in multiple non-covalent interactions in the active site of influenza neuraminidase N2, as it has previously been pointed out (Chapter 1.5).

Targeting this position together with the rest of the glycerol side chain has been a key feature in influenza neuraminidase inhibitor drug design.[99]

Therefore, it was anticipated that X-ray crystal structures of influenza neuraminidase N9 in complex with 9-deoxy-2,3-difluoro-sialic acid (**27**) would be useful to gain further understanding of the active site of influenza neuraminidase during the mechanism of inactivation.

Crystals of influenza neuraminidase N9 in complex with 9-deoxy-2,3-difluoro-sialic acid (**27**) were obtained by co-crystallisation. Diffraction data were collected from a single crystal that diffracted to 2.4 Å and refinement was performed using REFMAC 5.5.0110 on 3771 atoms (**Figure 33**).

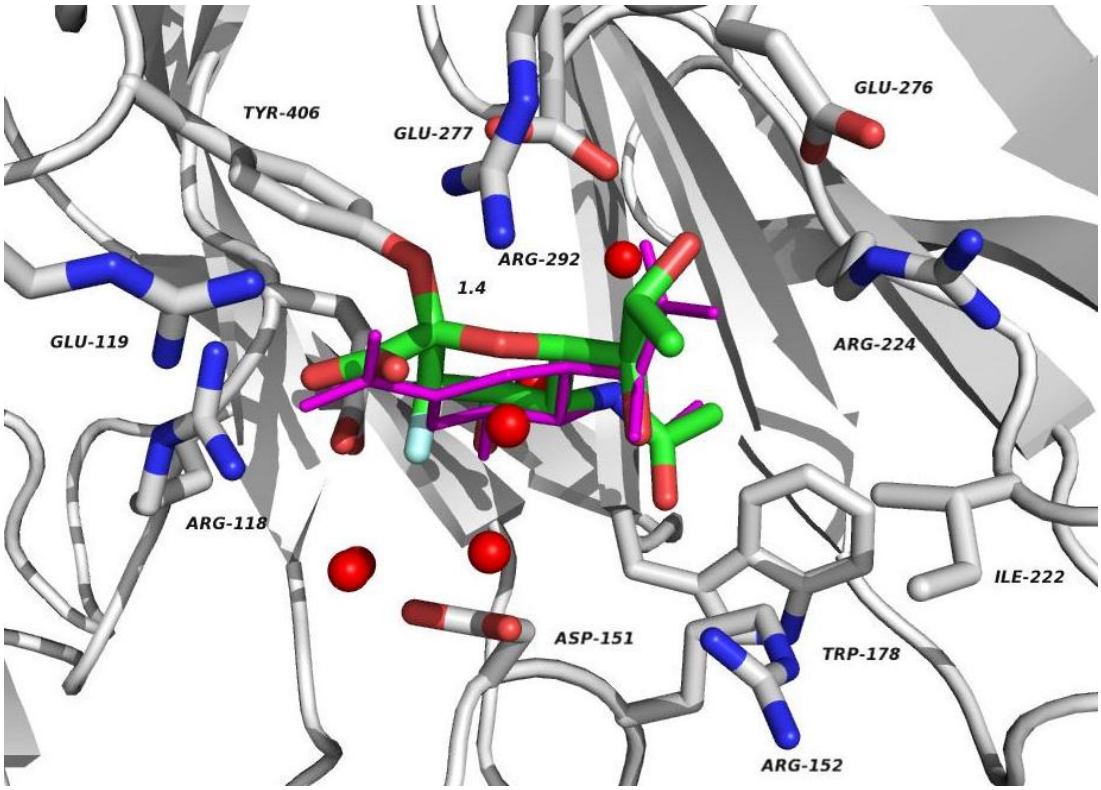

Figure 33 Key amino Acid residues and water molecules located within a 4 Å radius of the covalently bound β-9-deoxy-3-fluoro-sialosyl moiety in the active site of influenza neuraminidase N9. Amino acid residues are shown in stick representation and water molecules in spherical representation. The structure is shown with population of the DANA-like compound given in purple. Generated with PyMOL (unpublished work).

The refined model showed the covalently linked sialosyl-enzyme intermediate and in dual occupancy in an occurrence of 70% a DANA-like compound (shown in purple). The distortion of the ring moiety, the loss of a fluorine atom at position C-2 and the distance of ~ 1.4 Å between the oxygen of the residue Tyr406 and position C-2 all indicated covalent binding character (**Figure 33**). Unfortunately, the final proof of the covalent intermediate was not possible as the electron density map has not been provided.

To investigate conformational changes on the inactivator and the active site of Influenza neuraminidase, the X-ray crystal structure of influenza neuraminidase N9 in complex with 9-deoxy-2,3-difluoro-sialic acid (**27**) was superimposed with the structure of influenza neuraminidase N9 in complex with sialic acid (**2**) (**Figure 34**).

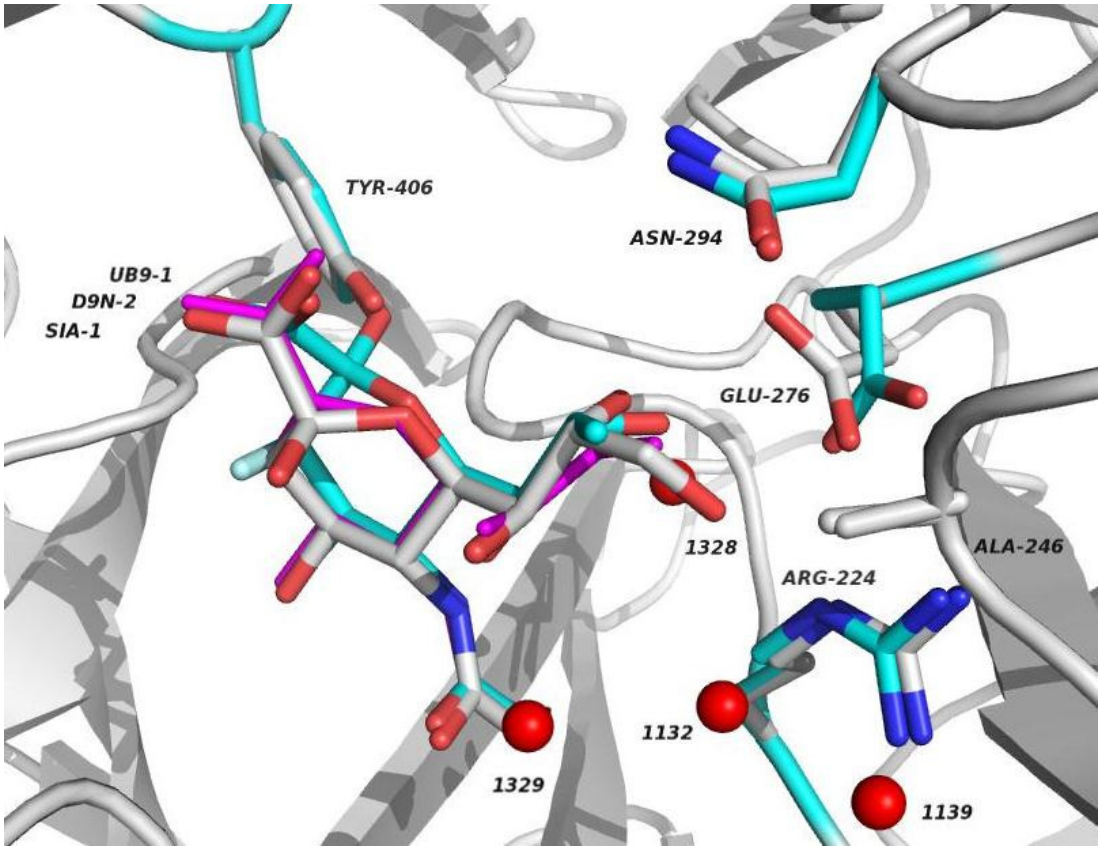

Figure 34 Superimposition of the active site of influenza neuraminidases N9 in complex with sialic acid (**2**) (SIA-1, grey) and β-9-deoxy-3-fluoro-sialosyl moiety (UB9-1, blue). The structure is shown with population of the DANA-like compound given in purple. Key amino acid residues and water molecules located within a 4 Å radius of the oxygen at position C-9 of sialic acid (**2**) in the active site of influenza neuraminidase N9. Amino acid residues are shown in stick representation and water molecules in spherical representation. Generated with PyMOL (PDB 1MWE, grey).[191]

The superimposition of the two X-ray crystal structures utilised the alignment tool in PyMOL on 367 atoms of the backbone and gave a root-mean-square deviation (RMSD) of 0.140.

The superimposition showed a twisted ring distortion of the β-9-deoxy-sialic acid moiety and is supporting the proposed formation of a covalent bond as previously demonstrated on 4-deoxy-2,3-difluoro-sialic acid (**24**). Furthermore, a re-orientation of the glycerol side chain and rotation of the amino acid residue Glu276 could be observed, which might correlate with the loss of hydrogen-bonding interaction at position C-9.

Finally, the X-ray crystal structure obtained from influenza neuraminidase N9 in complex 9-deoxy-2,3-difluoro-sialic acid (**27**) was superimposed with the structure of influenza neuraminidase N9 in complex with DANA (**16**), which as a competitive transition-state analogue inhibitor could be used to elucidate the behaviour of the 9-deoxy-2,3-difluoro-sialic acid (**27**) in the enzymatic catalytic cycle of influenza neuraminidase (**Figure 35**).

The alignment tool in PyMOL was used on 344 atoms of the backbone to give a root-mean-square deviation (RMSD) of 0.112.

The superimposition of the two structures showed that the second DANA-like ligand obtained in the X-ray crystal structure on 9-deoxy-2,3-difluoro-sialic acid (**27**) is congruent with the data obtained on influenza neuraminidase N9 in complex with DANA (**16**). The re-orientation of the glycerol side chain and rotation of the amino acid residue Glu276 is in support of the proposed correlation with the loss of hydrogen-bonding interaction at position C-9.

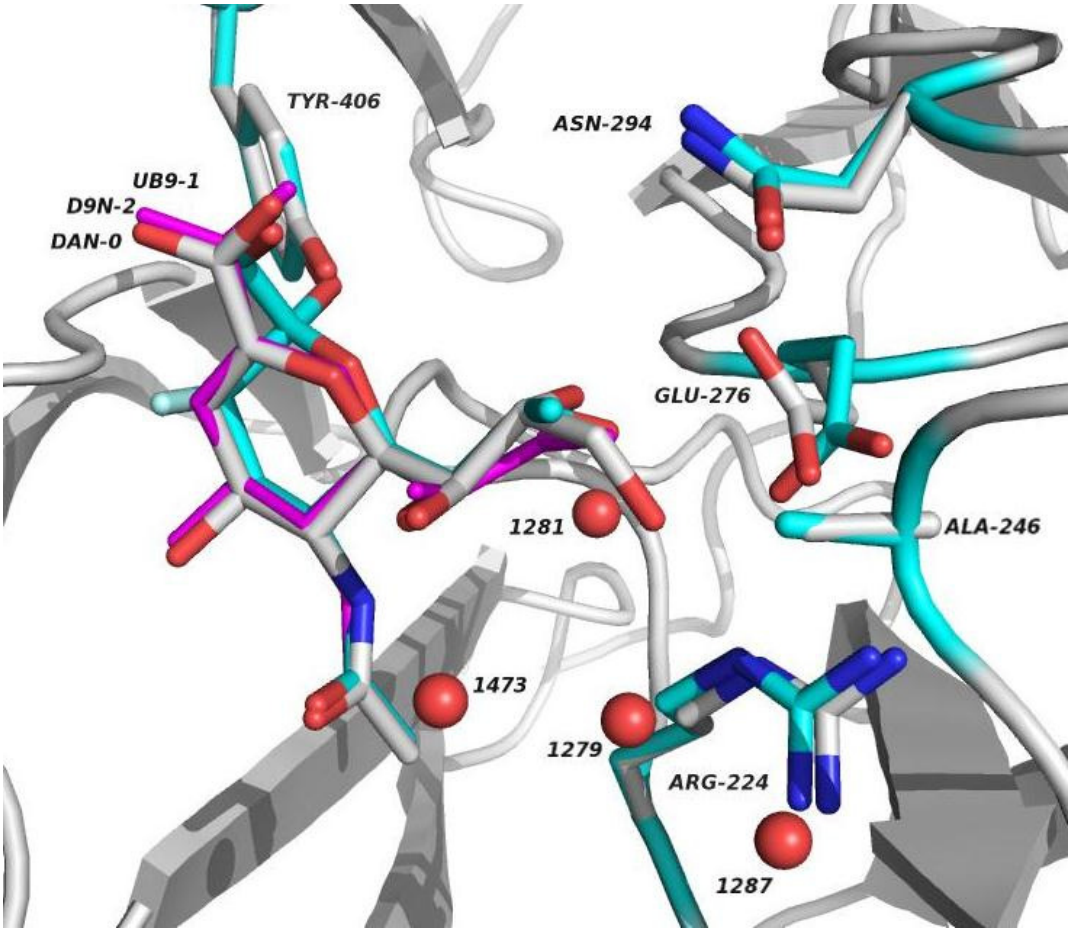

Figure 35 Superimposition of the active site of influenza neuraminidases N9 in complex with DANA (**16**) (DAN-0, grey) and β-9-deoxy-3-fluoro-sialosyl moiety (UB9-1, blue). The structure is shown with population of the DANA-like compound given in purple. Key amino acid residues and water molecules located within a 4 Å radius of the oxygen at position C-9 of DANA (**16**) in the active site of influenza neuraminidase N9. Amino acid residues are shown in stick representation and water molecules in spherical representation. Generated with PyMOL (PDB 1F8B, grey) (unpublished work).[196]

7.6 Conclusions

In conclusion, the X-ray crystal structure of influenza neuraminidase N9 in complex with monodeoxygenated 2,3-difluoro-sialic acid inactivators (**24**) - (**27**) allowed interpretation of the inhibition mechanisms on a physical basis. In detail, the superimposition of the structures of 4-deoxy-2,3-difluoro-sialic acid (**24**) (**Figure 36a**) and 7-deoxy-2,3-difluoro-sialic acid (**25**) in complex with influenza neuraminidase N9 showed a shift of the 7-deoxy-sialosyl moiety away from the Tyr406 amino acid residue (**Figure 36b**).

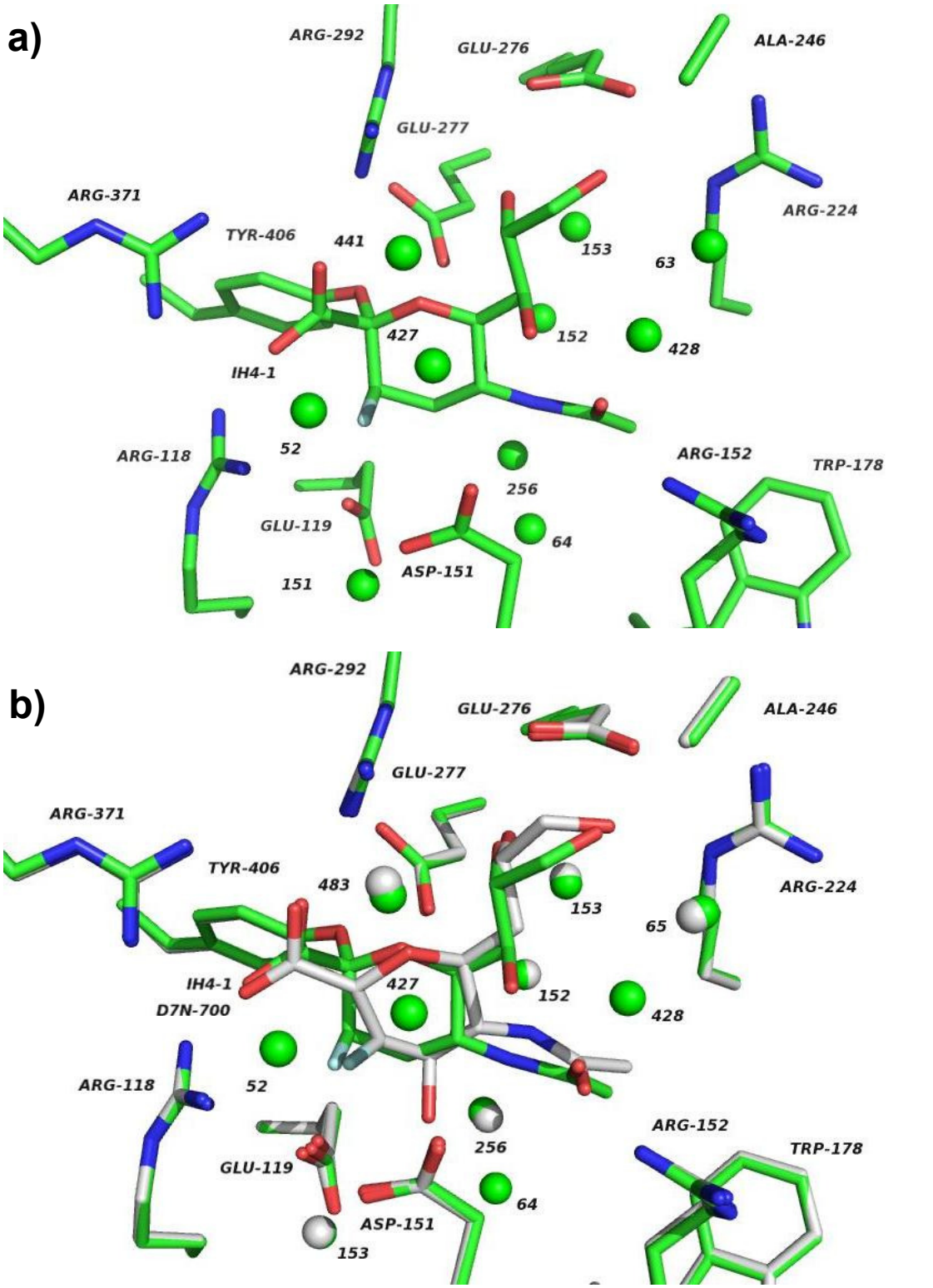

Figure 36 a) Key amino acid residues and water molecules located within a 4 Å radius of the covalently bound β-4-deoxy-3-fluoro-sialosyl moiety (IH4-1, green) in the active site of influenza neuraminidase N9. b) Superimposition of key amino acid residues and water molecules located within a 4 Å radius of the covalently bound β-4-deoxy-3-fluoro-sialosyl moiety (IH4-1, green) and β-7-deoxy-3-fluoro-sialosyl moiety (D7N-700, grey) in the active site of influenza neuraminidase N9. Amino acid residues are shown in stick representation and water molecules in spherical representation. Generated with PyMOL (unpublished work).

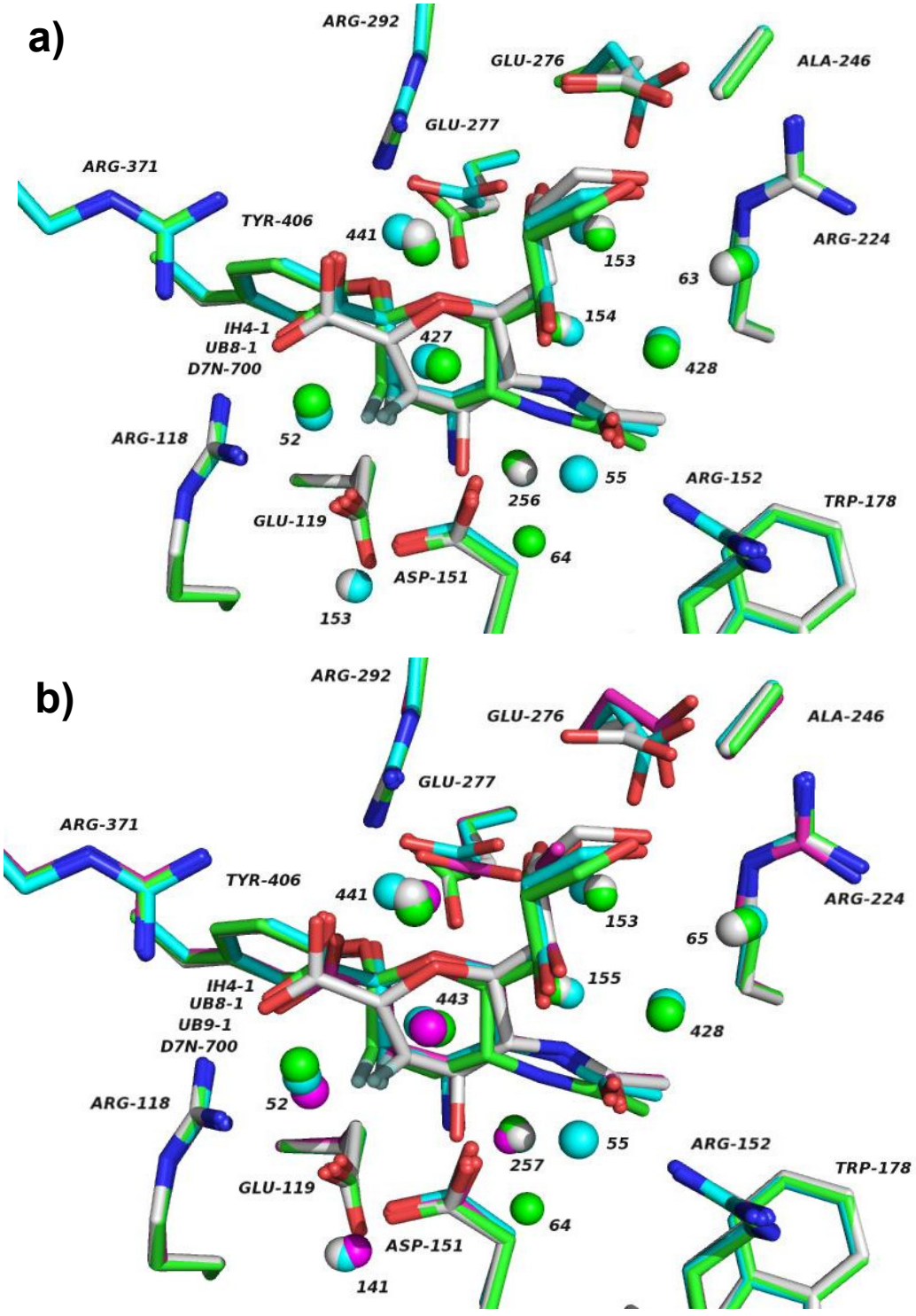

Figure 37 a) Superimposition of key amino acid residues and water molecules located within a 4 Å radius of the covalently bound β-4-deoxy-3-fluoro-sialosyl moiety (IH4-1, green), β-7-deoxy-3-fluoro-sialosyl moiety (D7N-700, grey) and β-8-deoxy-3-fluoro-sialosyl moiety (UB8-1, cyan) in the active site of influenza neuraminidase N9. b) Superimposition of key amino acid residues and water molecules located within a 4 Å radius of the covalently bound β-4-deoxy-3-fluoro-sialosyl moiety (IH4-1, green), β-7-deoxy-3-fluoro-sialosyl moiety (D7N-700, grey), β-8-deoxy-3-fluoro-sialosyl moiety (UB8-1, cyan) and β-9-deoxy-3-fluoro-sialosyl moiety (UB9-1, magenta) in the active site of influenza neuraminidase N9. Amino acid residues are shown in stick representation and water molecules in spherical representation. Generated with PyMOL (unpublished work).

This downwards shift could indicate that the 7-deoxy-2,3-difluoro-sialic acid (**25**) is not forming a covalent bond with Tyr406. In contrast to the 7-deoxy-2,3-difluoro-sialic acid (**25**), the 8-deoxy-2,3-difluoro-sialic acid (**26**) and 9-deoxy-2,3-difluoro-sialic acid (**27**) are congruent with 4-deoxy-2,3-difluoro-sialic acid (**24**) (**Figure 37b**) and are in compliance with the mechanism-based inhibitor design strategy, developed on the covalent glycosyl-enzyme intermediate mechanism for neuraminidases (**Scheme 8**, Chapter 1.5.1). Nevertheless, the structures of 8-deoxy-2,3-difluoro-sialic acid (**26**) and 9-deoxy-2,3-difluoro-sialic acid (**27**) showed a rotation of the amino acid residues Glu276 and Glu277 (**Figure 37b**). This rotation could be used to explain the poor inactivation previously envisaged against all influenza strains tested (Chapter 6.2). Furthermore, additional water molecules in 4-deoxy-2,3-difluoro-sialic acid (**24**) and in 8-deoxy-2,3-difluoro-sialic acid (**26**) respectively could be seen. To further investigate the role of this water molecules for catalysis, computer aided hydration free energy calculations could be performed, however this is beyond the scope of this project.[193]

However, the complex structure of IC_{50} values on different strains of influenza neuraminidases and the time-dependency thereof lead to the conclusion that minor differences in transition-state conformations in different neuraminidase strains result in major effects on Gibbs free energy of binding ($\Delta\Delta G^{\ddagger}$). Hence, the main focus will now be put on calculating the Gibbs free energy of binding ($\Delta\Delta G^{\ddagger}$) for the monodeoxygenated 2,3-difluoro-sialic acid inactivators (**24**) - (**27**). The systematic removal of each hydroxyl group not only produces analogues that differ in their hydrogen-bonding capabilities, but also influences electronic properties. In order to address differences in the electronic nature of the monodeoxygenated 2,3-difluoro-sialic acid derivatives (**24**) - (**27**) compared to the parent compound 2,3-difluoro-sialic acid (**23**) the monodeoxygenated natural substrates (**126**) - (**129**) with a 4-methylumbelliferone fluorescent tag are going to be generated.

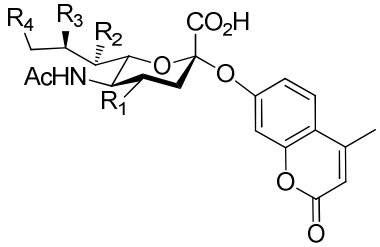

121 R_1, R_2, R_3, R_4 = OH

126 R_1 = H, R_2, R_3, R_4 = OH

127 R_2 = H, R_1, R_3, R_4 = OH

128 R_3 = H, R_1, R_2, R_4 = OH

129 R_4 = H, R_1, R_2, R_3 = OH

The difference in Gibbs free energy of binding ($\Delta\Delta G^{\ddagger}$) (**Figure 5**) for each monodeoxygenated natural substrate (**126**) - (**129**) compared to the natural substrate (**121**) consequent upon substitution of each hydroxyl by hydrogen are readily calculated from the relative values of V_m/K_i **(Equation 6**). $(V_m/K_i)_1$ and $(V_m/K_i)_2$ are the kinetic constants for the deoxygenated analogue and the parent compound respectively.[8]

$$\Delta\Delta G^{\ddagger} = RT \ln \frac{(V_{\mathrm{m}}/K_{\mathrm{i}})_2}{(V_{\mathrm{m}}/K_{\mathrm{i}})_1}$$

Equation 6 Difference in Gibbs free energy of binding ($\Delta\Delta G^{\ddagger}$) for monodeoxygenated compounds compared to parent compound.[8]

Chapter 8 - Towards the synthesis of monodeoxygenated sialic acids as substrates for influenza neuraminidase

We set out to generate a series of the monodeoxygenated natural substrates (**126**) - (**129**) with a 4-methylumbelliferone fluorescent tag to enable the determination of differences in Gibbs free energies of binding ($\Delta\Delta G^{\ddagger}$) to influenza neuraminidase (**Figure 5**) for each monodeoxygenated natural substrate (**126**) - (**129**) compared to the natural substrate (**121**).

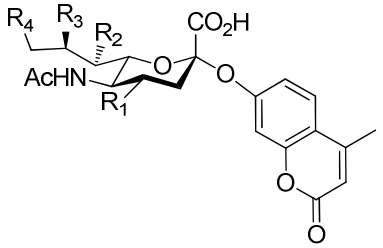

121 R_1, R_2, R_3, R_4 = OH

126 R_1 = H, R_2, R_3, R_4 = OH

127 R_2 = H, R_1, R_3, R_4 = OH

128 R_3 = H, R_1, R_2, R_4 = OH

129 R_4 = H, R_1, R_2, R_3 = OH

8.1 Attempted synthesis of 4-deoxy-2'-(4-methylumbelliferyl) α-*D*-sialic acid (126) via the C-4 Barton-McCombie deoxygenation

For the synthesis of 4-deoxy-2'-(4-methylumbelliferyl) α-*D*-sialic acid (**126**) we intended to utilise a 8,9-*O*-isopropylidene protection group on sialic acid (**2**) as an intermediate towards the synthesis of a C-4 xanthate (**130**).

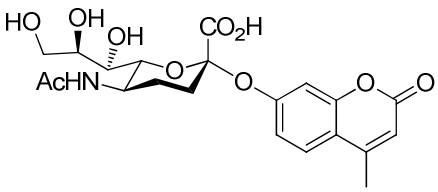

126

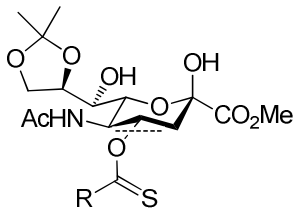

130

R = SMe (xanthate),
= OPh (thionocarbonate),
= 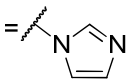 (*O*-thiocarbamate)

8.1.1 Retrosynthetic analysis

The 4-deoxy-2'-(4-methylumbelliferyl) α-*D*-sialic acid (**126**) could be yielded in a glycosylation step utilising 4-methylumbelliferone on the β-chloro-4-deoxy-sialic acid methyl ester (**131**) according to the procedure of Engstler *et al.* (**Scheme 70**).[199] It was anticipated to achieve formation of the β-chloro-4-deoxy-sialic acid methyl ester (**131**) by treatment of the 4-deoxy-sialic acid methyl ester derivative (**132**) with hydrochloric acid gaseous. By analogy with the previously accomplished synthesis of the 4-deoxy-2,3-difluoro-sialic acid (**24**) we considered to achieve the formation of 4-deoxy-sialic acid methyl ester (**132**) by Barton-McCombie deoxygenation of the C-4 Xanthate (**133**).[150,152]
The synthesis of the C-4 Xanthate (**133**) was considered possible from the 8,9-*O*-isopropylidene-sialic acid methyl ester, which itself can be produced from sialic acid (**2**).

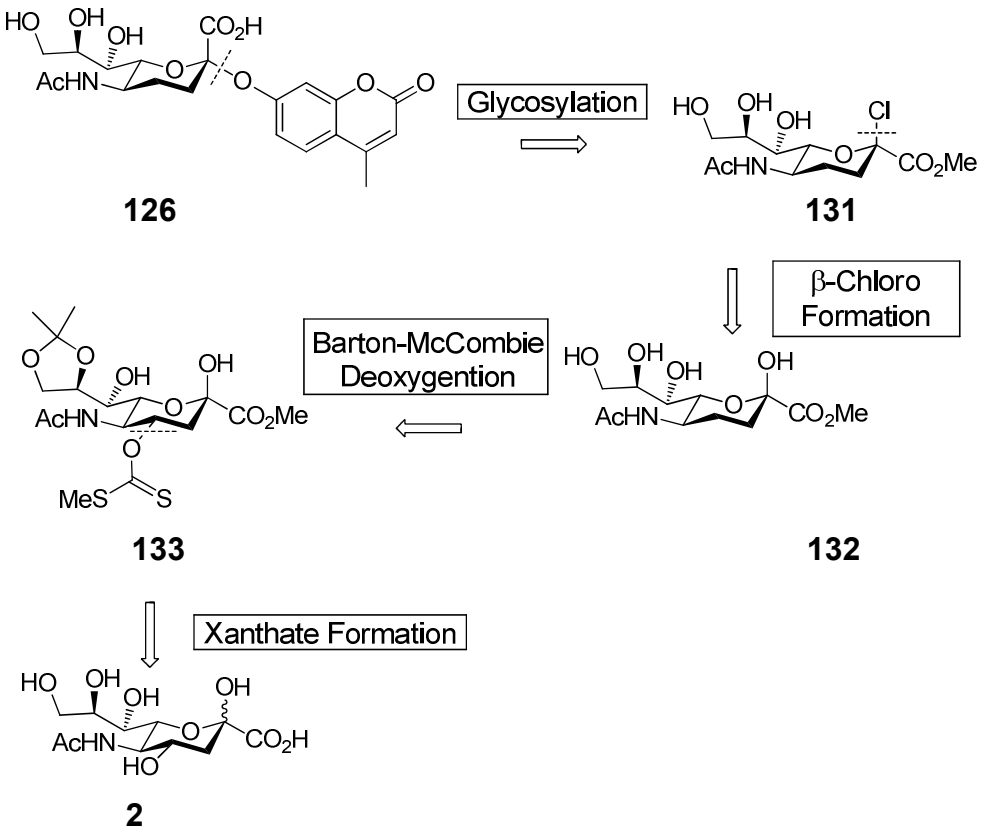

Scheme 70 Retrosynthetic strategy for the synthesis of 4-deoxy-2'-(4-methylumbelliferyl) α-*D*-sialic acid (**126**) via the C-4 xanthate (**133**).

8.1.2 Attempted formation of 4-deoxy-sialic acid methyl ester (132)

The synthesis of 4-deoxy-sialic acid methyl ester (**132**) started according to the procedure of Ogura *et al.* from sialic acid (**2**), which after esterification utilising trifluoroacetic acid in MeOH at room temperature and isopropylidene protection with 2,2'-dimethoxypropane and catalytic amounts of *p*-toluenesulfonic acid (*p*-TSA) in acetone gave the 8,9-*O*-isopropylidene-sialic acid methyl ester (**134**) (**Scheme 71**).[153]

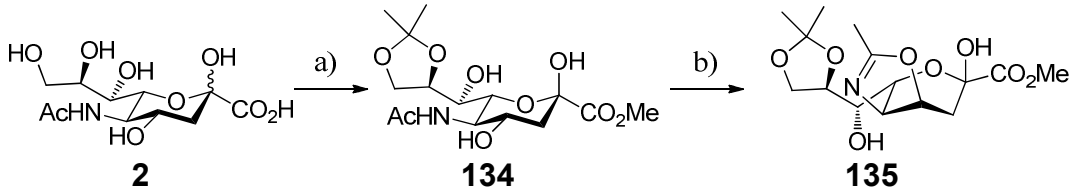

Scheme 71 Attempted synthesis of 8,9-*O*-isopropylidene-7-*O*-thiocarbamate-sialic acid methyl ester (**132**). a) (i) TFA, MeOH, r.t., O/N; (ii) 2,2'-Dimethoxypropane, *p*-TSA, acetone, r.t., O/N, 93% (**134**); b) 1,1'-Thiocarbonyldiimidazole, CH_2Cl_2, 40 °C, 2 d.

The introduction of a thiocarbamate at position C-4 using 1,1'-thiocarbonyldiimidazole was performed in accordance to the previously deployed method (Chapter 3.2) but resulted in formation of oxazoline (**135**) (**Scheme 71**).

However, treatment of 8,9-*O*-isopropylidene-sialic acid methyl ester (**134**) with phenyl chlorothionoformate according to the previously developed protocol (Chapter 2.3.2) gave the desired 4-*O*-(phenoxy)thiocarbonyl derivative (**136**) in 79% yield (**Scheme 72**).

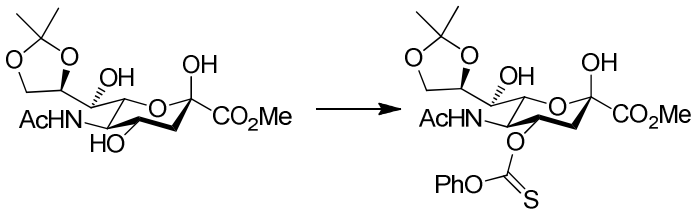

134 **136**

Scheme 72 Synthesis of 8,9-*O*-isopropylidene-4-*O*-(phenoxy)thiocarbonyl-sialic acid methyl ester (**136**). Phenyl chlorothionoformate, CH_2Cl_2/pyridine, - 40 ºC → r.t., 5 h, 79%.

In order to probe the optimal conditions for the Barton-McCombie deoxygenation, the thionocarbonate (**133**) was used as the model substrate, while radical initiator, radical carriers, solvents and temperatures were varied in an effort to generate 4-deoxy-8,9-*O*-isopropylidene-sialic acid methyl ester (**137**) in the highest possible yield.

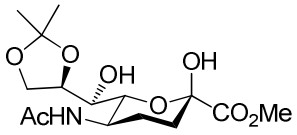

137

In the first set of reactions according to Lopez *et al.*, which has previously been described (Chapter 2.3.2), bis(tributyltin) oxide was used to generate tributyltin hydride in situ and subjected to thionocarbonate (**136**) with azobiscyanocyclohexane in toluene under reflux conditions (**Table 13, entry 1 and 2**).[151]

Table 13 Overview of the different conditions used for the attempted synthesis of 4-deoxy-8,9-*O*-isopropylidene-sialic acid derivative (**134**). **Condition A**: $(Bu_3Sn)_2O$ (0.037 eq.), PMHS (5 eq.), *n*-BuOH (5.5 eq.), azobiscyanocyclohexane (0.15 eq.), toluene; **Condition B**: $(Bu_3Sn)_2O$ (0.037 eq.), PMHS (5 eq.), *n*-BuOH (5.5 eq.), azobiscyanocyclohexane (0.15 eq.), toluene, solution was degassed and molecular sieves added; **Condition C**: $(Bu_4N)_2S_2O_8$ (3 eq.), $NaHCO_3$ (6 eq.), DMF; **Condition D**: $(Bu_4N)_2S_2O_8$ (3 eq.), $NaHCO_3$ (6 eq.), DMF, solution was degassed and molecular sieves added; **Condition E**: Bu_3SnH (2 eq.), azobiscyanocyclohexane (0.3 eq.), toluene; **Condition F**: Bu_3SnH (3.7 eq.), 50% 2,2-bis(*tert*-butylperoxy)-butane solution (0.45 eq.), 1,4-dioxane.

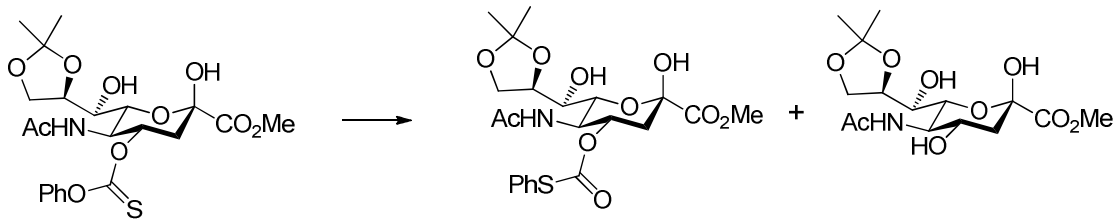

Entry	Condition	Time	T [°C]	Product	Yield (%), Ratio
1	A	O/N	80	**138**	n.d.
2	B	3.5 h	90	dec.	n.d.
3	C	2.5 h	60	**136**	67
4	C	1 d	60	**138 + 134**	8:1
5	D	5 h	70	**136**	n.d.
6	E	4 h	80	dec.	n.d.
7	F	4 h	100	**138**	n.d.

[a] Isolated yields after silica chromatography, dec. = decomposition, n.d. = not determined.

However, this reaction conditions gave *O*-thiocarbonyl (**138**) according to the rearrangement mechanism described by Powers *et al.* under Barton-McCombie conditions and also resulted in the formation of a highly polar side product.[160]

The method utilising tetrabutylammonium peroxydisulfate and sodium formate as described by Park *et al.* (**Table 13, entry 3 - 5**) was used in a facile Barton-McCombie deoxygenation.[157] The 4-*O*-(phenoxy)thiocarbonyl- derivative (**136**) was subjected to tetrabutylammonium peroxydisulfate and sodium formate in DMF at 60 °C for two and a half hours as previously described by Park *et al.* (**Table 13, entry 3**).[157]

An aqueous work up in order to remove the polar reagents was then performed. However, starting material (**136**) was recovered and an undesired side reaction gave a highly polar product that under these conditions could not be isolated.

To overcome the side product formation the solution was degassed and molecular sieves was added and in addition the reaction time under these conditions was extended (**Table 13, entry 4**). However, the reaction resulted in the formation of the sulfur oxygen exchanged derivative (**138**) and hydrolysis to give (**134**) in a ratio of 8:1.

The thionocarbonate (**136**) was next subjected to radical Barton-McCombie conditions using either 2,2-bis(*tert*-butylperoxy)-butane or azobiscyanocyclohexane as a radical initiator and the radical carrier tributyltin hydride under reflux conditions in either 1,4-dioxane or toluene (**Table 13, entry 6 - 7**).[150] However, the reaction conditions applied resulted in the formation of the sulfur oxygen exchanged derivative (**138**) and formation of a highly polar side product, which under these conditions could not be isolated.

As a consequence, it was concluded that acetylation of 8,9-*O*-isopropylidene-4-*O*-(phenoxy)thiocarbonyl-sialic acid methyl ester (**136**) could minimise the side reactions observed in the Barton-McCombie deoxygenation, which might be due to the polar character of the starting material. Hence, 8,9-*O*-isopropylidene-4-*O*-(phenoxy)thiocarbonyl-sialic acid methyl ester (**136**) was acetylated using acetic anhydride and subjected to Barton-McCombie conditions using tributyltin hydride in 1,4-dioxane (**Scheme 73**).

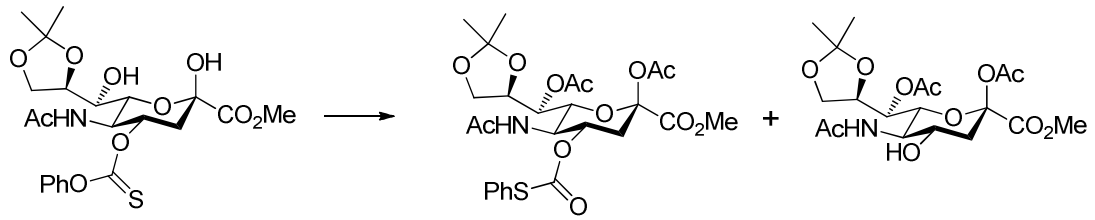

136 **139** **140**

Scheme 73 Attempted synthesis of 4-deoxy-8,9-*O*-isopropylidene-sialic acid derivative (**137**). (i) Ac_2O, DMAP, pyridine, r.t., O/N; (ii) Bu_3SnH, 50% 2,2-bis(*tert*-butylperoxy)-butane solution, 1,4-dioxane, 100 °C, 4 h.

However, these conditions gave the sulfur oxygen exchanged derivative (**139**) and the hydrolysed derivative (**140**) in a ratio of 6:1.

It was proposed that Barton-McCombie conditions are not applicable to this substrate. This might be due to the two protons at position C-3, which are next to the xanthate and might interfere under Barton-McCombie conditions. We investigated an alternative to the Barton-McCombie protocol to achieve deoxygenation, which had recently been proposed by Lam *et al.* and deploys toluates instead of xanthates utilising samarium under single electron transfer conditions.[200] The proposed mechanism proceeds via a toluate radical anion, which subsequently eliminates to give the toluate anion and the deoxygenated radical (**Scheme 74**).

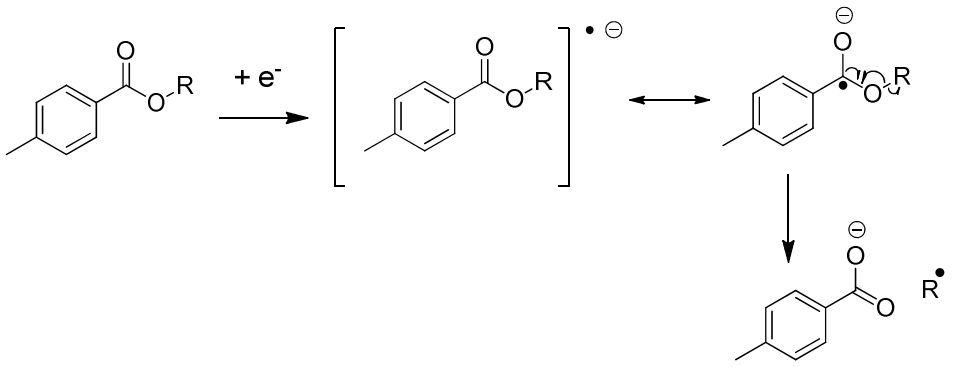

Scheme 74 Probable decomposition pathway of a toluate radical anion.[200]

The 8,9-*O*-isopropylidene-sialic acid methyl ester (**134**) was subjected to *p*-toluoyl chloride in dichloromethane in accordance to the protocol of Lam *et al.* to give the C-4 toluate, which was then acetylated to yield 4-*O*-toluoyl-sialic acid derivative (**141**) (**Scheme 75**).

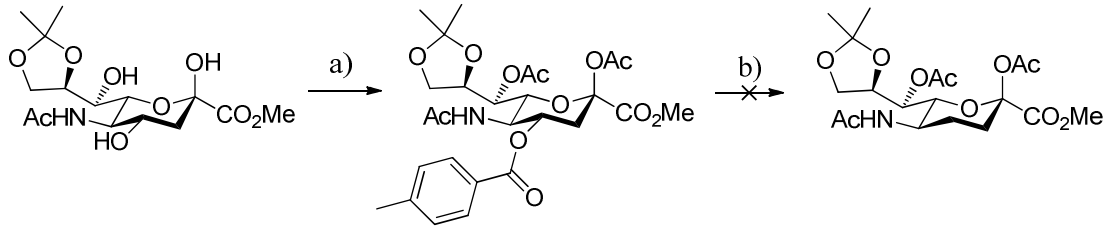

134 **141** **142**

Scheme 75 Attempted formation of 2,7-di-*O*-acetyl-4-deoxy-8,9-O-isopropylidene-sialic acid methyl ester (**142**). (a) (i) *p*-Toluoyl chloride, CH_2Cl_2, 0 ºC → r.t., 2 h; (ii) Ac_2O, DMAP, pyridine, r.t., O/N, 47% (over 2 steps) (**141**); (b) Sm, diiodoethane, HMPA, THF, 65 ºC.

In a flame-dried Schlenk flask samarium, diiodoethane, freshly distilled HMPA and anhydrous THF were heated to 65 °C and the C-4 toluate (**141**) was added. However, these conditions gave recovered starting material (**141**) and the formation of a highly polar side product. The protocol of Lam *et al.* applied to the C-4 toluate (**141**) led to comparable results obtained under Barton-McCombie conditions on thionocarbonate (**136**), which might support the proposed concept that radical conditions to form the 4-deoxy derivative on sialic acid are not applicable.

After re-evaluating the synthetic strategy and in search of a more vigorous method to form 4-deoxy-2'-(4-methylumbelliferyl) α-*D*-sialic acid (**126**) it was decided to explore previously accomplished studies towards the synthesis of a 4-deoxy derivative. A study performed by Hagedorn *et al.* utilised a 4-iodo-8,9-O-isopropylidene-sialic acid methyl ester methyl glycoside (**143**), which after dehalogen hydrogenation gave the 4-deoxy derivative. It was anticipated that this intermediate could provide a viable route towards the synthesis of 4-deoxy-2'-(4-methylumbelliferyl) α-*D*-sialic acid (**126**).

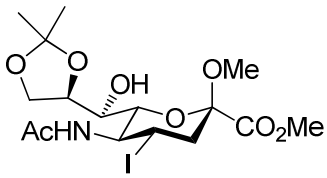

143

8.2 Attempted synthesis of 4-deoxy-2'-(4-methylumbelliferyl) α-*D*-sialic acid (126) via the 4-iodo-sialic acid methyl glycoside (143)

8.2.1 Retrosynthetic analysis

For the synthesis of 4-deoxy-2'-(4-methylumbelliferyl) α-*D*-sialic acid (**126**) we intended to utilise a glycosylation step utilising 4-methylumbelliferone on the β-chloro-4-deoxy-sialic acid methyl ester (**131**) according to the procedure of Engstler *et al.* (**Scheme 76**).[199]

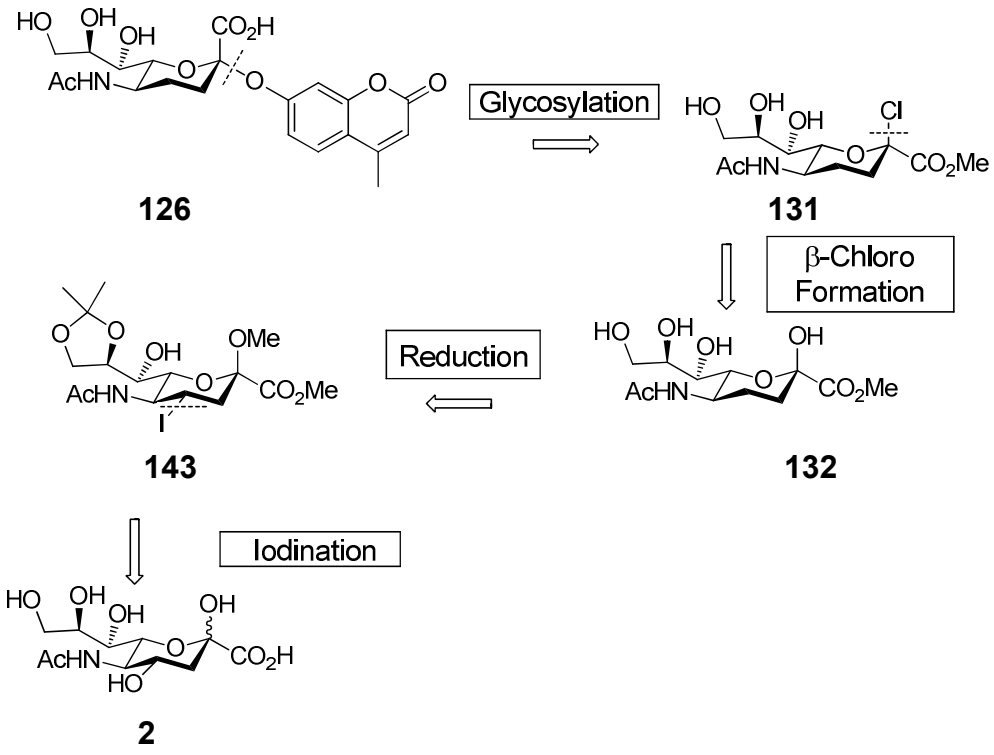

Scheme 76 Retrosynthetic strategy for the synthesis of 4-deoxy-2'-(4-methylumbelliferyl) α-*D*-sialic acid (**126**) via the 4-iodo methyl glycoside (**143**).

The formation of the β-chloro-4-deoxy-sialic acid methyl ester (**131**) could be achieved by treatment of 4-deoxy-sialic acid methyl ester derivative (**132**) with hydrochloric acid gaseous. It was anticipated to accomplish the synthesis of 4-deoxy-sialic acid methyl ester (**132**) via the 4-iodo-8,9-*O*-isopropylidene-sialic acid methyl ester methyl glycoside (**143**) which itself could be formed after iodination of protected sialic acid (**2**) in accordance to the procedure by Hagedorn *et al.*[137]

8.2.2 Attempted synthesis of 4-deoxy-sialic acid methyl ester (132)

Sialic acid (**2**) was treated with Dowex (acidic form) in methanol under reflux conditions to give the sialic acid methyl ester methyl glycoside according to the method by Kuhn *et al.* (**Scheme 77**).[201]

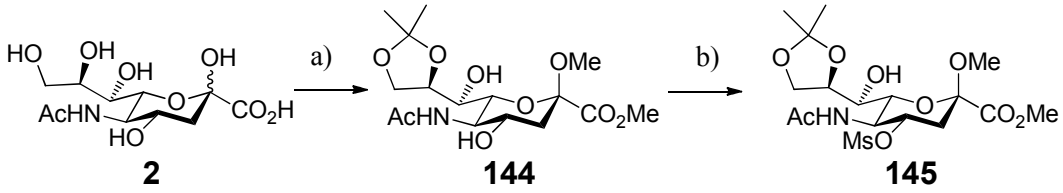

Scheme 77 Synthesis of 8,9-O-isopropylidene-4-methanesulfonyl-sialic acid methyl ester methyl glycoside (**145**). a) (i) Dowex 50x8, MeOH, 70 °C, O/N; (ii) 2,2'-Dimethoxypropane, *p*-TSA, acetone, r.t., O/N, 53% (over 2 steps) (**144**); b) MsCl, pyridine, 0 °C, O/N, 47% (**145**).[137]

Due to the high polarity the sialic acid methyl ester methyl glycoside was not purified and isolated at this stage. Subsequent isopropylidene protection with 2,2'-dimethoxypropane in acetone according to Ogura et al. was performed to give the 8,9-O-isopropylidene-sialic acid methyl ester methyl glycoside (**144**) in 53% over 2 steps.[153] Concurring with the procedure of Hagedorn *et al.* 8,9-*O*-isopropylidene-sialic acid methyl ester methyl glycoside (**144**) was subjected to methanesulfonyl chloride in pyridine to give 8,9-*O*-isopropylidene-4-methanesulfonyl-sialic acid derivative (**145**) in 47% yield.[137] The low yield is due to a side reaction forming a highly polar product which could not be isolated.

Then, the 8,9-*O*-isopropylidene-4-methanesulfonyl-sialic acid derivative (**145**) was subjected to sodium iodide in acetone at 100 °C in a pressure tube according to the procedure of Hagedorn *et al.* (**Scheme 78**).[137]

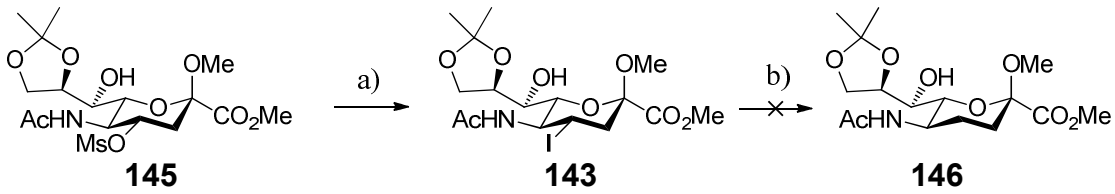

Scheme 78 Attempted formation of 4-deoxy-8,9-*O*-isopropylidene-sialic acid methyl ester methyl glycoside (**146**). a) NaI, acetone, 100 °C, 3 h; b) Pd/C, THF/AcOH, r.t., O/N.[137]

The molecular weight of 4-iodo-8,9-*O*-isopropylidene-sialic acid derivative (**143**) was confirmed by mass spectrometry of the crude mixture, but the desired product could not be isolated after silica column chromatography.

To overcome the difficulties in the purification of 4-iodo-8,9-*O*-isopropylidene-sialic acid derivative (**143**), subsequent hydrogenation was attempted to give the more stable 4-deoxy-8,9-*O*-isopropylidene-sialic acid methyl ester methyl glycoside (**146**). In conclusion, the formation of 4-deoxy-2'-(4-methylumbelliferyl) α-*D*-sialic acid (**126**) following the procedure of Hagedorn *et al.* could not be accomplished and need to be resolved in future studies.[137]

8.3 Attempted synthesis of 7-deoxy-2'-(4-methylumbelliferyl) α-*D*-sialic acid (127) via the C-7 Barton-McCombie deoxygenation

In parallel to the synthesis of 4-deoxy-2'-(4-methylumbelliferyl) α-*D*-sialic acid (**126**) we concurrently investigated the formation of 7-deoxy-2'-(4-methylumbelliferyl) α-*D*-sialic acid (**127**) and we intended to utilise a C-7 xanthate (**147**).

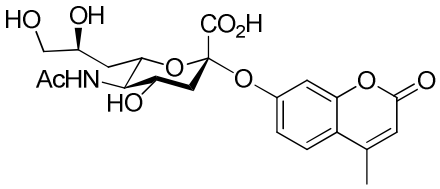

127

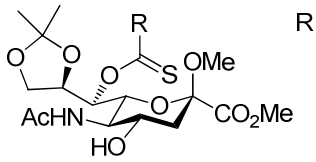

147

R = SMe (xanthate),

= OPh (thionocarbonate),

(*O*-thiocarbamate)

This strategy was based on a study performed by Miyazaki *et al.* utilising a C-7 *O*-thiocarbamate derivative, which was then subjected to Barton-McCombie conditions to give a 7-deoxy-sialic acid derivative.[155]

8.3.1 Retrosynthetic analysis

The 7-deoxy-2'-(4-methylumbelliferyl) α-*D*-sialic acid (**126**) could be yielded in a glycosylation step utilising 4-methylumbelliferone on the β-chloro-7-deoxy-sialic acid methyl ester (**145**) according to the procedure of Engstler *et al.* (**Scheme 79**).[199]

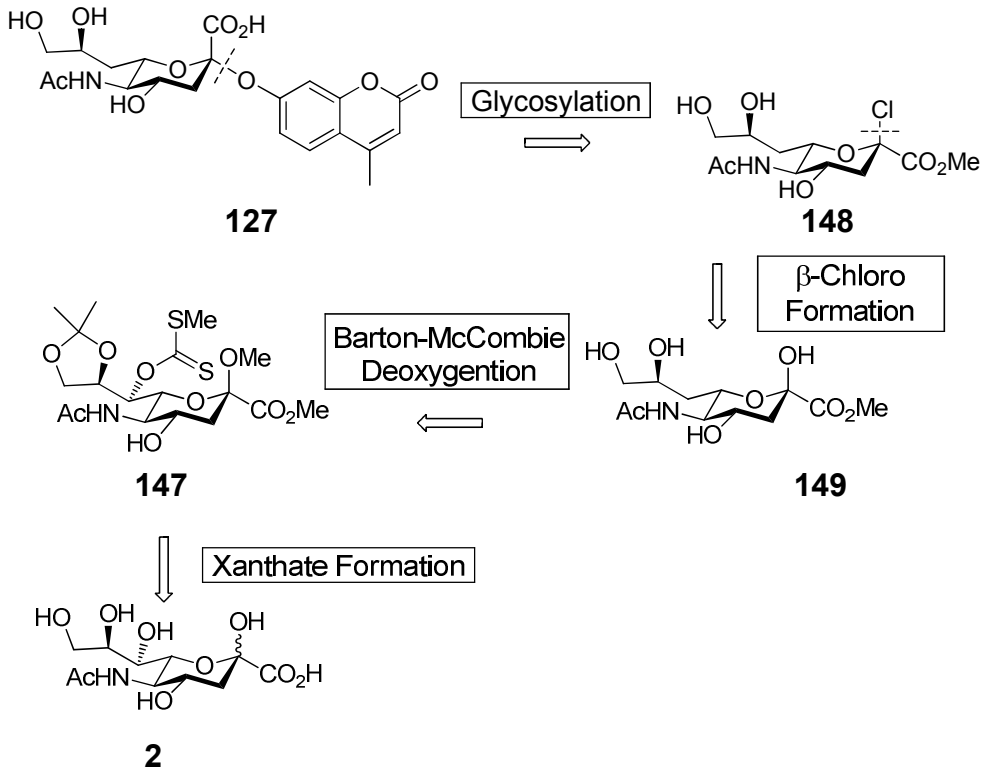

Scheme 79 Retrosynthetic strategy for the synthesis of 7-deoxy-2'-(4-methylumbelliferyl) α-*D*-sialic acid (**127**) via the C-7 xanthate methyl glycoside (**147**).

The formation of β-chloro-7-deoxy-sialic acid methyl ester (**148**) could be accomplished by treatment of 7-deoxy-sialic acid methyl ester derivative (**149**) with hydrochloric acid gaseous.

It was anticipated that following the approach of Miyazaki *et al.* the 7-deoxy-sialic acid methyl ester (**149**) could be yielded via a Barton-McCombie deoxygenation of the C-7 xanthate (**145**), which itself could be synthesised from sialic acid (**2**).[155]

8.3.2 Synthesis of 7-deoxy-8,9-*O*-isopropylidene-sialic acid derivative (152)

The previously synthesised 8,9-*O*-isopropylidene-sialic acid methyl ester methyl glycoside (**144**) (Chapter 8.2.2) was subjected to benzoyl chloride in pyridine according to the procedure of Miyazaki *et al.* to give 4-*O*-benzoyl-8,9-*O*-isopropylidene-sialic acid derivative (**150**) in 71% yield (**Scheme 80**).[155]

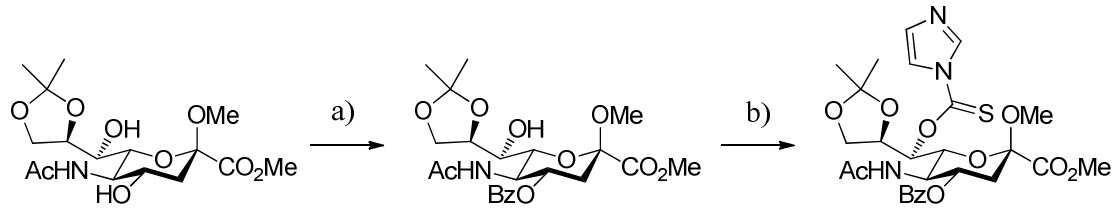

144 **150** **151**

Scheme 80 Synthesis of 7-*O*-thiocarbamate-sialic acid derivative (**151**). a) BzCl, pyridine, 0 °C, 40 min., 71% (**150**); b) 1,1'-Thiocarbonyldiimidazole, CH_2Cl_2, 40 °C, 48 h, 87% (**151**).[155]

Subsequent treatment with 1,1'-thiocarbonyldiimidazole in dichloromethane afforded the 7-*O*-thiocarbamate-sialic acid derivative (**151**) in 87% yield.

The 4-*O*-benzoyl-8,9-*O*-isopropylidene-7-*O*-thiocarbamate-sialic acid methyl ester methyl glycoside (**151**) was then subjected to the previously deployed Barton-McCombie protocol utilising tributyltin hydride in 1,4-dioxane to form 7-deoxy-8,9-*O*-isopropylidene-sialic acid derivative (**152**) in 54% yield (**Scheme 81**).

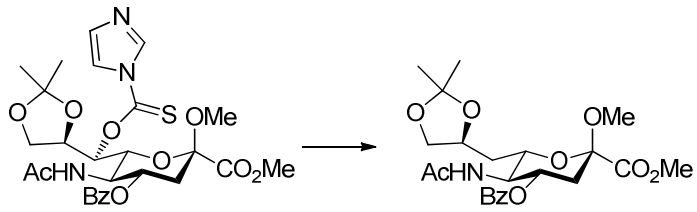

151 **152**

Scheme 81 Formation of 7-deoxy-8,9-*O*-isopropylidene-sialic acid methyl ester methyl glycoside (**152**). Luperox® 101, Bu_3SnH, 1,4-dioxane, 100 °C, 4 h, 54%.

8.3.3 Attempted synthesis of 7-deoxy-sialic acid methyl ester (149)

The 4-*O*-benzoyl-7-deoxy-8,9-*O*-isopropylidene-sialic acid methyl ester methyl glycoside (**152**) was then isopropylidene deprotected under acidic hydrolysis concurring with the procedure by Miyazaki *et al.* (**Scheme 82**).[155]

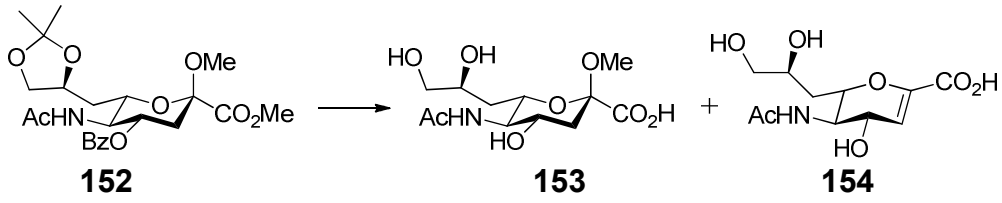

152 **153** **154**

Scheme 82 Attempted Synthesis of 7-deoxy-sialic acid methyl ester (**149**). (i) 80% AcOH/H_2O, 60 °C, 2 h; (ii) 0.3 N NaOH:MeOH = 1:1; 40 °C, 2 h; (iii) 25 mM HCl, Dowex 50x8, H_2O, 80 °C, 2 h.

Subsequent benzoyl deprotection with sodium hydroxide in methanol and hydrolysis of the methyl glycoside were attempted to give the 7-deoxy sialic acid derivative (**149**). However, after purification with a C18 reverse phase column an inseparable mixture of methyl glycoside (**153**) and a DANA-like derivative (**154**) was obtained. In conclusion the synthesis of 7-deoxy-2'-(4-methylumbelliferyl) α-*D*-sialic acid (**127**) could not be accomplished and need to be resolved in future studies.

8.4 Future works

The synthesis of the monodeoxygenated natural substrates (**126**) - (**129**) has previously been attempted (Chapter 8), but could not be accomplished.

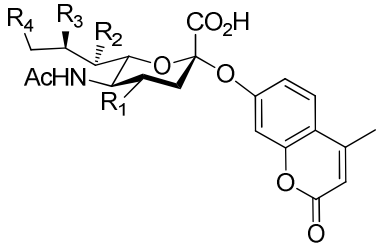

121 R_1, R_2, R_3, R_4 = OH

126 R_1 = H, R_2, R_3, R_4 = OH

127 R_2 = H, R_1, R_3, R_4 = OH

128 R_3 = H, R_1, R_2, R_4 = OH

129 R_4 = H, R_1, R_2, R_3 = OH

The measurement of Gibbs free energy of binding ($\Delta\Delta G^{\ddagger}$) for each monodeoxygenated natural substrate (**126**) - (**129**) needs to be highly accurate and the use of chromophoric tags, like 4-methylumbelliferone, to monitor enzyme kinetics is an established method.

However, the greater intrinsic reactivity towards hydrolysis of 4-methylumbelliferone compared to the natural substrates might mask the effects of individual hydroxyl group contribution towards transition-state stabilisation.[202] The differences in reactivity for spectroscopic useful non-natural substrates, compared to natural substrates on the example of *p*-nitrophenol has previously been addressed and was named '*p*-nitrophenol ester syndrome'.[203]

An elegant study utilising *Micromonospora viridifaciens* mutant Y370G highlighted the differences in Michaelis-Menten kinetic parameters by comparing the rate of hydrolysis of 4-methylumbelliferyl α-*D*-*N*-acetylneuraminylgalactopyranoside (**155**) to MUNANA (**121**) and was performed by Indurugalla *et al.*[202] Remarkably, the galactopyranoside (**155**) showed comparable rates of hydrolysis to the natural substrate 3'-sialyl lactose, but the chromophoric tag, 4-methylumbelliferone still could be used to monitor enzyme kinetics.

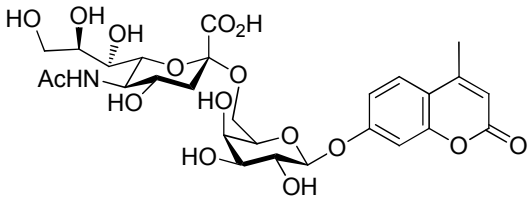

155

A possible new strategy based on 4-methylumbelliferyl α-*D*-*N*-acetylneuraminylgalactopyranoside (**155**) would involve the syntheses of the monodeoxygenated sialoside analogues (**156**) - (**159**), which could be useful in the measurement of accurate Gibbs free energies of binding ($\Delta\Delta G^{\ddagger}$) for individual hydroxyl group contribution towards transition-state stabilisation.

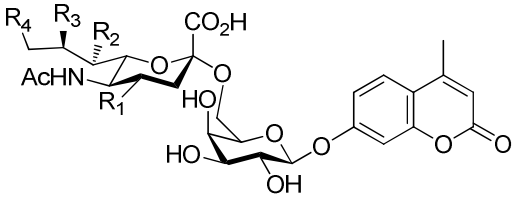

156 R_1 = H, R_2, R_3, R_4 = OH

157 R_2 = H, R_1, R_3, R_4 = OH

158 R_3 = H, R_1, R_2, R_4 = OH

159 R_4 = H, R_1, R_2, R_3 = OH

Chapter 9 - Conclusions

A number of approaches towards the syntheses of the four novel monodeoxygenated 2,3-difluorosialic acid inactivators (**24**) - (**27**) were investigated.

For the synthesis of 4-deoxy-2,3-difluorosialic acid (**24**) a Barton-McCombie protocol using Luperox® 101 as a radical initiator and the radical carrier tributyltin hydride under reflux conditions in 1,4-dioxane was developed and proved to be applicable to the synthesis of the remaining monodeoxygenated 2,3-difluorosialic acid derivatives (**25**) – (**27**). Following the formation of an α-/β-mixture of fluoride anomers in the fluorination of the hemiketal and ambiguous ^{19}F NMR coupling constants, X-ray crystallographic conformation of the β-anomer was accomplished.

The total synthesis from β-fluoropyruvic acid (**41**) to 4-deoxy-2,3-difluoro-sialic acid (**24**) was achieved in 11 steps, with an overall yield of 4%.

Time-dependent inactivation kinetics performed on wild type influenza neuraminidase N9 G70C and 4-deoxy-2,3-difluorosialic acid (**24**) showed no time-dependent inactivation with a fast rate of glycosylation (k_1) and a slow rate of deglycosylation (k_2).

Remarkably, IC_{50} measurements of 4-deoxy-2,3-difluorosialic acid (**24**) expressed tight-binding on FluB/Perth/wt. and mutant FluB/Perth/D197E with better inhibition than Oseltamivir (**6**), Zanamivir (**15**) and the parent compound 2,3-difluorosialic acid (**23**). The Oseltamivir (**6**) resistant mutant Miss/H1N1/H274Y did not have any effect on the inhibition of 4-deoxy-2,3-difluorosialic acid (**24**).

The X-ray crystal structure of influenza neuraminidase N9 in complex with 4-deoxy-2,3-difluorosialic acid (**24**) confirmed a covalently linked sialosyl-enzyme intermediate, supporting our proposed mechanism of influenza neuraminidase inactivation. An additional water molecule was identified, which could be an explanation for the behaviour of 4-deoxy-2,3-difluoro-sialic acid (**24**) in inactivation kinetics with better IC_{50} values than the parent inactivator 2,3-difluoro-sialic acid (**23**).

The total synthesis from β-fluoropyruvic acid (**41**) to 7-deoxy-2,3-difluorosialic acid (**25**) deploying the previously developed Barton-McCombie protocol on 4-deoxy-2,3-difluorosialic acid (**24**) was achieved in 13 steps, with an overall yield of 4.5%.

Time-dependent inactivation kinetics performed on wild type influenza neuraminidase N9 G70C and 7-deoxy-2,3-difluorosialic acid (**25**) showed no time-dependent inactivation with a fast rate of glycosylation (k_1) but no deglycosylation (k_2). IC_{50} measurements performed on a panel of influenza neuraminidases showed tight-binding and encouraging IC_{50} values across the panel, making position C-7 interesting for future drug discovery efforts. A study currently performed at Prof Stephen Withers laboratory is based on these findings of the 7-deoxy-2,3-difluorosialic acid (**25**) and investigates effects of *O*-alkylation at position C-7 of 2,3-difluorosialic acid with regards to inactivation and possible alternative breakdown mechanisms.

The X-ray crystal structure of influenza neuraminidase N9 in complex with 7-deoxy-2,3-difluorosialic acid (**25**) used soaking and co-crystallisation methods and gave an insight into the inactivation mechanism of the novel class of mechanism-based inactivators on a physical basis.

In brief, the total synthesis from β-fluoropyruvic acid (**41**) to 8-deoxy-2,3-difluorosialic acid (**26**) deploying the previously developed Barton-McCombie protocol on 4-deoxy-2,3-difluorosialic acid (**24**) was achieved in 12 steps, with an overall yield of 2%.

Time-dependent inactivation kinetics performed on wild type influenza neuraminidase N9 G70C and 8-deoxy-2,3-difluorosialic acid (**26**) showed time-dependent inactivation with a slow rate of glycosylation (k_1) and deglycosylation (k_2).

IC_{50} measurements showed poor inactivation against a panel of influenza neuraminidases, indicating a major contribution of the OH-8 group towards transition-state stabilisation.

The X-ray crystal structure of influenza neuraminidase N9 in complex with 8-deoxy-2,3-difluorosialic acid (**26**) confirmed a covalently linked sialosyl-enzyme intermediate and showed a rotation of the residues Glu276 and Glu277 with an additional water molecule, which could be an explanation for the poor performance of 8-deoxy-2,3-difluorosialic acid (**26**) in inactivation kinetics.

Finally, the total synthesis from β-fluoropyruvic acid (**41**) to 9-deoxy-2,3-difluorosialic acid (**27**) deploying the previously developed Barton-McCombie protocol on 4-deoxy-2,3-difluorosialic acid (**24**) was achieved in 14 steps, with an overall yield of 9%.

Time-dependent inactivation kinetics performed on wild type influenza neuraminidase N9 G70C and 9-deoxy-2,3-difluorosialic acid (**27**) showed time-dependent inactivation with a slow rate of glycosylation (k_1) and a calculated K_i = 12.1 $\pm$ 1.96 µM. The poor IC_{50} values might be an expression of the large dependency of inactivation on non-covalent interactions of the OH-9 group in the active-site of influenza neuraminidase.

The X-ray crystal structure of influenza neuraminidase N9 in complex with 9-deoxy-2,3-difluorosialic acid (**27**) showed a rotation of the amino acid residues Glu276 and Glu277 as previously deployed on the crystal structure of influenza neuraminidase N9 in complex with 8-deoxy-2,3-difluorosialic acid (**26**).

A principle inactivation mechanism of 2,3-difluorosialic acids on influenza neuraminidase has been proposed. However, uncertainties about the presence or formation of the second DANA like ligand in the active site of influenza neuraminidase need to be resolved.

Quite alarming is that none of the novel monodeoxygenated 2,3-difluorosialic acid inactivators (**24**) - (**27**) and Oseltamivir (**6**) and Zanamivir (**15**) retained activity across the panel of influenza strains tested, which could be seen as the crux of anti-viral drugs.[188]

Chapter 10 - Experimental

10.1 General

Chemical reagents were purchased from Sigma-Aldrich unless otherwise stated. Neu5Ac aldolase 9.2 U/mg EC 4.1.3.3 was purchased from Codexis®. Anhydrous dichloromethane and tetrahydrofuran were obtained by distillation over calcium hydride or sodium/benzophenone, respectively. All anhydrous solvents were used where indicated and were purchased from Sigma-Aldrich. All other solvents were purchased from Fisher Scientific and used without further purification.

Glassware for dry reactions was dried by heating in an oven at 120 ºC for at least 1h and heating with a hot air gun for 5 minutes. The glassware was then allowed to cool under a stream of N_2.

Analytical thin layer chromatography (TLC) was carried out on Merck aluminium backed TLC plates silica gel 60 F_{254} (0.25 mm thickness), viewed using UV light of wavelength 254 nm and then stained with ethanolic sulfuric acid. Reverse phase analytical TLC was performed with RP-18 F_{254}, pre-coated on aluminium sheets (0.27 mm thickness) purchased from Merck. Column chromatography was performed on silica gel 60 (35-70 micron) from Fisher Scientific. Compounds were loaded as an oil, appropriate organic solvent (mentioned) or dry loaded by adsorption onto silica.

Standard work up is referring to diluting the reaction residue in appropriate organic solvent (mentioned), washing with an aqueous saturated sodium bicarbonate solution, followed by washing with brine. The organic phases were then combined and dried over anhydrous magnesium sulfate, filtered and the filtrate concentrated *in vacuo*.

For slow addition a Razel Scientific Instruments INC. syringe pump was used.

Melting points were obtained using a Reichert-Jung heated-stage microscope and are uncorrected. Specific rotations were determined on an Optical Activity Ltd.: AA-10 automatic polarimeter.

^{1}H, ^{13}C and ^{19}F NMR were recorded using a Jeol Delta (270 MHz), Varian Mercury VX (400 MHz) or Bruker Avance III (400 and 500 MHz) spectrometers, with acquisition frequencies of 270, 400 or 500 for ^{1}H: 100 or 125 for ^{13}C and 376 or 470 for ^{19}F. The chemical shifts δ are recorded in parts per million (ppm) with reference to tetramethylsilane. The multiplicities are assigned as a singlet (s), doublet (d), triplet (t), quartet (q), doublet of doublets (dd), doublet of doublet of doublets (ddd), doublet of triplets (dt), triplet of doublets (td), broad (br) and multiplet (m).

High resolution mass spectrometry was performed using a Bruker MicrOTOF^{TM} electrospray ionisation mass spectrometer. X-ray crystallography was performed by Dr. Mary Mahon (Department of Chemistry, University of Bath). Single crystals were analysed at 150(2) K using graphite monochromated Mo(Kα) radiation and a Nonius Kappa CCD diffractometer. The structures were solved using SHELXS-97 and refined using SHELXL-97.

The kinetic measurements were performed on a BMG LABTECH FLUORStar Omega, Software Omega 1.30, double injector with a residual volume of 500 µL, the filters set to 355 nm excitation and 460 nm emission and a gain of 750. Black 96 well plates Greiner Bio-one were used at a temperature of 37 °C. The residual activity was measured over 30 minutes and the gradient calculated over the range of 8 to 28 minutes using Omega MARS BMG LABTECH software 2.10 R3. Fitting the residual activity to a single exponential equation with or without offset and the Lineweaver-Burk plot was generated using GraFit 5.0.13.

10.2 Synthesis

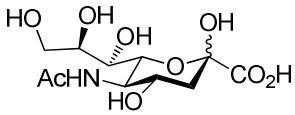

2

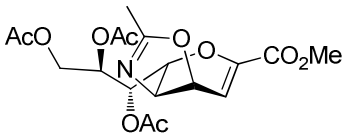

30

Methyl 7,8,9-tri-*O*-acetyl-2,3-didehydro-2,3,5-trideoxy-4',5'-dihydro-2'-methyloxazolo[5,4d]-*D-glycero-D*-talo-non-2-ulopyranosonate (30)

a) Trifluoroacetic acid (1.5 mL, 20 mmol) was added drop-wise to a stirred solution of sialic acid (**2**) (1.5 g, 4.9 mmol) in anhydrous methanol (50 mL) at room temperature and was stirred at this temperature overnight. The solution was then concentrated *in vacuo*, redissolved in methanol and concentrated *in vacuo* to give a white solid.

b) Acetic anhydride (6.9 mL, 73 mmol) was added drop-wise to the crude mixture in anhydrous pyridine (25 mL) at 4 ºC and the solution was then left to warm to room temperature and was stirred for 3 days. The solution was then concentrated *in vacuo* and residual pyridine was removed by azeotropic evaporation with toluene to give a yellow oil. The oil was subjected to a standard work up (CH_2Cl_2), filtered over a silica plug (EtOAc) and the filtrate concentrated *in vacuo*.

c) Trimethylsilyl trifluoromethanesulfonate (1.5 mL, 8 mmol) was added drop-wise under vigorous stirring to the crude mixture in anhydrous acetonitrile (45 mL) at room temperature and was then heated to 50 ºC overnight. The solution was then cooled to 4 ºC and potassium carbonate (2.2 g, 15.9 mmol) was added and stirred for 5 minutes. The mixture was filtered over Celite® and the filtrate was concentrated *in vacuo*. The crude mixture was then purified by silica column chromatography (EtOAc:Petroleum Ether 90:10) affording (**30**) as an off-white solid (1.53 g, 76% over 3 steps).

m.p. 90 - 94 °C (**lit. m.p**. 92.1 °C). $\mathbf{R_f}$ (EtOAc:MeOH 90:10, 0.7). **^{1}H NMR (400 MHz, $CDCl_3$)** δ 2.01, 2.05, 2.06 (3s, 9H, C(O)CH_3); 2.15 (s, 3H, CCH_3); 3.43 (dd, 1H, $J_{5,6}$ = 9.8, $J_{6,7}$ = 2.7 Hz, H-6); 3.81 (s, 3H, OCH_3); 3.95 (dd, 1H, $J_{5,6}$ = 9.8, $J_{4,5}$ = 8.5 Hz, H-5); 4.23 (dd, 1H, $J_{9,9'}$ = 12.5, $J_{8,9}$ = 6.3 Hz, H-9); 4.60 (dd, 1H, $J_{9,9'}$ = 12.5, $J_{8,9'}$ = 2.7 Hz, H-9'); 4.82 (dd, 1H, $J_{4,5}$ = 8.5, $J_{3,4}$ = 4.0 Hz, H-4); 5.44 (ddd, 1H, $J_{7,8}$ = $J_{8,9}$ = 6.3, $J_{8,9'}$ = 2.7 Hz, H-8); 5.63 (dd, 1H, $J_{7,8}$ = 6.3, $J_{6,7}$ = 2.7 Hz, H-7); 6.38 (d, 1H, $J_{3,4}$ = 4.0 Hz, H-3). **^{13}C NMR (100 MHz, $CDCl_3$)** δ 14.18 (C<u>C</u>H_3); 20.65, 20.81, 20.88 (C(O)<u>C</u>H_3); 52.57 (OCH_3); 62.02 (C-9); 62.10 (C-5); 68.89 (C-7); 70.32 (C-8); 72.27 (C-4); 76.78 (C-6); 107.59 (C-3); 147.19 (C-2); 161.90 (C-1); 167.20 (<u>C</u>CH_3); 169.60, 169.83, 170.68 (<u>C</u>(O)CH_3). **HRMS (ESI +ve)** *m/z* 414.1384 $[M+H]^+$ ($C_{18}H_{24}N_1O_{10}$ requires 414.1400). Melting point[204] and spectroscopic data are analogous to those reported in the literature.[145]

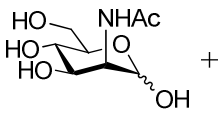

40

41

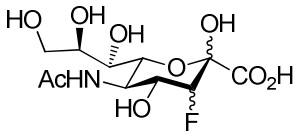

42+43+44

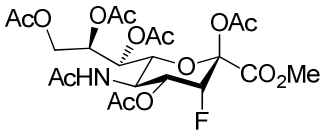

45

Methyl 5-*N*-acetyl-2,4,7,8,9-penta-*O*-acetyl-3,5-dideoxy-3-fluoro-*D*-*erythro*-α-L-manno-non-2ulopyranosonate (45)

a) A solution of β-fluoropyruvic acid (**41**) (3 g, 23.4 mmol), 2-*N*-acetyl-*D*-mannosamine (**40**) (10 g, 45.2 mmol) and Neu5Ac aldolase (200 mg, 9.2 U/mg) in water (200 mL) was left to stand at room temperature for 5 days. The reaction was monitored by the disappearing ^{19}F NMR signal corresponding to β-fluoropyruvic acid (**41**) at δ -229.1 ppm and the appearing signals corresponding to formation of axial 3-fluorosialic acid (**42**) at δ -208.1 ppm together with its epimer (**44**) at -217.7 ppm and the equatorial 3-fluorosialic acid (**43**) at -199.2 ppm.

After 3 days the mixture was filtered through a Sartorius Stedim Minisart® 1.2 µm to remove degraded enzyme. Further Neu5Ac aldolase (45 mg) was added and left to stand at room temperature for 2 days. The reaction mixture was then purified by ion-exchange chromatography (Dowex 1x2 200 ion exchange resin, conditioned with 6 M formic acid/H_2O) eluting with 0 → 1 M formic acid/H_2O. The eluate was concentrated *in vacuo* and the residue was lyophilised to give the 3-fluorosialic acids (**42**), (**43**) and (**44**) as a white solid which were used without further purification.

b) Trifluoroacetic acid (7 ml, 91.4 mmol) was added to a stirred solution of the 3-fluorosialic acids (**42**), (**43**) and (**44**) in anhydrous methanol (350 mL) and left at room temperature overnight. The mixture was then concentrated *in vacuo* three times with methanol affording 3-fluorosialic acid methyl ester as a white solid which was used without further purification.

c) Acetic anhydride (6.19 ml, 66 mmol) was added to a stirred solution of the crude methyl ester (1.5 g, 4.4 mmol) and catalytic amounts of 4-(dimethylamino)pyridine in pyridine (50 mL) at 4 °C and the solution was left to stir at room temperature for 17 hours. The solution was concentrated *in vacuo*, residual pyridine was removed by azeotropic evaporation with toluene and the residue was then subjected to a standard work up (EtOAc) and purified by silica chromatography (EtOAc) to give (**45**) as a white solid (1.809 g, 72% starting from β-fluoropyruvic acid (**41**)).

m.p. 192 - 194 °C (**lit. m.p.** 193 °C). **R_f** (EtOAc, 0.6). **^{1}H NMR (400 MHz, $CDCl_3$)** δ 1.91 (s, 3H, $NHC(O)CH_3$); 2.03, 2.10, 2.16, 2.17 (4s, 12H, $C(O)CCH_3$); 3.83 (s, 3H, OCH_3); 4.08 – 4.25 (m, 3H, H-5, H-6, H-9); 4.55 (dd, 1H, $J_{9,9'}$ = 12.4, $J_{8,9'}$ = 2.5 Hz, H-9'); 4.92 (dd, 1H, $J_{3,F3}$ = 49.0, $J_{3,4}$ = 2.5 Hz, H-3); 5.09 – 5.13 (m, 1H, H-8); 5.32 – 5.3 (m, 1H, H-7); 5.54 (ddd, 1H, $J_{4,F3}$ = 28.1, $J_{4,5}$ = 11.0, $J_{3,4}$ = 2.5 Hz, H-4). **HRMS (ESI +ve)** *m/z* 552.1714 $[M+H]^+$ ($C_{22}H_{31}F_1N_1O_{14}$ requires 552.1729). Melting point and spectroscopic data are analogous to those reported in the literature.[141]

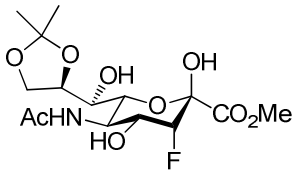

48

Methyl 5-*N*-acetyl-3,5-dideoxy-3-fluoro-8,9-*O*-isopropylidene-*D*-*erythro*-*α*-*L*-manno-non-2-ulopyranosonate (48)

a) In analogy to method a) for compound (**45**).

b) In analogy to method b) for compound (**45**).

c) A solution of 3-fluorosialic acid methyl ester, *p*-toluenesulfonic acid (156 mg, 0.82 mmol) and 2,2'-dimethoxypropane (14.4 mL, 117 mmol) in acetone (250 mL) was stirred at room temperature overnight. Triethylamine (555 µL, 3.99 mmol) was then added and the crude mixture was concentrated *in vacuo* and purified by silica column chromatography (EtOAc:MeOH 99:1 → 90:10) to give (**48**) as a white solid (6.3 g, 71% starting from β-fluoropyruvic acid (**41**)).

$[\alpha]_D^{24}$ = - 3° (c = 1, MeOH). **m.p.** 121 - 125 °C. **R_f** (EtOAc:MeOH 85:15, 0.5). **^{1}H NMR (400 MHz, CD_3OD)** δ 1.31 (s, 3H, CCH_3); 1.37 (s, 3H, CCH_3); 1.99 (s, 3H, $NHC(O)CH_3$); 3.52 (d, 1H, $J_{7,8}$ = 7.4 Hz, H-7); 3.82 (s, 3H, OCH_3); 3.97 – 4.25 (m, 6H, H-4, H-5, H-6, H-8, H-9, H-9'); 4.81 (dd, 1H, $J_{3,F3}$ = 49.3, $J_{3,4}$ = 2.7 Hz, H-3). **^{13}C NMR (100 MHz, CD_3OD)** δ 22.69 ($NHC(O)\underline{C}H_3$); 25.69 ($C\underline{C}H_3$); 27.20 ($C\underline{C}H_3$); 49.28 (d, $J_{5,F3}$ = 2.3 Hz, C-5); 53.32 (OCH_3); 67.99 (C-6); 68.95 (d, $J_{4,F3}$ = 18.4 Hz, C-4); 71.14 (C-7); 72.3 (C-8); 76.47 (C-9); 91.33 (d, $J_{3,F3}$ =178.7 Hz, C-3); 95.97 (d, $J_{2,F3}$ = 26.8 Hz, C-2); 110.2 ($\underline{C}CH_3$); 161.90 (C-1); 170.41 (C-1); 174.65 ($NH\underline{C}(O)CH_3$). **^{19}F NMR (376 MHz, CD_3OD)** – 209.4 (dd, $J_{F3,H3}$ = 50.4, $J_{F3,H4}$ = 28.9 Hz, F-3). **HRMS (ESI +ve)** *m/z* 382.1521 $[M+H]^+$ ($C_{15}H_{25}F_1N_1O_9$ requires 382.1513).

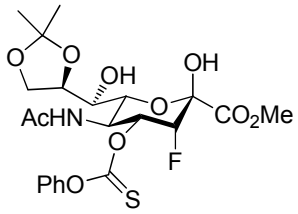

49

Methyl 5-*N*-acetyl-3,5-dideoxy-3-fluoro-8,9-*O*-isopropylidene-4-*O*-(phenoxy)thiocarbonyl-*D*-*erythro*-*α*-*L*-manno-non-2-ulopyranosonate (49)

Phenyl chlorothionoformate (0.76 mL, 5.6 mmol) was added drop-wise to a stirred solution of 3-fluoro-8,9-*O*-isopropylidenesialic acid methyl ester (**48**) (1.95 g, 5.1 mmol) in a mixture of anhydrous dichloromethane (70 mL) and anhydrous pyridine (23 mL) at – 40 ºC and was brought to room temperature over 1 hour. The mixture was left to stir at this temperature for further 3 hours. Methanol (1 mL) was added and after 10 minutes, the crude mixture was concentrated *in vacuo*, subjected to a standard work up (CH_2Cl_2) and purified by silica column chromatography (EtOAc:MeOH 99:1) to give (**49**) as an off-white solid (2.07 g, 76%).

$[\alpha]_D^{24}$ = - 8° (c = 1, CH_2Cl_2). **m.p.** 155 - 157 °C. $\mathbf{R_f}$ (EtOAc:MeOH 85:15, 0.5). **^{1}H NMR (400 MHz, $CDCl_3$)** δ 1.33 (s, 3H, CCH_3); 1.38 (s, 3H, CCH_3); 2.02 (s, 3H, $NHC(O)CH_3$); 3.48 (m, 1H, H-7); 3.82 (s, 3H, OCH_3); 3.99 (d, 1H, $J_{5,6}$ = 10.6 Hz, H-6); 4.06 (m, 2H, H-9, H-9'); 4.24 (m, 2H, H-8, OH); 4.63 (ddd, 1H, $J_{4,5}$ = 11.2, $J_{5,6}$ = 10.6, $J_{5,NH}$ = 8.1 Hz, H-5); 5.02 (dd, 1H, $J_{3,F3}$ = 50.3, $J_{3,4}$ = 2.1 Hz, H-3); 6.04 (dd, 1H, $J_{4,F3}$ = 25.5, $J_{4,5}$ = 11.2 Hz, H-4); 6.11 (d, 1H, $J_{5,NH}$ = 8.1 Hz, N<u>H</u>C(O)CH_3); 7.07 (d, 2H, $J_{Hb,Hc}$ = 7.6 Hz, H_b-PhOC(S)O); 7.32 (t, 1H, $J_{Hc,Hd}$ = 7.6 Hz, H_d-PhOC(S)O); 7.44 (t, 2H, $J_{Hb,Hc}$ = $J_{Hc,Hd}$ = 7.6 Hz, H_c-PhOC(S)O). **^{13}C NMR (100 MHz, $CDCl_3$)** δ 23.40 (NHC(O)<u>C</u>H_3); 25.52 (C<u>C</u>H_3); 27.35 (C<u>C</u>H_3); 47.78 (OCH_3); 53.80 (C-5); 67.70 (C-9); 69.88 (C-7); 72.24 (C-6); 74.42 (C-8); 78.74 (d, $J_{4,F3}$ = 17.0 Hz, C-4); 86.20 (d, $J_{3,F3}$ =189.2 Hz, C-3); 94.38 (d, $J_{2,F3}$ = 24.4 Hz, C-2); 109.53 (<u>C</u>CH_3); 121.68 (2C_c-PhOC(S)O); 127.30 (C_d-PhOC(S)O); 129.98 (2C_b-PhOC(S)O); 153.53 (C_a-PhOC(S)O); 168.18 (C-1); 172.58 (NH<u>C</u>(O)CH_3); 196.53 (PhO<u>C</u>(S)O).

^{19}F NMR (376 MHz, CD_3OD) – 208.36 (dd, $J_{F3,H3}$ = 50.4, $J_{F3,H4}$ = 27.5 Hz, F-3). **HRMS (ESI +ve)** *m/z* 540.1327 $[M+Na]^+$ ($C_{22}H_{28}F_1N_1O_{10}S_1Na_1$ requires 540.1316).

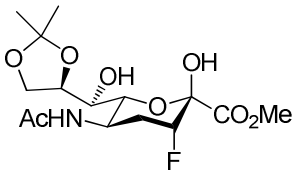

50

Methyl 5-*N*-acetyl-3,4,5-trideoxy-3-fluoro-8,9-*O*-isopropylidene-*D*-*erythro*-α-*L*-manno-non-2-ulopyranosonate (50)

3-Fluoro-8,9-*O*-isopropylidene-4-*O*-(phenoxy)thiocarbonyl sialic acid methyl ester (**49**) (265 mg, 0.51 mmol) was dissolved in anhydrous 1,4-dioxane (6 mL) concentrated *in vacuo*, ventilated under argon atmosphere, redissolved in 1,4-dioxane (12 mL) and molecular sieves (pellets, 4 Å) was added. The solution was then degassed and heated to 100 °C. A solution of 1,4-dioxane (6 mL), tributyltin hydride (0.51 mL, 1.89 mmol) and 50% 2,2-bis(*tert*-butylperoxy)-butane with molecular sieves was mixed in a flame-dried round-bottom flask and the mixture was then added drop-wise to the heated solution in 3 aliquots over 2 hours and left to stir at this temperature for further 2 hours. The crude mixture was then cooled, filtered, the filtrate concentrated *in vacuo* and purified by silica column chromatography (EtOAc:MeOH 90:10) to give (**50**) as a white solid (152 mg, 81%).

$[\alpha]_D^{24}$ = - 4° (c = 1, CH_2Cl_2). **m.p.** 165 - 168 °C. **R_f** (EtOAc:MeOH 90:10, 0.3). **^{1}H NMR (400 MHz, $CDCl_3$)** δ 1.32 (s, 3H, CCH_3); 1.37 (s, 3H, CCH_3); 2.02 (s, 3H, $NHC(O)CH_3$); 2.14 (dddd, 1H, $J_{4ax,F3}$ = 26.1, $J_{4ax,4eq}$ = 14.7, $J_{4ax,5}$ = 9.7, $J_{3,4ax}$ = 2.2 Hz, H-4_{ax}); 2.29 (m, 1H, H-4_{eq}); 3.48 (m, 2H, H-7, OH); 3.83 (s, 3H, OCH_3); 3.87 (d, 1H, $J_{5,6}$ = 10.8 Hz, H-6); 4.11 (m, 3H, H-9, H-9', OH); 4.25 (m, 1H, H-8); 4.36 (m, 1H, H-5); 4.76 (ddd, 1H, $J_{3,F3}$ = 47.3, $J_{3,4ax}$ = $J_{3,4eq}$ = 2.2 Hz, H-3); 5.36 (d, 1H, $J_{5,NH}$ = 8.4 Hz, N<u>H</u>C(O)CH_3).

^{13}C NMR (100 MHz, $CDCl_3$) δ 23.42 (NHC(O)$\underline{C}H_3$); 25.61 ($C\underline{C}H_3$); 27.31 ($C\underline{C}H_3$); 31.08 (d, $J_{4,F3}$ = 21.0 Hz, C-4); 40.9 (C-5); 53.55 (OCH_3); 66.06 (C-9); 67.61 (C-7); 70.07 (C-6); 74.54 (C-8); 86.78 (d, $J_{3,F3}$ =179.3 Hz, C-3); 93.23 (d, $J_{2,F3}$ = 26.1 Hz, C-2); 109.29 ($\underline{C}CH_3$); 169.50 (C-1); 171.86 ($NH\underline{C}(O)CH_3$).

^{19}F NMR (376 MHz, CD_3OD) – 193.30 (ddd, $J_{F3,H3}$ = 44.5, $J_{F3,H4ax}$ = 27.6, $J_{F3,H4eq}$ = 10.4 Hz, F-3). **HRMS (ESI +ve)** *m/z* 366.1557 $[M+H]^+$ ($C_{15}H_{25}F_1N_1O_8$ requires 366.1564).

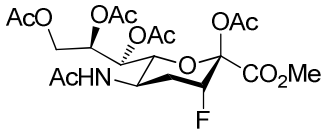

52

Methyl 5-*N*-acetyl-2,7,8,9-tetra-*O*-acetyl-3,4,5-trideoxy-3-fluoro-*D*-*erythro*-α-*L*-manno-non-2-ulopyranosonate (52)

a) A solution of 4-deoxy-3-fluoro-8,9-*O*-isopropylidenesialic acid methyl ester (**50**) (0.6 g, 1.7 mmol) in 80% acetic acid/H_2O (40 mL) was stirred at 60 °C for 2 hours. The crude mixture was then concentrated *in vacuo* and residual acetic acid was removed by azeotropic evaporation with toluene to give a white solid.

b) Acetic anhydride (7 mL, 75 mmol) was added to a solution of the crude mixture and catalytic amounts of 4-(dimethylamino)pyridine at 4 °C and the solution were left to stir at room temperature overnight. The solution was concentrated *in vacuo* and residual pyridine was removed by azeotropic evaporation with toluene. The crude was then subjected to a standard work up (EtOAc) and purified by silica chromatography (EtOAc) to give (**52**) as a white solid (643 mg, 76%).

$[\alpha]_D^{24}$ = - 4° (c = 1, CH_2Cl_2). **m.p.** 212 - 215 °C. **R_f** (EtOAc:MeOH 90:10, 0.5).

^{1}H NMR (400 MHz, $CDCl_3$) δ 1.94 (s, 3H, NHC(O)CH_3); 2.03, 2.04, 2.14, 2.16 (4s, 12H, C(O)CCH_3); 2.27 – 2.35 (m, 1H, H-4_{eq}); 2.46 (dddd, 1H, $J_{4ax,F3}$ = 25.6, $J_{4ax,4eq}$ = 14.6, $J_{4ax,5}$ = 10.2, $J_{3,4ax}$= 2.1 Hz, H-4_{ax}); 3.82 (s, 3H, OCH_3); 3.90 – 4.01 (m, 1H, H-5); 4.19 – 4.23 (m, 1H, H-6, H-9); 4.58 (dd, 1H, $J_{9,9'}$ = 12.5, $J_{8,9'}$ = 2.1 Hz, H-9'); 4.81 (ddd, 1H, $J_{3,F3}$ = 46.5, $J_{3,4ax}$ = $J_{3,4eq}$ = 2.1 Hz, H-3); 5.12 (ddd, 1H, $J_{7,8}$ = 7.4, $J_{8,9}$ = 5.1, $J_{8,9'}$ = 2.1 Hz, H-8); 5.34 (dd, 1H, $J_{7,8}$ = 7.4, $J_{6,7}$ = 2.3 Hz, H-7); 5.39 (d, 1H, $J_{5,NH}$ = 7.4 Hz, N<u>H</u>C(O)CH_3). **^{13}C NMR (100 MHz, $CDCl_3$)** δ 20.57, 20.78, 20.85, 20.94 (C(O)<u>C</u>H_3); 23.60 (NHC(O)<u>C</u>H_3); 30.44 (d, $J_{4,F3}$ = 20.7 Hz, C-4); 40.77 (C-5); 53.31 (OCH_3); 66.22 (C-9); 68.39 (C-7); 71.41 (C-8); 72.23 (C-6); 87.31 (d, $J_{3,F3}$ =177.8 Hz, C-3); 94.20 (d, $J_{2,F3}$ = 30.6 Hz, C-2); 166.12 (C-1); 167.31 (NH<u>C</u>(O)CH_3); 169.98, 170.34, 170.59, 170.87 (<u>C</u>(O)CH_3). **^{19}F NMR (376 MHz, $CDCl_3$)** - 194.27 (ddd, $J_{F3,H3}$ = 44.3, $J_{F3,H4ax}$ =26.5, $J_{F3,H4eq}$ = 11.6 Hz, F-3). **HRMS (ESI +ve)** *m/z* 494.1679 $[M+H]^+$ ($C_{20}H_{29}F_1N_1O_{12}$ requires 494.1674).

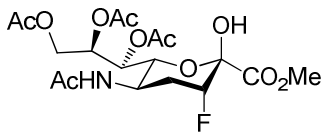

53

Methyl 5-*N*-acetyl-7,8,9-tri-*O*-acetyl-3,4,5-trideoxy-3-fluoro-*D*-*erythro*-α-*L*-manno-non-2-ulopyranosonate (53)

A solution of hydrazine acetate (99 mg, 1.1 mmol) in anhydrous methanol (2 mL) was cooled to 4 °C and added to a stirred solution of *per*-*O*-acetyl-4-deoxy-3-fluorosialic acid methyl ester (**52**) (132 mg, 0.3 mmol) in anhydrous dichloromethane (4 mL) at 4 °C and left at this temperature overnight. The mixture was then diluted with dichloromethane (10 mL), subjected to a standard work up and purified by silica column chromatography (EtOAc → EtOAc:MeOH 90:10) affording (**53**) as a white solid (62 mg, 51%).

$[\alpha]_D^{24}$ = + 4° (c = 1, CH_2Cl_2). **m.p.** 189 - 193 °C. **R_f** (EtOAc:MeOH 90:10, 0.5).

^{1}H NMR (400 MHz, $CDCl_3$) δ 1.93 (s, 3H, NHC(O)CH_3); 2.04, 2.05, 2.14 (3s, 9H, C(O)CCH_3); 2.19 – 2.30 (m, 1H, H-4_{eq}); 2.34 – 2.41 (m, 1H, H-4_{ax}); 3.86 (s, 3H, OCH_3); 4.15 (dd, 1H, $J_{9,9'}$ = 12.5, $J_{8,9}$ = 6.3 Hz, H-9); 4.19 – 4.25 (m, 1H, H-5); 4.25 – 4.29 (m, 2H, H-6, OH-2); 4.52 (dd, 1H, $J_{9,9'}$ = 12.5, $J_{8,9'}$ = 2.7 Hz, H-9'); 4.97 (ddd, 1H, $J_{3,F3}$ = 45.8, $J_{3,4ax}$ = $J_{3,4eq}$ = 2.3 Hz, H-3); 5.29 – 5.31 (m, 1H, H-8); 5.34 (dd, 1H, $J_{7,8}$ = 8.2, $J_{6,7}$ = 2.1 Hz, H-7); 5.37 (d, 1H, $J_{5,NH}$ = 9.3 Hz, N<u>H</u>C(O)CH_3). **^{13}C NMR (100 MHz, $CDCl_3$)** δ 20.85, 20.87, 21.10 (C(O)<u>C</u>H_3); 23.45 (NHC(O)<u>C</u>H_3); 31.25 (d, $J_{4,F3}$ = 20.6 Hz, C-4); 40.25 (C-5); 53.31 (OCH_3); 63.20 (C-9); 68.35 (C-7); 71.60 (C-6); 71.96 (C-8); 87.02 (d, $J_{3,F3}$ =177.7 Hz, C-3); 93.34 (d, $J_{2,F3}$ = 26.5 Hz, C-2); 168.58 (C-1); 169.72 (NH<u>C</u>(O)CH_3); 170.64, 171.10, 171.19 (<u>C</u>(O)CH_3). **^{19}F NMR (376 MHz, $CDCl_3$)** – 194.28 (ddd, $J_{F3,H3}$ = 43.2, $J_{F3,H4ax}$ = 26.3, $J_{F3,H4eq}$ = 11.7 Hz, F-3). **HRMS (ESI +ve)** *m/z* 452.1564 $[M+H]^+$ ($C_{18}H_{27}F_1N_1O_{11}$ requires 452.1568).

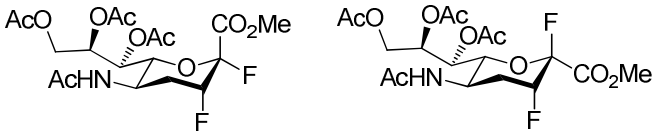

56 **57**

Methyl 5-*N*-acetyl-7,8,9-tri-*O*-acetyl-2,3,4,5-tetradeoxy-2,3-difluoro-*D*-*erythro*-*β*-*L*-manno-non-2-ulopyranosonate (56) and Methyl 5-*N*-acetyl-7,8,9-tri-*O*-acetyl-2,3,4,5-tetradeoxy-2,3-difluoro-*D*-*erythro*-*α*-*L*-manno-non-2-ulopyranosonate (57)

(Diethylamino)sulfur trifluoride (89 µL, 0.68 mmol) was added drop-wise to a stirred solution of hemiketal (**53**) (205 mg, 0.45 mmol) in anhydrous dichloromethane (15 mL) at – 40 °C and the temperature was increased to -10 °C within 1 hour. The reaction was then quenched by the addition of methanol (0.1 mL) and saturated $NaHCO_3$ solution (0.1 mL), subjected to a standard work up (CH_2Cl_2) and purified by silica column chromatography (EtOAc:MeOH 99:1 → EtOAc/MeOH 95:5) to give (**56**) and (**57**).

Data for (**56**): white solid (92 mg, 45%).

$[\alpha]_D^{24}$ = - 1° (c = 1, CH_2Cl_2). **m.p.** 63 - 65 °C. **R_f** (EtOAc:MeOH 90:10, 0.4).

^{1}H NMR (400 MHz, $CDCl_3$) δ 1.96 (s, 3H, NHC(O)CH_3); 2.03, 2.09, 2.14 (3s, 9H, C(O)CCH_3); 2.33 – 2.42 (m, 2H, H-4_{ax}, H-4_{eq}); 3.86 (s, 3H, OCH_3); 3.93 (ddd, 1H, $J_{5,NH}$ = $J_{4ax,5}$ = 8.2, $J_{4eq,5}$ = 2.5 Hz, H-5); 4.19 (dd, 1H, $J_{9,9'}$ = 12.9, $J_{8,9}$ = 5.5 Hz, H-9); 4.34 – 4.37 (m, 2H, H-6, H-9'); 5.09 (dddd, 1H, $J_{3,F3}$ = 47.7, $J_{3,4eq}$ = 5.2, $J_{3,4ax}$ = $J_{3,F2}$ = 2.1 Hz H-3); 5.29 (m, 1H, H-7); 5.41 (ddd, 1H, $J_{7,8}$ = 7.4, $J_{8,9}$ = 5.5, $J_{8,9'}$ = 2.3 Hz, H-8); 5.69 (d, 1H, $J_{5,NH}$ = 8.2 Hz, N<u>H</u>C(O)CH_3). **^{13}C NMR (100 MHz, $CDCl_3$)** δ 20.70, 20.72, 20.89 (C(O)<u>C</u>H_3); 23.50 (NHC(O)<u>C</u>H_3); 29.83 (dd, $J_{4,F3}$ = 21.0, $J_{4,F2}$ = 3.1 Hz, C-4); 41.86 (d, $J_{5,F3}$ = 5.4 Hz, C-5); 53.48 (OCH_3); 61.82 (C-9); 67.85 (C-7); 69.29 (C-8); 74.11 (d, $J_{6,F3}$ = 2.3 Hz, C-6); 83.61 (dd, $J_{3,F3}$ =187.1, $J_{3,F2}$ = 21.5 Hz, C-3); 104.99 (dd, $J_{2,F2}$ = 230.1, $J_{2,F3}$ = 19.2 Hz, C-2); 164.89 (d, $J_{1,F2}$ = 30.5 Hz, C-1); 169.89 (NH<u>C</u>(O)CH_3); 170.17, 170.55, 170.63 (<u>C</u>(O)CH_3). **^{19}F NMR (376 MHz, $CDCl_3$)** – 125.58 (dd, 1F, $J_{F2,F3}$ = 12.1, $J_{F2,H3}$ = 2.1 Hz, F-2); - 201.72 (dddd, 1F, $J_{F3,H3}$ = 48.1, $J_{F3,H4ax}$ = 27.5, $J_{F2,F3}$ = $J_{F3,H4eq}$ = 12.1 Hz, F-3). **HRMS (ESI +ve)** *m/z* 454.1506 $[M+H]^+$ ($C_{18}H_{26}F_2N_1O_{10}$ requires 454.1525).

Data for (**57**): white solid (62 mg, 30%).

$[\alpha]_D^{24}$ = + 2° (c = 1, CH_2Cl_2). **m.p.** 143 - 146 °C. **R_f** (EtOAc:MeOH 90:10, 0.5). **^{1}H NMR (400 MHz, $CDCl_3$)** δ 1.94 (s, 3H, NHC(O)CH_3); 2.04, 2.08, 2.15 (3s, 9H, C(O)CCH_3); 2.18 – 2.27 (m, 1H, H-4_{eq}); 2.30 (ddd, 1H, $J_{4ax,F3}$ = 25.3, $J_{4ax,4eq}$ = 14.7, $J_{3,4ax}$ = 2.1 Hz, H-4_{ax}); 3.86 (s, 3H, OCH_3); 4.10 (dd, 1H, $J_{9,9'}$ = 12.4, $J_{8,9}$ = 6.9 Hz, H-9); 4.11 – 4.19 (m, 1H, H-5); 4.28 (dd, 1H, $J_{5,6}$ = 10.6, $J_{6,7}$ = 2.1 Hz, H-6); 4.75 (dd, 1H, $J_{9,9'}$ = 12.4, $J_{8,9'}$ = 2.1 Hz, H-9'); 4.78 (dddd, 1H, $J_{3,F3}$ = 47.1, $J_{3,4eq}$ = 5.2, $J_{3,F2}$ = $J_{3,4ax}$ = 2.1 Hz, H-3); 5.28 (ddd, 1H, $J_{8,9}$ = $J_{7,8}$ = 6.9, $J_{8,9'}$ = 2.1 Hz, H-8); 5.41 (d, 1H, $J_{7,8}$ = 6.9, $J_{6,7}$ = 2.1 Hz, H-7); 5.49 (d, 1H, $J_{5,NH}$ = 9.0 Hz, N<u>H</u>C(O)CH_3). **^{13}C NMR (100 MHz, $CDCl_3$)** δ 20.74, 20.75, 20.78 (C(O)<u>C</u>H_3); 23.39 (NHC(O)<u>C</u>H_3); 30.81 (d, $J_{4,F3}$ = 21.5 Hz, C-4); 39.44 (C-5); 53.46 (OCH_3); 62.27 (C-9); 67.43 (C-7); 70.35 (C-8); 73.39 (d, $J_{6,F3}$ = 3.1 Hz, C-6); 84.87 (dd, $J_{3,F3}$ =177.1, $J_{3,F2}$ = 45.2 Hz, C-3); 104.01 (dd, $J_{2,F2}$ = 227.7, $J_{2,F3}$ = 29.9 Hz, C-2); 163.67 (d, $J_{1,F2}$ = 26.8 Hz, C-1); 169.81 (NH<u>C</u>(O)CH_3); 169.97, 170.43, 170.58 (<u>C</u>(O)CH_3).

^{19}F NMR (376 MHz, $CDCl_3$) – 121.54 (dd, 1F, $J_{F2,F3}$ = 10.7, $J_{F2,H3}$ = 2.1 Hz, F-2); - 193.11 (dddd, 1F, $J_{F3,H3}$ = 45.8, $J_{F3,H4ax}$ = 26.5, $J_{F3,H4eq}$ = 12.2, $J_{F2,F3}$ =10.7 Hz, F-3). **HRMS (ESI +ve)** *m/z* 454.1506 $[M+H]^+$ ($C_{18}H_{26}F_2N_1O_{10}$ requires 454.1525).

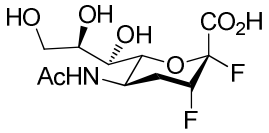

24

5-*N*-Acetyl-2,3,4,5-tetradeoxy-2,3-difluoro-*D*-*erythro*-*β*-*L*-manno-non-2-ulopyranosonic acid (24)

a) Sodium (8 mg, 0.35 mmol) was added to a stirred solution of *per*-*O*-acetyl-4-deoxy-2,3-difluorosialic acid methyl ester (**56**) (80 mg, 0.18 mmol) in anhydrous methanol (5 mL) at room temperature and was left to stir for 3 hours. The solution was then neutralised through addition of Dowex 50 Wx8 100 ion exchange resin, H^+ form, filtered, and the filtrate concentrated *in vacuo*.

b) A 0.5M aqueous NaOH solution (0.2 mL) was added to a stirred solution of the residue redissolved in water (1 mL) at room temperature and left to stir for 30 minutes. The solution was then neutralised through addition of Dowex 50 Wx8 100 ion exchange resin, H^+ form, filtered, the filtrate concentrated *in vacuo* and purified by silica column chromatography (EtOAc:MeOH 1:1) affording (**24**) as a white solid (29 mg, 52% over 2 steps).

$[\alpha]_D^{24}$ = - 2° (c = 1, H_2O). **m.p.** 127 - 131 °C. **R_f** (EtOAc:MeOH 70:30, 0.12). **^{1}H NMR (400 MHz, D_2O)** δ 1.91 (s, 3H, NHC(O)CH_3); 1.95 – 2.08 (m, 1H, H-4_{eq}); 2.38 (dddd, 1H, $J_{4ax,F3}$ = 23.8, $J_{4ax,4eq}$ = 15.1, $J_{4ax,5}$ = 11.2 $J_{3,4ax}$ = 2.5 Hz, H-4_{ax}); 3.49 (dd, 1H, $J_{7,8}$ = 8.6, $J_{6,7}$ = 1.8 Hz, H-7); 3.54 (dd, 1H, $J_{9,9'}$ = 12.3, $J_{8,9}$ = 6.9 Hz, H-9); 3.75 – 3.81 (m, 2H, H-8, H-9'); 3.83 (dd, 1H, $J_{5,6}$ = 11.2, $J_{6,7}$ = 1.8 Hz, H-6); 4.28 (ddd, 1H, $J_{5,6}$ = $J_{4ax,5}$ = 11.2, $J_{4eq,5}$ = 2.5 Hz, H-5); 5.12 (dddd, 1H, $J_{3,F3}$ = 48.4, $J_{3,4eq}$ = 5.7, $J_{3,4ax}$ = $J_{3,F2}$ = 2.5 Hz, H-3).

^{13}C NMR (100 MHz, D_2O) δ 22.09 (NHC(O)$\underline{C}H_3$); 31.25 (d, $J_{4,F3}$ = 19.9 Hz, C-4); 40.52 (d, $J_{5,F3}$ = 3.7 Hz, C-5); 63.03 (C-9); 68.37 (C-7); 70.68 (C-8); 76.19 (C-6); 86.41 (dd, $J_{3,F3}$ =180.6, $J_{3,F2}$ = 22.1 Hz, C-3); 105.23 (dd, $J_{2,F2}$ = 224.1, $J_{2,F3}$ = 19.2 Hz, C-2); 163.73 (d, $J_{1,F2}$ = 30.5 Hz, C-1); 174.4 (NH$\underline{C}$(O)CH_3). **^{19}F NMR (470 MHz, D_2O)** – 122.80 (dd, 1F, $J_{F2,F3}$ = 12.6, $J_{F2,H3}$ = 2.5 Hz, F-2); - 200.82 (dddd, 1F, $J_{F3,H3}$ = 47.9, $J_{F3,H4ax}$ = 24.5, $J_{F2,F3}$ = $J_{F3,H4eq}$ = 12.6 Hz, F-3). **HRMS (ESI -ve)** *m/z* 312.0900 $[M-H]^-$ ($C_{11}H_{16}F_2N_1O_7$ requires 312.0895). **Anal. Calcd. for $C_{11}H_{16}F_2N_1Na_1O_7$+1/2 H_2O**: C, 38.38; H, 4.98; N, 4.07. Found: C, 38.20; H, 5.26; N, 3.87.

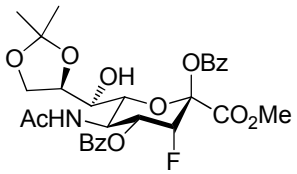

63

Methyl 5-*N*-acetyl-2,4-di-*O*-benzoyl-3,5-dideoxy-3-fluoro-8,9-*O*-isopropylidene-*D*-*erythro*-α-*L*-manno-non-2-ulopyranosonate (63)

Benzoyl chloride (2 mL, 17.3 mmol) was added drop-wise to a stirred solution of 3-fluoro-8,9-*O*-isopropylidenesialic acid methyl ester (**48**) (3 g, 7.9 mmol) in a mixture of anhydrous dichloromethane (36 mL) and anhydrous pyridine (12 mL) at – 40 ºC for 30 minutes and was then brought to – 20 ºC within 45 minutes. Methanol (1 mL) was added, the crude mixture was concentrated *in vacuo*, subjected to a standard work up (EtOAc) and was then purified by silica column chromatography (EtOAc:Petroleum Ether 80:20) to give (**63**) and (**64**).

Data for (**63**): white solid (2.41 g, 54%).

$[\alpha]_D^{24}$ = - 5° (c = 1, CH_2Cl_2). **m.p.** 124 - 128 °C. **R_f** (EtOAc:Petroleum Ether 90:10, 0.4).

^{1}H NMR (400 MHz, $CDCl_3$) δ 0.95 (s, 3H, CCH_3); 1.21 (s, 3H, CCH_3); 1.94 (s, 3H, $NHC(O)CH_3$); 3.47 (dd, 1H, $J_{7,8}$ = 8.5, $J_{7,OH}$ = 5.1 Hz, H-7); 3.91 (d, 1H, $J_{5,6}$ = 10.5 Hz, H-6); 3.92 (s, 3H, OCH_3); 3.96 (dd, 1H, $J_{9,9'}$ = 8.8, $J_{8,9}$ = 5.3 Hz, H-9); 4.10 (dd, 1H, $J_{9,9'}$ = 8.8, $J_{8,9'}$ = 2.1 Hz, H-9'); 4.24 (ddd, 1H, $J_{7,8}$ = 8.5, $J_{8,9}$ = 5.3 Hz, $J_{8,9'}$ = 2.1 Hz, H-8); 4.31 (d, 1H, $J_{7,OH}$ = 5.1 Hz, OH-7); 4.61 (ddd, 1H, $J_{4,5}$ = $J_{5,6}$ = 10.5, $J_{5,NH}$ = 7.8 Hz, H-5); 5.25 (dd, 1H, $J_{3,F3}$ = 48.5, $J_{3,4}$ = 2.2 Hz, H-3); 5.75 (ddd, 1H, $J_{4,F3}$ = 27.9, $J_{4,5}$ = 10.5, $J_{3,4}$ = 2.2 Hz, H-4); 6.12 (d, 1H, $J_{5,NH}$ = 7.8 Hz, $NHC(O)CH_3$); 7.51 (t, 4H, $J_{Hb,Hc}$ = 7.8 Hz, H_c-PhC(O)O, $H_{c'}$-PhC(O)O); 7.65 (dt, 2H, $J_{Hc,Hd}$ = 7.8, H_d-PhC(O)O, $H_{d'}$-PhC(O)O); 8.04 (d, 2H, $J_{Hb,Hc}$ = 7.8 Hz, H_b-PhC(O)O); 8.11 (d, 2H, $J_{Hb',Hc'}$ = 7.8 Hz, $H_{b'}$-PhC(O)O). **^{13}C NMR (100 MHz, $CDCl_3$)** δ 23.10 ($NHC(O)\underline{C}H_3$); 24.83 ($C\underline{C}H_3$); 26.48 ($C\underline{C}H_3$); 47.40 (C-5); 53.59 (OCH_3); 67.34 (C-9); 69.76 (C-7); 69.81 (d, $J_{4,F3}$ = 16.9 Hz, C-4); 73.87 (C-6); 74.13 (C-8); 87.48 (d, $J_{3,F3}$ = 186.3 Hz, C-3); 95.79 (d, $J_{2,F3}$ = 29.9 Hz, C-2); 108.58 ($\underline{C}CH_3$); 128.19 (C_a-PhC(O)O); 128.22 ($C_{a'}$-PhC(O)O); 128.69 ($2C_c$-PhC(O)O); 128.78 ($2C_{c'}$-PhC(O)O); 129.93 ($2C_b$-PhC(O)O); 130.17 ($2C_{b'}$-PhC(O)O); 134.10 (C_d-PhC(O)O); 134.35 ($C_{d'}$-PhC(O)O); 162.41 (Ph$\underline{C}$(O)O); 165.73 (C-1); 167.54 (Ph$\underline{C'}$(O)O); 172.51 ($NH\underline{C}(O)CH_3$). **^{19}F NMR (376 MHz, $CDCl_3$)** – 206.60 (dd, $J_{F3,H3}$ = 50.4, $J_{F3,H4}$ = 28.9 Hz, F-3). **HRMS (ESI +ve)** *m/z* 590.2050 $[M+H]^+$ ($C_{29}H_{33}F_1N_1O_{11}$ requires 590.2038).

Data for (**64**): white solid (0.8 g, 18%); further data shown below.

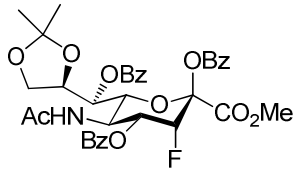

64

Methyl 5-*N*-acetyl-2,4,7-tri-*O*-benzoyl-3,5-dideoxy-3-fluoro-8,9-*O*-isopropylidene-*D*-*erythro*-α-*L*-manno-non-2-ulopyranosonate (64)

The 2,4,7-tri-*O*-benzoyl-3-fluoro-8,9-*O*-isopropylidenesialic acid methyl ester (**64**) was isolated as a side product in the formation of the 2,4-di-*O*-benzoyl-3-fluoro-8,9-*O*-isopropylidenesialic acid methyl ester (**63**) in 18% yield but was also prepared independently.

Benzoyl chloride (1.1 mL, 9.6 mmol) was added drop-wise to a stirred solution of 3-fluoro-8,9-*O*-isopropylidenesialic acid methyl ester (**48**) (0.9 g, 2.4 mmol) in anhydrous pyridine (15 mL) at 0 ºC and was then brought to room temperature and left to stir at this temperature for 5 hours. Methanol (1 mL) was added, the crude mixture was concentrated *in vacuo*, subjected to a standard work up (EtOAc) and was then purified by silica column chromatography (EtOAc:Petroleum Ether 60:40) to give (**64**) as a white solid (1.36 g, 82%).

$[\alpha]_D^{24}$ = - 1° (c = 1, CH_2Cl_2). **m.p.** 123 - 128 °C. **R_f** (EtOAc:Petroleum Ether 90:10, 0.8). **^{1}H NMR (400 MHz, $CDCl_3$)** δ 1.03 (s, 3H, CCH_3); 1.17 (s, 3H, CCH_3); 1.91 (s, 3H, $NHC(O)CH_3$); 3.92 (s, 3H, OCH_3); 3.94 -3.99 (m, 1H, H-5); 4.09 – 4.21 (m, 2H, H-9, H-9'); 4.34 (ddd, 1H, $J_{7,8}$ = 8.6, $J_{8,9}$ = 5.8, $J_{8,9'}$ = 2.2 Hz, H-8); 4.81 (d, 1H, $J_{5,6}$ = 10.6 Hz, H-6); 5.32 (dd, 1H, $J_{3,F3}$ = 49.3, $J_{3,4}$ = 2.5 Hz, H-3); 5.52 (d, 1H, $J_{7,8}$ = 8.6 Hz, H-7); 5.74 (d, 1H, $J_{5,NH}$ = 7.8 Hz, $NHC(O)CH_3$); 6.42 (ddd, 1H, $J_{4,F3}$ = 25.8, $J_{4,5}$ = 11.3, $J_{3,4}$ = 2.5 Hz, H-4); 7.43 (t, 2H, $J_{Hb,Hc}$ = 7.8 Hz, H_c-PhC(O)O); 7.50 (t, 2H, $J_{Hb',Hc'}$ = 7.8 Hz, $H_{c'}$-PhC(O)O); 7.55 (t, 2H, $J_{Hb'',Hc''}$ = 7.8 Hz, $H_{c''}$-PhC(O)O); 7.57 (d, 1H, $J_{Hc,Hd}$ = 8.6, H_d-PhC(O)O); 7.59 (d, 1H, $J_{Hc',Hd'}$ = 8.6, $H_{d'}$-PhC(O)O); 7.66 (t, 1H, $J_{Hc'',Hd''}$ = 7.4, $H_{d''}$-PhC(O)O); 8.04 (d, 2H, $J_{Hb,Hc}$ = 7.8 Hz, H_b-PhC(O)O); 8.15 (d, 2H, $J_{Hb',Hc'}$ = 7.8 Hz, $H_{b'}$-PhC(O)O); 8.17 (d, 2H, $J_{Hb'',Hc''}$ = 7.8 Hz, $H_{b''}$-PhC(O)O). **^{13}C NMR (100 MHz, $CDCl_3$)** δ 23.47 ($NHC(O)\underline{C}H_3$); 25.04 ($C\underline{C}H_3$); 26.27 ($C\underline{C}H_3$); 47.42 (C-5); 53.42 (OCH_3); 65.96 (C-9); 68.04 (d, $J_{4,F3}$ = 16.9 Hz, C-4); 70.26 (C-7); 70.99 (C-6); 75.02 (C-8); 87.31 (d, $J_{3,F3}$ =184.8 Hz, C-3); 95.50 (d, $J_{2,F3}$ = 29.1 Hz, C-2); 108.67 ($\underline{C}CH_3$); 127.93 (C_a-PhC(O)O); 128.54 ($2C_c$-PhC(O)O); 128.61 ($2C_{c'}$-PhC(O)O); 128.84 ($2C_{c''}$-PhC(O)O); 128.89 ($C_{a'}$-PhC(O)O); 129.35 ($C_{a''}$-PhC(O)O); 129.95 ($2C_b$-PhC(O)O); 130.10 ($2C_{b'}$-PhC(O)O); 130.29 ($2C_{b''}$-PhC(O)O); 133.54 (C_d-PhC(O)O); 133.66 ($C_{d'}$-PhC(O)O); 134.28 ($C_{d''}$-PhC(O)O); 162.41 (Ph$\underline{C}$(O)O); 165.12 (C-1); 165.74 (Ph$\underline{C'}$(O)O); 166.60 (Ph$\underline{C''}$(O)O); 170.73 ($NH\underline{C}(O)CH_3$). **^{19}F NMR (376 MHz, $CDCl_3$)** - 210.08 (dd, $J_{F3,H3}$ = 48.8, $J_{F3,H4}$ = 26.5 Hz, F-3). **HRMS (ESI +ve)** *m/z* 694.2293 $[M+H]^+$ ($C_{36}H_{37}F_1N_1O_{12}$ requires 694.2300).

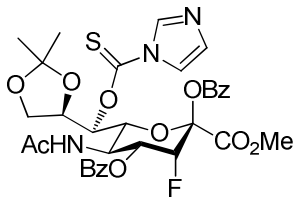

67

Methyl 5-*N*-acetyl-2,4-di-*O*-benzoyl-3,5-dideoxy-3-fluoro-7-*O*-(imidazol-1-ylthiocarbonyl)-8,9-*O*-isopropylidene-*D*-*erythro*-*α*-*L*-manno-non-2-ulopyranosonate (67)

1,1'-Thiocarbonyldiimidazole (3.8 g, 21.6 mmol) was added to a stirred solution of 2,4-di-*O*-benzoyl-3-fluoro-8,9-*O*-isopropylidenesialic acid methyl ester (**63**) (2.5 g, 4.3 mmol) in anhydrous dichloromethane (160 mL) and heated to 40 °C for 20 hours. The crude mixture was then concentrated *in vacuo* and purified by silica column chromatography (EtOAc:Petroleum Ether 80:20) affording (**67**) as a white solid (2.87g, 95%).

$[\alpha]_D^{24}$ = + 2° (c = 1, CH_2Cl_2). **m.p.** 129 - 132 °C. $\mathbf{R_f}$ (EtOAc:Petroleum Ether 80:20, 0.5). **^{1}H NMR (400 MHz, $CDCl_3$)** δ 1.05 (s, 3H, CCH_3); 1.16 (s, 3H, CCH_3); 1.88 (s, 3H, $NHC(O)CH_3$); 3.91 (s, 3H, OCH_3); 3.95 (m, 1H, H-5); 4.12 (dd, 1H, $J_{9,9'}$ = 12.1, $J_{8,9}$ = 5.4 Hz, H-9); 4.22 (dd, 1H, $J_{9,9'}$ = 12.1, $J_{8,9'}$ = 2.1 Hz, H-9'); 4.40 (ddd, 1H, $J_{7,8}$ = $J_{8,9}$ = 5.4, $J_{8,9'}$ = 2.1, Hz, H-8); 5.01 (d, 1H, $J_{5,6}$ = 10.5 Hz, H-6); 5.32 (dd, 1H, $J_{3,F3}$ = 49.2, $J_{3,4}$ = 2.3 Hz, H-3); 6.12 (d, 1H, $J_{7,8}$ = 5.4 Hz, H-7); 6.16 (d, 1H, $J_{5,NH}$ = 7.4 Hz, $NHC(O)CH_3$); 6.32 (ddd, 1H, $J_{4,F3}$ = 27.7, $J_{4,5}$ = 10.9, $J_{3,4}$ = 2.3 Hz, H-4); 7.04 (s, 1H, H_b-ImC(S)O); 7.44 (t, 2H, $J_{Hb,Hc}$ = 7.8 Hz, H_c-PhC(O)O); 7.54 (t, 2H, $J_{Hb',Hc'}$ = 7.8 Hz, $H_{c'}$-PhC(O)O); 7.59 (t, 1H, $J_{Hc,Hd}$ = 7.4, H_d-PhC(O)O); 7.65 (s, 1H, H_e-ImC(S)O); 7.67 (t, 1H, $J_{Hc',Hd'}$ = 7.4, $H_{d'}$-PhC(O)O); 8.10 (d, 2H, $J_{Hb,Hc}$ = 7.8 Hz, H_b-PhC(O)O); 8.15 (d, 2H, $J_{Hb',Hc'}$ = 8.2 Hz, $H_{b'}$-PhC(O)O); 8.43 (s, 1H, H_d-ImC(S)O).

^{13}C NMR (100 MHz, $CDCl_3$) δ 23.40 (NHC(O)$\underline{C}H_3$); 24.83 (C$\underline{C}H_3$); 26.13 (C$\underline{C}H_3$); 47.15 (C-5); 53.54 (OCH_3); 65.70 (C-9); 68.02 (d, $J_{4,F3}$ = 17.7 Hz, C-4); 70.67 (C-6); 74.83 (C-8); 78.08 (C-7); 87.41 (d, $J_{3,F3}$ =184.8 Hz, C-3); 95.41 (d, $J_{2,F3}$ = 29.1 Hz, C-2); 109.02 ($\underline{C}CH_3$); 117.61 (H_e-ImC(S)O); 127.78 (C_a-PhC(O)O); 128.62 ($2C_c$-PhC(O)O); 128.74 ($C_{a'}$-PhC(O)O); 128.80 ($2C_{c'}$-PhC(O)O); 129.92 ($2C_b$-PhC(O)O); 130.27 ($2C_{b'}$-PhC(O)O); 131.08 (H_b-ImC(S)O); 133.80 (C_d-PhC(O)O); 134.39 ($C_{d'}$-PhC(O)O); 137.97 (H_d-ImC(S)O); 162.95 (Ph$\underline{C}$(O)O); 164.91 (C-1); 165.68 (Ph$\underline{C'}$(O)O); 170.79 (NH$\underline{C}$(O)CH_3); 184.45 (Im$\underline{C}$(S)O. **^{19}F NMR (376 MHz, $CDCl_3$)** – 206.82 (dd, $J_{F3,H3}$ = 48.8, $J_{F3,H4}$ = 27.5 Hz, F-3). **HRMS (ESI +ve)** *m/z* 700.1947 $[M+H]^+$ ($C_{33}H_{35}F_1N_3O_{11}S_1$ requires 700.1976).

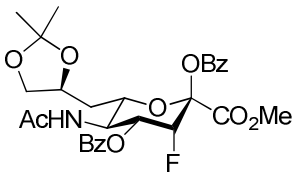

68

Methyl 5-*N*-acetyl-2,4-di-*O*-benzoyl-3,5,7-trideoxy-3-fluoro-8,9-*O*-isopropylidene-*D*-*erythro*-*α*-*L*-manno-non-2-ulopyranosonate (68)

In a flame-dried 100 mL round-bottom flask, 2,4-di-*O*-benzoyl-3-fluoro-8,9-*O*-isopropylidene-7-*O*-thiocarbamatesialic acid methyl ester (**67**) (0.5g mg, 0.7 mmol) was dissolved in anhydrous 1,4-dioxane (15 mL), concentrated *in vacuo*, ventilated under argon atmosphere, redissolved in anhydrous 1,4-dioxane (35 mL), degassed three times under argon atmosphere and then heated under stirring to 100 °C. In a flame-dried 25 mL round-bottom flask, tributyltin hydride (0.7 mL, 2.6 mmol) and Luperox® 101 (0.1 mL, 0.32 mmol) was added to 1,4-dioxane (8 mL) with molecular sieves (pellets, 4 Å). The tributyltin hydride solution was then added to the heated solution over 2 hours with a syringe pump under vigorous stirring and was left to stir at this temperature for further 2 hours. The solution was then cooled to room temperature, concentrated *in vacuo* and purified by silica column chromatography (EtOAc:Petroleum Ether 80:20) to give (**68**) as a white solid (365 mg, 89%).

$[\alpha]_D^{24}$ = - 3° (c = 1, CH_2Cl_2). **m.p.** 111 - 116 °C. **R_f** (EtOAc:Petroleum Ether 80:20, 0.4). **^{1}H NMR (400 MHz, $CDCl_3$)** δ 1.16 (s, 3H, CCH_3); 1.18 (s, 3H, CCH_3); 1.84 (s, 3H, $NHC(O)CH_3$); 1.86 (ddd, 1H, $J_{7,7'}$ = 14.2, $J_{7,8}$ = 5.3, $J_{6,7}$ = 2.1 Hz, H-7); 1.98 (ddd, 1H, $J_{7,7'}$ = 14.2, $J_{6,7'}$ = 10.5 $J_{7',8}$ = 7.8 Hz, H-7'); 3.52 (dd, 1H, $J_{9,9'}$ = 12.3, $J_{8,9}$ = 6.1 Hz, H-9); 3.87 (s, 3H, OCH_3); 3.95 (ddd, 1H, $J_{5,6}$ = $J_{6,7'}$ = 10.5, $J_{6,7}$ = 2.1 Hz, H-6); 4.06 – 4.10 (m, 1H, H-9'); 4.12 – 4.19 (m, 1H, H-8); 5.21 (ddd, 1H, $J_{4,5}$ = 11.2, $J_{5,6}$ = 10.5, $J_{5,NH}$ = 9.1 Hz, H-5); 5.21 (dd, 1H, $J_{3,F3}$ = 49.1, $J_{3,4}$ = 2.5 Hz, H-3); 5.52 (d, 1H, $J_{5,NH}$ = 9.1 Hz, $NHC(O)CH_3$); 5.67 (ddd, 1H, $J_{4,F3}$ = 27.9, $J_{4,5}$ = 11.2, $J_{3,4}$ = 2.5 Hz, H-4); 7.46 (t, 2H, $J_{Hb,Hc}$ = 7.8 Hz, H_c-PhC(O)O); 7.50 (t, 2H, $J_{Hb',Hc'}$ = 7.8 Hz, $H_{c'}$-PhC(O)O); 7.60 (t, 1H, $J_{Hc,Hd}$ = 7.4, H_d-PhC(O)O); 7.65 (t, 1H, $J_{Hc',Hd'}$ = 7.4, $H_{d'}$-PhC(O)O); 8.04 (dd, 4H, $J_{Hb,Hc}$ = $J_{Hb',Hc'}$ = 7.8 Hz, H_b-PhC(O)O, $H_{b'}$-PhC(O)O).

^{13}C NMR (100 MHz, $CDCl_3$) δ 23.43 ($NHC(O)\underline{C}H_3$); 25.07 ($C\underline{C}H_3$); 27.01 ($C\underline{C}H_3$); 35.22 (C-7); 49.55 (C-5); 53.73 (OCH_3); 67.31 (C-9); 70.06 (d, $J_{4,F3}$ = 17.6 Hz, C-4); 72.56 (C-6); 72.92 (C-8); 87.72 (d, $J_{3,F3}$ = 185.5 Hz, C-3); 95.79 (d, $J_{2,F3}$ = 29.2 Hz, C-2); 108.46 ($\underline{C}CH_3$); 128.27 (C_a-PhC(O)O); 128.81 ($C_{a'}$-PhC(O)O); 128.93 ($2C_c$-PhC(O)O); 129.00 ($2C_{c'}$-PhC(O)O); 130.29 ($2C_b$-PhC(O)O, $2C_{b'}$-PhC(O)O); 134.22 (C_d-PhC(O)O); 134.46 ($C_{d'}$-PhC(O)O); 162.92 ($Ph\underline{C}(O)O$); 165.54 (C-1); 166.97 ($Ph\underline{C'}(O)O$); 170.43 ($NH\underline{C}(O)CH_3$). **^{19}F NMR (470 MHz, $CDCl_3$)** – 207.35 (dd, $J_{F3,H3}$ = 48.9, $J_{F3,H4}$ = 27.9 Hz, F-3). **HRMS (ESI +ve)** *m/z* 574.2101 $[M+H]^+$ ($C_{29}H_{33}F_1N_1O_{10}$ requires 574.2089).

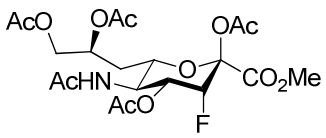

70

Methyl 5-*N*-acetyl-2,4,8,9-tetra-*O*-acetyl-3,5,7-trideoxy-3-fluoro-*D*-*erythro*-α-*L*-manno-non-2-ulopyranosonate (70)

a) 0.1M NaOMe/MeOH solution (2 mL) was added to a stirred solution of 2,4-di-*O*-benzoyl-7-deoxy-3-fluoro-8,9-*O*-isopropylidene sialic acid methyl ester (**68**) (1.3 g, 2.3 mmol) in anhydrous methanol (50 mL) at 40 °C and left to stir at this temperature for 36 hours. The solution was then neutralised through addition of Dowex 50 Wx8 100 ion exchange resin, H^+ form, filtered and the filtrate concentrated *in vacuo*.

b) The crude mixture was redissolved in 80% acetic acid/H_2O (80 mL) and stirred at 60 °C for 2 hours and was then concentrated *in vacuo*.

c) The residue was redissolved in anhydrous pyridine (50 mL) and acetic anhydride (2.55 mL, 27.2 mmol) and DMAP (11 mg, 0.09 mmol) were then added at 0 °C and left to stir at room temperature overnight. The crude mixture was then concentrated *in vacuo* and purified by silica column chromatography (EtOAc) affording (**70**) as a white solid (932 mg, 83% over 3 steps).

$[\alpha]_D^{24}$ = - 4° (c = 1, CH_2Cl_2). **m.p.** 77 - 79 °C. **R_f** (EtOAc:MeOH 90:10, 0.4). **^{1}H NMR (400 MHz, $CDCl_3$)** δ 1.84 – 1.99 (m, 2H, H-7, H-7'); 1.94 (s, 3H, NHC(O)CH_3); 2.01, 2.02, 2.11, 2.13 (4s, 12H, C(O)CCH_3); 3.76 (ddd, 1H, $J_{5,6}$ = $J_{6,7}$ = 10.2, $J_{6,7'}$ = 1.7 Hz, H-6); 3.81 (s, 3H, OCH_3); 4.06 (dd, 1H, $J_{9,9'}$ = 12.1, $J_{8,9}$ = 6.4 Hz, H-9); 4.24 (dd, 1H, $J_{9,9'}$ = 12.1, $J_{8,9'}$ = 3.2 Hz, H-9'); 4.27 (ddd, 1H, $J_{5,6}$ = $J_{4,5}$ = 10.2, $J_{5,NH}$ = 9.2 Hz H-5); 4.87 (dd, 1H, $J_{3,F3}$ = 49.1, $J_{3,4}$ = 2.5 Hz, H-3); 5.09 (dddd, 1H, $J_{7,8}$ = $J_{8,9}$ = 6.4, $J_{7',8}$ = $J_{8,9'}$ = 3.2 Hz, H-8); 5.28 (ddd, 1H, $J_{4,F3}$ = 28.2, $J_{4,5}$ = 10.2, $J_{3,4}$ = 2.5 Hz, H-4); 5.46 (d, 1H, $J_{5,NH}$ = 9.2 Hz, N<u>H</u>C(O)CH_3). **^{13}C NMR (100 MHz, $CDCl_3$)** δ 20.69, 20.93, 20.97, 21.19 (C(O)<u>C</u>H_3); 23.48 (NHC(O)<u>C</u>H_3); 33.41 (C-7); 49.48 (d, $J_{5,F3}$ = 2.1 Hz, C-5); 53.31 (OCH_3); 65.39 (C-9); 69.02 (d, $J_{4,F3}$ = 17.4 Hz, C-4); 69.64 (C-8); 72.02 (C-6); 87.55 (d, $J_{3,F3}$ = 185.1 Hz, C-3); 95.08 (d, $J_{2,F3}$ = 28.9 Hz, C-2); 165.60 (C-1); 167.27 (NH<u>C</u>(O)CH_3); 170.51, 170.56, 170.84, 171.51 (<u>C</u>(O)CH_3). **^{19}F NMR (470 MHz, $CDCl_3$)** - 207.28 (dd, $J_{F3,H3}$ = 49.3, $J_{F3,H4}$ = 28.5 Hz, F-3). **HRMS (ESI +ve)** *m/z* 494.1668 $[M+H]^+$ ($C_{20}H_{29}F_1N_1O_{12}$ requires 494.1674).

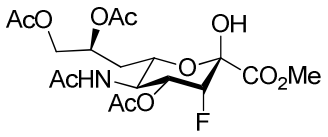

71

Methyl 5-*N*-acetyl-4,8,9-tri-*O*-acetyl-3,5,7-trideoxy-3-fluoro-*D*-*erythro*-α-*L*-manno-non-2-ulopyranosonate (71)

A solution of hydrazine acetate (902 mg, 9.8 mmol) in anhydrous methanol (20 mL) was cooled to 4 °C and added to a stirred solution of *per*-*O*-acetyl-7-deoxy-3-fluorosialic acid methyl ester (**70**) (1.2 g, 2.5 mmol) in anhydrous dichloromethane (40 mL) at 4 °C and left at this temperature overnight. The mixture was then diluted with dichloromethane (70 mL), subjected to a standard work up and purified by silica column chromatography (EtOAc) affording (**71**) as a white solid (933 mg, 84%).

$[\alpha]_D^{24}$ = - 1° (c = 1, CH_2Cl_2). **m.p.** 69 - 73 °C. **R_f** (EtOAc, 0.5). **^{1}H NMR (400 MHz, $CDCl_3$)** δ 1.85 – 1.93 (m, 2H, H-7, H-7'); 1.97 (s, 3H, NHC(O)CH_3); 2.05, 2.08, 2.12 (3s, 9H, C(O)CCH_3); 3.81 (ddd, 1H, $J_{5,6}$ = $J_{6,7}$ = 10.9, $J_{6,7'}$ = 2.1 Hz, H-6); 3.87 (s, 3H, OCH_3); 4.07 (dd, 1H, $J_{9,9'}$ = 12.1, $J_{8,9}$ = 6.8 Hz, H-9); 4.33 (ddd, 1H, $J_{4,5}$ = $J_{5,6}$ = 10.9, $J_{5,NH}$ = 9.6 Hz, H-5); 4.38 (dd, 1H, $J_{9,9'}$ = 12.1, $J_{8,9'}$ = 3.0 Hz, H-9'); 4.64 (s, 1H, OH-2); 4.87 (dd, 1H, $J_{3,F3}$ = 49.9, $J_{3,4}$ = 2.4 Hz, H-3); 5.24 – 5.29 (m, 1H, H-8); 5.28 (ddd, 1H, $J_{4,F3}$ = 28.2, $J_{4,5}$ = 10.9, $J_{3,4}$ = 2.4 Hz, H-4); 5.83 (d, 1H, $J_{5,NH}$ = 9.6 Hz, N<u>H</u>C(O)CH_3). **^{13}C NMR (100 MHz, $CDCl_3$)** δ 20.99, 21.00, 21.39, (C(O)<u>C</u>H_3); 23.29 (NHC(O)<u>C</u>H_3); 33.29 (C-7); 49.65 (C-5); 53.60 (OCH_3); 65.67 (C-9); 69.73 (d, $J_{4,F3}$ = 17.5 Hz, C-4); 69.89 (C-6); 69.92 (C-8); 87.39 (d, $J_{3,F3}$ = 185.2 Hz, C-3); 94.13 (d, $J_{2,F3}$ = 25.4 Hz, C-2); 168.05 (C-1); 170.66 (NH<u>C</u>(O)CH_3); 171.12, 171.60, 171.71, (<u>C</u>(O)CH_3). **^{19}F NMR (470 MHz, CD_3Cl_3)** – 204.71 (dd, $J_{F3,H3}$ = 50.2, $J_{F3,H4}$ = 29.1 Hz, F-3). **HRMS (ESI +ve)** *m/z* 474.1383 $[M+Na]^+$ ($C_{18}H_{26}F_1N_1Na_1O_{11}$ requires 474.1388).

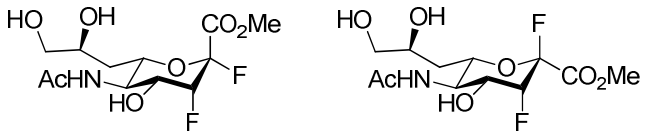

73 **74**

Methyl 5-*N*-acetyl-2,3,5,7-tetradeoxy-2,3-difluoro-*D*-*erythro*-*β*-*L*-manno-non-2-ulopyranosonate (73) and Methyl 5-*N*-acetyl-2,3,5,7-tetradeoxy-2,3-difluoro-*D*-*erythro*-*α*-*L*-manno-non-2-ulopyranosonate (74)

a) (Diethylamino)sulfur trifluoride (368 µL, 1.87 mmol) was added drop-wise to a stirred solution of hemiketal (**71**) (846 mg, 2.81 mmol) in anhydrous dichloromethane (40 mL) at – 40 °C and the temperature was increased to -10 °C during 1 hour. The reaction was then quenched by the addition of methanol (0.2 mL) and saturated $NaHCO_3$ solution (0.2 mL) and subjected to a standard work up (CH_2Cl_2).

b) The crude mixture was redissolved in methanol (40 mL) and sodium (20 mg) was then added to the stirred solution at room temperature and left to stir at this temperature for 3 hours.

The solution was then neutralised through addition of Dowex 50 Wx8 100 ion exchange resin, H^+ form, filtered, the filtrate concentrated *in vacuo* and purified by silica column chromatography (EtOAc:MeOH 99:1 → EtOAc:MeOH 70:30) to give (**73**) and (**74**).

Data for (**73**): white solid (254 mg, 41%).

$[\alpha]_D^{24}$ = + 2° (c = 1, CH_2Cl_2). **m.p.** 162 - 166 °C. **R_f** (EtOAc:MeOH 70:30, 0.4). **^{1}H NMR (400 MHz, CD_3OD)** δ 1.64 (ddd, 1H, $J_{7,7'}$ = 14.5, $J_{6,7}$ = 9.8, $J_{7,8}$ = 5.2 Hz, H-7); 1.71 (ddd, 1H, $J_{7,7'}$ = 14.5, $J_{7',8}$ = 9.8, $J_{6,7'}$ = 2.9 Hz, H-7'); 1.95 (s, 3H, NHC(O)CH_3); 3.41 (dd, 1H, $J_{9,9'}$ = 11.2, $J_{8,9}$ = 6.2 Hz, H-9); 3.48 (dd, 1H, $J_{9,9'}$ = 11.2, $J_{8,9'}$ = 4.6 Hz, H-9'); 3.75 (ddd, 1H, $J_{5,6}$ = $J_{6,7}$ = 9.8, $J_{6,7'}$ = 2.9 Hz, H-6); 3.81 -3.86 (m, 1H, H-8); 3.86 (s, 3H, OCH_3); 3.91 – 3.97 (m, 2H, H-4, H-5); 5.04 (ddd, 1H, $J_{3,F3}$ = 50.4, $J_{3,F2}$ = $J_{3,4}$ = 2.2 Hz, H-3).

^{13}C NMR (100 MHz, CD_3OD) δ 23.02 (NHC(O)$\underline{C}H_3$); 37.15 (C-7); 52.44 (d, $J_{5,F3}$ = 3.3 Hz, C-5); 53.97 (OCH_3); 67.88 (C-9); 69.29 (C-8); 70.06 (dd, $J_{4,F3}$ = 18.4, $J_{4,F2}$ = 5.0 Hz, C-4); 73.84 (d, $J_{6,F2}$ = 3.9 Hz, C-6); 89.34 (dd, $J_{3,F3}$ = 187.3, $J_{3,F2}$ = 18.4 Hz, C-3); 106.62 (dd, $J_{2,F2}$ = 220.6, $J_{2,F3}$ = 16.7 Hz, C-2); 167.03 (d, $J_{1,F2}$ = 34.9 Hz, C-1); 174.10 (NH$\underline{C}$(O)CH_3). **^{19}F NMR (470 MHz, CD_3OD)** - 123.74 (dd, 1F, $J_{F2,F3}$ = 11.2, $J_{H3,F2}$ = 2.2 Hz, F-2); – 200.74 (ddd, 1F, $J_{F3,H3}$ = 50.2, $J_{F3,H4}$ = 27.5, $J_{F2,F3}$ = 11.2 Hz, F-3). **HRMS (ESI +ve)** *m/z* 328.1215 $[M+H]^+$ ($C_{12}H_{20}F_2N_1O_7$ requires 328.1208).

Data for (**74**): white solid (121 mg, 20%).

$[\alpha]_D^{25}$ = - 3° (c = 1, MeOH). **m.p.** 86 - 89 °C. **R_f** (EtOAc:MeOH 70:30, 0.5) **^{1}H NMR (400 MHz, CD_3OD)** δ 1.64 (d, 1H, $J_{7,7'}$ = 11.8 Hz, H-7); 1.65 (d, 1H, $J_{7,7'}$ = 11.8 Hz, H-7'); 1.98 (s, 3H, NHC(O)CH_3); 3.42 (dd, 1H, $J_{9,9'}$ = 11.2, $J_{8,9}$ = 6.4 Hz, H-9); 3.49 (dd, 1H, $J_{9,9'}$ = 11.2, $J_{8,9'}$ = 2.3 Hz, H-9'); 3.84 (s, 3H, OCH_3); 3.87 – 4.11 (m, 4H, H-4, H-5, H-6, H-8); 4.98 (ddd, 1H, $J_{3,F3}$ = 45.8, $J_{3,4}$ = $J_{3,F2}$ = 2.2 Hz, H-3). **^{13}C NMR (100 MHz, CD_3OD)** δ 23.04 (NHC(O)$\underline{C}H_3$); 36.67 (C-7); 52.0 (d, $J_{5,F3}$ = 2.1 Hz, C-5); 54.04 (OCH_3); 67.85 (C-9); 68.67 (dd, $J_{4,F3}$ = 18.4, $J_{4,F2}$ = 5.1 Hz, C-4); 69.17 (C-8); 73.48 (d, $J_{6,F2}$ = 2.2 Hz, C-6); 88.85 (dd, $J_{3,F3}$ =179.4, $J_{3,F2}$ = 44.5 Hz, C-3); 106.82 (dd, $J_{2,F2}$ = 225.9, $J_{2,F3}$ = 28.5 Hz, C-2); 165.62 (d, $J_{1,F2}$ = 27.3 Hz, C-1); 174.15 (NH$\underline{C}$(O)CH_3). **^{19}F NMR (470 MHz, CD_3OD)** – 122.40 (dd, 1F, $J_{F2,F3}$ 15.5, $J_{F2,H3}$ = 2.2 Hz, F-2); – 210.08 (ddd, 1F, $J_{F3,H3}$ = 45.2, $J_{F3,H4}$ = 28.2, $J_{F2,F3}$ = 15.5 Hz, F-3). **HRMS (ESI +ve)** *m/z* 328.1215 $[M+H]^+$ ($C_{12}H_{20}F_2N_1O_7$ requires 328.1208).

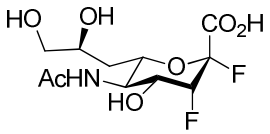

25

5-*N*-Acetyl-2,3,5,7-tetradeoxy-2,3-difluoro-*D*-*erythro*-*β*-*L*-manno-non-2-ulopyranosonic acid (25)

A 0.5M aqueous NaOH solution (1 mL) was added to a stirred solution of 7-deoxy-2,3-difluorosialic acid methyl ester (**73**) (198 mg) dissolved in water (2 mL) at room temperature and was left to stir for 45 minutes. The solution was then neutralised through addition of Dowex 50 Wx8 100 ion exchange resin, H^+ form, filtered, the filtrate concentrated *in vacuo* and purified by silica column chromatography (EtOAc:MeOH 1:1) affording (**25**) as a white solid (93 mg, 49%).

$[\alpha]_D^{24}$ = - 4° (c = 1, MeOH). **m.p.** 151 - 155 °C. **R_f** (EtOAc:MeOH 70:30, 0.1). **^{1}H NMR (400 MHz, D_2O)** δ 1.74 (d, 1H, $J_{7,7'}$ = 12.1 Hz, H-7); 1.75 (d, 1H, $J_{7,7'}$ = 12.1 Hz, H-7'); 2.10 (s, 3H, NHC(O)CH_3); 3.52 (dd, 1H, $J_{9,9'}$ = 11.3, $J_{8,9}$ = 7.0 Hz, H-9); 3.64 (dd, 1H, $J_{9,9'}$ = 11.3, $J_{8,9'}$ = 3.6 Hz, H-9'); 3.78 – 3.81 (m, 1H, H-6); 3.97 – 4.04 (m, 2H, H-5, H-8); 4.20 (ddd, 1H, $J_{4,F3}$ = 28.5, $J_{4,5}$ = 9.6, $J_{3,4}$ = 1.8 Hz, H-4); 5.25 (ddd, 1H, $J_{3,F3}$ = 51.1, $J_{3,4}$ = $J_{3,F2}$ = 1.8 Hz H-3). **^{13}C NMR (100 MHz, D_2O)** δ 22.19 (NHC(O)$\underline{C}H_3$); 34.83 (C-7); 50.95 (d, $J_{5,F3}$ = 3.1 Hz, C-5); 65.71 (C-9); 67.66 (C-8); 68.97 (dd, $J_{4,F3}$ = 17.9, $J_{4,F2}$ = 5.9 Hz, C-4); 71.44 (d, $J_{6,F2}$ = 4.7 Hz, C-6); 89.17 (dd, $J_{3,F3}$ =183.0, $J_{3,F2}$ = 18.9 Hz, C-3); 106.56 (dd, $J_{2,F2}$ = 219.6, $J_{2,F3}$ = 14.8 Hz, C-2); 169.46 (d, $J_{1,F2}$ = 26.6 Hz, C-1); 174.90 (NH$\underline{C}$(O)CH_3). **^{19}F NMR (470 MHz, D_2O)** – 120.23 (dd, 1F, $J_{F2,F3}$ = 11.9, $J_{F2,H3}$ = 1.8 Hz, F-2); - 217.10 (ddd, 1F, $J_{F3,H3}$ = 51.2, $J_{F3,H4}$ = 28.5, $J_{F2,F3}$ = 11.9 Hz, F-3). **HRMS (ESI -ve)** *m/z* 312.0891 $[M-H]^-$ ($C_{11}H_{16}F_2N_1O_7$ requires 312.0895). **Anal. Calcd. for $C_{11}H_{16}F_2N_1Na_1O_7$+1/2 H_2O**: C, 38.38; H, 4.98; N, 4.07. Found: C, 38.10; H, 5.20; N, 3.94.

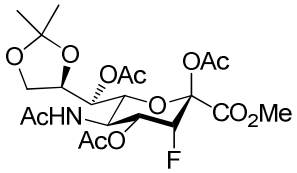

79

Methyl 5-*N*-acetyl-2,4,7-tri-*O*-acetyl-3,5-dideoxy-3-fluoro-8,9-*O*-isopropylidene-*D*-*erythro*-*α*-*L*-manno-non-2-ulopyranosonate (79)

Acetic anhydride (7.4 ml, 79 mmol) was added to a stirred solution of 3-fluoro-8,9-*O*-isopropylidenesialic acid methyl ester (**48**) (2.5 g, 6.6 mmol) in pyridine (70 mL) at 4 °C and the solution was left to stir at room temperature for 7 days. The solution was concentrated *in vacuo* and residual pyridine removed by azeotropic evaporation with toluene. The residue was then subjected to a standard work up (EtOAc) and purified by silica chromatography (EtOAc→ EtOAc:MeOH 90:10) to give (**79**) as a white solid (3.03 g, 91%).

$[\alpha]_D^{21}$ = - 2° (c = 1, CH_2Cl_2). **m.p.** 174 - 177 °C. **R_f** (EtOAc, 0.5). **^{1}H NMR (400 MHz, $CDCl_3$)** δ 1.30 (s, 3H, CCH_3); 1.34 (s, 3H, CCH_3); 1.92 (s, 3H, $NHC(O)CH_3$); 2.11, 2.15, 2.16 (3s, 9H, $C(O)CCH_3$); 3.84 (s, 3H, OCH_3); 3.95 (dd, 1H, $J_{9,9'}$ = 8.9, $J_{8,9}$ = 6.3 Hz, H-9); 4.04 (dd, 1H, $J_{9,9'}$ = 8.9, $J_{8,9'}$ = 6.3 Hz, H-9'); 4.12 (ddd, 1H, $J_{5,6}$ = $J_{4,5}$ = 10.9, $J_{5,NH}$ = 9.0 Hz, H-5); 4.23 (ddd, 1H, $J_{7,8}$ = $J_{8,9}$ = $J_{8,9'}$ = 6.3 Hz, H-8); 4.26 (dd, 1H, $J_{5,6}$ = 10.9, $J_{6,7}$ = 1.8 Hz, H-6); 4.94 (dd, 1H, $J_{3,F3}$ = 49.0, $J_{3,4}$ = 2.6 Hz, H-3); 5.23 (dd, 1H, $J_{7,8}$ = 6.3, $J_{6,7}$ = 1.8 Hz, H-7); 5.45 (d, 1H, $J_{5,NH}$ = 9.0 Hz, $N\underline{H}C(O)CH_3$); 5.60 (ddd, 1H, $J_{4,F3}$ = 28.0, $J_{4,5}$ = 10.9, $J_{3,4}$ = 2.6 Hz, H-4). **^{13}C NMR (100 MHz, $CDCl_3$)** δ 20.43, 20.66, 20.99 ($C(O)\underline{C}H_3$); 23.29 ($NHC(O)\underline{C}H_3$); 25.29 ($C\underline{C}H_3$); 26.59 ($C\underline{C}H_3$); 45.96 (C-5); 53.40 (OCH_3); 66.07 (C-9); 68.38 (d, $J_{4,F3}$ = 16.9 Hz, C-4); 69.11 (C-7); 71.55 (C-6); 74.38 (C-8); 87.08 (d, $J_{3,F3}$ = 184.8 Hz, C-3); 95.12 (d, $J_{2,F3}$ = 29.1 Hz, C-2); 165.15 (C-1); 166.98 ($NH\underline{C}(O)CH_3$); 170.37, 170.53, 171.02 ($\underline{C}(O)CH_3$). **^{19}F NMR (376 MHz, $CDCl_3$)** – 208.90 (dd, $J_{F3,H3}$ = 48.8, $J_{F3,H4}$ = 27.5 Hz, F-3). **HRMS (ESI +ve)** *m/z* 508.1817 $[M+H]^+$ ($C_{21}H_{31}F_1N_1O_{12}$ requires 508.1830).

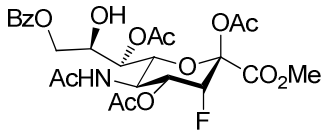

81

Methyl 5-*N*-acetyl-2,4,7-tri-*O*-acetyl-9-*O*-benzoyl-3,5-dideoxy-3-fluoro-*D*-*erythro*-α-*L*-manno-non-2-ulopyranosonate (81)

a) 2,4,7-Tri-*O*-acetyl-3-fluoro-8,9-*O*-isopropylidenesialic acid methyl ester (**79**) (3.5 g, 6.9 mmol) was dissolved in 80% acetic acid/H_2O (200 mL) and was then stirred at 60 °C for 2 hours. The crude mixture was concentrated *in vacuo* and residual acetic acid was removed by azeotropic evaporation with toluene to give a white solid.

b) The crude mixture was evaporated with pyridine (30 mL), redissolved in pyridine (75 mL) and cooled to 0 °C. Benzoyl chloride (0.88 mL, 7.6 mmol) was added to the cooled solution and was left to stir at this temperature for one hour and was then brought to room temperature and stirred for 6 hours. The solution was concentrated *in vacuo* and residual pyridine was removed by azeotropic evaporation with toluene. The crude was then purified by silica chromatography (EtOAc:MeOH 99:1) to give (**81**) as a white solid (2.76 g, 70% (over 2steps)).

$[\alpha]_D^{21}$ = + 1° (c = 1, CH_2Cl_2). **m.p.** 109 - 112 °C. **R_f** (EtOAc:MeOH 80:20, 0.5). **^{1}H NMR (400 MHz, $CDCl_3$)** δ 1.88 (s, 3H, NHC(O)CH_3); 2.05, 2.11, 2.17 (3s, 9H, C(O)CCH_3); 3.87 (s, 3H, OCH_3); 4.24 – 4.42 (m, 4H, H-5, H-6, H-8, H-9); 4.45 (dd, 1H, $J_{9,9'}$ = 11.4, $J_{8,9'}$ = 2.9 Hz, H-9'); 4.95 (dd, 1H, $J_{3,F3}$ = 49.0, $J_{3,4}$ = 2.5 Hz, H-3); 5.20 (dd, 1H, $J_{7,8}$ = 8.2, $J_{6,7}$ = 1.8 Hz, H-7); 5.32 (d, 1H, $J_{5,NH}$ = 7.6 Hz, N<u>H</u>C(O)CH_3); 5.50 (ddd, 1H, $J_{4,F3}$ = 27.8, $J_{4,5}$ = 10.6, $J_{3,4}$ = 2.5 Hz, H-4); 7.44 (t, 2H, $J_{Hb,Hc}$ = 7.9 Hz, H_c-PhC(O)O); 7.57 (t, 1H, $J_{Hc,Hd}$ = 7.9, H_d-PhC(O)O); 8.05 (d, 2H, $J_{Hb,Hc}$ = 7.8 Hz, H_b-PhC(O)O). **^{13}C NMR (100 MHz, $CDCl_3$)** δ 20.75, 20.87, 21.34 (C(O)<u>C</u>H_3); 23.41 (NHC(O)<u>C</u>H_3); 45.57 (C-5); 53.72 (OCH_3); 65.97 (C-9); 68.62 (C-8); 68.79 (C-7); 69.14 (d, $J_{4,F3}$ = 17.1 Hz, C-4); 71.76 (C-6); 87.15 (d, $J_{3,F3}$ = 185.5 Hz, C-3); 95.81 (d, $J_{2,F3}$ = 28.9 Hz, C-2); 128.65 (2C_c-PhC(O)O); 129.97 (2C_b-PhC(O)O); 133.28 (C_a-PhC(O)O); 133.48 (C_d-PhC(O)O); 165.73 (C-1); 167.07 (Ph<u>C</u>(O)O); 168.77, 170.44 (<u>C</u>(O)CH_3); 170.93 (NH<u>C</u>(O)CH_3); 171.08 (<u>C</u>(O)CH_3). **^{19}F NMR (470 MHz, $CDCl_3$)** – 208.76 (dd, 1F, $J_{F3,H3}$ = 49.1, $J_{F3,H4}$ = 28.1 Hz, F-3). **HRMS (ESI +ve)** *m/z* 594.1558 $[M+Na]^+$ ($C_{25}H_{30}F_1N_1Na_1O_{13}$ requires 594.1599).

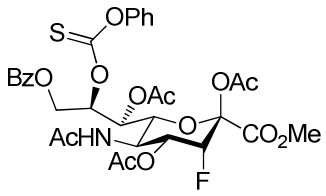

84

Methyl 5-*N*-acetyl-2,4,7-tri-*O*-acetyl-9-*O*-benzoyl-3,5-dideoxy-3-fluoro-8-*O*-(phenoxy)thiocarbonyl-*D*-*erythro*-*α*-*L*-manno-non-2-ulopyranosonate (84)

Phenyl chlorothionoformate (0.8 mL, 6 mmol) was added drop-wise to a stirred solution of 2,4,7-tri-*O*-acetyl-9-*O*-benzoyl-3-fluorosialic acid methyl ester (**81**) (1.4 g, 2.4 mmol) in anhydrous pyridine (50 mL) at 0 ºC The mixture was then left to stir at room temperature for 15 hours. Methanol (0.5 mL) was added, the crude mixture was concentrated *in vacuo* and purified by silica column chromatography (EtOAc) to give (**84**) as an off-white solid (1.43 g, 84%).

m.p. 133 - 136 °C. $\mathbf{R_f}$ (EtOAc, 0.5). **^{1}H NMR (270 MHz, $CDCl_3$)** δ 1.91 (s, 3H, $NHC(O)CH_3$); 2.11, 2.12, 2.20 (3s, 9H, $C(O)CCH_3$); 3.83 (s, 3H, OCH_3); 4.27 – 4.39 (m, 2H, H-5, H-6); 4.48 (dd, 1H, $J_{9,9'}$ = 12.7, $J_{8,9}$ = 5.5 Hz, H-9); 4.98 (dd, 1H, $J_{3,F3}$ = 49.0, $J_{3,4}$ = 2.5 Hz, H-3); 5.15 (dd, 1H, $J_{9,9'}$ = 12.7, $J_{8,9'}$ = 2.3 Hz, H-9'); 5.34 (d, 1H, $J_{5,NH}$ = 8.5 Hz, N<u>H</u>C(O)CH_3); 5.55 (ddd, 1H, $J_{4,F3}$ = 27.9, $J_{4,5}$ = 10.8, $J_{3,4}$ = 2.5 Hz, H-4); 5.69 (ddd, 1H, $J_{8,9}$ = $J_{7,8}$ = 5.5, $J_{8,9'}$ = 2.3 Hz, H-8); 5.79 (dd, 1H, $J_{7,8}$ = 5.5, $J_{6,7}$ = 2.1 Hz, H-7); 7.16 (d, 2H, $J_{Hb,Hc}$ = 7.4 Hz, H_b-PhC(S)O); 7.25 (t, 1H, $J_{Hc,Hd}$ = 7.4, H_d-PhC(S)O); 7.39 (t, 2H, $J_{Hb,Hc}$ = 7.9 Hz, H_c-PhC(S)O); 7.44 (t, 2H, $J_{Hb,Hc}$ = 7.9 Hz, H_c-PhC(O)O); 7.57 (t, 1H, $J_{Hc,Hd}$ = 7.9, H_d-PhC(O)O); 8.06 (d, 2H, $J_{Hb,Hc}$ = 7.9 Hz, H_b-PhC(O)O).

^{13}C NMR (100 MHz, $CDCl_3$) δ 20.50, 20.65, 20.79 (C(O)$\underline{C}H_3$); 23.25 (NHC(O)$\underline{C}H_3$); 45.52 (C-5); 53.50 (OCH_3); 61.72 (C-9); 67.39 (C-7); 68.46 (d, $J_{4,F3}$ = 17.6 Hz, C-4); 72.08 (C-6); 80.32 (C-8); 86.93 (d, $J_{3,F3}$ = 186.3 Hz, C-3); 95.09 (d, $J_{2,F3}$ = 28.4 Hz, C-2); 121.14 (C_a-PhC(S)O); 121.83 ($2C_b$-PhC(S)O); 126.71 (C_d-PhC(S)O); 128.35 ($2C_c$-PhC(O)O); 129.51 ($2C_c$-PhC(S)O); 129.80 ($2C_b$-PhC(O)O); 133.10 (C_d-PhC(O)O); 153.33 (C_a-PhC(O)O); 165.03 (C-1); 166.00 (Ph$\underline{C}$(O)O); 167.07, 170.26 ($\underline{C}$(O)CH_3); 170.34 (NH$\underline{C}$(O)CH_3); 170.57 ($\underline{C}$(O)CH_3); 193.70 (Ph$\underline{C}$(S)O). **^{19}F NMR (376 MHz, $CDCl_3$)** – 208.86 (dd, $J_{F3,H3}$ = 48.9, $J_{F3,H4}$ = 27.5 Hz, F-3). **HRMS (ESI +ve)** *m/z* 730.1562 $[M+Na]^+$ ($C_{32}H_{34}F_1N_1Na_1O_{14}S_1$ requires 730.1582).

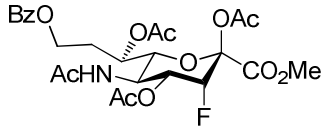

85

Methyl 5-*N*-acetyl-2,4,7-tri-*O*-acetyl-9-*O*-benzoyl-3,5,8-trideoxy-3-fluoro-*D*-*erythro*-α-*L*-manno-non-2-ulopyranosonate (85)

In a flame-dried 100 mL round-bottom flask 2,4,7-tri-*O*-acetyl-9-*O*-benzoyl-3-fluoro-8-*O*-phenyl-thionocarbonatesialic acid methyl ester (**84**) (0.3 g, 0.42 mmol) was dissolved in anhydrous 1,4-dioxane (25 mL), concentrated *in vacuo*, ventilated under argon atmosphere, redissolved in anhydrous 1,4-dioxane (35 mL), degassed three times under argon atmosphere and then heated under stirring to 100 °C.

In a flame-dried 25 mL round-bottom flask, tributyltin hydride (0.4 mL, 1.57 mmol) and Luperox® 101 (0.1 mL, 0.19 mmol) was added to 1,4-dioxane (10 mL) with molecular sieves. The tributyltin hydride solution was then added to the heated solution over 2 hours with a syringe pump under vigorous stirring and was left to stir at this temperature for further 2 hours. The solution was then cooled to room temperature, concentrated *in vacuo* and purified by silica column chromatography (EtOAc) to give (**85**) as a white solid (188 mg, 80%).

$[\alpha]_D^{21}$ = - 1° (c = 1, CH_2Cl_2). **m.p.** 164 - 166 °C. **R_f** (EtOAc:MeOH 90:10, 0.6). **^{1}H NMR (400 MHz, $CDCl_3$)** δ 1.82 (s, 3H, NHC(O)CH_3); 2.04 – 2.11 (m, 1H, H-8); 2.11, 2.13, 2.20 (3s, 9H, C(O)CCH_3); 2.27 – 2.36 (m, 1H, H-8'); 3.85 (s, 3H, OCH_3); 4.11 – 4.26 (m, 3H, H-5, H-6, H-9); 4.38 – 4.44 (m, 1H, H-9'); 4.96 (dd, 1H, $J_{3,F3}$ = 49.1, $J_{3,4}$ = 2.3 Hz, H-3); 5.23 (dd, 1H, $J_{7,8}$ = $J_{6,7}$ = 7.2 Hz, H-7); 5.34 (d, 1H, $J_{5,NH}$ = 8.1 Hz, N<u>H</u>C(O)CH_3); 5.60 (ddd, 1H, $J_{4,F3}$ = 27.9, $J_{4,5}$ = 10.7, $J_{3,4}$ = 2.3 Hz, H-4); 7.44 (t, 2H, $J_{Hb,Hc}$ = 7.9 Hz, H_c-PhC(O)O); 7.56 (t, 1H, $J_{Hc,Hd}$ = 7.8, H_d-PhC(O)O); 8.03 (d, 2H, $J_{Hb,Hc}$ = 7.8 Hz, H_b-PhC(O)O). **^{13}C NMR (100 MHz, $CDCl_3$)** δ 20.51, 20.63, 21.02, (C(O)<u>C</u>H_3); 23.07 (NHC(O)<u>C</u>H_3); 29.69 (C-8); 45.96 (C-5); 53.44 (OCH_3); 60.83 (C-9); 66.87 (C-7); 68.42 (d, $J_{4,F3}$ = 17.0 Hz, C-4); 72.66 (C-6); 86.93 (d, $J_{3,F3}$ = 185.0 Hz, C-3); 95.29 (d, $J_{2,F3}$ = 28.7 Hz, C-2); 128.38 (2C_c-PhC(O)O); 129.56 (2C_b-PhC(O)O); 129.56 (C_a-PhC(O)O); 133.10 (C_d-PhC(O)O); 165.09 (C-1); 166.65 (Ph<u>C</u>(O)O); 167.47 (NH<u>C</u>(O)CH_3); 170.30, 170.52, 171.12 (<u>C</u>(O)CH_3). **^{19}F NMR (376 MHz, $CDCl_3$)** – 209.35 (dd, $J_{F3,H3}$ = 47.9, $J_{F3,H4}$ = 27.7 Hz, F-3). **HRMS (ESI +ve)** *m/z* 556.1803 $[M+H]^+$ ($C_{25}H_{31}F_1N_1O_{12}$ requires 556.1830).

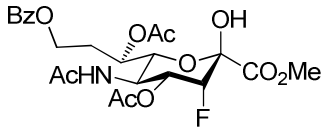

86

Methyl 5-*N*-acetyl-4,7-di-*O*-acetyl-9-*O*-benzoyl-3,5,8-trideoxy-3-fluoro-*D*-*erythro*-α-*L*-manno-non-2-ulopyranosonate (86)

A solution of hydrazine acetate (483 mg, 5.25 mmol) in anhydrous methanol (10 mL) was cooled to 4 °C and added to a stirred solution of 2,4,7-tri-*O*-acetyl-9-*O*-benzoyl-8-deoxy-3-fluorosialic acid methyl ester (**85**) (728 mg, 1.31 mmol) in anhydrous dichloromethane (20 mL) at 4 °C and left at this temperature overnight. The mixture was then diluted with dichloromethane (60 mL), subjected to a standard work up and purified by silica column chromatography (EtOAc:Petroleum ether, 90:10) affording (**86**) as a white solid (560 mg, 83%).

$[\alpha]_D^{23}$ = + 3° (c = 1, CH_2Cl_2). **m.p.** 107 - 111 °C. **R_f** (EtOAc, 0.4).

^{1}H NMR (400 MHz, $CDCl_3$) δ 1.87 (s, 3H, NHC(O)CH_3); 2.09, 2.13 (2s, 6H, C(O)CCH_3); 2.18 – 2.30 (m, 2H, H-8, H-8'); 3.84 (s, 3H, OCH_3); 4.20 (dd, 1H, $J_{5,6}$ = 10.4, $J_{6,7}$ = 2.0 Hz, H-6); 4.28 – 4.34 (m, 1H, H-9); 4.41 – 4.50 (m, 2H, H-5, H-9'); 4.90 (dd, 1H, $J_{3,F3}$ = 50.5, $J_{3,4}$ = 2.4 Hz, H-3); 5.17 (s, 1H, OH-2); 5.21 (dd, 1H, $J_{7,8}$ = 6.6, $J_{6,7}$ = 2.0 Hz, H-7); 5.45 (ddd, 1H, $J_{4,F3}$ = 27.8, $J_{4,5}$ = 11.0, $J_{3,4}$ = 2.4 Hz, H-4); 5.70 (d, 1H, $J_{5,NH}$ = 9.4 Hz, N<u>H</u>C(O)CH_3); 7.42 (t, 2H, $J_{Hb,Hc}$ = 7.8 Hz, H_c-PhC(O)O); 7.55 (t, 1H, $J_{Hc,Hd}$ = 7.8, H_d-PhC(O)O); 7.99 (d, 2H, $J_{Hb,Hc}$ = 7.8 Hz, H_b-PhC(O)O). **^{13}C NMR (100 MHz, $CDCl_3$)** δ 20.75, 21.12 (C(O)<u>C</u>H_3); 23.12 (NHC(O)<u>C</u>H_3); 29.62 (C-8); 45.73 (C-5); 53.54 (OCH_3); 61.50 (C-9); 76.64 (C-7); 69.56 (d, $J_{4,F3}$ = 16.9 Hz, C-4); 71.70 (C-6); 86.76 (d, $J_{3,F3}$ = 187.1 Hz, C-3); 94.06 (d, $J_{2,F3}$ = 24.5 Hz, C-2); 128.46 ($2C_c$-PhC(O)O); 129.58 ($2C_b$-PhC(O)O); 129.80 (C_a-PhC(O)O); 133.26 (C_d-PhC(O)O); 167.05 (C-1); 167.91 (Ph<u>C</u>(O)O); 170.22 (NH<u>C</u>(O)CH_3); 171.012, 171.22 (<u>C</u>(O)CH_3). **^{19}F NMR (376 MHz, $CDCl_3$)** – 205.06 (dd, $J_{F3,H3}$ = 50.4, $J_{F3,H4}$ = 27.5 Hz, F-3). **HRMS (ESI +ve)** *m/z* 514.1694 $[M+H]^+$ ($C_{23}H_{29}F_1N_1O_{11}$ requires 514.1725).

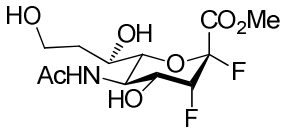

88

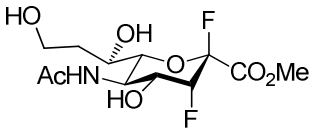

89

Methyl 5-*N*-acetyl-2,3,5,8-tetradeoxy-2,3-difluoro-*D*-*erythro*-*β*-*L*-manno-non-2-ulopyranosonate (88) and Methyl 5-*N*-acetyl-2,3,5,8-tetradeoxy-2,3-difluoro-*D*-*erythro*-*α*-*L*-manno-non-2-ulopyranosonate (89)

a) (Diethylamino)sulfur trifluoride (0.2 ml, 1.52 mmol) was added drop-wise to a stirred solution of hemiketal (**86**) (0.52 g, 1.01 mmol) in anhydrous dichloromethane (20 mL) at – 40 °C and the temperature was increased to -10 °C within 1 hour. The reaction was then quenched by the addition of methanol (0.2 mL) and saturated $NaHCO_3$ solution (0.2 mL) and subjected to a standard work up (CH_2Cl_2).

b) The crude mixture was redissolved in methanol (15 mL) and sodium (6 mg) was then added to the stirred solution at room temperature and left to stir at this temperature overnight. The solution was then neutralised through addition of Dowex 50 Wx8 100 ion exchange resin, H^+ form, filtered, the filtrate concentrated *in vacuo*. The crude mixture was redissolved in anhydrous methanol (15 mL) and trifluoroacetic acid (0.3 mL, 3.9 mmol) was added drop-wise to the stirred solution at room temperature and was stirred at this temperature overnight. The solution was then concentrated *in vacuo*, redissolved in methanol, concentrated *in vacuo* and purified by silica column chromatography (EtOAc:MeOH 99:1 → EtOAc:MeOH 90:10) to give (**88**) and (**89**).

Data for (**88**): white solid (82 mg, 25% (over 3 steps)).

$[\alpha]_D^{25}$ = - 1° (c = 1, MeOH). **m.p.** 113 - 117 °C. **R_f** (EtOAc:MeOH 80:20, 0.4). **^{1}H NMR (400 MHz, CD_3OD)** δ 1.69 – 1.76 (m, 1H, H-8); 1.92 – 1.99 (m, 1H, H-8'); 2.01 (s, 3H, NHC(O)CH_3); 3.39 (d, 1H, $J_{5,6}$ = 10.2 Hz, H-6); 3.68 – 3.71 (m, 2H, H-9, H-9'); 3.82 – 3.87 (m, 1H, H-7); 3.89 (s, 3H, OCH_3); 4.01 (ddd, 1H, $J_{4,F3}$ = 27.8, $J_{4,5}$ = 10.2, $J_{3,4}$ = 1.8 Hz, H-4); 4.20 (dd, 1H, $J_{4,5}$ = $J_{5,6}$ = 10.2 Hz, H-5); 5.08 (ddd, 1H, $J_{3,F3}$ = 51.2, $J_{3,F2}$ = $J_{3,4}$ = 1.8 Hz, H-3). **^{13}C NMR (100 MHz, CD_3OD)** δ 22.69 (NHC(O)$\underline{C}H_3$); 36.32 (C-8); 49.11 (d, $J_{5,F3}$ = 3.8 Hz, C-5); 49.64 (OCH_3); 59.54 (C-9); 66.40 (C-7); 69.55 (dd, $J_{4,F3}$ = 18.4, $J_{4,F2}$ = 6.2 Hz, C-4); 78.15 (d, $J_{6,F2}$ = 3.8 Hz, C-6); 89.25 (dd, $J_{3,F3}$ = 187.8, $J_{3,F2}$ = 17.6 Hz, C-3); 105.78 (dd, $J_{2,F2}$ = 219.3, $J_{2,F3}$ = 16.9 Hz, C-2); 166.62 (d, $J_{1,F2}$ = 25.3 Hz, C-1); 175.23 (NH$\underline{C}$(O)CH_3).**^{19}F NMR (470 MHz, CD_3OD)** – 123.66 (dd, 1F, $J_{F2,F3}$ = 11.3, $J_{F2,H3}$ = 1.8 Hz, F-2); – 221.14 (ddd, 1F, $J_{F3,H3}$ = 50.8, $J_{F3,H4}$ = 27.8, $J_{F2,F3}$ = 11.3 Hz, F-3). **HRMS (ESI +ve)** *m/z* 328.1208 $[M+H]^+$ ($C_{12}H_{20}F_2N_1O_7$ requires 328.1208).

Data for (**89**): colourless oil (35 mg, 11% (over 3 steps)).

$[\alpha]_D^{25}$ = - 2° (c = 1, MeOH). **R_f** (EtOAc:MeOH 80:20, 0.5) **^{1}H NMR (500 MHz, CD_3OD)** δ 1.61 – 1.64 (m, 1H, H-8); 1.83 – 1.87 (m, 1H, H-8'); 1.93 (s, 3H, NHC(O)CH_3); 3.29 (dd, 1H, $J_{5,6}$ = 10.8, $J_{6,7}$ = 1.3 Hz, H-6); 3.58 – 3.60 (m, 2H, H-9, H-9'); 3.73 – 3.77 (m, 1H, H-7); 3.89 (s, 3H, OCH_3); 4.01 (ddd, 1H, $J_{4,F3}$ = 27.8, $J_{4,5}$ = 10.8, $J_{3,4}$ = 2.1 Hz, H-4); 4.11 (dd, 1H, $J_{4,5}$ = $J_{5,6}$ = 10.8 Hz, H-5); 4.98 (ddd, 1H, $J_{3,F3}$ = 45.5, $J_{3,4}$ = $J_{3,F2}$ = 2.1 Hz, H-3).

^{13}C NMR (125 MHz, CD_3OD) δ 22.69 (NHC(O)$\underline{C}H_3$); 36.34 (C-8); 49.13 (C-5); 53.90 (OCH_3); 59.64 (C-9); 66.41 (C-7); 69.57 (dd, $J_{4,F3}$ = 18.2, $J_{4,F2}$ = 5.5 Hz, C-4); 78.17 (d, $J_{6,F2}$ = 3.4 Hz, C-6); 89.27 (dd, $J_{3,F3}$ = 188.0, $J_{3,F2}$ = 17.6 Hz, C-3); 106.89 (dd, $J_{2,F2}$ = 219.5, $J_{2,F3}$ = 16.8 Hz, C-2); 166.66 (d, $J_{1,F2}$ = 31.4 Hz, C-1); 175.25 (NH$\underline{C}$(O)CH_3). **^{19}F NMR (470 MHz, CD_3OD)** – 122.74 (dd, 1F, $J_{F2,F3}$ = 15.5, $J_{F2,H3}$ = 2.1 Hz, F-2); – 210.26 (ddd, 1F, $J_{F3,H3}$ = 45.2, $J_{F3,H4}$ = 27.8, $J_{F2,F3}$ = 15.5 Hz, F-3). **HRMS (ESI +ve)** *m/z* 328.1199 $[M+H]^+$ ($C_{12}H_{20}F_2N_1O_7$ requires 328.1208).

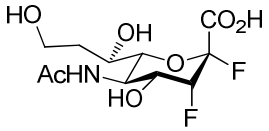

26

5-*N*-Acetyl-2,3,5,8-tetradeoxy-2,3-difluoro-*D*-*erythro*-*β*-*L*-manno-non-2-ulopyranosonic acid (26)

A 0.5M aqueous NaOH solution (0.6 mL) was added to a stirred solution of 8-deoxy-2,3-difluorosialic acid methyl ester (**88**) (82 mg) dissolved in water (1.5 mL) at room temperature and left to stir for 45 minutes. The solution was then neutralised through addition of Dowex 50 Wx8 100 ion exchange resin, H^+ form, filtered, the filtrate concentrated *in vacuo* and purified by silica column chromatography (EtOAc:MeOH 1:1) affording (**26**) as a white solid (17 mg, 22%).

$[\alpha]_D^{25}$ = - 3° (c = 1, H_2O). **m.p.** 76 - 79 °C. **R_f** (EtOAc:MeOH 70:30, 0.1). **^{1}H NMR (400 MHz, D_2O)** δ 1.68 – 1.71 (m, 1H, H-8); 1.86 – 1.91 (m, 1H, H-8'); 1.96 (s, 3H, NHC(O)CH_3); 3.38 (d, 1H, $J_{5,6}$ = 8.6 Hz, H-6); 3.59 – 3.69 (m, 2H, H-9, H-9'); 3.73 – 3.81 (m, 1H, H-7); 4.02 – 4.19 (m, 2H, H-4, H-5); 5.09 (ddd, 1H, $J_{3,F3}$ = 51.6, $J_{3,F2}$ = $J_{3,4}$ = 1.8 H-3). **^{13}C NMR (125 MHz, D_2O)** δ 22.06 (NHC(O)$\underline{C}H_3$); 35.02 (C-8); 47.42 (d, $J_{5,F3}$ = 3.4 Hz, C-5); 58.44 (C-9); 65.26 (C-7); 69.03 (dd, $J_{4,F3}$ = 18.0, $J_{4,F2}$ = 5.8 Hz, C-4); 75.65 (d, $J_{6,F2}$ = 4.2 Hz, C-6); 89.01 (dd, $J_{3,F3}$ =183.4, $J_{3,F2}$ = 18.7 Hz, C-3); 106.77 (dd, $J_{2,F2}$ = 219.6, $J_{2,F3}$ = 14.7 Hz, C-2); 169.48 (d, $J_{1,F2}$ = 23.5 Hz, C-1); 175.10 (NH$\underline{C}$(O)CH_3).

^{19}F NMR (470 MHz, D_2O) – 121.23 (dd, 1F, $J_{F2,F3}$ = 11.8, $J_{F2,H3}$ = 1.8 Hz, F-2); – 217.69 (ddd, 1F, $J_{F3,H3}$ = 51.3, $J_{F3,H4}$ = 28.2, $J_{F2,F3}$ = 11.8 Hz, F-3). **HRMS (ESI -ve)** *m/z* 312.0895 $[M-H]^-$ ($C_{11}H_{16}F_2N_1O_7$ requires 312.0895). **Anal. Calcd. for $C_{11}H_{16}F_2N_1Na_2O_7+H_2O$**: C, 35.12; H, 4.82; N, 3.72. Found: C, 35.50; H, 4.87; N, 3.54.

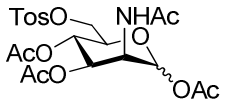

95

2-*N*-acetyl-1,3,4-tri-*O*-acetyl-2-deoxy-6-*O*-*p*-tolylsulfonyl-*D*-mannopyranose (95)

2-*N*-acetyl-*D*-mannosamine (**40**) (8 g, 36.2 mmol) was dissolved in anhydrous pyridine (20 mL) concentrated *in vacuo*, redissolved in anhydrous pyridine (100 mL), cooled to 0 °C and 4-toluenesulfonyl chloride (15.2 g, 79.6 mmol) dissolved in anhydrous pyridine (15 mL) was added over one hour and left to stir at this temperature for 7 hours. Acetic anhydride (11.2 mL, 119.3 mmol) was then added and the mixture was left to stir at room temperature overnight. The solution was concentrated *in vacuo* and residual pyridine removed by azeotropic evaporation with toluene. The crude was then subjected to a standard work up (EtOAc) and purified by silica chromatography (EtOAc:Petroleum Ether 90:10) to give (**95**) as a white solid (8.38 g, 48%).

m.p. 168 - 170 °C (**lit. m.p.** 170 -171 °C). **R_f** (EtOAc, 0.5). **^{1}H NMR (270 MHz, $CDCl_3$)** δ 1.95, 1.96, 2.02 (3s, 9H, $C(O)CCH_3$); 2.10 (s, 3H, $NHC(O)CH_3$); 2.41 (s, 3H, $CH_3Ph(SO_2)O$); 4.05 – 4.09 (m, 2H, H-5, H-6); 4.22 (dd, 1H, $J_{6,6'}$ = 11.3, $J_{5,6'}$ = 2.0 Hz, H-6'); 4.59 (ddd, 1H, $J_{2,NH}$ = 9.3, $J_{2,3}$ = 4.1, $J_{1,2}$ = 1.8 Hz, H-2); 5.18 – 5.30 (m, 2H, H-3, H-4); 5.95 (d, 1H, $J_{1,2}$ = 1.8 Hz, H-1); 6.26 (d, 1H, $J_{2,NH}$ = 9.3 Hz, $NHC(O)CH_3$); 7.31 (d, 2H, $J_{Hb,Hc}$ = 8.5 Hz, H_c-$CH_3Ph(SO_2)O$); 7.74 (d, 2H, $J_{Hb,Hc}$ = 8.5 Hz, H_b-$CH_3Ph(SO_2)O$). Melting point and spectroscopic data were analogous to those reported in the literature.[205]

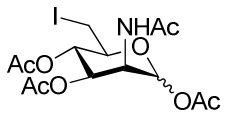

96

2-*N*-acetyl-1,3,4-tri-*O*-acetyl-2,6-dideoxy-6-iodo-*D*-mannopyranose (96)

Potassium iodide (0.34 g, 2.05 mmol) was added to a vigorously stirred solution of *per*-*O*-acetyl-2-*N*-acetyl-6-tosyl-*D*-mannosamine (**95**) (0.5 g, 1.03 mmol) in butanone (15 mL) and heated to 90 °C for 18 hours. The crude mixture was filtered over Celite® and the filtrate was then concentrated *in vacuo*, subjected to a standard work up (EtOAc) and purified by silica chromatography (EtOAc:Toluene 75:25) to give (**96**) as a white solid (235 mg, 50%).

$[\alpha]_D^{23}$ = + 7° (c = 1, CH_2Cl_2). **m.p.** 78 - 80 °C. $\mathbf{R_f}$ (EtOAc:Toluene 90:10, 0.3). **^{1}H NMR (400 MHz, $CDCl_3$)** δ 2.00 (s, 3H, C(O)CCH_3); 2.06 (s, 3H, NHC(O)CH_3); 2.08, 2.17 (2s, 6H, C(O)CCH_3); 3.18 (dd, 1H, $J_{6,6'}$ = 11.2, $J_{5,6}$ = 5.3 Hz, H-6); 3.37 (dd, 1H, $J_{6,6'}$ = 11.2, $J_{5,6'}$ = 3.1 Hz, H-6'); 3.60 – 3.64 (m, 1H, H-5); 4.59 (ddd, 1H, $J_{2,NH}$ = 9.1, $J_{2,3}$ = 4.2, $J_{1,2}$ = 1.9 Hz, H-2); 5.10 (dd, 1H, $J_{4,5}$ = $J_{3,4}$ = 9.8 Hz, H-4); 5.33 (dd, 1H, $J_{3,4}$ = 9.8, $J_{2,3}$ = 4.2 Hz, H-3); 5.78 (d, 1H, $J_{2,NH}$ = 9.1 Hz, NHC(O)CH_3); 6.03 (d, 1H, $J_{1,2}$ = 1.9 Hz, H-1). **^{13}C NMR (100 MHz, $CDCl_3$)** δ 5.74 (C-6); 20.70, 20.72, 20.81 (C(O)$\underline{C}H_3$); 23.30 (NHC(O)$\underline{C}H_3$); 49.12 (C-2); 68.52 (C-3); 69.77 (C-4); 70.50 (C-5); 91.50 (C-1); 168.09 (NH$\underline{C}$(O)CH_3); 169.59, 170.01, 170.08 ($\underline{C}$(O)CH_3). **HRMS (ESI +ve)** *m/z* 480.0120 $[M+H]^+$ ($C_{14}H_{20}I_1N_1Na_1O_8$ requires 480.0131).

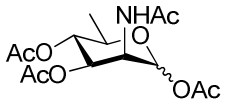

98

2-*N*-acetyl-1,3,4-tri-*O*-acetyl-2,6-dideoxy-*D*-mannopyranose (98)

Per-O-acetyl-2-*N*-acetyl-6-iodo-*D*-mannosamine (**96**) (0.2 g, 0.42 mmol) was dissolved in anhydrous 1,4-dioxane (15 mL) concentrated *in vacuo*, ventilated under argon atmosphere and redissolved in 1,4-dioxane (10 mL). The solution was then degassed and heated to 100 °C. A solution of 1,4-dioxane (5 mL), tributyltin hydride (0.42 mL, 1.56 mmol) and Luperox® 101 (0.1 mL, 0.19 mmol) with molecular sieves was mixed in a flame-dried round-bottom flask. The tributyltin hydride solution was then added to the heated solution over 2 hours with a syringe pump under vigorous stirring and was left to stir at this temperature for further 2 hours. The solution was then cooled to room temperature, concentrated *in vacuo* and purified by silica column chromatography (EtOAc:Petroleum Ether 65:35) to give (**98**) as a white solid (98 mg, 70%).

$[\alpha]_D^{23}$ = + 9° (c = 1, CH_2Cl_2). **m.p.** 71 - 73 °C. **R_f** (EtOAc, 0.3). **^{1}H NMR (400 MHz, $CDCl_3$)** δ 1.22 (d, 3H, $J_{5,6}$ = 6.3 Hz, H-6); 2.00, 2.06, 2.07 (3s, 9H, C(O)CCH_3); 2.16 (s, 3H, NHC(O)CH_3); 3.91 – 3.95 (m, 1H, H-5); 4.61 (ddd, 1H, $J_{2,NH}$ = 9.1, $J_{2,3}$ = 4.3, $J_{1,2}$ = 1.7 Hz, H-2); 4.91 (dd, 1H, $J_{4,5}$ = $J_{3,4}$ = 10.1 Hz, H-4); 5.29 (dd, 1H, $J_{3,4}$ = 10.1, $J_{2,3}$ = 4.3 Hz, H-3); 5.71 (d, 1H, $J_{2,NH}$ = 9.1 Hz, NHC(O)CH_3); 5.96 (d, 1H, $J_{1,2}$ = 1.7 Hz, H-1). **^{13}C NMR (100 MHz, $CDCl_3$)** δ 17.53 (C-6); 20.72, 20.74, 20.87 (C(O)$\underline{C}H_3$); 23.29 (NHC(O)$\underline{C}H_3$); 49.56 (C-2); 68.27 (C-5); 68.78 (C-3); 70.67 (C-4); 91.77 (C-1); 168.40 (NH$\underline{C}$(O)CH_3); 169.98, 170.0, 170.07 ($\underline{C}$(O)CH_3). **HRMS (ESI +ve)** *m/z* 354.1159 $[M+Na]^+$ ($C_{14}H_{21}N_1Na_1O_8$ requires 354.1165). Melting point and spectroscopic data were analogous to those reported in the literature.[206]

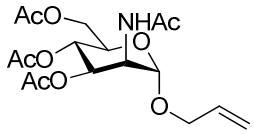

102

Allyl 2-*N*-acetyl-3,4,6-tri-*O*-acetyl-2-deoxy-α-*D*-mannopyranoside (102)

a) 2-*N*-acetyl-*D*-mannosamine (**40**) (0.11 g, 0.52 mmol) was dissolved in anhydrous pyridine (2 mL) concentrated *in vacuo*, redissolved in anhydrous pyridine (4 mL), cooled to 0 °C. Acetic anhydride (0.3 mL, 3.1 mmol) was then added and the mixture was left to stir at room temperature overnight. The solution was concentrated *in vacuo* and residual pyridine removed by azeotropic evaporation with toluene.

b) The crude was then redissolved in anhydrous nitromethane (15 mL) and allyl alcohol (0.35 mL, 5.1 mmol) and $BF_3 \bullet OEt_2$ (130 µL, 1.0 mmol) were added and the solution was heated to 40 °C for 3 hours. The mixture was then cooled, concentrated *in vacuo* and purified by silica chromatography (EtOAc) to give (**102**) as a white solid (71 mg, 36% (over 2 steps)).

R_f (EtOAc, 0.5). **^{1}H NMR (270 MHz, $CDCl_3$)** δ 1.96 (s, 3H, C(O)CH_3); 2.02 (s, 6H, 2C(O)CH_3); 2.04 (s, 3H, NHC(O)CH_3); 3.98 – 4.09 (m, 3H, H-5, OC$\underline{H}_2$CHCH_2); 4.12 (dd, 1H, $J_{6,6'}$ = 11.7, $J_{5,6}$ = 2.3 Hz, H-6); 4.28 (dd, 1H, $J_{6,6'}$ = 11.7, $J_{5,6'}$ = 5.1 Hz, H-6'); 4.61 (ddd, 1H, $J_{2,NH}$ = 9.1, $J_{2,3}$ = 4.4, $J_{1,2}$ = 1.6 Hz, H-2); 4.79 (d, 1H, $J_{1,2}$ = 1.6 Hz, H-1); 5.04 (dd, 1H, $J_{4,5}$ = $J_{3,4}$ = 9.8 Hz, H-4); 5.18 -5.27 (m, 3H, H-3, OCH_2CHC$\underline{H}_2$); 5.76 (d, 1H, $J_{2,NH}$ = 9.1 Hz, NHC(O)CH_3); 5.85 (m, 1H, OCH_2C$\underline{H}$CH_2). Spectroscopic data were analogous to those reported in the literature.[173]

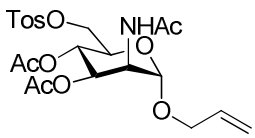

103

Allyl 2-*N*-acetyl-3,4-di-*O*-acetyl-2-deoxy-6-*O*-*p*-tolylsulfonyl-α-*D*-mannopyranoside (103)

a) Allyl-*per*-*O*-acetyl-2-*N*-acetyl-α-*D*-mannopyranoside (**102**) (55 mg, 0.14 mmol) was dissolved in methanol (3 mL) and sodium (1 mg) was then added to the stirred solution at room temperature and left to stir at this temperature for 3 hours. The solution was then neutralised through addition of Dowex 50 Wx8 100 ion exchange resin, H^+ form, filtered and the filtrate concentrated *in vacuo*.

b) The residue was dissolved in anhydrous pyridine (4 mL) concentrated *in vacuo*, redissolved in anhydrous pyridine (5 mL), cooled to 0 °C and 4-toluenesulfonyl chloride (60 mg, 0.32 mmol) dissolved in anhydrous pyridine (1 mL) was added over one hour and left to stir at this temperature for 7 hours. Acetic anhydride (80 µL, 0.85 mmol) was then added and the mixture was left to stir at room temperature overnight. The solution was concentrated *in vacuo* and residual pyridine removed by azeotropic evaporation with toluene. The crude was then subjected to a standard work up (EtOAc) and purified by silica chromatography (EtOAc) to give (**103**) as a white solid (71 mg, 36% (over 3 steps)).

R_f (EtOAc, 0.6). **^{1}H NMR (270 MHz, $CDCl_3$)** δ 1.96 (s, 6H, 2C(O)CCH_3); 2.06 (s, 3H, NHC(O)CH_3); 2.44 (s, 3H, CH_3Ph(SO_2)O); 3.98 – 4.01 (m, 4H, H-5, H-6, OC$\underline{H}_2$CHCH_2); 4.27 (dd, 1H, $J_{6,6'}$ = 11.7, $J_{5,6'}$ = 5.1 Hz, H-6'); 4.61 (ddd, 1H, $J_{2,NH}$ = 9.4, $J_{2,3}$ = 4.2, $J_{1,2}$ = 1.7 Hz, H-2); 4.77 (d, 1H, $J_{1,2}$ = 1.7 Hz, H-1); 5.12 (dd, 1H, $J_{4,5}$ = $J_{3,4}$ = 9.5 Hz, H-4); 5.21 -5.38 (m, 3H, H-3, $OCH_2CHC\underline{H}_2$); 5.85 (m, 1H, $OCH_2C\underline{H}CH_2$); 6.08 (d, 1H, $J_{2,NH}$ = 9.4 Hz, NHC(O)CH_3); 7.34 (d, 2H, $J_{Hb,Hc}$ = 8.4 Hz, H_c-CH_3Ph(SO_2)O); 7.79 (d, 2H, $J_{Hb,Hc}$ = 8.4 Hz, H_b-CH_3Ph(SO_2)O). **HRMS (ESI +ve)** *m/z* 500.1571 $[M+H]^+$ ($C_{22}H_{30}N_1O_{10}S_1$ requires 500.1590). Spectroscopic data were analogous to those reported in the literature.[173]

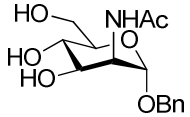

104

Benzyl 2-*N*-acetyl-2-deoxy-α-*D*-mannopyranoside (104)

a) 2-*N*-Acetyl-*D*-mannosamine (**40**) (0.28 g, 1.26 mmol) was dissolved in anhydrous pyridine (4 mL) concentrated *in vacuo*, redissolved in anhydrous pyridine (6 mL), cooled to 0 °C. Acetic anhydride (1.42 mL, 15.1 mmol) was then added and the mixture was left to stir at room temperature overnight. The solution was concentrated *in vacuo* and residual pyridine removed by azeotropic evaporation with toluene.

b) The residue was then redissolved in anhydrous nitromethane (5 mL) and benzyl alcohol (0.4 mL, 3.9 mmol) and $BF_3 \bullet OEt_2$ (20 µL, 0.15 mmol) were added and the solution was heated to 80 °C for 3 hours. The mixture was then cooled, concentrated *in vacuo* and residual $BF_3 \bullet OEt_2$ removed by azeotropic evaporation with toluene.

(c) The crude mixture was redissolved in methanol (2 mL) and sodium (2 mg) was then added to the stirred solution at room temperature and left to stir at this temperature for 1.5 hours. The solution was then neutralised through addition of Dowex 50 Wx8 100 ion exchange resin, H^+ form, filtered, the filtrate concentrated *in vacuo* and purified by silica column chromatography (EtOAc:MeOH 80:20 → EtOAc:MeOH 70:30) to give (**104**) as a white solid (188 mg, 48% (over 3 steps)).

R_f (EtOAc:MeOH, 70:30, 0.3). **^{1}H NMR (270 MHz, $CDCl_3$)** δ 2.01 (s, 3H, NHC(O)CH_3); 3.35 (br s, 1H, OH); 3.61 – 3.66 (m, 2H, H-6, H-6'); 3.90 – 3.95 (m, 1H, H-2); 4.07 (br s, 1H, OH); 4.08 – 4.12 (m, 1H, H-5); 4.30 (br s, 1H, OH); 4.32 – 4.46 (m, 1H, H-4); 4.60 (m, 2H, OC$\underline{H}_2$Ph); 4.77 (m, 1H, H-1); 4.81 (m, 1H, NHC(O)CH_3); 7.25 – 7.40 (m, 5H, OCH_2Ph). **HRMS (ESI +ve)** *m/z* 312.1446 $[M+H]^+$ ($C_{15}H_{22}N_1O_6$ requires 312.1447). Spectroscopic data were analogous to those reported in the literature.[207]

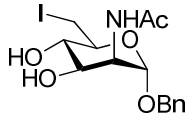

105

Benzyl 2-*N*-acetyl-2,6-dideoxy-6-iodo-α-*D*-mannopyranoside (105)

a) Benzyl 2-*N*-acetyl-α-*D*-mannopyranoside (**104**) (185 mg, 0.59 mmol) was dissolved in anhydrous pyridine (2 mL) concentrated *in vacuo*, redissolved in anhydrous pyridine (3 mL), cooled to 0 °C and 4-toluenesulfonyl chloride (0.19 g, 1.0 mmol) dissolved in anhydrous pyridine (1 mL) was added over 30 minutes and left to stir at this temperature for 3 hours. The mixture was then put to room temperature and left to stir at this temperature for 3 hours. The solution was then concentrated *in vacuo* and residual pyridine removed by azeotropic evaporation with toluene and was subjected to a standard work up (EtOAc)

b) The crude mixture was redissolved in acetone (10 mL) and under vigorous stirring sodium iodide (250 mg, 1.67 mmol) was added. The solution was heated to 50 °C and stirred at this temperature for 32 hours. The reaction mixture was cooled, concentrated *in vacuo,* redissolved in EtOAc, washed with an aqueous saturated sodium thiosulfate solution and followed by washing with brine. The organic phases were then combined and dried over anhydrous magnesium sulfate, filtered and the filtrate concentrated *in vacuo* and purified by silica column chromatography (EtOAc:MeOH 90:10) to give (**105**) as a white solid (168 mg, 52% (over 2 steps)).

$[\alpha]_D^{23}$ = + 10° (c = 1, CH_2Cl_2). **m.p.** 168 - 171 °C. **R_f** (EtOAc:MeOH, 90:10, 0.4). **^{1}H NMR (400 MHz, CD_3OD)** δ 1.98 (s, 3H, NHC(O)CH_3); 3.26 (dd, 1H, $J_{6,6'}$ = 10.4, $J_{5,6}$ = 9.2 Hz, H-6); 3.41 (dd, 1H, $J_{4,5}$ = $J_{3,4}$ = 9.2 Hz, H-4); 3.61 (ddd, 1H, $J_{4,5}$ = $J_{5,6}$ = 9.2, $J_{5,6'}$ = 2.0 Hz, H-5); 3.67 (dd, 1H, $J_{6,6'}$ = 10.4, $J_{5,6'}$ = 2.0 Hz, H-6'); 3.92 (dd, 1H, $J_{3,4}$ = 9.2, $J_{2,3}$ = 4.9 Hz, H-3); 4.28 (dd, 1H, $J_{2,3}$ = 4.9, $J_{1,2}$ = 1.3 Hz, H-2); 4.52 (d, 1H, J = 11.5 Hz, OC$\underline{H}_2$Ph); 4.76 (d, 1H, $J_{1,2}$ = 1.3 Hz, H-1); 4.82 (d, 1H, J = 11.5 Hz, OC$\underline{H}_2$Ph). **^{13}C NMR (100 MHz, CD_3OD)** δ 6.33 (C-6); 22.70 (NHC(O)$\underline{C}H_3$); 54.80 (C-2); 70.19 (O$\underline{C}H_2$Ph); 70.45 (C-3); 72.89 (C-4); 74.62 (C-5); 99.61 (C-1); 129.07 168.09 (C_d-OCH_2Ph); 129.48 ($2C_b$-OCH_2Ph); 129.59 ($2C_c$-OCH_2Ph); 138.72 (C_a-OCH_2Ph); 174.23 (NH$\underline{C}$(O)CH_3). **HRMS (ESI +ve)** *m/z* 422.0453 $[M+H]^+$ ($C_{15}H_{21}I_1N_1O_5$ requires 422.0464).

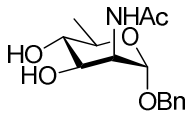

106

Benzyl 2-*N*-acetyl-2,6-dideoxy-6-iodo-α-*D*-mannopyranoside (106)

Benzyl 2-*N*-acetyl-6-iodo-α-*D*-mannopyranoside (**105**) (0.16 g, 0.38 mmol) was dissolved in methanol (3 mL) and water (1.5 mL). The solution was degassed before and after 20% $Pd(OH)_2/C$ (65 mg) was added. A balloon filled with hydrogen gas was put on top of the stirred solution and left to stir for 4 days. The mixture was filtered over Celite® and the filtrate was concentrated *in vacuo*. The crude mixture was then purified by silica column chromatography (EtOAc:MeOH 80:20) affording (**106**) as a colourless oil (73 mg, 65%).

R_f (EtOAc:MeOH, 70:30, 0.8). **^{1}H NMR (270 MHz, CD_3OD)** δ 1.29 (d, 3H, $J_{5,6}$ = 6.3 Hz, H-6); 2.01 (s, 3H, $NHC(O)CH_3$); 3.30 – 3.41 (m, 1H, H-4); 3.58 - 3.63 (m, 1H, H-5); 3.92 (dd, 1H, $J_{3,4}$ = 9.9, $J_{2,3}$ = 4.7 Hz, H-3); 4.32 (d, 1H, $J_{1,2}$ = 1.3 Hz, H-1); 4.28 (d, 1H, $J_{2,3}$ = 4.7 Hz, H-2); 4.55 (d, 1H, *J* = 11.8 Hz, OCH_2Ph); 4.72 (d, 1H, *J* = 11.8 Hz, OCH_2Ph); 7.28 – 7.34 (m, 5H, OCH_2Ph). **HRMS (ESI +ve)** *m/z* 318.1309 $[M+H]^+$ ($C_{15}H_{21}N_1Na_1O_5$ requires 318.1317).

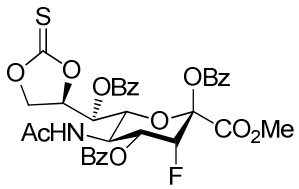

114

Methyl 5-*N*-acetyl-2,4,7-tri-*O*-benzoyl-3,5-dideoxy-3-fluoro-8,9-*O*-carbonothoate-*D*-*erythro*-α-*L*-manno-non-2-ulopyranosonate (114)

a) A solution of 2,4,7-tri-*O*-benzoyl-3-fluoro-8,9-*O*-isopropylidenesialic acid methyl ester (**64**) (3.2 g, 4.55 mmol) in 80% acetic acid/H_2O (275 mL) was stirred at 60 °C for 2 hours.

The crude mixture was then concentrated *in vacuo* and residual acetic acid was removed by azeotropic evaporation with toluene and the residue was then subjected to a standard work up (EtOAc) to give a white solid.

b) The crude was redissolved in anhydrous dichloromethane (250 mL) and 1,1'-thiocarbonyldiimidazole (0.8 g, 4.55 mmol) was added to the stirred solution and heated to 40 °C for 20 hours. The crude mixture was concentrated *in vacuo*, and the procedure was repeated again. The reaction mixture was then concentrated *in vacuo* and purified by silica column chromatography (EtOAc:Petroleum Ether 70:30) affording (**114**) as a white solid (2.58 g, 81%).

$[\alpha]_D^{23}$ = + 6° (c = 1, CH_2Cl_2). **m.p.** 146 - 150 °C. **R_f** (EtOAc:Petroleum Ether 80:20, 0.8). **^{1}H NMR (400 MHz, $CDCl_3$)** δ 1.90 (s, 3H, NHC(O)CH_3); 3.90 (s, 3H, OCH_3); 4.08 – 4.18 (m, 1H, H-5); 4.77 (d, 1H, $J_{5,6}$ = 10.6 Hz, H-6); 4.93 (dd, 1H, $J_{9,9'}$ = $J_{8,9}$ = 9.2 Hz, H-9); 4.99 (dd, 1H, $J_{8,9}$ = $J_{8,9'}$ = 9.2 Hz, H-8); 5.23 – 5.37 (m, 2H, H-3, H-9'); 5.95 – 5.97 (m, 2H, H-7, NHC(O)CH_3); 6.30 (dd, 1H, $J_{4,F3}$ = 25.8, $J_{4,5}$ = 11.3, H-4); 7.43 (t, 2H, $J_{Hb,Hc}$ = 7.8 Hz, H_c-PhC(O)O); 7.51 (t, 2H, $J_{Hb',Hc'}$ = 7.8 Hz, $H_{c'}$-PhC(O)O); 7.56 (t, 2H, $J_{Hb'',Hc'}$ = 7.8 Hz, $H_{c''}$-PhC(O)O); 7.58 (t, 1H, $J_{Hc'',Hd''}$ = 7.4, H_d-PhC(O)O); 7.64 (t, 1H, $J_{Hc'',Hd''}$ = 7.4, $H_{d'}$-PhC(O)O); 7.68 (t, 1H, $J_{Hc'',Hd''}$ = 7.4, $H_{d''}$-PhC(O)O); 8.04 (d, 2H, $J_{Hb,Hc}$ = 7.8 Hz, H_b-PhC(O)O); 8.07 (d, 2H, $J_{Hb',Hc'}$ = 7.8 Hz, $H_{b'}$-PhC(O)O); 8.14 (d, 2H, $J_{Hb'',Hc''}$ = 7.8 Hz, $H_{b''}$-PhC(O)O). **^{13}C NMR (100 MHz, $CDCl_3$)** δ 23.40 (NHC(O)<u>C</u>H_3); 46.43 (C-5); 53.68 (OCH_3); 67.83 (d, $J_{4,F3}$ = 17.6 Hz, C-4); 68.47 (C-7); 70.63 (C-9); 71.45 (C-6); 81.98 (C-8); 86.98 (d, $J_{3,F3}$ = 185.6 Hz, C-3); 95.42 (d, $J_{2,F3}$ = 29.1 Hz, C-2); 127.18 (C_a-PhC(O)O); 128.39 ($C_{a'}$-PhC(O)O); 128.54 ($C_{a''}$-PhC(O)O); 128.61 ($2C_c$-PhC(O)O); 128.83 ($2C_{c'}$-PhC(O)O); 129.05 ($2C_{c''}$-PhC(O)O); 129.97 ($2C_b$-PhC(O)O); 130.05 ($2C_{b'}$-PhC(O)O); 130.39 ($2C_{b''}$-PhC(O)O); 133.82 (C_d-PhC(O)O); 134.07 ($C_{d'}$-PhC(O)O); 134.84 ($C_{d''}$-PhC(O)O); 163.41 (Ph<u>C</u>(O)O); 164.32 (C-1); 165.72 (Ph<u>C'</u>(O)O); 165.84 (Ph<u>C''</u>(O)O); 171.16 (NH<u>C</u>(O)CH_3); 190.81 (OC(S)O). **^{19}F NMR (376 MHz, $CDCl_3$)** – 210.43 (dd, $J_{F3,H3}$ = 48.6, $J_{F3,H4}$ = 26.2 Hz, F-3). **HRMS (ESI +ve)** *m/z* 696.1482 $[M+H]^+$ ($C_{34}H_{31}F_1N_1O_{12}S_1$ requires 696.1531).

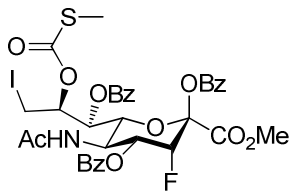

115

Methyl 5-*N*-acetyl-2,4,7-tri-*O*-benzoyl-3,5-dideoxy-3-fluoro-9-iodo-8-*O*-methylthiocarbonyl-*D*-*erythro*-α-*L*-manno-non-2-ulopyranosonate (115)

Iodomethane was freshly distilled prior to use at 60 °C in the dark. 2,4,7-tri-*O*-benzoyl-8,9-*O*-carbonothioate-3-fluorosialic acid methyl ester (**114**) (0.43 g, 0.62 mmol) was dissolved in freshly distilled iodomethane (12 mL) and heated in the dark to 56 °C for 20 hours. The reaction mixture was concentrated *in vacuo* and purified by silica column chromatography (EtOAc:Petroleum Ether 80:20) to give (**115**) as a white solid (490 mg, 95%). $[\alpha]_D^{23}$ = + 1° (c = 1, CH_2Cl_2). **m.p.** 112 - 117 °C. $\mathbf{R_f}$ (EtOAc:Petroleum Ether 80:20, 0.8). **^{1}H NMR (400 MHz, $CDCl_3$)** δ 1.92 (s, 3H, NHC(O)CH_3); 2.02 (s, 3H, CH_3SC(O)O); 3.34 (dd, 1H, $J_{9,9'}$ = 11.5, $J_{8,9}$ = 6.1 Hz, H-9); 3.82 (dd, 1H, $J_{9,9'}$ = 11.5, $J_{8,9'}$ = 3.1 Hz, H-9'); 3.91 (s, 3H, OCH_3); 4.06 – 4.12 (m, 1H, H-5); 4.69 (d, 1H, $J_{5,6}$ = 11.0 Hz, H-6); 5.16 (ddd, 1H, $J_{7,8}$ = $J_{8,9}$ = 6.1, $J_{8,9'}$ = 3.1 Hz, H-8); 5.30 (dd, 1H, $J_{3,F3}$ = 49.2, $J_{3,4}$ = 2.1 Hz, H-3); 5.59 (d, 1H, $J_{7,8}$ = 6.1 Hz, H-7); 5.74 (d, $J_{5,NH}$ = 8.2 Hz, N<u>H</u>C(O)CH_3); 6.34 (ddd, 1H, $J_{4,F3}$ = 27.8, $J_{4,5}$ = 11.3, $J_{3,4}$ = 2.1 Hz H-4); 7.42 (t, 2H, $J_{Hb,Hc}$ = 7.8 Hz, H_c-PhC(O)O); 7.51 (t, 2H, $J_{Hb',Hc'}$ = 7.8 Hz, $H_{c'}$-PhC(O)O); 7.53 (t, 2H, $J_{Hb'',Hc''}$ = 7.8 Hz, $H_{c''}$-PhC(O)O); 7.57 (t, 1H, $J_{Hc'',Hd''}$ = 7.4, H_d-PhC(O)O); 7.62 – 7.67 (m, 2H, $H_{d'}$-PhC(O)O, $H_{d''}$-PhC(O)O); 8.03 (d, 2H, $J_{Hb,Hc}$ = 7.8 Hz, H_b-PhC(O)O); 8.15 (dd, 4H, $J_{Hb',Hc'}$ = $J_{Hb'',Hc''}$ = 7.8 Hz, $H_{b'}$-PhC(O)O, $H_{b''}$-PhC(O)O).

^{13}C NMR (100 MHz, $CDCl_3$) δ 4.11 (C-9); 13.31 ($\underline{C}H_3SC(O)O$); 23.44 ($NHC(O)\underline{C}H_3$); 46.86 (C-5); 53.48 (OCH_3); 68.15 (d, $J_{4,F3}$ = 16.9 Hz, C-4); 70.43 (C-7); 70.66 (C-6); 73.14 (C-8); 87.24 (d, $J_{3,F3}$ = 184.8 Hz, C-3); 95.36 (d, $J_{2,F3}$ = 29.1 Hz, C-2); 128.03 (C_a-PhC(O)O); 128.55 ($2C_c$-PhC(O)O); 128.74 ($2C_{c'}$-PhC(O)O, $2C_{c''}$-PhC(O)O); 128.78 ($C_{a'}$-PhC(O)O); 128.83 ($C_{a''}$-PhC(O)O); 129.96 ($2C_b$-PhC(O)O); 130.17 ($2C_{b'}$-PhC(O)O); 130.33 ($2C_{b''}$-PhC(O)O); 133.70 (C_d-PhC(O)O); 133.84 ($C_{d'}$-PhC(O)O); 134.22 ($C_{d''}$-PhC(O)O); 162.84 (Ph$\underline{C}$(O)O); 164.79 (C-1); 165.80 (Ph$\underline{C'}$(O)O); 165.94 (Ph$\underline{C''}$(O)O); 170.46 ($NH\underline{C}(O)CH_3$); 170.55 ($CH_3S\underline{C}(O)O$). **^{19}F NMR (376 MHz, $CDCl_3$)** – 209.82 (dd, $J_{F3,H3}$ = 48.8, $J_{F3,H4}$ = 27.5 Hz, F-3). **HRMS (ESI +ve)** *m/z* 838.0765 $[M+H]^+$ ($C_{35}H_{34}F_1I_1N_1O_{12}S_1$ requires 838.0803).

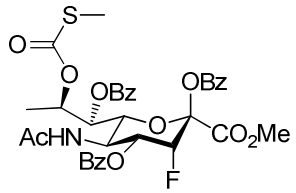

116

Methyl 5-*N*-acetyl-2,4,7-tri-*O*-benzoyl-3,5,9-trideoxy-3-fluoro-8-*O*-methylthiocarbonyl-*D*-*erythro*-*α*-*L*-manno-non-2-ulopyranosonate (116)

In a flame-dried 250 mL round-bottom flask, 2,4,7-tri-*O*-benzoyl-3-fluoro-9-iodo-8-*O*-methylthiocarbonylsialic acid methyl ester (**115**) (3 g, 3.6 mmol) was dissolved in anhydrous 1,4-dioxane (100 mL), concentrated *in vacuo*, ventilated under argon atmosphere, redissolved in anhydrous 1,4-dioxane (150 mL), degassed three times under argon atmosphere and then heated under stirring to 100 °C. In a flame-dried 50 mL round-bottom flask tributyltin hydride (3.55 mL, 13.2 mmol) and Luperox® 101 (0.54 mL, 1.6 mmol) was added to 1,4-dioxane (30 mL) with molecular sieves. The tributyltin hydride solution was then added to the heated solution over 2 hours with a syringe pump under vigorous stirring and was left to stir at this temperature for further 2 hours.

The solution was then cooled to room temperature, concentrated *in vacuo* and purified by silica column chromatography (EtOAc:Petroleum Ether 60:40) to give (**116**) as a white solid (2.5 g, 98%).

$[\alpha]_D^{25}$ = - 2° (c = 1, CH_2Cl_2). **m.p.** 112 - 115 °C. **R_f** (EtOAc:Petroleum Ether 80:20, 0.8). **^{1}H NMR (400 MHz, $CDCl_3$)** δ 1.36 (d, 3H, $J_{8,9}$ = 6.4 Hz, H-9, H-9', H-9''); 1.87 (s, 3H, NHC(O)CH_3); 2.00 (s, 3H, CH_3SC(O)O); 3.89 (s, 3H, OCH_3); 4.21 (ddd, 1H, $J_{5,6}$ = $J_{4,5}$ = 10.8, $J_{5,NH}$ = 9.0 Hz, H-5); 4.59 (d, 1H, $J_{5,6}$ = 10.8 Hz, H-6); 5.26 (dd, 1H, $J_{3,F3}$ = 49.8, $J_{3,4}$ = 2.5 Hz, H-3); 5.34 (dddd, 1H, $J_{8,9}$ = $J_{8,9'}$ = $J_{8,9''}$ = $J_{7,8}$ = 6.4 Hz, H-8); 5.47 (dd, 1H, $J_{7,8}$ = 6.4, $J_{6,7}$ = 1.5 Hz, H-7); 5.58 (d, $J_{5,NH}$ = 9.0 Hz, N<u>H</u>C(O)CH_3); 6.19 (ddd, 1H, $J_{4,F3}$ = 27.8, $J_{4,5}$ = 10.8, $J_{3,4}$ = 2.5 Hz, H-4); 7.40 (t, 2H, $J_{Hb,Hc}$ = 7.8 Hz, H_c-PhC(O)O); 7.47 (t, 2H, $J_{Hb',Hc'}$ = 7.8 Hz, $H_{c'}$-PhC(O)O); 7.50 (t, 2H, $J_{Hb'',Hc''}$ = 7.8 Hz, $H_{c''}$-PhC(O)O); 7.55 (t, 1H, $J_{Hc'',Hd''}$ = 7.4, H_d-PhC(O)O); 7.57 – 7.64 (m, 2H, $H_{d'}$-PhC(O)O, $H_{d''}$-PhC(O)O); 7.99 (d, 2H, $J_{Hb,Hc}$ = 7.8 Hz, H_b-PhC(O)O); 8.11 (dd, 4H, $J_{Hb',Hc'}$ = $J_{Hb'',Hc''}$ = 7.8 Hz, $H_{b'}$-PhC(O)O, $H_{b''}$-PhC(O)O). **^{13}C NMR (100 MHz, $CDCl_3$)** δ 13.48 (<u>C</u>H_3SC(O)O); 23.44 (NHC(O)<u>C</u>H_3); 46.83 (C-5); 53.64 (OCH_3); 68.93 (d, $J_{4,F3}$ = 17.2 Hz, C-4); 71.17 (C-7); 71.35 (C-6); 72.26 (C-8); 87.58 (d, $J_{3,F3}$ = 185.2 Hz, C-3); 95.78 (d, $J_{2,F3}$ = 28.9 Hz, C-2); 128.39 (C_a-PhC(O)O); 128.79 (2C_c-PhC(O)O); 128.86 (2$C_{c'}$-PhC(O)O); 128.92 (2$C_{c''}$-PhC(O)O); 129.07 ($C_{a'}$-PhC(O)O); 129.56 ($C_{a''}$-PhC(O)O); 130.22 (2C_b-PhC(O)O); 130.37 (2$C_{b'}$-PhC(O)O); 130.53 (2$C_{b''}$-PhC(O)O); 133.77 (C_d-PhC(O)O); 133.92 ($C_{d'}$-PhC(O)O); 134.38 ($C_{d''}$-PhC(O)O); 163.03 (Ph<u>C</u>(O)O); 165.22 (C-1); 166.20 (Ph<u>C'</u>(O)O); 166.44 (Ph<u>C''</u>(O)O); 170.43 (NH<u>C</u>(O)CH_3), 170.53 (CH_3S<u>C</u>(O)O).

^{19}F NMR (376 MHz, $CDCl_3$) – 209.32 (dd, $J_{F3,H3}$ = 48.7, $J_{F3,H4}$ = 27.8 Hz, F-3). **HRMS (ESI +ve)** *m/z* 712.1828 $[M+H]^+$ ($C_{35}H_{35}F_1N_1O_{12}S_1$ requires 712.1864).

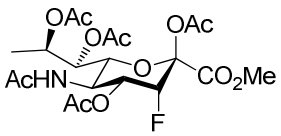

117

Methyl 5-*N*-acetyl-2,4,7,8-tetra-*O*-acetyl-3,5,9-trideoxy-3-fluoro-*D*-*erythro*-α-*L*-manno-non-2-ulopyranosonate (117)

a) To a solution of 2,4,7-tri-*O*-benzoyl-9-deoxy-3-fluoro-8-*O*-methylthiocarbonylsialic acid methyl ester (**116**) (2.5 g, 3.5 mmol) in anhydrous methanol (120 mL) sodium (75 mg) was added at room temperature and left to stir at this temperature for 3 hours. More sodium (75 mg) was then added and left to stir at room temperature overnight. The solution was then neutralised through addition of Dowex 50 Wx8 100 ion exchange resin, H^+ form, filtered and the filtrate concentrated *in vacuo*.

b) The residue was redissolved in anhydrous pyridine (150 mL) and acetic anhydride (4.9 mL, 51.9 mmol) and DMAP (17 mg, 0.14 mmol) were then added at 0 °C and left to stir at room temperature overnight. The solution was concentrated *in vacuo* and residual pyridine removed by azeotropic evaporation with toluene. The crude was then subjected to a standard work up (EtOAc) and purified by silica column chromatography (EtOAc:MeOH 98:2) affording (**117**) as a white solid (1.31 g, 77% over 2 steps).

$[\alpha]_D^{25}$ = - 2° (c = 1, CH_2Cl_2). **m.p.** 192 - 197 °C. **R_f** (EtOAc, 0.4). **^{1}H NMR (400 MHz, $CDCl_3$)** δ 1.27 (d, 3H, $J_{8,9}$ = 6.4 Hz, H-9, H-9', H-9''); 1.89 (s, 3H, NHC(O)CH_3); 1.98, 2.07, 2.15, 2.16 (4s, 12H, C(O)CCH_3); 3.82 (s, 3H, OCH_3); 4.17 (dd, 1H, $J_{5,6}$ = 10.6, $J_{6,7}$ = 1.7 Hz, H-6); 4.24 (ddd, 1H, $J_{5,6}$ = $J_{4,5}$ = 10.6, $J_{5,NH}$ = 9.0 Hz, H-5); 4.90 (dd, 1H, $J_{3,F3}$ = 49.4, $J_{3,4}$ = 1.4 Hz, H-3); 4.96 (dddd, 1H, $J_{8,9}$ = $J_{8,9'}$ = $J_{8,9''}$ = $J_{7,8}$ = 6.4 Hz, H-8); 5.19 (dd, 1H, $J_{7,8}$ = 6.4, $J_{6,7}$ = 1.7 Hz, H-7); 5.27 (d, 1H, $J_{5,NH}$ = 9.0 Hz, N<u>H</u>C(O)CH_3); 5.47 (ddd, 1H, $J_{4,F3}$ = 27.9, $J_{4,5}$ = 10.6, $J_{3,4}$ = 1.4 Hz, H-4). **^{13}C NMR (100 MHz, $CDCl_3$)** δ 15.82 (C-9); 20.77, 20.89, 21.11, 21.33 (C(O)<u>C</u>H_3); 23.51 (NHC(O)<u>C</u>H_3); 45.98 (C-5); 53.66 (OCH_3); 68.86 (d, $J_{4,F3}$ = 17.1 Hz, C-4); 70.44 (C-8); 70.51 (C-7); 72.51 (C-6); 87.29 (d, $J_{3,F3}$ = 185.4 Hz, C-3); 95.52 (d, $J_{2,F3}$ = 28.8 Hz, C-2); 165.28 (C-1); 167.28 (NH<u>C</u>(O)CH_3); 170.37, 170.56, 170.85, 171.23 (<u>C</u>(O)CH_3). **^{19}F NMR (470 MHz, $CDCl_3$)** – 208.54 (dd, $J_{F3,H3}$ = 48.9, $J_{F3,H4}$ = 27.9 Hz, F-3). **HRMS (ESI +ve)** *m/z* 494.1668 $[M+H]^+$ ($C_{20}H_{29}F_1N_1O_{12}$ requires 494.1674).

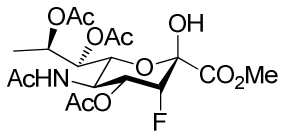

118

Methyl 5-*N*-acetyl-4,7,8-tri-*O*-acetyl-3,5,9-trideoxy-3-fluoro-*D*-*erythro*-α-*L*-manno-non-2-ulopyranosonate (118)

A solution of hydrazine acetate (0.97 g, 10.6 mmol) in anhydrous methanol (20 mL) was cooled to 4 °C and added to a stirred solution of *per*-*O*-acetyl-9-deoxy-3-fluorosialic acid methyl ester (**117**) (1.3 g, 2.6 mmol) in anhydrous dichloromethane (40 mL) at 4 °C and left at this temperature overnight. The mixture was then diluted with dichloromethane (70 mL), subjected to a standard work up and purified by silica column chromatography (EtOAc) affording (**118**) as a white solid (806 mg, 68%).

$[\alpha]_D^{25}$ = + 4.5° (c = 0.67, CH_2Cl_2). **m.p.** 205 - 211 °C. **R_f** (EtOAc, 0.3). **^{1}H NMR (400 MHz, $CDCl_3$)** δ 1.26 (d, 3H, $J_{8,9}$ = 6.3 Hz, H-9, H-9', H-9''); 1.90 (s, 3H, NHC(O)CH_3); 2.04, 2.08, 2.15, (3s, 9H, C(O)CCH_3); 3.85 (s, 3H, OCH_3); 4.24 (dd, 1H, $J_{5,6}$ = 10.4, $J_{6,7}$ = 1.7 Hz, H-6); 4.36 (ddd, 1H, $J_{5,6}$ = $J_{4,5}$ = 10.4, $J_{5,NH}$ = 9.7 Hz, H-5); 4.72 (s, 1H, OH-2); 4.87 (dd, 1H, $J_{3,F3}$ = 50.0, $J_{3,4}$ = 2.4 Hz, H-3); 5.16 (dd, 1H, $J_{7,8}$ = 6.3, $J_{6,7}$ = 1.7 Hz, H-7); 5.20 (dddd, 1H, $J_{8,9}$ = $J_{8,9'}$ = $J_{8,9''}$ = $J_{7,8}$ = 6.3 Hz, H-8); 5.42 (ddd, 1H, $J_{4,F3}$ = 27.8, $J_{4,5}$ = 10.4, $J_{3,4}$ = 2.4 Hz, H-4); 5.55 (d, 1H, $J_{5,NH}$ = 9.7 Hz, N<u>H</u>C(O)CH_3). **^{13}C NMR (100 MHz, $CDCl_3$)** 16.34 (C-9); 20.98, 21.17, 21.58 (C(O)<u>C</u>H_3); 23.44 (NHC(O)<u>C</u>H_3); 45.86 (C-5); 53.71 (OCH_3); 69.87 (d, $J_{4,F3}$ = 17.4 Hz, C-4); 70.21 (C-8); 70.50 (C-7); 70.81 (C-6); 87.16 (d, $J_{3,F3}$ = 186.0 Hz, C-3); 94.42 (d, $J_{2,F3}$ = 25.2 Hz, C-2); 168.02 (C-1); 170.47 (NH<u>C</u>(O)CH_3); 171.13 (2<u>C</u>(O)CH_3); 171.79 (<u>C</u>(O)CH_3). **^{19}F NMR (470 MHz, CD_3Cl_3)** – 207.74 (dd, $J_{F3,H3}$ = 49.7, $J_{F3,H4}$ = 27.8 Hz, F-3). **HRMS (ESI +ve)** *m/z* 474.1384 $[M+Na]^+$ ($C_{18}H_{26}F_1N_1Na_1O_{11}$ requires 474.1388).

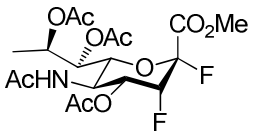

119

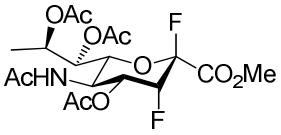

120

Methyl 5-*N*-acetyl-4,7,8-tri-*O*-acetyl-2,3,5,9-tetradeoxy-2,3-difluoro-*D*-*erythro*-*β*-*L*-manno-non-2-ulopyranosonate (119) and Methyl 5-*N*-acetyl-4,7,8-tri-*O*-acetyl-2,3,5,9-tetradeoxy-2,3-difluoro-*D*-*erythro*-*α*-*L*-manno-non-2-ulopyranosonate (120)

(Diethylamino)sulfur trifluoride (0.35 mL, 2.7 mmol) was added drop-wise to a stirred solution of hemiketal (**118**) (0.8 g, 1.8 mmol) in anhydrous dichloromethane (40 mL) at – 40 °C and the temperature was increased to -10 °C during 1 hour. The reaction was then quenched by the addition of methanol (0.2 mL) and saturated $NaHCO_3$ solution (0.2 mL), subjected to a standard work up (CH_2Cl_2) and purified by silica column chromatography (EtOAc:Petroleum Ether 80:20 → EtOAc) to give (**119**) and (**120**).

Data for (**119**): white solid (304 mg, 38%).

$[\alpha]_D^{25}$ = - 4° (c = 1, MeOH). **m.p.** 161 - 164 °C. **R_f** (EtOAc, 0.3) **^{1}H NMR (500 MHz, $CDCl_3$)** δ 1.24 (d, 3H, $J_{8,9}$ = 6.1 Hz, H-9, H-9', H-9''); 1.93 (s, 3H, $NHC(O)CH_3$); 2.06, 2.10, 2.18 (3s, 9H, $C(O)CCH_3$); 3.90 (s, 3H, OCH_3); 4.21 – 4.26 (m, 2H, H-5, H-6); 5.16 (ddd, 1H, $J_{3,F3}$ = 50.7, $J_{3,4}$ = $J_{3,F2}$ = 2.1 Hz, H-3); 5.24 (d, 1H, $J_{7,8}$ = 6.3, H-7); 5.22 (dddd, 1H, $J_{8,9}$ = $J_{8,9'}$ = $J_{8,9''}$ = $J_{7,8}$ = 6.3 Hz, H-8); 5.32 (d, 1H, $J_{5,NH}$ = 8.3 Hz, $N\underline{H}C(O)CH_3$); 5.40 (ddd, 1H, $J_{4,F3}$ = 26.2, $J_{4,5}$ = 10.2, $J_{3,4}$ = 2.1 Hz, H-4). **^{13}C NMR (125 MHz, $CDCl_3$)** 16.58 (C-9); 20.86, 21.06, 21.38 ($C(O)\underline{C}H_3$); 23.50 ($NHC(O)\underline{C}H_3$); 45.78 (d, $J_{5,F3}$ = 4.1 Hz, C-5); 53.96 (OCH_3); 68.42 (C-8); 68.93 (dd, $J_{4,F3}$ = 17.3, $J_{4,F2}$ = 6.1 Hz, C-4); 70.36 (C-7); 72.57 (d, $J_{6,F2}$ = 4.4 Hz, C-6); 85.80 (dd, $J_{3,F3}$ = 194.4, $J_{3,F2}$ = 19.4 Hz, C-3); 104.92 (dd, $J_{2,F2}$ = 225.1, $J_{2,F3}$ = 17.3 Hz, C-2); 164.67 (d, $J_{1,F2}$ = 30.2 Hz, C-1); 170.17 ($NH\underline{C}(O)CH_3$); 170.41, 170.68, 171.07 ($\underline{C}(O)CH_3$).**^{19}F NMR (470 MHz, $CDCl_3$)** – 123.27 (dd, 1F, $J_{F2,F3}$ = 11.3, $J_{F2,H3}$ = 2.1 Hz, F-2); – 216.50 (ddd, 1F, $J_{F3,H3}$ = 50.8, $J_{F3,H4}$ = 26.1, $J_{F2,F3}$ = 11.3 Hz, F-3). **HRMS (ESI +ve)** *m/z* 476.1365 $[M+Na]^+$ ($C_{18}H_{25}F_2N_1Na_1O_{10}$ requires 476.1344).

Data for (**120**): white solid (302 mg, 38%).
$[\alpha]_D^{25}$ = + 1° (c = 1, MeOH). **m.p.** 194 - 197 °C. $\mathbf{R_f}$ (EtOAc, 0.4). **^{1}H NMR (400 MHz, $CDCl_3$)** δ 1.27 (d, 3H, $J_{8,9}$ = 6.2 Hz, H-9, H-9', H-9''); 1.89 (s, 3H, NHC(O)CH_3); 2.00, 2.09, 2.12 (3s, 9H, C(O)CCH_3); 3.86 (s, 3H, OCH_3); 4.28 (dd, 1H, $J_{5,6}$ = 10.8, $J_{6,7}$ = 1.7 Hz, H-6); 4.46 (ddd, 1H, $J_{5,6}$ = $J_{4,5}$ = 10.8, $J_{5,NH}$ = 9.9 Hz, H-5); 5.08 (ddd, 1H, $J_{3,F3}$ = 46.6, $J_{3,4}$ = $J_{3,F2}$ = 2.4 Hz, H-3); 5.12 (dddd, 1H, $J_{8,9}$ = $J_{8,9'}$ = $J_{8,9''}$ = $J_{7,8}$ = 6.2 Hz, H-8); 5.24 (dd, 1H, $J_{7,8}$ = 6.2, $J_{6,7}$ = 1.7 Hz, H-7); 5.32 (ddd, 1H, $J_{4,F3}$ = 27.9, $J_{4,5}$ = 10.8, $J_{3,4}$ = 2.4 Hz, H-4); 5.46 (d, 1H, $J_{5,NH}$ = 9.9 Hz, N<u>H</u>C(O)CH_3). **^{13}C NMR (100 MHz, $CDCl_3$)** 16.39 (C-9); 20.79, 21.05, 21.21 (C(O)<u>C</u>H_3); 23.36 (NHC(O)<u>C</u>H_3); 44.92 (d, $J_{5,F3}$ = 2.2 Hz, C-5); 53.85 (OCH_3); 68.93 (d, $J_{4,F3}$ = 17.2 Hz, C-4); 69.45 (C-8); 70.02 (C-7); 73.22 (d, $J_{6,F2}$ = 3.0 Hz, C-6); 85.07 (dd, $J_{3,F3}$ = 185.0, $J_{3,F2}$ = 43.9 Hz, C-3); 105.37 (dd, $J_{2,F2}$ = 228.5, $J_{2,F3}$ = 28.0 Hz, C-2); 162.98 (d, $J_{1,F2}$ = 26.7 Hz, C-1); 170.31 (NH<u>C</u>(O)CH_3, <u>C</u>(O)CH_3); 170.84, 170.87 (<u>C</u>(O)CH_3). **^{19}F NMR (470 MHz, $CDCl_3$)** – 122.15 (dd, 1F, $J_{F2,F3}$ = 16.6, $J_{F2,H3}$ = 2.4 Hz, F-2); – 206.51 (ddd, 1F, $J_{F3,H3}$ = 46.2, $J_{F3,H4}$ = 27.4, $J_{F2,F3}$ = 16.6 Hz, F-3). **HRMS (ESI +ve)** *m/z* 476.1379 $[M+Na]^+$ ($C_{18}H_{25}F_2N_1Na_1O_{10}$ requires 476.1344).

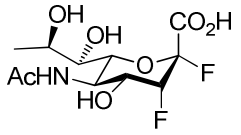

27

5-*N*-acetyl-2,3,5,9-tetradeoxy-2,3-difluoro-*D*-*erythro*-*β*-*L*-manno-non-2-ulopyranosonic acid (27)

a) Sodium (45 mg, 2 mmol) was added to a stirred solution of *per*-*O*-acetyl-9-deoxy-2,3-difluorosialic acid methyl ester (**119**) (0.3 g, 0.6 mmol) in anhydrous methanol (15 mL) at room temperature and was left to stir for 7 hours. The solution was then neutralised through addition of Dowex 50 Wx8 100 ion exchange resin, H^+ form, filtered and the filtrate concentrated *in vacuo*.

b) A 0.5M aqueous NaOH solution (1.2 mL) was added to a stirred solution of the residue redissolved in water (3 mL) at room temperature and left to stir for 3 hours. The solution was then neutralised through addition of Dowex 50 Wx8 100 ion exchange resin, H^+ form, filtered, the filtrate concentrated *in vacuo* and purified by silica column chromatography (EtOAc:MeOH 1:1) affording (**27**) as a white solid (196 mg, 99% over 2 steps).

$[\alpha]_D^{25}$ = - 2° (c = 1, H_2O). **m.p.** 175 - 179 °C. **R_f** (EtOAc:MeOH 50:50, 0.4). **^{1}H NMR (400 MHz, D_2O)** δ 1.32 (d, 3H, $J_{8,9}$ = 6.4 Hz, H-9, H-9', H-9''); 2.10 (s, 3H, NHC(O)CH_3); 3.39 -3.43 (m, 1H, H-7); 3.85 (d, 1H, $J_{5,6}$ = 10.4 Hz, H-6); 4.01 (dddd, 1H, $J_{8,9}$ = $J_{8,9'}$ = $J_{8,9''}$ = $J_{7,8}$ = 6.4 Hz, H-8); 4.32 (ddd, 1H, $J_{4,F3}$ = 28.4, $J_{4,5}$ = 10.4, $J_{3,4}$ = 2.1Hz, H-4); 4.46 (dd, 1H, $J_{5,6}$ = $J_{4,5}$ = 10.4 Hz, H-5); 5.27 (ddd, 1H, $J_{3,F3}$ = 51.4, $J_{3,4}$ = $J_{3,F2}$ = 2.1 Hz, H-3). **^{13}C NMR (100 MHz, D_2O)** δ 18.88 (C-9); 22.12 (NHC(O)$\underline{C}H_3$); 47.10 (d, $J_{5,F3}$ = 3.3 Hz, C-5); 66.75 (C-8); 69.28 (dd, $J_{4,F3}$ = 17.9, $J_{4,F2}$ = 6.1 Hz, C-4); 72.43 (C-7); 72.67 (d, $J_{6,F2}$ = 4.3 Hz, C-6); 89.07 (dd, $J_{3,F3}$ =183.8, $J_{3,F2}$ = 18.6 Hz, C-3); 106.36 (dd, $J_{2,F2}$ = 219.5, $J_{2,F3}$ = 14.8 Hz, C-2); 169.60 (dd, $J_{1,F2}$ = 26.5, $J_{1,F3}$ = 3.6 Hz, C-1); 175.0 (NH$\underline{C}$(O)CH_3). **^{19}F NMR (470 MHz, D_2O)** – 121.34 (dd, 1F, $J_{F2,F3}$ = 11.5, $J_{3,F2}$ = 2.1 Hz, F-2); – 217.92 (dddd, 1F, $J_{F3,H3}$ = 51.3, $J_{F3,H4}$ = 28.7, $J_{F2,F3}$ = 11.5 Hz, F-3). **HRMS (ESI -ve)** *m/z* 312.0881 $[M-H]^-$ ($C_{11}H_{16}F_2N_1O_7$ requires 312.0895). **Anal. Calcd. for $C_{11}H_{16}F_2N_1Na_1O_7$+1/2 H_2O**: C, 38.38; H, 4.98; N, 4.07. Found: C, 37.9; H, 5.28; N, 3.78.

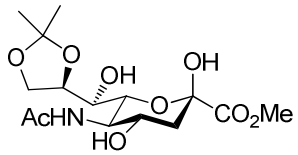

134

Methyl 5-*N*-acetyl-3,5-dideoxy-8,9-*O*-isopropylidene-*D*-*erythro*-*α*-*L*-manno-non-2-ulopyranosonate (134)

a) Trifluoroacetic acid (8 ml, 104.5 mmol) was added to a stirred solution of sialic acid (**2**) (ordered from Carbosynth®) in anhydrous methanol (300 mL) and left at room temperature overnight. The mixture was then concentrated *in vacuo* three times with methanol affording sialic acid methyl ester as a white solid which was used without further purification.

b) A solution of sialic acid methyl ester, *p*-toluenesulfonic acid (0.2 g, 1.1 mmol) and 2,2'-dimethoxypropane (19 mL, 155 mmol) in acetone (300 mL) was stirred at room temperature overnight. Triethylamine (0.7 mL, 5.3 mmol) was then added and the crude mixture was concentrated *in vacuo* and purified by silica column chromatography (EtOAc:MeOH 99:1 → 85:15) to give (**134**) as a white solid (10.46 g, 93%).

m.p. 113 - 116 °C. $\mathbf{R_f}$ (EtOAc:MeOH 80:20, 0.5). **^{1}H NMR (270 MHz, CD_3OD)** δ 1.31 (s, 3H, CCH_3); 1.36 (s, 3H, CCH_3); 1.84 (dd, 1H, $J_{3ax,3eq}$ = $J_{3ax,4}$ = 11.8 Hz, H-3_{ax}); 2.00 (s, 3H, NHC(O)CH_3); 2.21 (dd, 1H, $J_{3ax,3eq}$ = 11.8, $J_{3,4}$ = 4.7 Hz, H-3_{eq}); 3.52 (m, 1H, H-7); 3.77 (s, 3H, OCH_3); 3.75 – 4.05 (m, 6H, H-4, H-5, H-6, H-8, H-9, H-9'). **HRMS (ESI +ve)** *m/z* 364.1606 $[M+H]^+$ ($C_{15}H_{26}N_1O_9$ requires 364.1608). Melting point and spectroscopic data are analogous to those reported in the literature.[153]

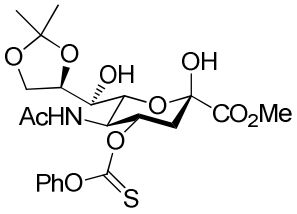

136

Methyl 5-*N*-acetyl-3,5-dideoxy-8,9-*O*-isopropylidene-4-*O*-(phenoxy)thiocarbonyl-*D*-*erythro*-α-*L*-manno-non-2-ulopyranosonate (136)

Phenyl chlorothionoformate (1.2 mL, 9.1 mmol) was added drop-wise to a stirred solution of 8,9-*O*-isopropylidenesialic acid methyl ester (**134**) (3 g, 8.3 mmol) in a mixture of anhydrous dichloromethane (60 mL) and anhydrous pyridine (30 mL) at – 40 ºC and brought to room temperature over 1 hour. The mixture was left to stir at this temperature for further 4 hours.

Methanol (1 mL) was added and after 10 minutes the crude mixture was concentrated *in vacuo*, subjected to a standard work up (CH_2Cl_2) and purified by silica column chromatography (EtOAc:MeOH 99:1) to give (**136**) as an off-white solid (3.27 g, 79%).

m.p. 131 – 135 °C. $\mathbf{R_f}$ (EtOAc:MeOH 90:10, 0.5).

^{1}H NMR (400 MHz, CD_3OD) δ 1.33 (s, 3H, CCH_3); 1.38 (s, 3H, CCH_3); 1.99 (s, 3H, $NHC(O)CH_3$); 2.04 (dd, 1H, $J_{3ax,3eq}$ = $J_{3ax,4}$ = 11.8 Hz, H-3_{ax}); 2.60 (dd, 1H, $J_{3ax,3eq}$ = 11.8, $J_{3eq,4}$ = 5.5 Hz, H-3_{eq}); 3.60 (d, 1H, $J_{5,6}$ = 9.8 Hz, H-6); 3.80 (s, 3H, OCH_3); 4.00 (dd, 1H, $J_{9,9'}$ = 8.6, $J_{8,9}$ = 5.5 Hz, H-9); 4.07 (dd, 1H, $J_{9,9'}$ = $J_{8,9'}$ = 8.6 Hz, H-9'); 4.14 – 4.19 (m, 2H, H-7, H-8); 4.33 (dd, 1H, $J_{4,5}$ = $J_{5,6}$ = 9.8 Hz, H-5); 5.86 (ddd, 1H, $J_{3ax,4}$ = 11.8, $J_{4,5}$ = 9.8, $J_{3eq,4}$ = 5.5 Hz, H-4); 7.07 (d, 2H, $J_{Hb,Hc}$ = 7.6 Hz, H_b-PhOC(S)O); 7.29 (t, 1H, $J_{Hc,Hd}$ = 7.6 Hz, H_d-PhOC(S)O); 7.42 (t, 2H, $J_{Hb,Hc}$ = $J_{Hc,Hd}$ = 7.6 Hz, H_c-PhOC(S)O). **^{13}C NMR (100 MHz, $CDCl_3$)** δ 22.76 ($NHC(O)\underline{C}H_3$); 25.70 ($C\underline{C}H_3$); 27.15 ($C\underline{C}H_3$); 36.87 (OCH_3); 50.94 (C-3); 53.27 (C-5); 67.69 (C-9); 70.63 (C-7); 72.24 (C-6); 76.71 (C-8); 81.15 (C-4); 96.46 (C-2); 110.22 ($\underline{C}CH_3$); 122.93 ($2C_c$-PhOC(S)O); 127.60 (C_d-PhOC(S)O); 130.60 ($2C_b$-PhOC(S)O); 154.87 (C_a-PhOC(S)O); 171.15 (C-1); 173.97 ($NH\underline{C}(O)CH_3$); 195.89 ($PhO\underline{C}(S)O$). **HRMS (ESI +ve)** *m/z* 500.1581 $[M+H]^+$ ($C_{22}H_{30}N_1O_{10}S_1$ requires 500.1590).

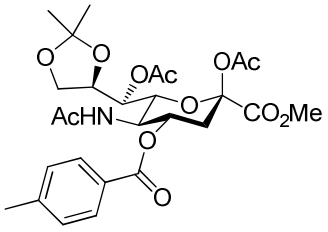

141

Methyl 5-*N*-acetyl-2,7-di-*O*-acetyl-3,5-dideoxy-8,9-*O*-isopropylidene-4-*O*-toluoyl-*D*-*erythro*-α-*L*-manno-non-2-ulopyranosonate (141)

a) *p*-Toluoyl chloride (44 µL, 0.33 mmol) and tetramethylethylenediamine (TMEDA) (50 µL, 0.33 mmol) were added to a stirred solution of 8,9-*O*-isopropylidenesialic acid methyl ester (**134**) (100 mg, 0.3 mmol) in anhydrous dichloromethane (3 mL) at 0 ºC and brought to room temperature over 45 minutes.

After 2 hours the solution was diluted with dichloromethane (3 mL) and subjected to a standard work up (CH_2Cl_2).

b) The residue was redissolved in anhydrous pyridine (2 mL) and acetic anhydride (83 µL, 0.9 mmol) and DMAP (1 mg, 0.01 mmol) were then added at 0 °C and left to stir at room temperature overnight. The crude mixture was then concentrated *in vacuo* and purified by silica column chromatography (EtOAc:Petroleum Ether 8:2) affording (**141**) as a white solid (73 mg, 47% over 2 steps).

m.p. 151 – 154 °C. **R_f** (EtOAc:MeOH 90:10, 0.7). **^{1}H NMR (270 MHz, $CDCl_3$)** δ 1.30 (s, 3H, CCH_3); 1.34 (s, 3H, CCH_3); 1.79 (s, 3H, $NHC(O)CH_3$); 2.03 - 2.07 (m, 1H, H-3_{ax}); 2.14, 2.15 (2s, 6H, $C(O)CCH_3$); 2.38 (s, 3H, $PhCH_3$); 2.63 (dd, 1H, $J_{3ax,3eq}$ = 11.8, $J_{3eq,4}$ = 5.5 Hz, H-3_{eq}); 3.79 (s, 3H, OCH_3); 3.89 – 4.19 (m, 5 H, H-6, H-7, H-8, H-9, H-9'); 5.26 – 5.28 (m, 2H, H-5, $NHC(O)CH_3$); 5.52 (ddd, 1H, $J_{3ax,4}$ = 11.8, $J_{4,5}$ = 9.8, $J_{3eq,4}$ = 5.5 Hz, H-4); 7.22 (d, 2H, $J_{Hb,Hc}$ = 8.7 Hz, H_b-$PhCH_3$); 7.85 (d, 2H, $J_{Hc,Hd}$ = 8.7 Hz, H_c-$PhCH_3$). **HRMS (ESI +ve)** *m/z* 566.2247 $[M+H]^+$ ($C_{27}H_{36}N_1O_{12}$ requires 566.2238).

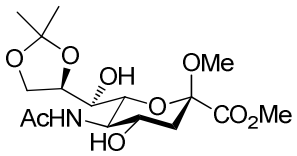

144

Methyl (methyl-5-*N*-acetyl-3,5-dideoxy-8,9-*O*-isopropylidene-*D*-*erythro*-*α*-*L*-manno-non-2-ulopyranos)onate (144)

a) To a stirred solution of sialic acid (**2**) (8 g, 26 mmol) in anhydrous methanol (300 mL) Dowex 50x8 (24 g) was added, heated to 70 °C and left at this temperature overnight. The solution was then filtered, washed with methanol and concentrated *in vacuo* affording sialic acid methyl ester methyl glycoside as an off-white solid which was used without further purification.

b) A solution of sialic acid methyl ester methyl glycoside, *p*-toluenesulfonic acid (172 mg, 0.01 mmol) and 2,2'-dimethoxypropane (16 mL, 155 mmol) in acetone (200 mL) was stirred at room temperature overnight.

Triethylamine (0.6 mL, 5.3 mmol) was then added and the crude mixture was concentrated *in vacuo* and purified by silica column chromatography (EtOAc:MeOH 95:5 → 90:10) to give (**144**) as a white solid (5.2 g, 53% over 2 steps).

m.p. 178 - 182 °C. **R_f** (EtOAc:MeOH 80:20, 0.5). **^{1}H NMR (400 MHz, $CDCl_3$)** δ 1.31 (s, 3H, CCH_3); 1.36 (s, 3H, CCH_3); 1.74 (dd, 1H, $J_{3ax,3eq}$ = $J_{3ax,4}$ = 12.9 Hz, H-3_{ax}); 2.04 (s, 3H, $NHC(O)CH_3$); 2.21 (dd, 1H, $J_{3ax,3eq}$ = 12.9, $J_{3eq,4}$ = 4.9 Hz, H-3_{eq}); 3.24 (s, 3H, OCH_3); 3.44 – 3.49 (m, 1H, H-7); 3.56 (d, 1H, $J_{4,OH}$ = 10.4 Hz, OH-4); 3.79 (s, 3H, $C(O)OCH_3$); 3.75 – 3.81 (m, 2H, H-5, H-9); 3.92 - 4.01(m, 2H, H-6, H-9'); 4.10 (m, 1H, H-4); 4.24 - 4.29 (m, 1H, H-8); 4.60 (d, 1H, $J_{7,OH}$ = 6.1 Hz, OH-7); 6.39 (d, 1H, $J_{5,NH}$ = 8.1 Hz, N<u>H</u>$C(O)CH_3$). Spectroscopic data are analogous to those reported in the literature.[137]

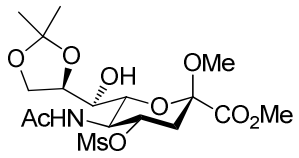

145

Methyl (methyl-5-*N*-acetyl-3,5-dideoxy-8,9-*O*-isopropylidene-4-*O*-methanesulfonyl-*D*-*erythro*-*α*-*L*-manno-non-2-ulopyranos)onate (145)

Methanesulfonyl chloride (68 µL, 0.87 mmol) was added drop-wise over 40 minutes to a stirred solution of 8,9-*O*-isopropylidenesialic acid methyl ester methyl glycoside (**144**) (0.3 g, 0.8 mmol) in anhydrous pyridine (4 mL) at 0 ºC. The mixture was left to stand at this temperature overnight. The crude mixture was then poured on ice-water, extracted with dichloromethane, concentrated *in vacuo* and purified by silica column chromatography (Toluene:EtOAc:EtOH 5:1:1) to give (**145**) as a white solid (171 mg, 47%).

m.p. 128 – 130°C (**lit. m.p.** 129 °C). **R_f** (EtOAc:MeOH 80:20, 0.5).

^{1}H NMR (400 MHz, $CDCl_3$) δ 1.31 (s, 3H, CCH_3); 1.36 (s, 3H, CCH_3); 2.01 – 2.07 (m, 1H, H-3_{ax}); 2.04 (s, 3H, $NHC(O)CH_3$); 2.59 (dd, 1H, $J_{3ax,3eq}$ = 12.1, $J_{3eq,4}$ = 4.8 Hz, H-3_{eq}); 3.05 (s, 3H, OCH_3); 3.30 (s, 3H, $SOCH_3$); 3.44 – 3.49 (m, 2H, H-7, OH-7); 3.64 (d, 1H, $J_{6,7}$ = 7.8 Hz, H-6); 3.79 (s, 3H, $C(O)OCH_3$); 3.98 – 4.08 (m, 2H, H-5, H-9'); 4.10 - 4.15 (m, 1H, H-9'); 4.28 - 4.33 (m, 1H, H-8); 5.07 (ddd, 1H, $J_{3ax,4}$ = 7.8, $J_{4,5}$ = 6.3, $J_{3eq,4}$ = 4.8 Hz, H-4); 6.13 (d, 1H, $J_{5,NH}$ = 8.3 Hz, N<u>H</u>C(O)CH_3). **HRMS (ESI +ve)** *m/z* 456.1524 $[M+H]^+$ ($C_{17}H_{30}N_1O_{11}S_1$ requires 456.1540). Melting point and spectroscopic data are analogous to those reported in the literature.[137]

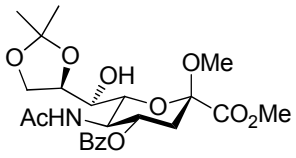

150

Methyl (methyl-5-*N*-acetyl-4-*O*-benzoyl-3,5-dideoxy-8,9-*O*-isopropylidene-*D*-*erythro*-*α*-*L*-manno-non-2-ulopyranos)onate (150)

Benzoyl chloride (0.6 mL, 5.4 mmol) was added drop-wise to a stirred solution of 8,9-O-isopropylidenesialic acid methyl ester methyl glycoside (**144**) (1.9 g, 4.9 mmol) in anhydrous pyridine (45 mL) at 0 ºC for 5 minutes and was then left to stir at this temperature for 35 minutes. Methanol (0.5 mL) was then added, the crude mixture was concentrated *in vacuo*, subjected to a standard work up (CH_2Cl_2) and purified by silica column chromatography (EtOAc:Petroleum Ether 80:20) to give (**150**) as a white solid (1.69 g, 71%).

m.p. 146 – 149 °C. **R_f** (EtOAc:Petroleum Ether 90:10, 0.5).

^{1}H NMR (400 MHz, $CDCl_3$) δ 1.27 (s, 3H, CCH_3); 1.40 (s, 3H, CCH_3); 1.94 (s, 3H, $NHC(O)CH_3$); 2.12 (dd, 1H, $J_{3ax,3eq}$ = 12.8, $J_{3ax,4}$ = 11.5 Hz, H-3_{ax}); 2.54 (dd, 1H, $J_{3ax,3eq}$ = 12.8, $J_{3eq,4}$ = 5.1 Hz, H-3_{eq}); 3.34 (s, 3H, OCH_3); 3.47 – 3.51 (m, 1H, H-7); 3.72 (dd, 1H, $J_{5,6}$ = 10.5, $J_{6,7}$ = 1.4 Hz, H-6); 3.81 (s, 3H, $C(O)OCH_3$); 4.03 (dd, 1H, $J_{9,9'}$ = 10.5, $J_{8,9}$ = 5.3 Hz, H-9); 4.07 - 4.18 (m, 2H, H-5, H-9'); 4.35 - 4.40 (m, 1H, H-8); 4.66 (d, 1H, $J_{7,OH}$ = 4.9 Hz, OH-7); 5.61 (ddd, 1H, $J_{3ax,4}$ = 11.5, $J_{4,5}$ = 6.8, $J_{3eq,4}$ = 5.1 Hz, H-4); 6.21 (d, 1H, $J_{5,NH}$ = 7.8 Hz, N<u>H</u>$C(O)CH_3$); 7.44 (t, 2H, $J_{Hb,Hc}$ = 7.4 Hz, H_c-PhC(O)O); 7.59 (t, 1H, $J_{Hc,Hd}$ = 7.4, H_d-PhC(O)O); 7.99 (d, 2H, $J_{Hb,Hc}$ = 7.4 Hz, H_b-PhC(O)O). Spectroscopic data are analogous to those reported in the literature.[155]

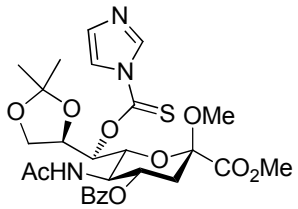

151

Methyl (methyl-5-*N*-acetyl-4-*O*-benzoyl-3,5-dideoxy-8,9-*O*-isopropylidene-7-*O*-(imidazol-1-ylthiocarbonyl)-*D*-*erythro*-*α*-*L*-manno-non-2-ulopyranos)onate (151)

1,1'-Thiocarbonyldiimidazole (0.9 g, 5.1 mmol) was added to a stirred solution of 4-*O*-benzoyl-8,9-*O*-isopropylidenesialic acid methyl ester methyl glycoside (**150**) (0.8 mg, 1.7 mmol) in anhydrous dichloromethane (40 mL) and heated to 40 °C for 48 hours. The crude mixture was then concentrated *in vacuo* and purified by silica column chromatography (EtOAc:Petroleum Ether 90:10) affording (**151**) as a white solid (880 mg, 87%).
m.p. 117 – 121 °C. **R_f** (EtOAc:Petroleum Ether 80:20, 0.6).

^{1}H NMR (400 MHz, $CDCl_3$) δ 1.35 (s, 3H, CCH_3); 1.38 (s, 3H, CCH_3); 1.79 (s, 3H, $NHC(O)CH_3$); 2.02 (dd, 1H, $J_{3ax,3eq}$ = 12.8, $J_{3ax,4}$ = 11.5 Hz, H-3_{ax}); 2.61 (dd, 1H, $J_{3ax,3eq}$ = 12.8, $J_{3eq,4}$ = 5.1 Hz, H-3_{eq}); 3.36 (s, 3H, OCH_3); 3.84 (s, 3H, $C(O)OCH_3$); 4.07 - 4.11 (m, 2H, H-5, H-9); 4.23 (dd, 1H, $J_{9,9'}$ = 9.2, $J_{8,9'}$ = 5.6 Hz, H-9'); 4.29 (dd, 1H, $J_{5,6}$ = 10.9, $J_{6,7}$ = 1.5 Hz, H-6); 4.56 - 4.60 (m, 1H, H-8); 5.33 (d, 1H, $J_{5,NH}$ = 9.7 Hz, $NHC(O)CH_3$); 5.57 (ddd, 1H, $J_{3ax,4}$ = 11.5, $J_{4,5}$ = 6.5, $J_{3eq,4}$ = 5.1 Hz, H-4); 6.05 (dd, 1H, $J_{7,8}$ = 7.1, $J_{6,7}$ = 1.5 Hz, H-7); 7.07 (s, 1H, H_b-ImC(S)O); 7.38 (t, 2H, $J_{Hb,Hc}$ = 7.4 Hz, H_c-PhC(O)O); 7.52 (t, 1H, $J_{Hc,Hd}$ = 7.4, H_d-PhC(O)O); 7.70 (s, 1H, H_e-ImC(S)O); 7.94 (d, 2H, $J_{Hb,Hc}$ = 7.4 Hz, H_b-PhC(O)O); 8.41 (s, 1H, H_d-ImC(S)O). **HRMS (ESI +ve)** *m/z* 592.1963 $[M+H]^+$ ($C_{27}H_{34}N_3O_{10}S_1$ requires 592.1965). Spectroscopic data are analogous to those reported in the literature.[155]

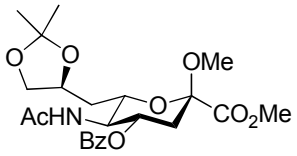

152

Methyl (methyl-5-*N*-acetyl-4-*O*-benzoyl-3,5,7-trideoxy-8,9-*O*-isopropylidene-*D*-*erythro*-*α*-*L*-manno-non-2-ulopyranos)onate (152)

In a flame-dried 250 mL round-bottom flask, 4-*O*-benzoyl-8,9-*O*-isopropylidene-7-*O*-thiocarbamate methyl ester methyl glycoside (**151**) (0.9 g, 1.5 mmol) was dissolved in anhydrous 1,4-dioxane (30 mL), concentrated *in vacuo*, ventilated under argon atmosphere, redissolved in anhydrous 1,4-dioxane (70 mL), degassed three times under argon atmosphere and then heated under stirring to 100 °C. In a flame-dried 25 mL round-bottom flask, tributyltin hydride (1.5 mL, 5.4 mmol) and Luperox® 101 (220 µL, 0.66 mmol) was added to 1,4-dioxane (16 mL) with molecular sieves. The tributyltin hydride solution was then added to the heated solution over 2 hours with a syringe pump under vigorous stirring and was left to stir at this temperature for further 2 hours.

The solution was then cooled to room temperature, concentrated *in vacuo* and purified by silica column chromatography (EtOAc:Petroleum Ether 90:10) to give (**152**) as a white solid (369 mg, 54%).

m.p. 103 – 107 °C. **R_f** (EtOAc, 0.4). **^{1}H NMR (400 MHz, $CDCl_3$)** δ 1.33 (s, 3H, CCH_3); 1.39 (s, 3H, CCH_3); 1.86 (s, 3H, $NHC(O)CH_3$); 1.84 - 2.12 (m, 2H, H-7, H-7'); 2.02 (dd, 1H, $J_{3ax,3eq}$ = 12.8, $J_{3ax,4}$ = 11.5 Hz, H-3_{ax}); 2.54 (dd, 1H, $J_{3ax,3eq}$ = 12.8, $J_{3eq,4}$ = 5.1 Hz, H-3_{eq}); 3.31 (s, 3H, OCH_3); 3.06 (dd, 1H, $J_{9,9'}$ = $J_{8,9}$ = 7.6 Hz, H-9); 3.77 – 3.86 (m, 4H, H-6, $C(O)OCH_3$); 4.07 - 4.15 (m, 2H, H-5, H-9'); 4.31 - 4.36 (m, 1H, H-8); 5.40 (ddd, 1H, $J_{3ax,4}$ = 11.5, $J_{4,5}$ = 6.6, $J_{3eq,4}$ = 5.1 Hz, H-4); 5.53 (d, 1H, $J_{5,NH}$ = 9.4 Hz, N<u>H</u>$C(O)CH_3$); 7.42 (t, 2H, $J_{Hb,Hc}$ = 7.4 Hz, H_c-PhC(O)O); 7.56 (t, 1H, $J_{Hc,Hd}$ = 7.4, H_d-PhC(O)O); 7.98 (d, 2H, $J_{Hb,Hc}$ = 7.4 Hz, H_b-PhC(O)O). **HRMS (ESI +ve)** *m/z* 466.2063 $[M+H]^+$ ($C_{23}H_{32}N_1O_9$ requires 466.2077). Spectroscopic data are analogous to those reported in the literature.[155]

10.3 Biology

Sodium acetate trihydrate (6.8 g, 50 mmol) was dissolved in minimal amounts of milli-q water, adjusted to pH 5.5 with 50 % acetic acid and filled up to 50 mL with milli-q water to give 1 mM NaOAc buffer pH 5.5. Calcium chloride (147 mg, 1 mmol) was dissolved in milli-q water (10 mL) to give 0.1 mM $CaCl_2$. 2′-(4-Methylumbelliferyl) α-*D*-N-acetylneuraminic acid (**121**) (MUNANA) (1 mg, 2 mmol) was dissolved in milli-q water (1 mL) to give 2 mM MUNANA. The G70C H1N9 egg derived neuraminidase 28/01/11 provided by Dr. Jennifer McKimm-Breschkin (Materials Science and Engineering, CSIRO, Australia) 1.4 mg/mL was diluted 1:6000 with BSA 1 mg/mL.

10.3.1 Protocol for the inactivation kinetics of 4-deoxy-2,3-difluorosialic acid (24)

The incubation solutions in a black 96 Greiner Bio-one well plate in duplicate were prepared in the layout shown below (**Figure 38**) following the assay (**Table 14**) with final concentrations of 4-deoxy-2,3-difluorosialic acid (**24**) inactivator in X1 = 200, X2 = 100, X3 = 50, X4 = 25, X5 = 10 nM and control (C).

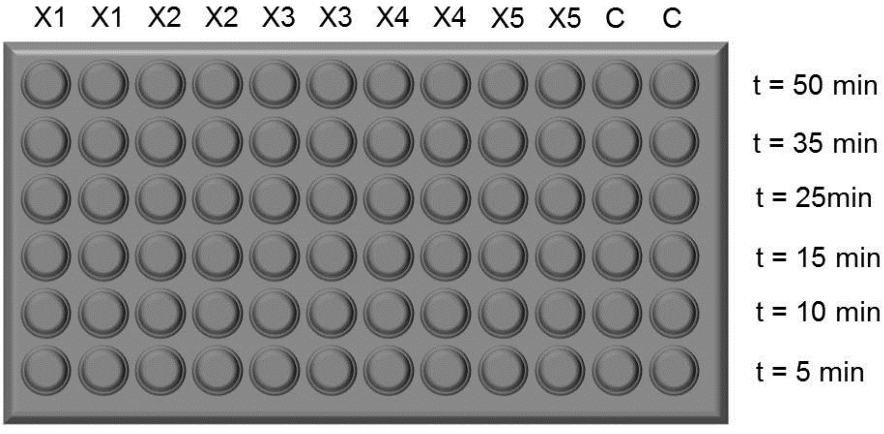

Figure 38 Layout of the 96 Greiner Bio-one well plates for inactivation kinetics.

Table 14 Assay of 4-deoxy-2,3-difluorosialic acid (**24**). (A) 1 mM NaOAc pH 5.5, (B) 0.1 mM $CaCl_2$.

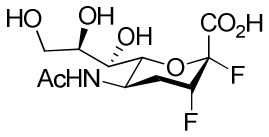

24

200 nM (X1)	100 nM (X2)	50 nM (X3)
10 μL (A)	10 μL (A)	10 μL (A)
10 μL (B)	10 μL (B)	10 μL (B)
10 μL 2 μM (**24**)	10 μL 1 μM (**24**)	10 μL 0.5 μM (**24**)
55 μL H_2O	55 μL H_2O	55 μL H_2O

25 nM (X4)	10 nM (X5)	Control (C)
10 μL (A)	10 μL (A)	10 μL (A)
10 μL (B)	10 μL (B)	10 μL (B)
10 μL 0.25 μM (**24**)	10 μL 0.1 μM (**24**)	
55 μL H_2O	55 μL H_2O	60 μL H_2O

G70C H1N9 egg-derived neuraminidase diluted with BSA 1mg/mL 1:6000 gave high activity, but BSA had to be added in order to minimise activity loss due to neuraminidase being stuck to the plastic tubing of the injector.

At each of the time points 5 µL of diluted G70C H1N9 neuraminidase was injected using pump 1 with an injection speed of 100 µL/sec. Finally, 2 mM MUNANA (10 µL) was injected in all wells using pump 2 with an injection speed of 100 µL/sec and subsequently the plate was shaken with 500 rpm for 15 seconds.

The fluorescence intensity was measured for 30 minutes for each concentration and each time point. The gradients in an interval of 8 to 28 minutes of all concentrations and all time points measured were divided by the gradients of the control and gave the residual activity.

10.3.2 Protocol for the inactivation kinetics of 7-deoxy-2,3-difluorosialic acid (25)

The incubation solutions were made in accordance to the previously developed protocol and the same plate layout was used (**Figure 38**, Chapter 10.3.1) following the assay (**Table 15**) with final concentrations of 7-deoxy-2,3-difluorosialic acid (**25**) inactivator in X1 = 50, X2 = 25, X3 = 10, X4 = 5, X5 = 1 µM and control (C).

Table 15 Assay of 7-deoxy-2,3-difluorosialic acid (**25**). (A) 1 mM NaOAc pH 5.5, (B) 0.1 mM $CaCl_2$.

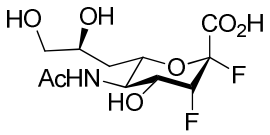

25

50 µM (X1)	25 µM (X2)	10 µM (X3)
10 µL (A)	10 µL (A)	10 µL (A)
10 µL (B)	10 µL (B)	10 µL (B)
10 µL 500 µM (**25**)	10 µL 250 µM (**25**)	10 µL 100 µM (**25**)
55 µL H_2O	55 µL H_2O	55 µL H_2O

5 µM (X4)	1 µM (X5)	Control (C)
10 µL (A)	10 µL (A)	10 µL (A)
10 µL (B)	10 µL (B)	10 µL (B)
10 µL 50 µM (**25**)	10 µL 10 µM (**25**)	
55 µL H_2O	55 µL H_2O	60 µL H_2O

10.3.3 Protocol for the inactivation kinetics of 8-deoxy-2,3-difluorosialic acid (26)

The incubation solutions were made in accordance to the previously developed protocol and the same plate layout was used (**Figure 38**, Chapter 10.3.1) following the assay (**Table 16**) with final concentrations of 8-deoxy-2,3-difluorosialic acid (**26**) inactivator in X1 = 50, X2 = 25, X3 = 10, X4 = 5, X5 = 1 µM and control (C).

Table 16 Assay of 8-deoxy-2,3-difluorosialic acid (**26**). (A) 1 mM NaOAc pH 5.5, (B) 0.1 mM $CaCl_2$.

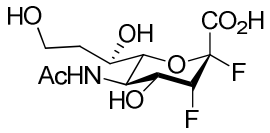

26

50 µM (X1)	25 µM (X2)	10 µM (X3)
10 µL (A)	10 µL (A)	10 µL (A)
10 µL (B)	10 µL (B)	10 µL (B)
10 µL 500 µM (**26**)	10 µL 250 µM (**26**)	10 µL 100 µM (**26**)
55 µL H_2O	55 µL H_2O	55 µL H_2O

5 µM (X4)	1 µM (X5)	Control (C)
10 µL (A)	10 µL (A)	10 µL (A)
10 µL (B)	10 µL (B)	10 µL (B)
10 µL 50 µM (**26**)	10 µL 10 µM (**26**)	
55 µL H_2O	55 µL H_2O	60 µL H_2O

10.3.4 Protocol for the inactivation kinetics of 9-deoxy-2,3-difluorosialic acid (27)

The incubation solutions with final concentrations of 9-deoxy-2,3-difluorosialic acid (**27**) inactivator in X1 = 25, X2 = 10, X3 = 5, X4 = 2, X5 = 1 µM and control (C) were made in compliance to the previously developed protocol and the same plate layout was used (**Figure 38**, Chapter 10.3.1) following the assay (**Table 17**).

Table 17 Assay of 9-deoxy-2,3-difluorosialic acid (**27**). (A) 1 mM NaOAc pH 5.5, (B) 0.1 mM $CaCl_2$.

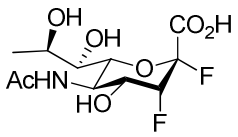

27

25 µM (X1)	10 µM (X2)	5 µM (X3)
10 µL (A)	10 µL (A)	10 µL (A)
10 µL (B)	10 µL (B)	10 µL (B)
10 µL 250 µM (**27**)	10 µL 100 µM (**27**)	10 µL 50 µM (**27**)
55 µL H_2O	55 µL H_2O	55 µL H_2O

2 µM (X4)	1 µM (X5)	Control (C)
10 µL (A)	10 µL (A)	10 µL (A)
10 µL (B)	10 µL (B)	10 µL (B)
10 µL 20 µM (**27**)	10 µL 10 µM (**27**)	
55 µL H_2O	55 µL H_2O	60 µL H_2O

Chapter 11 - References

(1) Varki, A. *Glycobiology* **1992**, *2*, 25.

(2) Zechel, D. L.; Withers, S. G. *Acc. Chem. Res.* **2000**, *33*, 11.

(3) Dharan, N. J.; Gubareva, L. V.; Meyer, J. J.; Okomo-Adhiambo, M.; McClinton, R. C.; Marshall, S. A.; St. George, K.; Epperson, S.; Brammer, L.; Klimov, A.; Bresee, J. S.; Fry, A. M. *JAMA* **2009**, *301*, 1034.

(4) Wang, B.; Dwyer, D. E.; Blyth, C. C.; Soedjono, M.; Shi, H.; Kesson, A.; Ratnamohan, M.; McPhie, K.; Cunningham, A. L.; Saksena, N. K. *Antivir. Res.* **2010**, *87*, 16.

(5) Le Quynh, M.; Wertheim Heiman, F. L.; Tran Nhu, D.; van Doorn, H. R.; Nguyen Tran, H.; Horby, P. *N. Engl. J. Med.* **2010**, *362*, 86.

(6) Fersht, A. R.; Shi, J. P.; Knill-Jones, J.; Lowe, D. M.; Wilkinson, A. J.; Blow, D. M.; Brick, P.; Carter, P.; Waye, M. M.; Winter, G. *Nature* **1985**, *314*, 235.

(7) Street, I. P.; Armstrong, C. R.; Withers, S. G. *Biochemistry* **1986**, *25*, 6021.

(8) Street, I. P.; Rupitz, K.; Withers, S. G. *Biochemistry* **1989**, *28*, 1581.

(9) Withers, S. G.; Street, I. P.; Bird, P.; Dolphin, D. H. *J. Am. Chem. Soc.* **1987**, *109*, 7530.

(10) Withers, S. G.; Rupitz, K.; Street, I. P. *J. Biol. Chem.* **1988**, *263*, 7929.

(11) Watts, A. G.; Damager, I.; Amaya, M. L.; Buschiazzo, A.; Alzari, P.; Frasch, A. C.; Withers, S. G. *J. Am. Chem. Soc.* **2003**, *125*, 7532.

(12) Watts, A. G.; Oppezzo, P.; Withers, S. G.; Alzari, P. M.; Buschiazzo, A. *J. Biol. Chem.* **2006**, *281*, 4149.

(13) Amaya, M. F.; Watts, A. G.; Damager, I.; Wehenkel, A.; Nguyen, T.; Buschiazzo, A.; Paris, G.; Frasch, A. C.; Withers, S. G.; Alzari, P. M. *Structure* **2004**, *12*, 775.

(14) Traving, C.; Schauer, R. *Cell. Mol. Life Sci.* **1998**, *54*, 1330.

(15) Chen, X.; Varki, A. *ACS Chem. Biol.* **2010**, *5*, 163.

(16) Schauer, R. *Zoology* **2004**, *107*, 49.

(17) Hilleman, M. R. *Vaccine* **2002**, *20*, 3068.

(18) Vimr, E.; Lichtensteiger, C. *Trends Microbiol.* **2002**, *10*, 254.

(19) Cantarel, B. L.; Coutinho, P. M.; Rancurel, C.; Bernard, T.; Lombard, V.; Henrissat, B. *Nucleic Acids Res.* **2009**, *37*, D233.

(20) Varghese, J. N.; Laver, W. G.; Colman, P. M. *Nature* **1983**, *303*, 35.

(21) Crennell, S. J.; Garman, E. F.; Laver, W. G.; Vimr, E. R.; Taylor, G. L. *Proc. Natl. Acad. Sci. USA* **1993**, *90*, 9852.

(22) Luo, Y.; Li, S.-C.; Chou, M.-Y.; Li, Y.-T.; Luo, M. *Structure* **1998**, *6*, 521.

(23) *The PyMOL Molecular Graphics System, Version 1.3, Schrödinger, LLC.*

(24) Varghese, J. N.; McKimm-Breschkin, J. L.; Caldwell, J. B.; Kortt, A. A.; Colman, P. M. *Proteins* **1992**, *14*, 327.

(25) Carapito, R.; Imberty, A.; Jeltsch, J.-M.; Byrns, S. C.; Tam, P.-H.; Lowary, T. L.; Varrot, A.; Phalip, V. *J. Biol. Chem.* **2009**, *284*, 12285.

(26) Wolfenden, R.; Lu, X.; Young, G. *J. Am. Chem. Soc.* **1998**, *120*, 6814.

(27) Sinnott, M. L. *Chem. Rev.* **1990**, *90*, 1171.

(28) Davies, G.; Henrissat, B. *Structure* **1995**, *3*, 853.

(29) Withers, S. G. *Carbohydr. Polym.* **2001**, *44*, 325.

(30) Koshland, D. E. *Biol. Rev. Camb. Philos. Soc.* **1953**, *28*, 416.

(31) Phillips, D. C. *Proc. Natl. Acad. Sci. USA* **1967**, *57*, 484.

(32) Heightman, T. D.; Vasella, A. T. *Angew. Chem. Int. Ed.* **1999**, *38*, 750.

(33) Treadway, J. L.; Mendys, P.; Hoover, D. J. *Expert Opin. Invest. Drugs* **2001**, *10*, 439.

(34) Groopman, J. E. *Rev. Infect Dis.* **1990**, *12*, 908.

(35) Zitzmann, N.; Mehta, A. S.; Carrouee, S.; Butters, T. D.; Platt, F. M.; McCauley, J.; Blumberg, B. S.; Dwek, R. A.; Block, T. M. *Proc. Natl. Acad. Sci. USA* **1999**, *96*, 11878.

(36) Laver, W. G.; Bischofberger, N.; Webster, R. G. *Sci. Am.* **1999**, *280*, 78.

(37) Gloster, T. M.; Davies, G. J. *Org. Biomol. Chem.* **2010**, *8*, 305.

(38) Legler, G. *Adv. Carbohydr. Chem. Biochem.* **1990**, *48*, 319.

(39) Mooser, G. *Enzymes* **1992**, *20*, 187.

(40) Copeland, R. A. *Evaluation of Enzyme Inhibitors in Drug Discovery: A Guide to Medicinal Chemists and Pharmacologists*, **2005**; Wiley-Interscience, ISBN-10: 0471686964

(41) Lillelund, V. H.; Jensen, H. H.; Liang, X.; Bols, M. *Chem. Rev.* **2002**, *102*, 515.

(42) Hammond, G. S. *J. Am. Chem. Soc.* **1955**, *77*, 334.

(43) Mobashery, S.; Kotra, L. P. *Handbook of Proteins* **2007**, *1*, 534; John Wiley & Sons, ISBN-13: 978-0-470-06098-8.

(44) Eyring, H. *J. Chem. Phys.* **1935**, *3*, 107.

(45) Fersht, A. *Enzyme Structure and Mechanism*, **1985**; W H Freeman & Co, ISBN-10: 0716716143.

(46) Peters, B. *J. Chem. Theory Comput.* **2010**, *6*, 1447.

(47) Schramm, V. L. *Curr. Opin. Struc. Biol.* **2005**, *15*, 604.

(48) Shan, S.-O.; Herschlag, D. *Method Enzymol.* **1999**, *308*, 246.

(49) Gerlt, J. A.; Kreevoy, M. M.; Cleland, W. W.; Frey, P. A. *Chem. Biol.* **1997**, *4*, 259.

(50) Cleland, W. W.; Kreevoy, M. M. *Science* **1994**, *264*, 1887.

(51) Warshel, A. *Computer Modeling of Chemical Reactions in Enzymes and Solutions*, **1991**; John Wiley & Sons, ISBN-10: 0471533955.

(52) Schramm, V. L. *Annu. Rev. Biochem.* **1998**, *67*, 693.

(53) Asano, N. *Glycobiology* **2003**, *13*, 93R.

(54) Barrett, S.; Mohr, P. G.; Schmidt, P. M.; McKimm-Breschkin, J. L. *PLoS One* **2011**, *6*, e23627.

(55) Rempel, B. P.; Withers, S. G. *Glycobiology* **2008**, *18*, 570.

(56) Withers, S. G.; Aebersold, R. *Protein Sci.* **1995**, *4*, 361.

(57) Sauve, A. A.; Schramm, V. L. *Biochemistry* **2002**, *41*, 8455.

(58) Presti, R. M.; Zhao, G.; Beatty, W. L.; Mihindukulasuriya, K. A.; Travassos da Rosa, A. P. A.; Popov, V. L.; Tesh, R. B.; Virgin, H. W.; Wang, D. *J. Virol.* **2009**, *83*, 11599.

(59) Pinto Da Silva, E. V.; Travassos Da Rosa, A. P. A.; Nunes, M. R. T.; Diniz, J. A. P.; Tesh, R. B.; Cruz, A. C. R.; Vieira, C. M. A.; Vasconcelos, P. F. C. *Am. J. Trop. Med. Hyg.* **2005**, *73*, 1050.

(60) Van Reeth, K. *Vet. Res.* **2007**, *38*, 243.

(61) Suzuki, Y. *Biol. Pharm. Bull.* **2005**, *28*, 399.

(62) Anonymous *Bull. World Health Organ.* **1980**, *58*, 585.

(63) Epstein, S. L.; Price, G. E. *Expert Rev. Vaccines* **2010**, *9*, 1325.

(64) Zambon, M. C. *Rev. Med. Virol.* **2001**, *11*, 227.

(65) Johnson, N. P. A. S.; Mueller, J. *Bull. Hist. Med.* **2002**, *76*, 105.

(66) Das, K.; Aramini, J. M.; Ma, L.-C.; Krug, R. M.; Arnold, E. *Nat. Struct. Mol. Biol.* **2010**, *17*, 530.

(67) Peiris, J. S. M.; Tu, W.-w.; Yen, H.-l. *Eur. J. Immunol.* **2009**, *39*, 2946.

(68) Jordan, D. *Centers for Disease Control and Prevention (CDC), Public Health Image Library (PHIL), ID# 11822, 26/04/2011,* http://www.cdc.gov/h1n1flu/images/3D_Influenza_transparent_key_pieslice_lrg.gif *(This image is in the public domain and thus free of any copyright restrictions)*.

(69) Webster, R. G.; Bean, W. J.; Gorman, O. T.; Chambers, T. M.; Kawaoka, Y. *Microbiol. Rev.* **1992**, *56*, 152.

(70) von Itzstein, M. *Nat. Rev. Drug Discov.* **2007**, *6*, 967.

(71) Hayden, F. G. *N. Engl. J. Med.* **2006**, *354*, 785.

(72) Schiek, W. *Deut. Med. Wochenschr.* **1969**, *94*, 857.

(73) Bright, R. A.; Medina, M.-j.; Xu, X.; Perez-Oronoz, G.; Wallis, T. R.; Davis, X. M.; Povinelli, L.; Cox, N. J.; Klimov, A. I. *Lancet* **2005**, *366*, 1175.

(74) Houck, P.; Hemphill, M.; LaCroix, S.; Hirsh, D.; Cox, N. *Arch. Intern. Med.* **1995**, *155*, 533.

(75) Masuda, H.; Suzuki, H.; Oshitani, H.; Saito, R.; Kawasaki, S.; Nishikawa, M.; Satoh, H. *Microbiol. Immunol.* **2000**, *44*, 833.

(76) Englund, J. A.; Champlin, R. E.; Wyde, P. R.; Kantarjian, H.; Atmar, R. L.; Tarrand, J.; Yousuf, H.; Regnery, H.; Klimov, A. I.; Cox, N. J.; Whimbey, E. *Clin. Infect. Dis.* **1998**, *26*, 1418.

(77) De Clercq, E.; Neyts, J. *Trends Pharmacol. Sci.* **2007**, *28*, 280.

(78) De Clercq, E. *Nat. Rev. Drug Discov.* **2006**, *5*, 1015.

(79) Beigel, J.; Bray, M. *Antivir. Res.* **2008**, *78*, 91.

(80) Furuta, Y.; Takahashi, K.; Kuno-Maekawa, M.; Sangawa, H.; Uehara, S.; Kozaki, K.; Nomura, N.; Egawa, H.; Shiraki, K. *Antimicrob. Agents Chemother.* **2005**, *49*, 981.

(81) Smee, D. F.; Hurst, B. L.; Wong, M.-H.; Bailey, K. W.; Tarbet, E. B.; Morrey, J. D.; Furuta, Y. *Antimicrob. Agents Chemother.* **2010**, *54*, 126.

(82) Lentz, M. R.; Webster, R. G.; Air, G. M. *Biochemistry* **1987**, *26*, 5351.

(83) Wallace, A. C.; Laskowski, R. A.; Thornton, J. M. *Protein Eng.* **1995**, *8*, 127.

(84) Horenstein, B. A.; Bruner, M. *J. Am. Chem. Soc.* **1996**, *118*, 10371.

(85) Chong, A. K. J.; Pegg, M. S.; Taylor, N. R.; Von Itzstein, M. *Eur. J. Biochem.* **1992**, *207*, 335.

(86) Taylor, N. R.; von Itzstein, M. *J. Med. Chem.* **1994**, *37*, 616.

(87) Watts, A. G.; Withers, S. G. *Can. J. Chem.* **2004**, *82*, 1581.

(88) Patrick, G. L. *An Introduction to Medicinal Chemistry; 3rd ed.*, **2005**; Oxford University Press, ISBN-10: 0199275009

(89) Holzer, C. T.; Von Itzstein, M.; Jin, B.; Pegg, M. S.; Stewart, W. P.; Wu, W. Y. *Glycoconjugate J.* **1993**, *10*, 40.

(90) von Itzstein, M.; Wu, W. Y.; Kok, G. B.; Pegg, M. S.; Dyason, J. C.; Jin, B.; Phan, T. V.; Smythe, M. L.; White, H. F.; Oliver, S. W.; Colman, P.M.; Varghese, J.N.; Ryan, D. M.; Woods, J. M.; Bethell, R. C.; Hotham, V. J.; Cameron, J. M.; Penn, C. R. *Nature* **1993**, *363*, 418.

(91) Chavas, L. M. G.; Kato, R.; Suzuki, N.; von Itzstein, M.; Mann, M. C.; Thomson, R. J.; Dyason, J. C.; McKimm-Breschkin, J.; Fusi, P.; Tringali, C.; Venerando, B.; Tettamanti, G.; Monti, E.; Wakatsuki, S. *J. Med. Chem.* **2010**, *53*, 2998.

(92) von Itzstein, M.; Dyason, J. C.; Oliver, S. W.; White, H. F.; Wu, W.-Y.; Kok, G. B.; Pegg, M. S. *J. Med. Chem.* **1996**, *39*, 388.

(93) Gubareva, L. V.; Matrosovich, M. N.; Brenner, M. K.; Bethell, R. C.; Webster, R. G. *J. Infect. Dis.* **1998**, *178*, 1257.

(94) Blick, T. J.; Sahasrabudhe, A.; McDonald, M.; Owens, I. J.; Morley, P. J.; Fenton, R. J.; McKimm-Breschkin, J. L. *Virology* **1998**, *246*, 95.

(95) Staschke, K. A.; Colacino, J. M.; Baxter, A. J.; Air, G. M.; Bansal, A.; Hornback, W. J.; Munroe, J. E.; Laver, W. G. *Virology* **1995**, *214*, 642.

(96) Jones, M.; Del Mar, C. *Expert Opin. Drug Saf.* **2006**, *5*, 603.

(97) Vorwerk, S.; Vasella, A. *Angew. Chem. Int. Ed.* **1998**, *37*, 1732.

(98) Kim, C. U.; Lew, W.; Williams, M. A.; Liu, H.; Zhang, L.; Swaminathan, S.; Bischofberger, N.; Chen, M. S.; Mendel, D. B.; Tai, C. Y.; Laver, W. G.; Stevens, R. C. *J. Am. Chem. Soc.* **1997**, *119*, 681.

(99) Kim, C. U.; Lew, W.; Williams, M. A.; Wu, H.; Zhang, L.; Chen, X.; Escarpe, P. A.; Mendel, D. B.; Laver, W. G.; Stevens, R. C. *J. Med. Chem.* **1998**, *41*, 2451.

(100) Shi, D.; Yang, J.; Yang, D.; LeCluyse, E. L.; Black, C.; You, L.; Akhlaghi, F.; Yan, B. *J. Pharmacol. Exp. Ther.* **2006**, *319*, 1477.

(101) Russell, R. J.; Haire, L. F.; Stevens, D. J.; Collins, P. J.; Lin, Y. P.; Blackburn, G. M.; Hay, A. J.; Gamblin, S. J.; Skehel, J. J. *Nature* **2006**, *443*, 45.

(102) Hurt, A. C.; Holien, J. K.; Parker, M. W.; Barr, I. G. *Drugs* **2009**, *69*, 2523.

(103) Baranovich, T.; Saito, R.; Suzuki, Y.; Zaraket, H.; Dapat, C.; Caperig-Dapat, I.; Oguma, T.; Shabana, I. I.; Saito, T.; Suzuki, H. *J. Clin. Virol.* **2010**, *47*, 23.

(104) Valinotto, L. E.; Diez, R. A.; Barrero, P. R.; Farias, J. A.; Lopez, E. L.; Mistchenko, A. S. *Antiv. Ther.* **2010**, 923.

(105) de Jong, M. D.; Thanh, T. T.; Khanh, T. H.; Hien, V. M.; Smith, G. D.; Chau, N. V.; Cam, B. V.; Qui, P. T.; Ha, D. Q.; Guan, Y.; Peiris, J. S. M.; Phil, D.; Hien, T. T.; Farrar, J. *N. Engl. J. Med.* **2005**, *353*, 2667.

(106) Dulek, D. E.; Williams, J. V.; Creech, C. B.; Schulert, A. K.; Frangoul, H. A.; Domm, J.; Denison, M. R.; Chappell, J. D. *Clin. Infect. Dis.* **2010**, *50*, 1493.

(107) Monto, A. S.; McKimm-Breschkin, J. L.; Macken, C.; Hampson, A. W.; Hay, A.; Klimov, A.; Tashiro, M.; Webster, R. G.; Aymard, M.; Hayden, F. G.; Zambon, M. *Antimicrob. Agents Chemother.* **2006**, *50*, 2395.

(108) Kiso, M.; Mitamura, K.; Sakai-Tagawa, Y.; Shiraishi, K.; Kawakami, C.; Kimura, K.; Hayden, F. G.; Sugaya, N.; Kawaoka, Y. *Lancet* **2004**, *364*, 759.

(109) McKimm-Breschkin, J. L.; Sahasrabudhe, A.; Blick, T. J.; McDonald, M.; Colman, P. M.; Hart, G. J.; Bethell, R. C.; Varghese, J. N. *J. Virol.* **1998**, *72*, 2456.

(110) Gubareva, L. V.; Robinson, M. J.; Bethell, R. C.; Webster, R. G. *J. Virol.* **1997**, *71*, 3385.

(111) Gubareva, L. V.; Bethell, R.; Hart, G. J.; Murti, K. G.; Penn, C. R.; Webster, R. G. *J. Virol.* **1996**, *70*, 1818.

(112) Gubareva, L. V.; Kaiser, L.; Matrosovich, M. N.; Soo-Hoo, Y.; Hayden, F. G. *J. Infect. Dis.* **2001**, *183*, 523.

(113) Sheu, T. G.; Deyde, V. M.; Okomo-Adhiambo, M.; Garten, R. J.; Xu, X.; Bright, R. A.; Butler, E. N.; Wallis, T. R.; Klimov, A. I.; Gubareva, L. V. *Antimicrob. Agents Chemother.* **2008**, *52*, 3284.

(114) McKimm-Breschkin, J. L. *Antivir. Res.* **2000**, *47*, 1.

(115) Ison, M. G.; Gubareva, L. V.; Atmar, R. L.; Treanor, J.; Hayden, F. G. *J. Infect. Dis.* **2006**, *193*, 760.

(116) Sahasrabudhe, A.; Lawrence, L.; Epa, V. C.; Varghese, J. N.; Colman, P. M.; McKimm-Breschkin, J. L. *Virology* **1998**, *247*, 14.

(117) Okomo-Adhiambo, M.; Demmler-Harrison, G. J.; Deyde, V. M.; Sheu, T. G.; Xu, X.; Klimov, A. I.; Gubareva, L. V. *Antimicrob. Agents Chemother.* **2010**, *54*, 1834.

(118) Blick, T. J.; Tiong, T.; Sahasrabudhe, A.; Varghese, J. N.; Colman, P. M.; Hart, G. J.; Bethell, R. C.; McKimm-Breschkin, J. L. *Virology* **1995**, *214*, 475.

(119) McKimm-Breschkin, J.; Sahasrabudhe, A.; Blick, T.; McDonald, M. *Int. Congr. Ser.* **2001**, *1219*, 855.

(120) Matsuzaki, Y.; Mizuta, K.; Aoki, Y.; Suto, A.; Abiko, C.; Sanjoh, K.; Sugawara, K.; Takashita, E.; Itagaki, T.; Katsushima, Y.; Ujike, M.; Obuchi, M.; Odagiri, T.; Tashiro, M. *Virol. J.* **2010**, *7*, 53.

(121) Anonymous *Wkly Epidemiol Rec* **2009**, *84*, 289.

(122) Varghese, J. N.; Smith, P. W.; Sollis, S. L.; Blick, T. J.; Sahasrabudhe, A.; McKimm-Breschin, J. L.; Colman, P. M. *Structure* **1998**, *6*, 735.

(123) Collins, P. J.; Haire, L. F.; Lin, Y. P.; Liu, J.; Russell, R. J.; Walker, P. A.; Skehel, J. J.; Martin, S. R.; Hay, A. J.; Gamblin, S. J. *Nature* **2008**, *453*, 1258.

(124) Bantia, S.; Arnold, C. S.; Parker, C. D.; Upshaw, R.; Chand, P. *Antivir. Res.* **2006**, *69*, 39.

(125) Memoli, M. J.; Hrabal, R. J.; Hassantoufighi, A.; Eichelberger, M. C.; Taubenberger, J. K. *Clin. Infect. Dis.* **2010**, *50*, 1252.

(126) Nguyen, H. T.; Sheu, T. G.; Mishin, V. P.; Klimov, A. I.; Gubareva, L. V. *Antimicrob. Agents Chemother.* **2010**, *54*, 3671.

(127) Baz, M.; Abed, Y.; Boivin, G. *Antivir. Res.* **2007**, *74*, 159.

(128) Smith, B. J.; McKimm-Breshkin, J. L.; McDonald, M.; Fernley, R. T.; Varghese, J. N.; Colman, P. M. *J. Med. Chem.* **2002**, *45*, 2207.

(129) Memoli, M. J.; Hrabal, R. J.; Hassantoufighi, A.; Jagger, B. W.; Sheng, Z.-M.; Eichelberger, M. C.; Taubenberger, J. K. *J. Infect. Dis.* **2010**, *201*, 1397.

(130) van der Vries, E.; Stelma, F. F.; Boucher, C. A. B. *N. Engl. J. Med.* **2010**, *363*, 1381.

(131) MacDonald, S. J. F.; Cameron, R.; Demaine, D. A.; Fenton, R. J.; Foster, G.; Gower, D.; Hamblin, J. N.; Hamilton, S.; Hart, G. J.; Hill, A. P.; Inglis, G. G. A.; Jin, B.; Jones, H. T.; McConnell, D. B.; McKimm-Breschkin, J.; Mills, G.; Nguyen, V.; Owens, I. J.; Parry, N.; Shanahan, S. E.; Smith, D.; Watson, K. G.; Wu, W.-Y.; Tucker, S. P. *J. Med. Chem.* **2005**, *48*, 2964.

(132) Kiso, M.; Shinya, K.; Shimojima, M.; Takano, R.; Takahashi, K.; Katsura, H.; Kakugawa, S.; Le, M. t. Q.; Yamashita, M.; Furuta, Y.; Ozawa, M.; Kawaoka, Y. *PLoS Pathog.* **2010**, e1001079.

(133) Macdonald, S. J. F.; Watson, K. G.; Cameron, R.; Chalmers, D. K.; Demaine, D. A.; Fenton, R. J.; Gower, D.; Hamblin, J. N.; Hamilton, S.; Hart, G. J.; Inglis, G. G. A.; Jin, B.; Jones, H. T.; McConnell, D. B.; Mason, A. M.; Nguyen, V.; Owens, I. J.; Parry, N.; Reece, P. A.; Shanahan, S. E.; Smith, D.; Wu, W.-Y.; Tucker, S. P. *Antimicrob. Agents Chemother.* **2004**, *48*, 4542.

(134) Zürcher, T.; Yates, P. J.; Daly, J.; Sahasrabudhe, A.; Walters, M.; Dash, L.; Tisdale, M.; McKimm-Breschkin, J. L. *J. Antimicrob. Chemother.* **2006**, *58*, 723.

(135) McKimm-Breschkin, J. L.; McDonald, M.; Blick, T. J.; Colman, P. M. *Virology* **1996**, *225*, 240.

(136) Colacino, J. M.; Chirgadze, N. Y.; Garman, E.; Murti, K. G.; Loncharich, R. J.; Baxter, A. J.; Staschke, K. A.; Laver, W. G. *Virology* **1997**, *236*, 66.

(137) Hagedorn, H. W.; Brossmer, R. *Helv. Chim. Acta* **1986**, *69*, 2127.

(138) Baumberger, F.; Vasella, A. *Helv. Chim. Acta* **1986**, *69*, 1535.

(139) Estenne, G.; Saroli, A.; Doutheau, A. *J. Carbohydr. Chem.* **1991**, *10*, 181.

(140) Ooi, H. C.; Marcuccio, S. M.; Jackson, W. R. *Aust. J. Chem.* **1999**, *52*, 937.

(141) Nakajima, T.; Hori, H.; Ohrui, H.; Meguro, H.; Ido, T. *Agr. Biol. Chem.* **1988**, *52*, 1209.

(142) Meindl, P.; Tuppy, H. *Monatsh. Chem.* **1969**, *100*, 1295.

(143) Burkart, M. D.; Zhang, Z.; Hung, S.-C.; Wong, C.-H. *J. Am. Chem. Soc.* **1997**, *119*, 11743.

(144) Vincent, S. P.; Burkart, M. D.; Tsai, C.-Y.; Zhang, Z.; Wong, C.-H. *J. Org. Chem.* **1999**, *64*, 5264.

(145) Schreiner, E.; Zbiral, E.; Kleineidam, R. G.; Schauer, R. *Liebigs Ann. Chem.* **1991**, 129.

(146) Lin, C.-C.; Lin, C.-H.; Wong, C.-H. *Tetrahedron Lett.* **1997**, *38*, 2649.

(147) Gijsen, H. J. M.; Qiao, L.; Fitz, W.; Wong, C.-H. *Chem. Rev.* **1996**, *96*, 443.

(148) Baumann, W.; Freidenreich, J.; Weisshaar, G.; Brossmer, R.; Friebolin, H. *Biol. Chem.* **1989**, *370*, 141.

(149) Beliczey, J.; Kragl, U.; Liese, A.; Wandrey, C.; Hamacher, K.; Coenen, H. H.; Tierling, T.; Method for making fluorinated sugars having a side chain and use thereof: US Patent 6,355,453, March 12, 2002.

(150) Barton, D. H. R.; McCombie, S. W. *J. Chem. Soc. Perkin Trans. 1* **1975**, 1574.

(151) Lopez, R. M.; Hays, D. S.; Fu, G. C. *J. Am. Chem. Soc.* **1997**, *119*, 6949.

(152) Boyer, I. J. *Toxicology* **1989**, *55*, 253.

(153) Ogura, H.; Furuhata, K.; Sato, S.; Anazawa, K.; Itoh, M.; Shitori, Y. *Carbohydr. Res.* **1987**, *167*, 77.

(154) Barton, D. H. R.; Motherwell, W. B.; Stange, A. *Synthesis* **1981**, 743.

(155) Miyazaki, T.; Sato, H.; Sakakibara, T.; Kajihara, Y. *J. Am. Chem. Soc.* **2000**, *122*, 5678.

(156) Barton, D. H. R.; Jang, D. O.; Jaszberenyi, J. C. *Tetrahedron* **1993**, *49*, 7193.

(157) Park, H. S.; Lee, H. Y.; Kim, Y. H. *Org. Lett.* **2005**, *7*, 3187.

(158) Tsuda, Y.; Sato, Y.; Kanemitsu, K.; Hosoi, S.; Shibayama, K.; Nakao, K.; Ishikawa, Y. *Chem. Pharm. Bull.* **1996**, *44*, 1465.

(159) Barton, D. H. R.; Dalko, P. I.; Gero, S. D. *Tetrahedron Lett.* **1992**, *33*, 1883.

(160) Powers, D. H.; Tarbell, D. S. *J. Am. Chem. Soc.* **1956**, *78*, 70.

(161) Anazawa, K.; Furuhata, K.; Ogura, H. *Chem. Pharm. Bull.* **1988**, *36*, 4976.

(162) Excoffier, G.; Gagnare, D.; Utille, J. P. *Carbohydr. Res.* **1975**, *39*, 368.

(163) Dax, K.; Albert, M.; Ortner, J.; Paul, B. J. *Carbohydr. Res.* **2000**, *327*, 47.

(164) Resende, R. *PhD. Thesis*; Universtiy of Bath, 2010.

(165) Zemplén, G.; Pacsu, E. *Ber.* **1929**, *62B*, 1613.

(166) Varki, A.; Diaz, S. *Anal. Biochem.* **1984**, *137*, 236.

(167) Kamerling, J. P.; Schauer, R.; Shukla, A. K.; Stoll, S.; Van Halbeek, H.; Vliegenthart, J. F. G. *Eur. J. Biochem.* **1987**, *162*, 601.

(168) Buchini, S.; Buschiazzo, A.; Withers, S. G. *Angew. Chem. Int. Ed.* **2008**, *47*, 2700.

(169) Saxon, E.; Luchansky, S. J.; Hang, H. C.; Yu, C.; Lee, S. C.; Bertozzi, C. R. *J. Am. Chem. Soc.* **2002**, *124*, 14893.

(170) Horita, Y.; Takii, T.; Chiba, T.; Kuroishi, R.; Maeda, Y.; Kurono, Y.; Inagaki, E.; Nishimura, K.; Yamamoto, Y.; Abe, C.; Mori, M.; Onozaki, K. *Bioorg. Med. Chem. Lett.* **2009**, *19*, 6313.

(171) Yeom, C.-E.; Lee, S. Y.; Kim, Y. J.; Kim, B. M. *Synlett* **2005**, 1527.

(172) Kartha, K. P. R.; Mukhopadhyay, B.; Field, R. A. *Carbohydr. Res.* **2004**, *339*, 729.

(173) Liu, J. L. C.; Shen, G. J.; Ichikawa, Y.; Rutan, J. F.; Zapata, G.; Vann, W. F.; Wong, C. H. *J. Am. Chem. Soc.* **1992**, *114*, 3901.

(174) Garegg, P. J.; Samuelsson, B. *J. Chem. Soc. Chem. Commun.* **1979**, 978.

(175) Garegg, P. J.; Samuelsson, B. *J. Chem. Soc. Perkin Trans. 1* **1980**, 2866.

(176) Garegg, P. J.; Johansson, R.; Ortega, C.; Samuelsson, B. *J. Chem. Soc. Perkin Trans. 1* **1982**, 681.

(177) Schreiner, E.; Christian, R.; Zbiral, E. *Liebigs Ann. Chem.* **1990**, 93.

(178) Wetherall, N. T.; Trivedi, T.; Zeller, J.; Hodges-Savola, C.; McKimm-Breschkin, J. L.; Zambon, M.; Hayden, F. G. *J. Clin. Microbiol.* **2003**, *41*, 742.

(179) Howard, S.; He, S.; Withers, S. G. *J. Biol. Chem.* **1998**, *273*, 2067.

(180) Leatherbarrow, R. J. *GraFit Version 5, Erithacus Software Ltd., Horley, UK*, 2001.

(181) Lineweaver, H.; Burk, D. *J. Am. Chem. Soc.* **1934**, *56*, 658.

(182) Oakley, A. J.; Barrett, S.; Peat, T. S.; Newman, J.; Streltsov, V. A.; Waddington, L.; Saito, T.; Tashiro, M.; McKimm-Breschkin, J. L. *J. Med. Chem.* **2010**, *53*, 6421.

(183) Baum, E. Z.; Wagaman, P. C.; Ly, L.; Turchi, I.; Le, J.; Bucher, D.; Bush, K. *Antivir. Res.* **2003**, *59*, 13.

(184) Kati, W. M.; Saldivar, A. S.; Mohamadi, F.; Sham, H. L.; Laver, W. G.; Kohlbrenner, W. E. *Biochem. Biophys. Res. Commun.* **1998**, *244*, 408.

(185) Pegg, M. S.; von Itzstein, M. *Biochem. Mol. Biol. Int.* **1994**, *32*, 851.

(186) Hart, G. J.; Bethell, R. C. *Biochem. Mol. Biol. Int.* **1995**, *36*, 695.

(187) McKimm-Breschkin, J. L.; Blick, T. J.; Sahasrabudhe, A.; Tiong, T.; Marshall, D.; Hart, G. J.; Bethell, R. C.; Penn, C. R. *Antimicrob. Agents Chemother.* **1996**, *40*, 40.

(188) Hayden, F. G. *Antivir. Res.* **2006**, *71*, 372.

(189) Woods, J. M.; Bethell, R. C.; Coates, J. A.; Healy, N.; Hiscox, S.; Pearson, B. A.; Ryan, D.; Ticehurst, J.; Tilling, J.; Walcott, S. M.; Penn, C. R. *Antimicrob. Agents Chemother.* **1993**, *37*, 1473.

(190) Trampuz, A.; Prabhu, R. M.; Smith, T. F.; Baddour, L. M. *Mayo Clin. Proc.* **2004**, *79*, 523.

(191) Varghese, J. N.; Colman, P. M.; van Donkelaar, A.; Blick, T. J.; Sahasrabudhe, A.; McKimm-Breschkin, J. L. *Proc. Natl. Acad. Sci. USA* **1997**, *94*, 11808.

(192) Burmeister, W. P.; Henrissat, B.; Bosso, C.; Cusack, S.; Ruigrok, R. W. H. *Structure* **1993**, *1*, 19.

(193) Woods, C. J.; King, M. A.; Essex, J. W. *J. Comput.-Aided Mol. Des.* **2001**, *15*, 129.

(194) Varghese, J. N.; Epa, V. C.; Colman, P. M. *Protein Sci.* **1995**, *4*, 1081.

(195) Yang, G.; Yang, Z.; Zu, Y.; Wu, X.; Fu, Y. *Internet Electron. J. Mol. Des.* **2008**, *7*, 97.

(196) Smith, B. J.; Colman, P. M.; Von Itzstein, M.; Danylec, B.; Varghese, J. N. *Protein Sci.* **2001**, *10*, 689.

(197) Koyama, K.; Takahashi, M.; Nakai, N.; Takakusa, H.; Murai, T.; Hoshi, M.; Yamamura, N.; Kobayashi, N.; Okazaki, O. *Xenobiotica* **2010**, *40*, 207.

(198) Andrews, D. M.; Cherry, P. C.; Humber, D. C.; Jones, P. S.; Keeling, S. P.; Martin, P. F.; Shaw, C. D.; Swanson, S. *Eur. J. Med. Chem.* **1999**, *34*, 563.

(199) Engstler, M.; Talhouk, J. W.; Smith, R. E.; Schauer, R. *Anal. Biochem.* **1997**, *250*, 176.

(200) Lam, K.; Markó, I. E. *Org. Lett.* **2008**, *10*, 2773.

(201) Kuhn, R.; Lutz, P.; MacDonald, D. L. *Chem. Ber.* **1966**, *99*, 611.

(202) Indurugalla, D.; Watson, J. N.; Bennet, A. J. *Org. Biomol. Chem.* **2006**, *4*, 4453.

(203) Menger, F. M.; Ladika, M. *J. Am. Chem. Soc.* **1987**, *109*, 3145.

(204) Chandler, M.; Bamford, M. J.; Conroy, R.; Lamont, B.; Patel, B.; Patel, V. K.; Steeples, I. P.; Storer, R.; Weir, N. G.; Wright, M.; Williamson, C. *J. Chem. Soc. Perkin Trans. 1* **1995**, 1173.

(205) Thomson, R.; von Itzstein, M. *Carbohydr. Res.* **1995**, *274*, 29.

(206) Bock, K.; Lundt, I.; Pedersen, C. *Acta Chem. Scand. B* **1987**, *41*, 435.

(207) Halcomb, R. L.; Fitz, W.; Wong, C.-H. *Tetrahedron-Asymmetry* **1994**, *5*, 2437.

Chapter 12 - Appendix

12.1 Crystallographic data for *per*-O-acetyl-4-deoxy-β-2,3-difluorosialic acid methyl ester (57)

Table 18 Crystal data and structure refinement for *per-O*-acetyl-4-deoxy-β-2,3-difluorosialic acid methyl ester (**57**).

Identification code	k08farm4
Empirical formula	C18 H25 F2 N O10
Formula weight	453.39
Temperature	150(2) K
Wavelength	0.71073 Å
Crystal system	Monoclinic
Space group	P21
Unit cell dimensions	a = 8.9500(2)Å $\alpha = 90^{o}$ b = 9.2930(2)Å $\beta = 106.533(1)^{o}$ c = 14.1660(3)Å $\gamma = 90^{o}$
Volume	1129.51(4) $Å^3$
Z	2
Density (calculated)	1.333 Mg/m^3
Absorption coefficient	0.119 mm^{-1}
F(000)	476
Crystal size	0.45 x 0.20 x 0.08 mm
Theta range for data collection	3.92 to 27.49^{o}
Index ranges	-11<=h<=11; -12<=k<=11; -18<=l<=18
Reflections collected	16738
Independent reflections	5040 [R(int) = 0.0415]
Reflections observed (>2σ)	4363
Data Completeness	0.991

Absorption correction	Semi-empirical from equivalents
Max. and min. transmission	0.99 and 0.91
Refinement method	Full-matrix least-squares on F^2
Data / restraints / parameters	5040 / 49 / 333
Goodness-of-fit on F^2	1.039
Final R indices [I>2σ(I)]	R1 = 0.0366 wR2 = 0.0869
R indices (all data)	R1 = 0.0469 wR2 = 0.0928
Absolute structure parameter	0.2(6)
Largest diff. peak and hole	0.209 and -0.146 eÅ^{-3}

Notes: 55:45 disorders modeled for O2, C3, C7, O10 and C18. The ADPs of partial occupancy atoms were refined subject to some restraints. Lattice consists of hydrogen-bonded chains.

Hydrogen bonds with H..A < r(A) + 2.000 Ångstroms and <DHA > 110 deg.

D-H	d(D-H)	d(H..A)	<DHA	d(D..A)	A
N1-H1	0.880	2.011	150.78	2.812	O4 [-x+1, y-1/2, -z]

Table 19 Atomic coordinates (x 10^4) and equivalent isotropic displacement parameters (Å^2 x 10^3) for 1. U(eq) is defined as one third of the trace of the orthogonalised Uij tensor.

Atom	x	y	z	U(eq)
F(1)	8663(1)	6892(1)	3024(1)	45(1)
F(2)	8787(2)	10529(2)	2344(1)	55(1)
O(1)	6697(1)	8486(1)	2849(1)	32(1)
O(2)	10461(9)	8636(8)	4404(6)	84(2)
O(2A)	10472(11)	9346(9)	4261(7)	72(2)
O(3)	8156(14)	9069(9)	4601(8)	61(2)
O(3A)	8235(15)	9557(11)	4455(9)	63(3)
O(4)	3931(2)	10343(1)	-358(1)	33(1)
O(5)	3530(1)	9423(1)	1796(1)	29(1)
O(6)	1361(2)	8746(2)	629(1)	43(1)
O(7)	2283(1)	6580(1)	2549(1)	30(1)
O(8)	3210(2)	4814(2)	1789(1)	42(1)
O(9)	3846(2)	7516(2)	4481(1)	47(1)
O(10)	4525(17)	9515(13)	5361(9)	83(3)
O(10A)	4900(30)	9300(20)	5420(11)	143(8)
N(1)	5261(2)	8273(2)	135(1)	26(1)
C(1)	8280(2)	8354(2)	3016(1)	37(1)
C(2)	8880(2)	9042(2)	2220(2)	41(1)
C(3)	7915(2)	8626(2)	1199(1)	35(1)
C(4)	6171(2)	8786(2)	1090(1)	27(1)
C(5)	5786(2)	7925(2)	1911(1)	25(1)
C(6)	9119(2)	8924(3)	4045(2)	53(1)
C(7)	8804(12)	9516(11)	5618(7)	82(3)
C(7A)	9003(14)	10169(12)	5427(8)	77(3)

C(8)	4229(2)	9089(2)	-522(1)	26(1)
C(9)	3431(2)	8363(2)	-1476(1)	37(1)
C(10)	2132(2)	9668(2)	1127(1)	34(1)
C(11)	1709(3)	11227(2)	1131(2)	45(1)
C(12)	4090(2)	7947(2)	1894(1)	26(1)
C(13)	3816(2)	7242(2)	2811(1)	28(1)
C(14)	2146(2)	5343(2)	2031(1)	32(1)
C(15)	534(2)	4748(2)	1793(2)	44(1)
C(16)	3844(2)	8317(2)	3621(1)	35(1)
C(17)	4316(4)	8217(3)	5332(2)	70(1)
C(18)	3969(9)	7295(13)	6143(7)	71(2)
C(18A)	4698(12)	7246(12)	6222(8)	67(2)

Table 20 Bond lengths [Å] and angles [°] for *per-O*-acetyl-4-deoxy-β-2,3-difluorosialic acid methyl ester (**57**).

F(1)-C(1)	1.400(2)	F(2)-C(2)	1.398(2)
O(1)-C(1)	1.375(2)	O(1)-C(5)	1.4449(19)
O(2)-C(6)	1.193(8)	O(2A)-C(6)	1.226(9)
O(3)-C(6)	1.329(12)	O(3)-C(7)	1.452(14)
O(3A)-C(6)	1.252(13)	O(3A)-C(7A)	1.468(17)
O(4)-C(8)	1.232(2)	O(5)-C(10)	1.357(2)
O(5)-C(12)	1.4527(19)	O(6)-C(10)	1.196(2)
O(7)-C(14)	1.351(2)	O(7)-C(13)	1.452(2)
O(8)-C(14)	1.205(2)	O(9)-C(17)	1.329(3)
O(9)-C(16)	1.428(2)	O(10)-C(17)	1.219(13)
O(10A)-C(17)	1.119(17)	N(1)-C(8)	1.344(2)
N(1)-C(4)	1.447(2)	N(1)-H(1)	0.8800
C(1)-C(2)	1.520(3)	C(1)-C(6)	1.532(3)
C(2)-C(3)	1.509(3)	C(2)-H(2)	1.0000
C(3)-C(4)	1.532(2)	C(3)-H(3A)	0.9900
C(3)-H(3B)	0.9900	C(4)-C(5)	1.529(2)
C(4)-H(4)	1.0000	C(5)-C(12)	1.512(2)
C(5)-H(5)	1.0000	C(7)-H(7A1)	0.9800
C(7)-H(7A2)	0.9800	C(7)-H(7A3)	0.9800
C(7A)-H(7A)	0.9800	C(7A)-H(7B)	0.9800
C(7A)-H(7C)	0.9800	C(8)-C(9)	1.498(2)
C(9)-H(9A)	0.9800	C(9)-H(9B)	0.9800
C(9)-H(9C)	0.9800	C(10)-C(11)	1.497(3)
C(11)-H(11A)	0.9800	C(11)-H(11B)	0.9800
C(11)-H(11C)	0.9800	C(12)-C(13)	1.536(2)
C(12)-H(12)	1.0000	C(13)-C(16)	1.515(2)
C(13)-H(13)	1.0000	C(14)-C(15)	1.492(3)
C(15)-H(15A)	0.9800	C(15)-H(15B)	0.9800

C(15)-H(15C)	0.9800	C(16)-H(16A)	0.9900
C(16)-H(16B)	0.9900	C(17)-C(18A)	1.508(12)
C(17)-C(18)	1.534(10)	C(18)-H(18A)	0.9800
C(18)-H(18B)	0.9800	C(18)-H(18C)	0.9800
C(18A)-H(18D)	0.9800	C(18A)-H(18E)	0.9800
C(18A)-H(18F)	0.9800		
C(1)-O(1)-C(5)	114.21(12)	C(6)-O(3)-C(7)	118.2(9)
C(6)-O(3A)-C(7A)	115.3(11)	C(10)-O(5)-C(12)	116.74(13)
C(14)-O(7)-C(13)	115.62(13)	C(17)-O(9)-C(16)	116.23(19)
C(8)-N(1)-C(4)	123.71(14)	C(8)-N(1)-H(1)	118.1
C(4)-N(1)-H(1)	118.1	O(1)-C(1)-F(1)	109.01(16)
O(1)-C(1)-C(2)	113.54(15)	F(1)-C(1)-C(2)	106.07(14)
O(1)-C(1)-C(6)	109.56(15)	F(1)-C(1)-C(6)	105.97(16)
C(2)-C(1)-C(6)	112.30(18)	F(2)-C(2)-C(3)	109.55(17)
F(2)-C(2)-C(1)	106.03(16)	C(3)-C(2)-C(1)	112.13(16)
F(2)-C(2)-H(2)	109.7	C(3)-C(2)-H(2)	109.7
C(1)-C(2)-H(2)	109.7	C(2)-C(3)-C(4)	111.11(15)
C(2)-C(3)-H(3A)	109.4	C(4)-C(3)-H(3A)	109.4
C(2)-C(3)-H(3B)	109.4	C(4)-C(3)-H(3B)	109.4
H(3A)-C(3)-H(3B)	108.0	N(1)-C(4)-C(5)	110.48(13)
N(1)-C(4)-C(3)	110.37(14)	C(5)-C(4)-C(3)	108.48(14)
N(1)-C(4)-H(4)	109.2	C(5)-C(4)-H(4)	109.2
C(3)-C(4)-H(4)	109.2	O(1)-C(5)-C(12)	108.10(12)
O(1)-C(5)-C(4)	108.69(13)	C(12)-C(5)-C(4)	115.08(13)
O(1)-C(5)-H(5)	108.3	C(12)-C(5)-H(5)	108.3
C(4)-C(5)-H(5)	108.3	O(2)-C(6)-O(2A)	33.2(5)
O(2)-C(6)-O(3A)	126.9(7)	O(2A)-C(6)-O(3A)	116.3(7)
O(2)-C(6)-O(3)	121.0(7)	O(2A)-C(6)-O(3)	125.5(7)
O(3A)-C(6)-O(3)	22.6(7)	O(2)-C(6)-C(1)	119.2(4)
O(2A)-C(6)-C(1)	122.0(5)	O(3A)-C(6)-C(1)	113.6(6)
O(3)-C(6)-C(1)	111.9(5)	O(3A)-C(7A)-H(7A)	109.5
O(3A)-C(7A)-H(7B)	109.5	H(7A)-C(7A)-H(7B)	109.5
O(3A)-C(7A)-H(7C)	109.5	H(7A)-C(7A)-H(7C)	109.5
H(7B)-C(7A)-H(7C)	109.5	O(4)-C(8)-N(1)	123.06(16)
O(4)-C(8)-C(9)	121.58(16)	N(1)-C(8)-C(9)	115.36(15)
C(8)-C(9)-H(9A)	109.5	C(8)-C(9)-H(9B)	109.5
H(9A)-C(9)-H(9B)	109.5	C(8)-C(9)-H(9C)	109.5
H(9A)-C(9)-H(9C)	109.5	H(9B)-C(9)-H(9C)	109.5
O(6)-C(10)-O(5)	123.64(17)	O(6)-C(10)-C(11)	126.22(18)
O(5)-C(10)-C(11)	110.13(17)	C(10)-C(11)-H(11A)	109.5
C(10)-C(11)-H(11B)	109.5	H(11A)-C(11)-H(11B)	109.5
C(10)-C(11)-H(11C)	109.5	H(11A)-C(11)-H(11C)	109.5
H(11B)-C(11)-H(11C)	109.5	O(5)-C(12)-C(5)	109.34(12)
O(5)-C(12)-C(13)	110.50(13)	C(5)-C(12)-C(13)	112.48(13)
O(5)-C(12)-H(12)	108.1	C(5)-C(12)-H(12)	108.1
C(13)-C(12)-H(12)	108.1	O(7)-C(13)-C(16)	106.50(13)
O(7)-C(13)-C(12)	109.34(13)	C(16)-C(13)-C(12)	112.75(14)
O(7)-C(13)-H(13)	109.4	C(16)-C(13)-H(13)	109.4
C(12)-C(13)-H(13)	109.4	O(8)-C(14)-O(7)	123.04(16)
O(8)-C(14)-C(15)	125.24(17)	O(7)-C(14)-C(15)	111.71(15)

C(14)-C(15)-H(15A)	109.5	C(14)-C(15)-H(15B)	109.5
H(15A)-C(15)-H(15B)	109.5	C(14)-C(15)-H(15C)	109.5
H(15A)-C(15)-H(15C)	109.5	H(15B)-C(15)-H(15C)	109.5
O(9)-C(16)-C(13)	107.35(15)	O(9)-C(16)-H(16A)	110.2
C(13)-C(16)-H(16A)	110.2	O(9)-C(16)-H(16B)	110.2
C(13)-C(16)-H(16B)	110.2	H(16A)-C(16)-H(16B)	108.5
O(10A)-C(17)-O(10)	17.9(18)	O(10A)-C(17)-O(9)	123.8(8)
O(10)-C(17)-O(9)	121.4(6)	O(10A)-C(17)-C(18A)	117.1(10)
O(10)-C(17)-C(18A)	124.6(7)	O(9)-C(17)-C(18A)	113.7(4)
O(10A)-C(17)-C(18)	127.1(9)	O(10)-C(17)-C(18)	126.2(7)
O(9)-C(17)-C(18)	109.0(5)	C(18A)-C(17)-C(18)	24.0(4)
C(17)-C(18)-H(18A)	109.5	C(17)-C(18)-H(18B)	109.5
C(17)-C(18)-H(18C)	109.5	C(17)-C(18A)-H(18D)	109.5
C(17)-C(18A)-H(18E)	109.5	H(18D)-C(18A)-H(18E)	109.5
C(17)-C(18A)-H(18F)	109.5	H(18D)-C(18A)-H(18F)	109.5
H(18E)-C(18A)-H(18F)	109.5		

Symmetry transformations used to generate equivalent atoms.

Table 21 Anisotropic displacement parameters ($Å^2$ x 10^3) for *per-O*-acetyl-4-deoxy-β-2,3-difluorosialic acid methyl ester (**57**). The anisotropic displacement factor exponent takes the form: $-2\ gpi^2\ [\ h^2\ a^{*2}\ U11 + ... + 2\ h\ k\ a^*\ b^*\ U$.

Atom	U11	U22	U33	U23	U13	U12
F(1)	45(1)	50(1)	36(1)	1(1)	6(1)	23(1)
F(2)	47(1)	45(1)	69(1)	-12(1)	9(1)	-12(1)
O(1)	26(1)	39(1)	27(1)	-9(1)	4(1)	5(1)
O(2)	44(2)	131(5)	61(3)	-40(4)	-11(2)	17(4)
O(2A)	32(2)	113(6)	60(3)	-26(4)	-2(2)	-6(4)
O(3)	52(3)	89(5)	38(3)	-27(3)	4(2)	-3(4)
O(3A)	49(4)	86(6)	44(4)	-38(4)	-3(3)	26(4)
O(4)	40(1)	22(1)	37(1)	3(1)	10(1)	2(1)
O(5)	29(1)	24(1)	33(1)	1(1)	10(1)	5(1)
O(6)	31(1)	45(1)	48(1)	9(1)	2(1)	-2(1)
O(7)	33(1)	25(1)	33(1)	-3(1)	14(1)	-2(1)
O(8)	42(1)	33(1)	56(1)	-10(1)	22(1)	0(1)
O(9)	68(1)	44(1)	30(1)	-1(1)	18(1)	-2(1)
O(10)	157(6)	52(4)	55(5)	-16(2)	53(4)	-21(3)
O(10A)	280(19)	91(10)	38(4)	-29(5)	15(7)	-73(11)
N(1)	32(1)	20(1)	28(1)	0(1)	10(1)	1(1)
C(1)	29(1)	44(1)	34(1)	-9(1)	2(1)	10(1)
C(2)	26(1)	45(1)	50(1)	-6(1)	9(1)	2(1)
C(3)	28(1)	40(1)	38(1)	0(1)	12(1)	1(1)
C(4)	28(1)	24(1)	30(1)	-2(1)	9(1)	0(1)
C(5)	28(1)	23(1)	24(1)	-3(1)	6(1)	4(1)

C(6)	34(1)	76(2)	43(1)	-17(1)	-1(1)	9(1)
C(7)	79(4)	113(6)	45(4)	-39(4)	4(3)	-8(5)
C(7A)	74(5)	91(6)	52(5)	-40(5)	-2(4)	16(5)
C(8)	30(1)	22(1)	27(1)	2(1)	11(1)	-1(1)
C(9)	42(1)	32(1)	32(1)	-3(1)	4(1)	2(1)
C(10)	29(1)	38(1)	37(1)	10(1)	14(1)	5(1)
C(11)	44(1)	40(1)	55(1)	12(1)	19(1)	15(1)
C(12)	29(1)	22(1)	26(1)	-2(1)	8(1)	1(1)
C(13)	29(1)	28(1)	27(1)	-1(1)	8(1)	0(1)
C(14)	40(1)	25(1)	33(1)	-1(1)	12(1)	-2(1)
C(15)	44(1)	36(1)	54(1)	-12(1)	19(1)	-9(1)
C(16)	42(1)	34(1)	30(1)	-4(1)	14(1)	-3(1)
C(17)	114(2)	64(2)	36(1)	-10(1)	28(1)	-12(2)
C(18)	87(5)	94(5)	37(3)	7(3)	25(4)	4(5)
C(18A)	113(7)	58(4)	34(3)	-7(3)	28(5)	-14(5)

Table 22 Hydrogen coordinates (x 10^4) and isotropic displacement parameters ($Å^2$ x 10^3) for *per-O*-acetyl-4-deoxy-β-2,3-difluorosialic acid methyl ester (**57**).

Atom	x	y	z	U(eq)
H(1)	5391	7376	-24	32
H(2)	9991	8757	2315	49
H(3A)	8143	7616	1066	42
H(3B)	8200	9245	708	42
H(4)	5927	9824	1159	32
H(5)	6100	6902	1859	30
H(7A1)	9470	8748	5988	122
H(7A2)	7955	9709	5911	122
H(7A3)	9425	10391	5642	122
H(7A)	9636	9427	5848	115
H(7B)	8211	10518	5728	115
H(7C)	9673	10971	5355	115
H(9A)	2440	7953	-1440	56
H(9B)	4099	7593	-1601	56
H(9C)	3232	9067	-2013	56
H(11A)	840	11440	547	68
H(11B)	2610	11819	1121	68
H(11C)	1399	11441	1726	68
H(12)	3481	7397	1303	31
H(13)	4628	6489	3068	33
H(15A)	128	4607	1080	66
H(15B)	-138	5423	2013	66
H(15C)	553	3824	2129	66

H(16A)	4789	8925	3750	41
H(16B)	2916	8949	3424	41
H(18A)	4759	7479	6770	107
H(18B)	3989	6275	5972	107
H(18C)	2936	7542	6205	107
H(18D)	5432	6501	6149	100
H(18E)	3741	6791	6281	100
H(18F)	5170	7814	6815	100

Table 23 Dihedral angles [°] for *per-O*-acetyl-4-deoxy-β-2,3-difluorosialic acid methyl ester (**57**).

Atom1 - Atom2 - Atom3 - Atom4	Dihedral
C(5) - O(1) - C(1) - F(1)	-62.09(18)
C(5) - O(1) - C(1) - C(2)	55.9(2)
C(5) - O(1) - C(1) - C(6)	-177.64(17)
O(1) - C(1) - C(2) - F(2)	71.98(19)
F(1) - C(1) - C(2) - F(2)	-168.33(14)
C(6) - C(1) - C(2) - F(2)	-53.0(2)
O(1) - C(1) - C(2) - C(3)	-47.5(2)
F(1) - C(1) - C(2) - C(3)	72.14(18)
C(6) - C(1) - C(2) - C(3)	-172.54(17)
F(2) - C(2) - C(3) - C(4)	-70.1(2)
C(1) - C(2) - C(3) - C(4)	47.4(2)
C(8) - N(1) - C(4) - C(5)	118.22(16)
C(8) - N(1) - C(4) - C(3)	-121.81(16)
C(2) - C(3) - C(4) - N(1)	-175.36(16)
C(2) - C(3) - C(4) - C(5)	-54.19(19)
C(1) - O(1) - C(5) - C(12)	171.93(14)
C(1) - O(1) - C(5) - C(4)	-62.52(17)
N(1) - C(4) - C(5) - O(1)	-179.03(12)
C(3) - C(4) - C(5) - O(1)	59.87(16)
N(1) - C(4) - C(5) - C(12)	-57.66(17)
C(3) - C(4) - C(5) - C(12)	-178.76(14)
C(7A) - O(3A) - C(6) - O(2)	8.9(13)
C(7A) - O(3A) - C(6) - O(2A)	-28.4(12)
C(7A) - O(3A) - C(6) - O(3)	91(3)
C(7A) - O(3A) - C(6) - C(1)	-177.7(7)
C(7) - O(3) - C(6) - O(2)	27.4(10)
C(7) - O(3) - C(6) - O(2A)	-12.1(11)
C(7) - O(3) - C(6) - O(3A)	-85(3)
C(7) - O(3) - C(6) - C(1)	176.3(7)

O(1) - C(1) - C(6) - O(2)	164.7(5)
F(1) - C(1) - C(6) - O(2)	47.2(5)
C(2) - C(1) - C(6) - O(2)	-68.1(5)
O(1) - C(1) - C(6) - O(2A)	-156.7(5)
F(1) - C(1) - C(6) - O(2A)	85.8(5)
C(2) - C(1) - C(6) - O(2A)	-29.5(5)
O(1) - C(1) - C(6) - O(3A)	-9.2(6)
F(1) - C(1) - C(6) - O(3A)	-126.7(6)
C(2) - C(1) - C(6) - O(3A)	117.9(6)
O(1) - C(1) - C(6) - O(3)	15.3(5)
F(1) - C(1) - C(6) - O(3)	-102.2(4)
C(2) - C(1) - C(6) - O(3)	142.4(4)
C(4) - N(1) - C(8) - O(4)	-2.2(2)
C(4) - N(1) - C(8) - C(9)	178.79(15)
C(12) - O(5) - C(10) - O(6)	0.0(2)
C(12) - O(5) - C(10) - C(11)	178.80(14)
C(10) - O(5) - C(12) - C(5)	134.17(14)
C(10) - O(5) - C(12) - C(13)	-101.51(15)
O(1) - C(5) - C(12) - O(5)	72.72(15)
C(4) - C(5) - C(12) - O(5)	-48.96(17)
O(1) - C(5) - C(12) - C(13)	-50.44(17)
C(4) - C(5) - C(12) - C(13)	-172.12(13)
C(14) - O(7) - C(13) - C(16)	-163.54(14)
C(14) - O(7) - C(13) - C(12)	74.36(17)
O(5) - C(12) - C(13) - O(7)	89.03(15)
C(5) - C(12) - C(13) - O(7)	-148.46(13)
O(5) - C(12) - C(13) - C(16)	-29.23(19)
C(5) - C(12) - C(13) - C(16)	93.27(17)
C(13) - O(7) - C(14) - O(8)	-0.5(2)
C(13) - O(7) - C(14) - C(15)	-179.74(15)
C(17) - O(9) - C(16) - C(13)	161.2(2)
O(7) - C(13) - C(16) - O(9)	69.79(17)
C(12) - C(13) - C(16) - O(9)	-170.29(14)
C(16) - O(9) - C(17) - O(10A)	-11.4(15)
C(16) - O(9) - C(17) - O(10)	9.7(8)
C(16) - O(9) - C(17) - C(18A)	-164.8(5)
C(16) - O(9) - C(17) - C(18)	170.0(4)

Symmetry transformations used to generate equivalent atoms.

12.2 Curriculum Vitae

Stefan Hader

39 Shakespeare Avenue
Bath
Avon
BA2 4RF
United Kingdom

Nationality: Austrian

Mobile: 0044 7794162164

E-mail: stefan.b.hader@gmail.com

Education

PhD in Medicinal Chemistry, University of Bath 2007 - Present

- **Thesis Title**: *Synthesis and evaluation of fluorinated sialic acid derivatives as novel 'mechanism-based' neuraminidase inhibitors*

- **Brief Synopsis of Research**:
  The aim of the project is to translate the approach of Street et al. (*Biochemistry*, **1989**) to the generation of deoxygenated and fluorinated sialic acid derivatives towards a more detailed understanding of individual hydroxyl group contribution to transition-state stabilisation in influenza neuraminidases. This is achievable by using the kinetic behaviour of the deoxygenated and fluorinated sialic acid derivatives towards neuraminidase, as well as gaining structural information by X-ray crystallographic studies of these derivatives in complex with neuraminidase.

  During my PhD I was given the duty as a casual demonstrator, involving supervision of undergraduate students in the laboratory and in workshops.

Mag. rer. nat. in Organic Chemistry, University of Vienna, 1998 – 2006

- **Thesis Title**: *Cu(I)-catalysed 'Click chemistry' of 1,2,3 triazole derivatives of 6,6'-diazido-α,α'-trehalose*

- **Modules included**: Mathematics, Physics, Analytical-, Physical-, Organic-, Inorganic-, Theoretical-, and Bio-Chemistry.

A Levels at Bundesrealgymnasium Waidhofen/Ybbs 1998

- Chemistry (A), Biology (A)

Employment

- **Compulsory Community Service – GIN (2006)**: The job entailed guidance of mentally and physically disabled clients in daily life routines.
- **Assistant of the Deanery – Department of Chemistry (2005)**: Duties involved office work plus dealing with any of the Dean's inquiries.
- **Servant – Call&Mail (2001)**: General managing duties and dealing with customers enquiries.

Skills

- **Chemical synthesis**: Organic synthesis including enzymatic reactions and the handling of air, moisture and light sensitive compounds.
- **Biochemical work**: Inactivation kinetics, cell breakage, enzyme and immunoassays, protein purification SDS-PAGE and Western Blot analysis.
- **Analytical methods**: Skilled in spectroscopic techniques, analytical and preparative HPLC, high resolution mass spectrometry, AES and AAS of trace compounds.
- **Computer skills**: Proficient in the use of Windows 7, MS Office, ChemDraw, SciFinder Scholar, GraFit and PyMol.
- **Willingness to learn**: I am keen to develop and acquire new skills through employment.
- **Teamwork**: I have successfully undertaken a variety of team projects within both academic and non-academic environments.
- **Language skills**: German (native speaker), English (fluently spoken and written), French and Swedish (basics).

Publications, oral and poster presentations

- Telford, J. C.; Yeung, J. H. F.; Xu, G.; Kiefel, M. J.; Watts, A. G.; Hader, S.; Chan, J.; Bennet, A. J.; Moore, M. M.; Taylor, G. L. J. Biol. Chem. **2011**, 286, 10783.
- **15th European Carbohydrate Symposium, Vienna, July 2009**, oral presentation.
- **RSC Carbohydrate and Bioorganic Interest Groups Joint Meeting, London, April 2011**, poster presentation.
- **Sialoglyco Meeting, Potsdam, August 2010**, poster presentation.
- **8th Carbohydrate Bioengineering Meeting, Ischia, Mai 2009**, poster presentation.
- **23rd International Carbohydrate Symposium, Whistler Mountain, July 2006**, poster presentation.

Fellowships, grants, and prizes

- **MRC Capacity Building Studentship 2007 – 2011**
- **University of Bath, Department of Pharmacy and Pharmacology Travel Grant 2009**
- **Postgraduate Research Symposium 2008, Prize for best presentation**
- **University of Vienna, Travel Grant 2006**

References

Dr. A. G. Watts (Supervisor)
Department of Pharmacy and Pharmacology
University of Bath
Claverton Down
Bath
BA2 7AY
a.watts@bath.ac.uk
Telephone: 01225 386788

Prof. M. Threadgill (Internal Examiner)
Department of Pharmacy and Pharmacology
University of Bath
Claverton Down
Bath
BA2 7AY
m.d.threadgill@bath.ac.uk
Telephone: 01225 386840